

THESE

UNIVERSITE DE PAU ET DES PAYS DE L'ADOUR

École doctorale des Sciences Exactes et de leur Applications

Soutenance prévu le 04 mai 2018

par **Ekaterina POLEKH EPOVA**

pour obtenir le grade de docteur
de l'Université de Pau et des Pays de l'Adour
Spécialité : Environnement et Matériaux

ÉVALUATION DU POTENTIEL DES RAPPORTS ISOTOPIQUES STABLES DU STRONTIUM ET DU PLOMB POUR L'ORIGINE GÉOGRAPHIQUE ET L'AUTHENTICITÉ DES PRODUITS ALIMENTAIRES

MEMBRES DU JURY

RAPPORTEURS

- Miguel DE LA GUARDIA Professeur / Université de Valence, Valence, Espagne
- Douglas RUTLEDGE Professeur / AGROPARISTECH, Paris, France

EXAMINATEURS

- Isabel CASTANHEIRA Directeur de recherche / INSA, Porto, Portugal
- Milena HORVAT Professeur / Institute « Jožef Stefan », Ljubljana, Slovénie
- Joanna SZPUNAR Ingénieur de recherche / CNRS, Pau, France
- Gilles BAREILLE Chargé de recherche / CNRS, Pau, France
- Jiubin CHEN Professeur / Institute of Geochemistry, Chinese Academy of Sciences, Chine

DIRECTEUR

- Olivier DONARD Directeur de recherche / CNRS, Pau, France

INVITÉS

- Bernard MÉDINA Consultant et Conseiller Scientifique / CNRS, Pau, France
- Laurence SARTHOU Responsable développement Pôle Chimie / LPL, Lagor, France
- Francis GROUSSET Directeur de recherche retraité / CNRS, Bordeaux, France

Acknowledgments

First, I would like to thank the Laboratoire de Chimie Analytique Bio-Inorganique et Environnement, IPREM (LCABIE-IPREM, Pau) and Laboratoires des Pyrénées et des Landes (LPL, Lagor) for the support and contribution toward this project.

I express my appreciation for the financial support of this research by the ORQUE SUDOE INTERREG project № SOE3/P2/F591, MASSTWIN project № 692241, PROMETROFOOD project, Spanish contribution was supported by Ministry MINECO (project CTM2015-65414-C2-1-R).

My sincere gratitude goes to my advisor Dr. Olivier Donard, who encouraged me through out these years and allowing me the room to work in my own way.

My sincere thanks to Dr. Fabienne Séby, responsable d'Ultra-Traces Analyses Aquitaine, to Dr. Bernard Médina, Scientific Consultant of Société des Experts Chimistes de France, to Dr. Gilles Bareille, chargé de recherche, LCABIE, IPREM, to Dr. Francis Grousset, retired staff member of Laboratory of Environnements et Paléoenvironnements Océaniques et Continentaux CNRS, for their helpful suggestions and discussions.

I am grateful to Lydia Gauthier, to Dr. Bernard Médina, to Dr. Manuel Valiente, and also to PYRAGENA - Consortium du Jambon de Bayonne, and to Societe d'Exploitation Des Salines De Salies-De-Bearn for the collaboration in working out the sampling collection.

Last, but not least, I want to thank all my colleagues, friends and family for continued support over the years.

Table of contents

Abstract	9
Resumé (Français).....	10
List of figures and tables	11
List of abbreviations and acronyms	15
General introduction	17
Introduction générale (Français)	21

Chapter A

Stable isotope ratios of Strontium and Lead as tracers for food

provenance assessment 25

Abstract	25
A.1. Strontium isotope ratio as a tracer of food geological provenance	26
A.1.1. Strontium: general information and environmental impact	27
A.1.2. Strontium isotope ratio $^{87}\text{Sr}/^{86}\text{Sr}$	27
A.1.3. Ratio $^{87}\text{Sr}/^{86}\text{Sr}$ as a geological tracer: theoretical substantiation.....	29
A.1.3.1. Natural variability and transferability of $^{87}\text{Sr}/^{86}\text{Sr}$ ratios in the Earth ecosystem. . .	29
A.1.3.2. Influence from other Sr sources on a value $^{87}\text{Sr}/^{86}\text{Sr}$ in environmental samples. . .	33
A.1.4. Ratio $^{87}\text{Sr}/^{86}\text{Sr}$ as a food provenance tracer: experimental evidence	36
A.1.4.1. Beverages.....	37
A.1.4.2. Gramineae	40
A.1.4.3. Other food of vegetable origin	42
A.1.4.4. Food products of animal origin	46
A.1.5. Limitation of the method, problems in data interpretation and solutions	49
A.2. Isotope ratios of Lead as tracers of environmental ambient pollution	51
A.2.1. General information and environmental impact.....	51
A.2.1.1. Exposure pathways to the environment.....	51
A.2.1.2. Effects on terrestrial and aquatic systems	52
A.2.2. Lead isotopes: systematics and applications	51
A.2.3. Principles of lead isotopic fingerprinting for food traceability	55
A.2.4. Food origin by means of Pb isotopes	56
A.2.5. Perspectives and limitation	58
A.3. Conclusion	59

Chapter B**Analytical procedures for determining Sr and Pb isotopic compositions by MC-ICP-MS**

Introduction	77
B.1. A fit-for purpose procedure for sample preparation	79
B.1.1. Sample conditioning, sample pretreatment	80
B.1.2. Sample digestion	80
B.1.2.1. Wine	81
B.1.2.2. Ham	82
B.1.2.3. Tea	83
B.1.2.4. Salt	83
B.1.3. Multielemental analysis	83
B.1.4. Ion exchange chemistry	86
B.1.4.1. Sr column chemistry	86
B.1.4.2. Pb column chemistry	88
B.2. Isotopic analysis	89
B.2.1. Instrumentation, method description and operating parameters	89
B.2.2. Isotope ratio measurement and precision	90
B.2.2.1. Mass discrimination and mass bias correction	91
B.2.2.2. Sr isotope ratio measurement	92
B.2.2.3. Pb isotope ratio measurement	95
B.4. Chemometric technics	97
B.5. Conclusion	98

Chapter C**Authentic and regional discrimination of Bordeaux wines using elemental and non-traditional isotopic fingerprinting**

Abstract	101
C.1. Relevance of the issue	102
C.1.1. Sample description	104
C.2. Strontium elemental and isotopic compositions of Bordeaux wines	105
C.2.1. Introduction	105
C.2.2. Strontium elemental concentration	107
C.2.3. Strontium isotope ratios	110
C.2.3.1. Authentic Bordeaux wines	110
C.2.3.2. "Other wines" purchased in China	113
C.2.4. Combination of $^{87}\text{Sr}/^{86}\text{Sr}$ and Sr concentrations	114

C.2.4.1. Case of Pomerol wine	114
C.2.4.2. Variability of Sr isotope ratios and Sr elemental profile	116
C.2.4.3. Testing of wine authenticity by means of $^{87}\text{Sr}/^{86}\text{Sr}$ and Sr concentrations	118
C.2.5. Factors of influence on variability of Sr isotope and Sr elemental content	119
C.3. Lead elemental and isotopic compositions of Bordeaux wines	122
C.3.1. Introduction	122
C.3.2. Results.	123
C.3.2.1. Lead concentrations	123
C.3.2.2. Lead isotope ratios.	125
C.3.3. Temporal evolution of lead content during the period of 1962-2012	126
C.3.3.1. Changes of Pb concentrations	126
C.3.3.2. Changes of the $^{208}\text{Pb}/^{204}\text{Pb}$ ratio	129
C.3.4. Geographical provenance of wines by means of $^{208}\text{Pb}/^{206}\text{Pb}$ and $^{206}\text{Pb}/^{207}\text{Pb}$ ratios . . .	131
C.3.4.1. Bordeaux wines of vintages of 1969-2012	131
C.3.4.2. Wines with the suspicious Bordeaux provenance, vintages 1998-2009.	133
C.3.5. Geographic provenance of wines by means of non-radiogenic isotope ^{204}Pb	134
C.3.6. Wine dating	136
C.4. Elemental composition of Bordeaux wine for classification purposes	137
C.4.1. Authentic Bordeaux versus imitated Bordeaux and Chinese wines.	137
C.4.2. Differences in elemental content of red and white wines.	138
C.4.3. Is it possible to identify one Bordeaux winery from others?	138
C.5. Wine authenticity by means of trace elements, Sr- and Pb isotope ratios	141
C.6. Conclusion.	143
Chapter D	
$^{87}\text{Sr}/^{86}\text{Sr}$ isotope ratio and multielemental signatures as indicators of origin of European cured hams: The role of salt.	147
Abstract	147
D.1. Introduction	148
D.1.1. Sample description	151
D.2. Elemental composition	151
D.2.1. Selected trace and ultra-trace elements in dry-cured hams	151
D.2.2. Variability of elements composition of dry-cured ham	157
D.2.3. Elemental content of salt samples	158
D.3. Strontium isotopic signatures	161
D.3.1. $^{87}\text{Sr}/^{86}\text{Sr}$ in dry-cured hams	161
D.3.2. $^{87}\text{Sr}/^{86}\text{Sr}$ in salts	162

D.4. Is strontium in ham mostly sourced from salt?	163
D.5. Statistical approach	165
D.6. Conclusion	167

Chapter E

A comparative evaluation of Sr-, Pb- isotopic compositions and elemental profiles of teas for geographical origin discrimination. 171

E.1. Relevance of the issue.	171
E.1.1. Geographical origins of tea samples.	173
E.2. Strontium isotopic compositions and Sr concentrations of teas	176
E.2.1. China and Taiwan.	177
E.2.2. Japan	179
E.2.3. South Korea.	180
E.2.4. Vietnam	180
E.2.5. India, Sri Lanka and Nepal	181
E.2.6. Turkey	181
E.2.7. Rwanda	181
E.3. Lead concentrations and lead isotopic compositions of teas	184
E.4. Lead isotopic compositions of teas from China, Japan and South Korea as the signatures of the regional atmosphere and geology	185
E.4.1. Geographical origins of teas according to geochemical zoning of the Asian region	185
E.4.2. Lead isotopic signatures of teas as a record of regional atmospheric composition	189
E.4.3. Distinguishing of teas originated from Japan and South Korea	191
E.5. Distinguishing of geographical origin of Asian teas a by means of $^{87}\text{Sr}/^{86}\text{Sr}$, lead isotope ratios and multielemental concentrations	195
E.6. Conclusion	198

General conclusion and Perspectives 207

Appendix 1. Elemental concentrations in Bordeaux wines.	213
Appendix 2. Trace metals in teas origin China, Japan and South Korea	227
Appendix 3. Scientific contribution.	229
Appendix 4. Curriculum vitae	232

References 235

Abstract

Assessing the Potential of Stable Isotope Ratios of Strontium and Lead for Geographical Origin and Authenticity of Food Products.

Food authenticity and traceability have received an increasing interest during the last decade since the knowledge of food provenance is regarded as an additional warranty of its quality. The world's globalization brought to the consumers is more and more concerned with the origin of the food they eat because various products are subjected to adulteration or false denomination. The augmentative interest in anti-fraud and consumer protection has led to the extension of scientific research and development of effective tools of food authenticity control. Among the analytical technics applied to food authenticity and traceability, one of the most rapidly developing and promising method is based on fingerprinting of heavy elements detected by atomic spectroscopy. The multicollection inductively coupled plasma mass spectrometry (MC-ICP-MS) is recognized as a method of choice for the high precision measurement of numerous elements of the periodic table as well as ratios of their stable isotopes. This study present a new analytical strategy based on combined non-traditional stable isotopes and trace elements determination by ICP-MS. The benefits of combining information from two isotopic systems, one tracing the soil (Sr), and the other tracing environmental ambient pollution (Pb), allowed to obtain an exceptional new information about traceability and authenticity of selected food matrixes: prestigious Bordeaux wines, dry-cured hams and tea. Using complementary analytical techniques such as traditional elemental fingerprinting, the regional specification, as well as tracing of the food preparation process are possible. When combined with chemometrics, these analytical advances constitute an efficient and promising tool to detect food frauds, including adulteration of high value products with cheaper substitutes, forgery and falsification.

Key words: Food Authenticity – Geographic Origin – Strontium Isotope Ratio – Lead isotope ratios – Multi-Collection ICP-MS – Bordeaux Wine – Dry-Cured Ham – Salt – Tea

Résumé

Évaluation du Potentiel des Rapports Isotopiques Stables du Strontium et du Plomb pour l'Origine Géographique et l'Authenticité des Produits Alimentaires.

L'authenticité et la traçabilité des aliments gagnent un intérêt croissant au cours de la dernière décennie puisque la connaissance de la provenance des aliments est considérée comme une garantie supplémentaire de leur qualité. Les consommateurs ont également des inquiétudes et des préoccupations par l'origine de la nourriture qu'ils consomment car divers produits sont sujets à l'adultération ou à la fausse dénomination. L'intérêt accru à l'égard de la protection des consommateurs et de la lutte antifraude ont entraîné un accroissement de la recherche scientifique appliquée et le développement d'outils efficaces pour contrôler l'authenticité des produits alimentaires. Entre techniques analytiques appliquées à l'authenticité et à la traçabilité des aliments, les méthodes les plus prometteuses sont basées sur les empreintes d'éléments lourds mesurées par la spectroscopie atomique. La spectrométrie de masse à multicollection à couplage à plasma induit (MC-ICP-MS) est reconnue comme la méthode optimale pour effectuer des mesures de haute précision de nombreux éléments du tableau périodique en contrôlant simultanément les rapports entre leurs isotopes stables. Cette étude présente une nouvelle stratégie analytique basée sur des isotopes stables non-traditionnels combinés avec des éléments traces déterminés par ICP-MS. Les avantages de combiner les informations de deux systèmes isotopiques, l'un traçant le sol (Sr), et l'autre traçant la pollution environnementale ambiante (Pb), ont permis d'obtenir de nouvelles informations exceptionnelles sur la traçabilité et l'authenticité des matrices alimentaires sélectionnées : vins de Bordeaux, jambons secs et thé. En utilisant des techniques analytiques complémentaires telles que les empreintes des éléments traditionnelles, la spécification régionale, ainsi que le traçage du processus de préparation des aliments sont possibles. Traitée par la chimiométrie, cette approche analytique constitue un nouvel outil efficace et prometteur pour détecter des fraudes alimentaires, y compris l'imitation de produits de grande valeur, l'étiquetage erroné et la substitution par des produits moins cher.

Mots clés: Authenticité des produits alimentaires – Origine géographique – Rapport isotopique du Strontium – Rapports Isotopiques du Plomb – Multi-Collection ICP-MS – Vin de Bordeaux – Jambon sec – Sel – Thé

List of figures and tables

Chapter A

Stable isotope ratios of Strontium and Lead as tracers for food provenance assessment

Figure A.1. $^{87}\text{Sr}/^{86}\text{Sr}$ ratios in bedrocks, bulk soil, soil fractions, and plant parts	33
Figure A.2. Correspondence between levels of $^{87}\text{Sr}/^{86}\text{Sr}$ ratio in soil, water, and meat samples from different geographical areas.	33
Figure A.3. $^{87}\text{Sr}/^{86}\text{Sr}$ vs Sr concentration for rice samples	41
Figure A.4. Box plot diagram displaying $^{87}\text{Sr}/^{86}\text{Sr}$ of authentic beef samples ordered by geological settings of the sampling sites	48
Figure A.5. Box plot diagram displaying $^{87}\text{Sr}/^{86}\text{Sr}$ of beef origin of different Argentinian regions.	48
Table A.1. Concentrations of strontium in food and feed plants, mg kg^{-1}	60
Table A.2. Food product studied for authenticity, provenance and geographic origin using the strontium isotope ratio, analytical and statistical methods, precision of isotopic ratio determination	61
Table A.3. Strontium Isotope ratio in different food products reported from the region over the world . .	64
Table A.4. Relative abundances of Pb stable isotopes.	54
Table A.5. Lead isotope ratios in food product. Instrumentation, analytical methods, precision of isotope determination	74

Chapter B

Analytical procedures for determining Sr and Pb isotopic compositions by MC-ICP-MS

Figure B.1. A schema of analytical approach applied in the study	79
Figure B.2. A schema of a multi- collector mass spectrometer Nu Plasma 2.	90
Figure B.3. The reproducibility, accuracy and precision of measurement on example of 2 days measurement sequence	94
Table B.1. Materials used in the experiment	99
Table B.2. Reagents used in the experiment.	99
Table B.3. Apparatus used during in experiment	100
Table B.4. Analyzed elements and operating detection modes	84
Table B.5. Instrumental settings and data acquisition parameters of the NexION-300S	85
Table B.6. Certified and determined concentrations of elements in reference materials SLRS-5, RM 8414 and NIES 23.	85
Table B.7. The procedure for the sample matrix removal for Sr isotopic analysis.	87
Table B.8. The procedure for the sample matrix removal for Pb isotopic analysis	89
Table B.9. Mass assignment to Faraday cup detectors of Nu-Plasma HR for Sr and Pb isotopic determination	93
Table B.10. Instrument settings, data acquisition parameters for wet plasma operating conditions of Nu-Plasma HR and typical sensitivity for Sr isotopic analysis.	93
Table B.11. Summarized precision of Sr isotope measurements	94

Table B.12. Precision of Sr isotope measurements during a typical session of 5 days	94
Table B.13. Instrument settings, data acquisition parameters for dry plasma operating conditions of Nu-Plasma HR and typical sensitivity for Pb isotopic analysis	96
Table B.14. Comparison of the obtained and certified values of NIST 981	96
Table B.15. Comparison of the Pb isotope ratios, obtained in this study, and previously reported values for BCR 482.	97
Table B.16. The values of Pb isotope ratios of NIES 23 obtained in this study.	97

Chapter C

A comparative evaluation of Sr-, Pb- isotopic compositions and elemental profiles of Bordeaux wines with a view of authenticity and geographical origin

Figure C.1. Geographical map of the origin of the Bordeaux wines	105
Figure C.2. Sr concentrations in wines.	108
Figure C.3. $^{87}\text{Sr}/^{86}\text{Sr}$ in the wines and comparison with wines from different world origin, as reported in literature	111
Figure C.4. Evolution of $^{87}\text{Sr}/^{86}\text{Sr}$ ratios in Jurassic and Cretaceous sea water with respect of the period of geological formation of Saint-Émilion limestone plateau (red bound) and alluvial terraces of Pomerol (blue bound)	111
Figure C.5. Time dependent changes of Sr concentrations and $^{87}\text{Sr}/^{86}\text{Sr}$ ratios in wines from Pomerol	115
Figure C.6. Ratios of $^{87}\text{Sr}/^{86}\text{Sr}$ as a function of $1/\text{Sr}$ concentrations the wines studied, A – wines of authentic and suspicious Bordeaux origins; B – wines of Bordeaux origin	117
Figure C.7. Box plots of the Pb concentrations determined in studied wine samples	125
Figure C.8. Ranges of values of lead isotope ratios: (A) – $^{206}\text{Pb}/^{207}\text{Pb}$, (B) – $^{208}\text{Pb}/^{206}\text{Pb}$, (C) – $^{206}\text{Pb}/^{204}\text{Pb}$, (D) – $^{208}\text{Pb}/^{204}\text{Pb}$, and (E) – $^{206}\text{Pb}/^{204}\text{Pb}$ for wines from different geographical origin world over, as reported in literature	127
Figure C.9. Evolution of Pb concentration (A) and $^{208}\text{Pb}/^{204}\text{Pb}$ ratio in French wines during period of 1965-2012, observed in the wine from south-east (Rosman et al., 1998) and wine from Bordeaux (this study)	130
Figure C.10. Ratios $^{208}\text{Pb}/^{204}\text{Pb}$ and $^{207}\text{Pb}/^{204}\text{Pb}$ in authentic Bordeaux wines and wines with suspicious Bordeaux origin (purchased in China) in comparison with the predominant anthropogenic lead sources	132
Figure C.11. Comparison of linear regressions of ratios $^{208}\text{Pb}/^{204}\text{Pb}$ and $^{207}\text{Pb}/^{204}\text{Pb}$ in authentic Bordeaux wines and wines with suspicious Bordeaux origin, purchased in China	135
Figure C.12. Classification of different Bordeaux wineries by means of selected elemental concentrations: A) Sr and Li; B) Sr and B; C) B and V	139
Figure C.13. Comparison of elemental and isotopic compositions in authentic and adulterated wines from Pauillac: (A) - of Sr vs Li; (B) - Fe vs Mn; (C) - $^{87}\text{Sr}/^{86}\text{Sr}$ vs Sr elemental concentrations; (D) – $^{208}\text{Pb}/^{206}\text{Pb}$ vs $^{208}\text{Pb}/^{204}\text{Pb}$	142
Table C.1. Studied wines, Sr elemental concentrations and Sr isotope ratios	108
Table C.2. Interval and means of Pb isotopic ratios and Pb concentrations determined in wines	124
Table C.3. Pb isotopic ratios and Pb concentrations determined in wines	144

Table C.4. <i>P</i> - values and significance of the differences between the Pb concentrations and Pb isotope ratios for authentic and imitated Bordeaux wines	123
---	-----

Chapter D

⁸⁷Sr/⁸⁶Sr Isotope ratio and multielemental signatures as indicators of origin of European cured hams: The role of salt

Figure D.1. Analytical protocol	150
Figure D.2. Sr isotope ratios in dry-cured ham and salt samples	164
Figure D.3. Correlation of Sr isotope ratios in dry-cured ham and salt samples	165
Figure D.4. PCA for discrimination of dry-cured ham's geographic origin	166
Table D.1. Dry-cured ham and salt: geographical provenance of studied samples	152
Table D.2. Concentrations of selected elements (on dry weight basis) and values of the ratio ⁸⁷ Sr/ ⁸⁶ Sr in dry cured hams	154
Table D.3. Elemental content and Sr isotope ratio in individual dry-cured ham samples.	168
Table D.4. Elemental content and ratios ⁸⁷ Sr/ ⁸⁶ Sr in salt samples (mg kg ⁻¹)	160
Table D.5. Elemental content and Sr isotope ratio in individual rock salts.	170
Table D.6. Elemental content and Sr isotope ratio in individual sea salts.	170

Chapter E

Geographic origin classification of tea by means of Sr-, Pb- isotopic and elemental compositions

Figure E.1. Known geographical origins of Chinese teas including provinces: Yunnan, Guangxi, Guangdong, Fujian, Zhejiang, Anhui, Hubei, and Jiangxi	171
Figure E.2. Known geographical origins of tea samples from Japan (A) and South Korea (B)	174
Figure E.3. Known geographical origins of tea samples from Vietnam (B), and India, Sri Lanka and Nepal (B).	175
Figure E.4. Geographical origins of tea samples from Turkey (A) and Rwanda (B)	176
Figure E.5. Comparison of the isotopic composition of tea samples from China, Taiwan and Vietnam (A), and Japan (B) with previously published data	182
Figure E.6. Comparison of the isotopic composition of tea samples from South Korea (A); India, Sri Lanka, Nepal (B), Turkey (C), and Rwanda (D) with previously published data	183
Figure E.7. Known geographical origins of teas on a sketch map of China, South Korea and Japan with selected geochemical zones - Northern China Block (NCB), Yangtze Block (YB), and Southern China Block (SCB), modified after Bingquan (1995)	186
Figure E.8. A comparison plot of ²⁰⁶ Pb/ ²⁰⁴ Pb and ²⁰⁸ Pb/ ²⁰⁴ Pb ratios determined in tea samples and previously reported ratios in basalts, granites and ores from China, South Korea and Japan . .	187
Figure E.9. A comparison plot of ²⁰⁷ Pb/ ²⁰⁶ Pb and ²⁰⁸ Pb/ ²⁰⁶ Pb ratios determined in tea samples and previously reported ratios in aerosols and predominant Pb emission sources from China, South Korea and Japan	190
Figure E.10. A comparison plot of ²⁰⁷ Pb/ ²⁰⁶ Pb and ²⁰⁸ Pb/ ²⁰⁶ Pb ratios determined in tea samples origin Japan, South Korea and Chinese provinces with previously reported ratios in aerosols and dominant Pb emission sources in regions considered	193

Figure E.11. Origin differentiation in tea leaves from China (blue triangles), Japan (red circles), South Korea (gray squares) obtained by: (A) - plot of Sr concentration versus $^{87}\text{Sr}/^{86}\text{Sr}$ ratio; (B) - plot of $^{207}\text{Pb}/^{206}\text{Pb}$ and $^{208}\text{Pb}/^{206}\text{Pb}$ 196

Figure E.12. Origin differentiation of tea leaves from China (blue triangles), Japan (red circles), South Korea (gray squares) obtained by PCA: (A) - using 16 elemental concentration; (B) - using 16 elemental concentration completed with isotope ratios of Sr and Pb 196

Table E.1. Geographical origin and provenance of studied tea samples 199

Table E.2. Mean values, minimum and maximum values of Sr elemental concentrations and $^{87}\text{Sr}/^{86}\text{Sr}$ ratios in tea samples 178

Table E.3. Sr concentrations and $^{87}\text{Sr}/^{86}\text{Sr}$ in teas 202

Table E.4. Pb concentrations and Pb isotope ratios in teas 204

Appendix 1

Elemental concentrations of wines and tea for geographical origin classification

Figure 1.1. Comparison of elemental concentrations in authentic and imitated Bordeaux wines. 218

Table 1.1. Concentrations of selected elements in the studied wines 221

Table 2.1. Median values, minimum and maximum values of metal content in tea samples origin of China, Japan and South Korea 228

List of abbreviations and acronyms

ANOVA – Analysis of Variance
AOC – Controlled Designation of Origin
CCA – Canonical Correlation Analysis
CDA – Canonical Discriminant Analysis
CRM – Certified Reference Material
FA – Factor Analysis
GFAAS – Graphite Furnace Atomic Absorption Spectrometry
GPA – Generalized Procrustes Analysis
HCA – Hierarchical Cluster Analysis
IA – Isotopic Abundances
ICP-MS – Inductively Coupled Plasma Mass Spectrometry
IQR – Interquartile Ranges
IRM – Internal Reference Material
IRMM – Institute for Reference Materials and Measurements
IRMS – Isotope Ratio Mass Spectrometry
KNN – Nearest Neighbors Algorithm
LDA – Linear Discriminant Analysis
LOD – Limit of Detection
LOQ – Limit of Quantification
MC-ICPMS – Multicollector Inductively Coupled Plasma Mass Spectrometry
MHC – Multivariate Hierarchical Clustering
NIES – National Institute for Environmental Studies
NIST – *National Institute of Standards and Technology*
NMR – Nuclear Magnetic Resonance
NRCC – National Research Council of Canada
OIV code – International Code of Oenological Practices
PCA – Principal Component Analysis
PDO – Protected Designation of Origin
PGI – Protected geographical indication
PLS-DA – Partial Least Squares Discriminant Analysis
Q-ICP-MS – Quadrupole Inductively Coupled Plasma Mass Spectrometry
RM – Reference Material
SIMCA – Soft Independent Modelling by Class Analogy
SRM – Standard Reference Material
TIMS – Thermal Ionization Mass Spectrometry
TOF-ICP-MS – Inductively Coupled Plasma Time-of-Flight Mass Spectrometry
TSG – Traditional Specialties Guaranteed
UPGMA – Unweighted Pair Group Method with Arithmetic Mean
WHO – World Health Organization

General Introduction

The quality of food is a highly important subject worldwide and is of prime importance for the future of humankind. The possibility to assess provenance and authenticity of food products is regarded by customers as an additional warranty of their quality. In Europe, the priority is given to the products whose quality is guaranteed by European Union schemes of geographical indications, known as Protected Designation of Origin (PDO), Protected Geographical Indications (PGI), Traditional Specialties Guaranteed (TSG), and corresponding to them national legal protection systems, that promote and protect names of quality agricultural products and foodstuffs, and ensures that only genuinely products are allowed to be identified as such in commerce (Huygens et al., 2012). By the concept of PDO, PGI, TSG, food products are closely associated with their special geographical provenance and special preparation process, because their taste and nutritional value are significantly or even exclusively determined by the geographical environment, including natural and human factors. However, any higher quality and value products that can be substituted or diluted with a lower cost item are vulnerable. Hence, today the control of food authenticity is becoming crucial, since more and more products are subject to adulteration or false denomination. These problems are extremely important issues for the food production and distribution sector due to substantial health risks for the customers and, eventually, to enormous economic damage caused by frauds. For example, while a national legal protection system Appellation d'Origine Contrôlée (AOC) protect names of quality French wines, today the damage from counterfeit wine is estimated only for the French wine market to be around 36 million euros (Lecat et al., 2016).

For testing authenticity and providing analytical data on traceability, different analytical techniques are used and recognized by the various regulatory authorities. Often, their performance is based on considering of a large amount of chemical parameters, and the reliable data interpretation includes statistical treatment having regard to limits of reading the results obtained in actual cases (Danezis et al., 2016). However, food authentication and geographical origin can be assessed by a limited number of highly specific criteria which are closely related to the place of origin and/or features of the production process.

In this context, analytical methods dealing with stable isotope ratios determination have taken the lead in this field. Stable isotope ratio determination is one of the robust and most discriminant methods with traditional approach based on ratios of light bio elements such as hydrogen, nitrogen, oxygen, carbon and sulfur, determined often by isotope ratio mass spectrometry (IRMS)

and nuclear magnetic resonance (NMR). The ratios of $^2\text{H}/^1\text{H}$, and $^{18}\text{O}/^{16}\text{O}$ are strongly latitude dependent, while local agricultural practices and animal diet will rather affect the ratios $^{15}\text{N}/^{14}\text{N}$, and $^{13}\text{C}/^{12}\text{C}$, respectively. Stable isotope ratios of light elements have been used in food control since around 1975 to detect adulteration of food products of vegetable (Camin et al., 2017) and animal (Camin et al., 2016) origins.

The recent instrumental development of MC-ICP-MS (multi-collector inductively coupled plasma mass-spectrometry) have expanded the potential of isotopic analysis by adding the so-called “non-traditional” elements – strontium (Sr), lead (Pb) (Balcaen et al., 2010). Isotopes of Sr and Pb can be used as environmental indicators of food provenance assessment as they provide experimentally confirmed sustainable linkage between a food isotopic composition and lithosphere (isotopes of Sr), and anthroposphere (isotopes of Pb). Over the last decade there has been a noticeable increase of interest in the Sr and Pb isotopes application as a sensitive geochemical tracer in food sciences (Balcaen et al., 2010). Despite the first preliminary proposals having emerged in the 1990s, the real practical expansion of Sr and Pb isotopes for provenance assessment has only been available in recent years due to the introduction of MC-ICP-MS, whose outstanding precision and accuracy of simultaneous multi-isotopes detection offer information competitive with data obtained by TIMS as one of the reference techniques in the field of isotopic analysis (Walczyk, 2004). Authenticity testing and geographical origin assignment by Sr and Pb isotopes requires understanding and correct usage of a large data base, as well as input of detailed isotopic compositions of genuine food products or those of the regional environment being concerned. Overcoming such complexities, the food geographical origin can be defined with varying degrees of proximity to the respective region. For authenticity testing, the comparison of obtained data with isotopic ratios of authentic product is necessary. For example, recently created an extensive database of Sr isotopic map is able to objectively support the Lambrusco PDO wines (Durante et al., 2018).

This doctoral thesis focuses on the demonstration of potential of the use of Sr and Pb stable isotope ratios for food authenticity and provenance assessment. Based on extensive previous investigations, this research gathered the experimental evidences concerning the direct linkage of Sr isotopic composition of a food to the soil of its origin, and those of Pb to the regional atmospheric Pb isotopic specification, and applied them to the authentic Bordeaux wines, PDO/PGI dry-cured ham and original teas from all over the world. The present research is focused on the specificity of Sr and Pb isotopic compositions of genuine food products with a special goal to gain an informed understanding of the natural processes which assist with their formation. General understanding of such regularities within and between all constituents will contribute to further

develop applications of this analytical approach providing both geographic origin identification and authentic individuation of a food product.

The manuscript is organized in five chapters. The opening Chapter A highlights the main consistency in formation of Sr- and Pb- isotopic compositions of food products in view of all influential impacts from nature and humankind, and it places focus on the state of the art of practical applications, including limits of reliable interpretations. Then, the Chapter B is aimed to present an accurate and a high precise analytical approach for Sr- and Pb isotopes determination in different food matrixes of vegetable and animal origin, which is necessary to achieve reliable experimental results. Chapters C through E examine selected food products and discuss the general results.

Introduction générale

La qualité des aliments est actuellement un sujet de grande importance au niveau mondial qui va devenir crucial ces prochaines années. Tout particulièrement, l'obtention d'informations sur la provenance et l'authenticité des produits alimentaires est considérée par les consommateurs comme une garantie supplémentaire de la qualité des produits. En Europe, la priorité est donnée aux produits pour lesquels la qualité est garantie par des labels prouvant l'origine géographique, connus sous les mentions Appellations d'Origine Protégée (AOP), Indications Géographiques Protégées (IGP) ou Spécialités Traditionnelles Garanties (STG) et auxquels correspondent des protections légales nationales. Ces labels favorisent et protègent la qualité des produits alimentaires et permettent d'assurer leur authenticité quand ils sont retrouvés sur le marché (Huygens et al., 2012). Par ces mentions, les produits alimentaires peuvent être étroitement associés à leur provenance géographique et aux procédés de préparation qui leur sont spécifiques. En effet, la saveur et la valeur nutritionnelle des produits sont significativement, voire exclusivement, déterminés par l'environnement géographique. Toutefois, la qualité et la valeur des produits restent toujours vulnérables. De ce fait, le contrôle de l'authenticité des produits alimentaires est actuellement crucial car de plus en plus de produits sont affectés par des falsifications et/ou de fausses dénominations. Ces problèmes constituent des enjeux très importants pour la production agroalimentaire ainsi que pour le secteur de la grande distribution en raison des risques de santé substantiels qui existent pour les consommateurs. Des dommages économiques importants peuvent également être engendrés par ces fraudes. Par exemple, bien que des systèmes de protection nationaux comme l'Appellation d'Origine Contrôlée (AOC) protègent la qualité des vins français, les dommages dus à la contrefaçon sont estimés autour de 36 millions d'euros en ne considérant que le marché français seulement (Lecat et al., 2016).

Pour obtenir des informations sur l'authenticité et accéder à des données analytiques sur la traçabilité, différentes techniques reconnues par les autorités de régulation sont disponibles. Leur performance est souvent basée sur la mesure de nombreux paramètres chimiques et une interprétation fiable des données nécessite un traitement statistique au minimum (Danezis et al., 2016). Cependant, l'authenticité des produits et la détermination de leur origine géographique peuvent également être obtenues par un nombre plus limité de critères spécifiques qui peuvent être plus facilement reliés à l'origine et/ou au procédé de production.

Dans ce contexte, des méthodes analytiques permettant de mesurer des rapports isotopiques deviennent incontournables. Ce sont des méthodes robustes et discriminantes dont l'approche est

basée sur la mesure des isotopes d'éléments dits légers comme les isotopes de l'hydrogène, l'azote, l'oxygène, le carbone et le soufre. Les techniques utilisées sont le plus souvent la spectrométrie de masse de rapport isotopique (IRMS) et la résonance magnétique nucléaire (RMN). Les rapports isotopiques $^2\text{H}/^1\text{H}$, and $^{18}\text{O}/^{16}\text{O}$ dépendent fortement de la latitude alors que les rapports $^{15}\text{N}/^{14}\text{N}$, and $^{13}\text{C}/^{12}\text{C}$ sont affectés respectivement par les pratiques agricoles locales et l'alimentation animale. La mesure des rapports isotopiques des éléments légers est utilisée pour le contrôle alimentaire depuis 1975 pour détecter les falsifications sur l'origine de végétaux (Camin et al., 2017) et de produits alimentaires d'origine animale (Camin et al., 2016).

Le développement récent de la spectrométrie de masse à plasma inductif à multi-collection (MC-ICP-MS) a élargi le potentiel de l'analyse isotopique en permettant d'accéder à des éléments moins traditionnels comme le strontium (Sr) ou le plomb (Pb) (Balcaen et al., 2010). Ces isotopes peuvent être utilisés comme traceurs environnementaux de la provenance des aliments, les isotopes du strontium donnant des informations sur la lithosphère et ceux du plomb sur l'anthroposphère. Ces dernières années, la détermination des isotopes du plomb et du strontium a connu un grand intérêt en raison de leur sensibilité en tant que traceurs géochimiques dans le domaine de l'agroalimentaire (Balcaen et al., 2010). Bien que les premières études aient été publiées dans les années 90, les applications pratiques de la mesure des isotopes de ces deux éléments pour accéder à la provenance des produits agroalimentaires sont relativement récentes. Elles sont liées à l'introduction du MC-ICP-MS qui permet une détection simultanée de plusieurs isotopes avec d'excellentes justesse et précision et qui offre ainsi une information compétitive avec celle obtenue par le TIMS, technique considérée comme une référence dans le domaine de l'analyse isotopique (Walczyk, 2004). Les études sur l'authenticité et l'origine géographique au moyen des isotopes du plomb et du strontium nécessitent l'utilisation d'une base de données de qualité ainsi que des informations détaillées sur la composition isotopique du produit alimentaire authentique ou sur l'environnement immédiat d'où ils sont issus. En dehors de ces aspects complexes, l'origine géographique peut être définie selon divers degrés de proximité par rapport à la région respective. Par exemple, une base de donnée très complète sur la cartographie des isotopes du strontium a été récemment publiée qui permet de supporter l'AOP des vins Lambrusco (Durante et al., 2018).

Cette thèse de doctorat a pour objectif de démontrer le potentiel de l'utilisation des rapports isotopiques stables du plomb et du strontium pour déterminer l'authenticité et la provenance de certains produits agroalimentaires. A partir de travaux de recherche précédents, cette étude porte sur l'obtention de données expérimentales qui devrait permettre d'obtenir un lien direct entre la composition isotopique du strontium d'un aliment et celle du sol où il a été produit. Dans le cas du

plomb, ce lien est basé sur la composition isotopique atmosphérique. Ces mesures ont été appliquées à l'authenticité des vins de Bordeaux, du jambon possédant des labels AOP/IGP et des échantillons de thé prélevés dans le monde entier. Ce travail s'est particulièrement intéressé à la composition isotopique de Sr et Pb des produits authentiques pour mieux comprendre les processus naturels qui sont à leur origine.

Ce manuscrit est organisé en cinq chapitres. Le premier chapitre traite des rapports isotopiques du strontium dans les produits agroalimentaires recensés dans la bibliographie et des paramètres qui peuvent influencer leur composition. Dans un second chapitre, l'approche analytique retenue pour une mesure juste et précise des isotopes de Sr et Pb est présentée pour différentes matrices alimentaires végétales et animales. Enfin, les trois chapitres suivants portent sur les résultats obtenus pour les trois matrices étudiées.

Chapter A

Stable isotope ratios of Strontium and Lead as tracers for food provenance assessment

Abstract

Food traceability has received an increasing interest during the last decade and has led to the extension of scientific research in development of suitable and effective analytical methods to support modern legislative tools aimed at guaranteeing food authenticity and geographical origin. This review summarizes the practical results obtained with the use of the Strontium (Sr) and Lead (Pb) isotopic ratios, when applied to the traceability of the origin of different foods products, including vegetables, meat, beverages and dairy products. The principle of isotopic fingerprinting for both isotopic systems, natural variability of Sr- and Pb- isotopes in the environment, factors of influence, perspectives and limitation will be examined and commented.

A.1. Strontium isotope ratio as a tracer of food geological provenance

A.1.1. Strontium: general information and environmental impact

Strontium (Sr) is a chemical element, one of the alkaline-earth metals of Group №2 of the Periodic table with atomic number 38 and atomic weight 87.62. Strontium commonly occurs in nature, and it is the 15th most abundant element on Earth, composing about 0.04% of Earth's crust. Estimated content of Sr ranges between 260 and 360 mg kg⁻¹ in common rock types. It concentrates predominantly in mafic igneous rocks and in calcareous sediments. Strontium is found chiefly in the form of the sulfate mineral celestite (SrSO₄) and the carbonate strontianite (SrCO₃). Both geochemical and biochemical characteristics of Sr are similar to those of Ca. It is not an essential element, and its salts are generally non-toxic. Strontium is usually immobile in the environment because of its rapid precipitation as strontium carbonate.

Strontium content in soil is highly controlled by parent rock (Capo et al., 1998). Its compounds are moderately mobile in soil, with the predominant cation Sr²⁺ which is likely to be sorbed in its hydrated form by clay minerals and for this reason its concentration is higher in heavy loamy soils and can reach up to 3.1 g kg⁻¹. The distribution of Sr in soil follows the general trends: Sr can be concentrated in upper horizons of calcareous soils and can be leached down to the profile in acid soils. Strontium accumulation occurs preferably in roots with the highest uptake of Sr from high acid sandy soils. The highest strontium concentrations are found in deserts and forest soils (Kabata-Pendias, 2010).

The average Sr concentration in sea water is about 8 mg L⁻¹, in fresh water about 50 µg L⁻¹. This element is only a dietary requirement in a few exceptional cases for deep sea organisms who use strontium sulfate in shells. Strontium is water insoluble, but it does react with water and its compounds can be water soluble. Examples include strontium carbonate with a water solubility of 10 mg L⁻¹, and strontium chromate with a water solubility of 9 mg L⁻¹. When dissolved in water, Sr mainly occurs as Sr²⁺ and its another possible form is SrOH⁺.

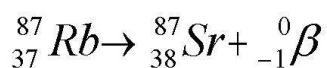
Strontium is considered as a non-essential element for plants with highly variable content: from a few micrograms per kilogram to around hundred milligrams per kilogram on dry mass basis, the average concentrations of Sr in food and feed plants are presented in the Table A.1, placed at the end of this chapter. The lowest concentrations are attributed to the grains (1.5-2.5 mg kg⁻¹) and the highest can be found in vegetable leaves (45-74 mg kg⁻¹) and in top parts of legumes and feed plants (219-662 mg kg⁻¹). The source of this element is presently still unclear, especially for land

plants: it can be originated either from soil exchange complexes, from soil solutions or from atmospheric particles (Techer et al., 2011). Biochemically, strontium is an analogue of calcium due to the same valence and similar ionic radius, it is taken up by plant roots from soil solutions following the plant metabolic requirements for calcium and it physiologically incorporated like calcium. Strontium assimilation is not identical in the different plant species since parts of the plant are strongly influenced by numerous parameters, such as type and pH of soil, nature of the plants, and presence of water. Strontium is likely accumulated in roots and the highest uptake of Sr is from acid light sandy soils. (Kabata-Pendias, 2010). The Sr absorption by plants is related to both mechanisms of mass flow and exchange diffusion (Nakano et al., 2001).

Living organisms obtain the strontium through the interaction with each other and the environment of its habitat. Strontium quantities in living organisms vary inversely to the organism position on the trophic pyramid: plants display higher levels of Sr than animals; herbivores, by the nature of their diet, display higher strontium than carnivores. Incorporated strontium accumulates in animal body tissues with higher concentrations in bones and teeth (Kabata-Pendias, 2010).

A.1.2. Strontium isotope ratio $^{87}\text{Sr}/^{86}\text{Sr}$

Strontium in nature occurs as a mixture of four stable isotopes: ^{88}Sr (82.6%), ^{86}Sr (9.9 %), ^{87}Sr (7.0 %) and ^{84}Sr (0.56 %). While ^{84}Sr , ^{86}Sr and ^{88}Sr are non-radiogenic (i.e., they are not the products of the radioactive decay), only ^{87}Sr is produced by β -decay from the radioactive alkali metal ^{87}Rb with a half-life of 4.88×10^{10} years:



On geological time scales, the abundances of isotopes 84, 86, and 88 are invariant. In contrast, the abundance of ^{87}Sr naturally increases with time and the present day quantity of ^{87}Sr depends on its initial stock (^{87}Sr at time zero) and the amount of radiogenic Sr generated from ^{87}Rb over geological timescales:

$${}^{87}\text{Sr}_{(sample)} = {}^{87}\text{Sr}_{(initial)} + {}^{87}\text{Rb}(e^{\lambda t} - 1)$$

where: t - is the age of the rocks, either that of primary crystallization, metamorphosis and/or sedimentary deposition (Veizer, 1989).

Thus, there are two sources of ^{87}Sr in any material: first, the initial portion formed in stars along with the isotopes ^{84}Sr , ^{86}Sr , and ^{88}Sr ; and second, the portion formed by radioactive decay $^{87}\text{Rb} \rightarrow$

^{87}Sr . This radioactive decay produced therefore distinctly different ^{87}Sr abundances in different parts of the Earth over its 4.5 billion year history. To measure differences in the ^{87}Sr abundances in various rocks or other samples, ^{87}Sr abundances are typically normalized to a non-radiogenic isotope ^{86}Sr , which absolute amount remains constant since the elements formation: any natural or instrumental mass dependent fractionation of the $^{87}\text{Sr}/^{86}\text{Sr}$ ratio is normalized against an $^{86}\text{Sr}/^{88}\text{Sr}$ ratio of 0.1194 (Faure, 1986).

The use of the $^{87}\text{Sr}/^{86}\text{Sr}$ ratio gives two great advantages over the use absolute ^{87}Sr abundances: a) it removes variations in ^{87}Sr abundances that reflect natural variations in total Sr; and b) allows to isolate the variations in ^{87}Sr abundances that are solely a function of $^{87}\text{Rb} \rightarrow ^{87}\text{Sr}$ decay (Beard & Johnson, 2000).

The dating of Precambrian and Proterozoic rocks was the first application of Sr isotope ratio (Sr IR) in chronological geosciences (Faure & Powell, 1972). Soon after, the first published study about Sr IR application to investigate the origin of groundwater opened new possibilities in hydrology (Chaudhuri & Claurer, 1992). Åberg (1995) presented the applicability of the Sr IR method to various aspects of earth and water sciences. Over the last decade there has been an increasing interest in the Sr IR technique and its application as a sensitive geochemical tracer, what has resulted in new applications of this method in paleontology, archeology and food sciences. At the present time the isotope ratio $^{87}\text{Sr}/^{86}\text{Sr}$ is widely applied in the following scientific areas:

- a) Geology: dating of formation and origin of rocks and minerals (Faure, 1986; Banner, 2004); soil genesis: tracing of metal sources and isotope mobility, chemical weathering (Prohaska et al., 2005);
- b) Hydrology: groundwater origin, tracing the sources and recharging of water pathways, provenance of sediment in natural water systems, temporal changes in the hydrologic and sedimentary cycles, (Graustein, 1989; Brenot et al., 2008; Banner, 2004; Capo et al., 1998; Prohaska et al., 2005; Lahd Geagea et al., 2008);
- c) Mechanisms of interactions within different ecosystems: transportation of cations through variable ecosystems (Nakano et al., 2001; Bailey et al., 1996; Grousset & Biscaye, 2005);
- d) Archeology: identification of the provenance of ancient archaeological biomaterials and artifacts (Capo et al., 1998; Balcaen et al., 2010; Rich et al., 2012, Coelho et al., 2017);
- e) Human and animal migrations studies: tracking spatial and temporal variability (Beard & Johnson, 2000; Hobson et al., 2010; Porder et al., 2003; Szostek et al., 2015; Maurer et al., 2012; Coelho et al., 2017);
- f) Ecology: tracking actual and historic anthropogenic contamination of ecosystems (Maurer et al., 2012; Balcaen et al., 2010; Miller et al., 2014; Sherman et al., 2015);

- g) Criminal forensics (Balcaen et al., 2010; Degryse et al., 2012; Coelho et al., 2017);
- h) Food authenticity and geographical provenance (Kelly et al., 2005; González et al., 2009; Balcaen et al., 2010; Zhao et al., 2014 ; Baffi & Trincherini, 2016 ; Coelho et al., 2017).

Extensive summaries of strontium isotope geochemistry have been given by Faure et al. (1972) and Faure (1986).

A.1.3. Ratio $^{87}\text{Sr}/^{86}\text{Sr}$ as a geological tracer: theoretical substantiation

For the last two decades, natural variations of Sr IR have been increasingly used to conduct provenance studies. The principle of application of Sr IR as a geological tracer for provenance assessment is based on the fact that the Sr isotope composition of the bedrock and soil are variable as a result of long-lived radioactive decay, and Sr isotopes are not fractionated during their cycle through the food chain. Plants from one geographic location, first, uptake strontium, then, concentrate it, and finally, their Sr isotopic composition became similar or closely approximate to this of soil and rock upon which they grew. Herbivore animals obtained Sr from the plants that they eat. Carnivores, in their turn, receive the Sr isotope composition similar to those of the herbivores that they eat. The different theoretical substantiation of this chain will be further discussed, such as: the natural variability of $^{87}\text{Sr}/^{86}\text{Sr}$ ratios in Earth's lithology, moving of Sr isotopes through the system rock-soil, its transferring through water sources and its entry into the food chain, uptake by plants and living organisms, and the influence of various factors on strontium isotope ratio composition of a substance.

A.1.3.1. Natural variability and transferability of $^{87}\text{Sr}/^{86}\text{Sr}$ ratios in the Earth ecosystem

Strontium constantly moves through a natural cycle which allows it to move around the earth. Any Sr naturally released by weathering rocks, sea spray in coastal regions, entrainment of dust particles and resuspension of soil, is transferring with air as dust particles and is subsequently settling down by wet deposition on the earth surface, or moving through soil, ground and stream water, vegetation, animals, and eventually enters the oceans, primarily by rivers. The compound annual flux of Sr into the ocean is about 5.4 million tons (Veizer, 1989). Strontium leaves the oceans, primarily by deposition in marine carbonate. A small amount of Sr is also transferred directly from the oceans to the atmosphere and transferred to the continents in precipitation (Capo et al., 1998). The principles of strontium isotope geology suggest that any Sr released primarily as a result of natural mechanisms has an isotopic signature that reflects only the

difference in source of contributions (Faure et al., 1972; Faure, 1986). Human activities including milling and processing of strontium-containing products, coal combustion, land application of phosphate fertilizers, and the use of pyrotechnic devices release Sr into the atmosphere, and then, this anthropogenically emitted Sr joins the flow of the natural cycle. Stable strontium can neither be created nor destroyed, it is becoming a component of the soil and water, and after, it is taken up and retained by aquatic and terrestrial plants.

Terrestrial rocks and minerals. A wide natural variation in the isotopic composition of Sr has been observed in different rock types and formations due to different initial concentrations and chemical behavior of Sr and Rb in geological processes in the timescale. The most primitive meteorite showed an initial $^{87}\text{Sr}/^{86}\text{Sr}$ value of 0.69899 (Capo et al., 1998). However, the minimal value currently encountered in the Earth's crust is about 0.702 (Rosner, 2010). The ancient granitic rocks and alluvial sands derived from similar felsic rocks have elevated $^{87}\text{Sr}/^{86}\text{Sr}$ ratios, ranged 0.720-0.780, that reflect their high Rb/Sr ratios and the age of the continental crust from which these rocks and sediments were derived (Voerkelius et al., 2010). Young volcanic rocks and oceanic basalts as well as sediments derived from them will generally have lower $^{87}\text{Sr}/^{86}\text{Sr}$ values, typically ranged from 0.702 to 0.705. However, igneous rocks with very young radiometric age have extremely high values of $^{87}\text{Sr}/^{86}\text{Sr}$ (up to 0.8) due to the formation by melting of old crustal gneisses, or derived from a sourced mineral rich in ^{87}Sr and ^{87}Rb , such as biotite. More typical values for common geologic materials may be found in literature (Faure, 1986; Capo et al., 1998).

Soils plays a key role in the Earth's ecosystem due to the interaction between the atmosphere, biosphere, hydrosphere, and lithosphere. Soil mineral composition is greatly influenced by the factors of soil formation. The process of soil formation starts from weathering of bed rock with associated erosion. Different types of parent rocks (sedimentary, metamorphic, and igneous) and different conditions which are present during soil formation, cause differences in soil mineral composition. The utility of the Rb-Sr isotope system results from the fact that different minerals in a given geologic setting can have distinct ratio $^{87}\text{Sr}/^{86}\text{Sr}$ as a consequence of different ages, original Rb/Sr values and the initial $^{87}\text{Sr}/^{86}\text{Sr}$. Thus, the first important concept for isotopic tracing using Sr IR was formulated in early studies: Sr in soil derived from any mineral through weathering will have the same $^{87}\text{Sr}/^{86}\text{Sr}$ as the mineral of source (Faure, 1986; Graustein, 1989; Kendall et al, 1995; Capo et al., 1998; Kennedy et al., 1998), i.e., the ratio $^{87}\text{Sr}/^{86}\text{Sr}$ in soils depend upon Rb/Sr ratios and the geological age of the rocks and soil developed on it. Durante et al. (2013) have demonstrated that Sr isotopic ratio variations in the soil extract fractions are the function of the geology of the area as well as of the chemical form in which the strontium is present.

However, as has been shown by Nakano et al. (2001), the Sr IR of initial bedrock are slightly lower than those in weathered rocks fragments: values of $^{87}\text{Sr}/^{86}\text{Sr}$ were observed in range 0.7039–0.7040 and 0.7042–0.7046 respectively. The recent study (Song et al., 2014) pointed out again this difference: all investigated sub-soil fractions had higher $^{87}\text{Sr}/^{86}\text{Sr}$ than bedrock. The authors explain this by higher weathering ability of radiogenic, mafic, and bedrock-forming minerals (such as biotite and hornblende) in comparison with felsic minerals, thus releasing their Sr easily into the soil, resulting in higher radiogenic $^{87}\text{Sr}/^{86}\text{Sr}$ values in soil than in bedrock.

Ground-, stream-, and sea waters. Ground and spring waters moving along specific flow paths slowly react with rocks and soils and gradually approach chemical equilibrium over long time periods and getting specific stable Sr isotopic compositions which reflect the $^{87}\text{Sr}/^{86}\text{Sr}$ of the soluble minerals of subsoil and bedrock (Voerkelius et al., 2010). For example, the values of $^{87}\text{Sr}/^{86}\text{Sr}$ of stream water have been found almost identical to those of sub soil, 0.7043 ± 0.0001 and 0.7044 ± 0.0002 , respectively (Nakano et al., 2001). This suggests that secondary minerals with high cation exchange capacity and wide distribution in the lower soil horizon and water-saturated zone are controlling the $^{87}\text{Sr}/^{86}\text{Sr}$ ratio and strontium concentrations in stream water through the exchange reaction. The study of (Song et al., 2014) confirmed that the Sr concentrations and $^{87}\text{Sr}/^{86}\text{Sr}$ in water come mainly from mineral dissolution with a minor contribution from atmospheric deposition and anthropogenic input: the $^{87}\text{Sr}/^{86}\text{Sr}$ in water samples were found within the range of: 0.70698 – 0.75753, which were close to those in the exchangeable soil fraction (0.70646 – 0.76283) and the carbonate soil fraction (0.70787 – 0.74561). For waters developed in multi-mineral rocks or soils, $^{87}\text{Sr}/^{86}\text{Sr}$ in any water parcel usually represents a mixture of Sr released from several sources, and, therefore, the exact contributions from individual minerals might be difficult to determine. In such a case, the Sr IR in plants from a given geological area reflects to a greater extent the Sr isotopic composition in ground water than subsoils and weathered rock (Kendall et al., 1998).

The $^{87}\text{Sr}/^{86}\text{Sr}$ ratios of most of the world's rivers range between 0.703 and 0.730, although some rivers have ratios close to 1 (Nakano, 2016). This variability caused by the differences in Sr isotopic composition of the aquifer rocks, resulting that the waters contacting older rocks have a more radiogenic signature than those contacting younger rocks. The study of more than 650 different European mineral waters demonstrated a significant correlation between $^{87}\text{Sr}/^{86}\text{Sr}$ of the water samples and the local surface geology (Voerkelius et al., 2010). The Sr isotope determination in British mineral waters sources (Montgomery et al., 2006) and in those located in France (Brach-Papa et al., 2009) also found a wide range of $^{87}\text{Sr}/^{86}\text{Sr}$ ratios that broadly reflect the age and lithology of the host aquifers. As water is completely bio-available to plants and animals, it

transfers the Sr isotope signature correlated with local surface geology and hydrology up the food chain without significant modification (Horn et al., 1998; Beard et al., 2000; Voerkelius et al., 2010) and becomes the main Sr source for plants and animals.

Contrary to fresh water, sea water has an extremely homogeneous $^{87}\text{Sr}/^{86}\text{Sr}$ isotopic composition due to its long residence time of several million years, and oceanic mixing time about a thousand years (Capo et al., 1998). The actual value $^{87}\text{Sr}/^{86}\text{Sr}$ of sea water is 0.709176 ± 0.000003 (Allègre et al., 2010). However, over long time scales, in order of 10^7 – 10^9 years, the Sr isotopic composition of seawater has changed significantly due to major tectonic events, such as uplift of the Himalayas (Veizer, 1989). Many studies have been dedicated to the determination of strontium isotopic composition of pre-historical sea water by measurements of unaltered marine fossils and deep sediments. It has been found that the value $^{87}\text{Sr}/^{86}\text{Sr}$ varied in the course of geological periods to a large extent, from 0.7068 up to 0.7091 (e.g. Jones et al., 1994; Koepnick et al., 1985).

Terrestrial plants. During growth and development plants uptake water-dissolved Sr, mainly sourced from the soil. Any biological processes, whether involved in plant metabolism, do not significantly cause the Sr isotope fractionation (Capo et al., 1998). In this hypothesis, the Sr absorbed by a plant is supposed to have the same value of $^{87}\text{Sr}/^{86}\text{Sr}$ as the water soluble fraction of soil in the growing area, which is linked to the geological bedrock (Graustein, 1989). Many studies have since confirmed that among different Sr sources, the exchangeable and carbonate fractions in soil and water together influence the plant $^{87}\text{Sr}/^{86}\text{Sr}$ ratio (Green et al., 2004; Swoboda et al., 2008; Brunner et al., 2010; Zampella et al., 2011; Song et al., 2014; Petrini et al., 2015; Song et al., 2015; Vinciguerra et al., 2016; Liu et al., 2016; Liu et al., 2017; Zannella et al., 2017). Apart from this, the seasonal and annual variations of the investigated $^{87}\text{Sr}/^{86}\text{Sr}$ isotope ratio in agriculture products are not significant (Swoboda et al., 2008), as well as isotopic fractionation of the Sr isotopic composition through the transport from the soil to the parts of plant (Brunner et al., 2010; Song et al., 2015). Figure A.1 illustrate the proximity of Sr isotopic signatures, obtain within the entire studied chain “rock – soil – soil’s extract – plant – fruits” on tree in region of South Korea (Song et al., 2015).

All these findings demonstrate the potential of the use of Sr IR as a marker in the provenance study of food vegetation origin. However, it should be noted that the ratio $^{87}\text{Sr}/^{86}\text{Sr}$ in plant might be affected by the Sr from the sources, other than geological. For example, some agricultural activity (Green et al., 2004; Song et al., 2014) and atmosphere deposition (Techer et al., 2011; Song et al., 2014) might be considered as a factor of influence. The most significant aspects will be discussed further.

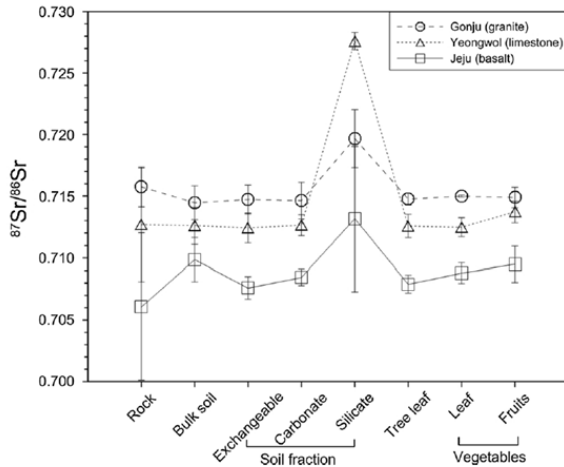


Fig. A.1: $^{87}\text{Sr}/^{86}\text{Sr}$ ratios in bedrocks, bulk soil, soil fractions, and plant parts (from *Song et al., 2015*).

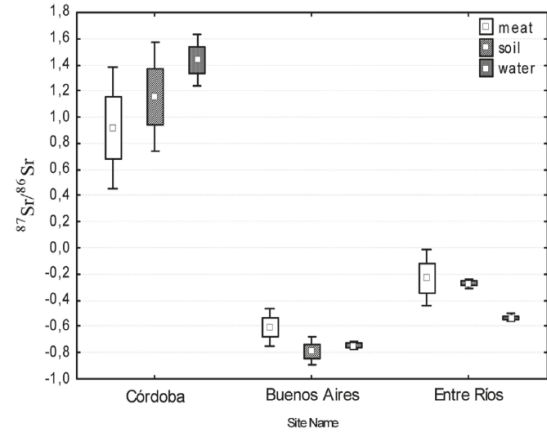


Fig. A.2: Correspondence between levels of $^{87}\text{Sr}/^{86}\text{Sr}$ ratio in soil, water, and meat samples from different geographical areas (from *Baroni et al., 2011*).

Living organisms. The strontium isotope composition reflects the concentration-weighted average of the Sr that was uptake (Beard et al., 2000). There are two important facts concerning the transfer of strontium through the food chain: a) terrestrial vegetation, available for nutrition purposes reflecting the Sr isotopic composition of labile cations in the soil, which are themselves influenced by bedrock, soil water properties, and atmospheric inputs (Graustein, 1989; Capo et al., 1998) and: b) any biological processes in plant or animal metabolism do not significantly fractionate strontium isotopes (Capo et al., 1998; Brunner et al., 2010). It can be resumed that Sr IR in animal tissue reflect to a certain extent the geological characteristics of the area growth or habitat. This hypothesis was confirmed by the experiment performed on soil, water and beef samples from three major cattle-producing regions of Argentina (Baroni et al., 2011), illustrated the correlation between Sr isotope composition of animal's muscle tissues and the geological settings from the site of the habitat. The beef samples from different cattles had the values of Sr IR close to those in soil and water from the same site (Fig. A.2).

A.1.3.2. Influence from other Sr sources on a value $^{87}\text{Sr}/^{86}\text{Sr}$ in environmental samples

Apart the ground waters, which dissolve and transport Sr from bedrock to plants, the atmosphere is the second major transport pathways for suspended Sr-contained particles in the environment, which are important to consider when assessing the potential for cation transportation through

variable ecosystems. Strontium released into the atmosphere is primarily taken from natural sources: rock weathering, resuspension of soil, entrainment of dust particles and sea spray dispersion, although the presence of Sr of anthropogenic origin cannot be ruled out. The atmospheric impact on the formation of local Sr isotopic signature can be significant: according to Pourcelot et al. (2008), from 50% to 80% of the Sr in the topsoil of a small catchment in the Vosges Mountains (eastern France, near its border with Germany) were of atmospheric origin. Examining of the ratio $^{87}\text{Sr}/^{86}\text{Sr}$ of plant roots pointed to the presence of an atmospheric and soil component, but the main source was a dust input coming from the atmosphere substantially exposes the upper layers of the soil. In contrary, in a region with lower industrial activity, such Réunion Island, the influence of atmospheric impact has been estimated as insignificant: the ratio $^{87}\text{Sr}/^{86}\text{Sr}$ in coffee beans was close to those of soil extracts (Techer et al., 2011). Therefore, the atmospheric impact is closely related also to human activity, which might be considered as the next important contributor of Sr releases as a consequence of agricultural and industrial activity.

Dust and sea spray transportation. The transport of continental dust through the atmosphere can be considered as a factor of influence for the Sr isotopic composition of aerosols (Grousset & Biscaye, 2005). For example, Saharan dust is lifted from its source in West Africa by strong winds and is blown northwards into weather systems heading to Southern Europe towards to Central Europe and eventually reaching the UK. Such large dust events can transport a large amounts of atmospheric suspended weathered rock particles over long distances and, thus, represent a significant impact of Sr from Sahara on the local ecosystems. The influence from volcanic dust on the Sr isotopic composition of coffee beans was observed in Hawaii (Rodrigues et al., 2011a).

In coastal areas the influence of sea spray is more important than in zones remote from the coast. Wet precipitation rich in components derived from sea salt particles have relatively constant $^{87}\text{Sr}/^{86}\text{Sr}$ ratio (0.70917-0.70935) through the year, they mix in different proportions with continental dust and may result spatial and temporal changes in $^{87}\text{Sr}/^{86}\text{Sr}$ of plants, as it has been shown on the example of coffee beans were correlation between the ratios $^{87}\text{Sr}/^{86}\text{Sr}$ of coffee and the distance from coast for each sampling site was observed (Rodrigues et al., 2011a).

In arid regions such as a desert with very low rainfall, the transfer of strontium from the bedrock and soil to the plant cannot be fully carried out because of lack of water in soil. In these climatic conditions often accompanied by strong winds, the relative contributions of atmospheric sources to bioavailable strontium in local soils prevails over the geogenic bedrock source. The wind brings not only weathered rock particles from other geological sites, but also anthropogenic dust, which

may increase the relative contribution of atmospheric Sr sources from different soil and climatic zones. As an example, the $^{87}\text{Sr}/^{86}\text{Sr}$ ratio measured in ligneous plants in Northern Israel and the Golan regions growing on volcanic bedrock show time dependent increase that confirm the significant impact of easily weathered radiogenic strontium brought by atmospheric deposition (Hartman et al., 2014). The $^{87}\text{Sr}/^{86}\text{Sr}$ results for cedar wood from Cyprus reflect a closer correlation with seawater than with bedrock, indicating greater influence of sea-induced rainfall and sea-spray in the island environment (Rich et al., 2012).

Precipitation. Assessing the impact of atmospheric wet deposition on the ratios $^{87}\text{Sr}/^{86}\text{Sr}$ of ecosystems is important because the amount of Sr-contained particles deposited on the Earth's surface could seasonally change around the year. As it has been observed in Japan, the seasonal changing of $^{87}\text{Sr}/^{86}\text{Sr}$ in local precipitation were found to be affected by contributions from Sr ultimately derived from volcanic rocks (Nakano, 2016). The Sr apportionment from different sources in Kawakami stream (Central Japan) has been calculated from the comparison of $^{87}\text{Sr}/^{86}\text{Sr}$ ratio of rainwater, stream water, bedrock; and the results indicated that about 10% of Sr in the stream water were precipitated with rains (Nakano et al., 2001). Atmospheric precipitations forming under the Atlantic Ocean, can bring significant wet dissolved Sr elemental flux with a strong dependency on seasonal to inter-annual scales (Maneux et al, 1999). Considerable amount of water passing through the soils horizons with different $^{87}\text{Sr}/^{86}\text{Sr}$ can change the hydrochemical dynamics in them resulting the release of extra-amount of bioavailable Sr sourced from soil or sub-soil substrata (Green et al., 2004). Also, an interaction between rain and plants was observed, when Sr cations were leached from the plants by the interaction of the rainwater with the leaves and bark, and later may be adsorbed through roots (Nakano et al., 1993).

Human activity. Despite the fact that in the beginning of the application of Sr isotopes ratio to trace provenance and geographic origin, it was pointed out that the agricultural activity does not affect the Sr IR significantly (Kawasaki et al., 2002, Green et al., 2004), some recent studies noted a significant variation of Sr ratio in different segment of geo- and ecosystems due to 'conventional cultivation' modalities to some extent (Horn et al., 1998; Kawasaki et al., 2002; Techer et al., 2011; Zampella et al., 2011; Techer et al., 2017). As great examples, two studies of Techer et al. (2011 and 2017) describe a significant disturbing influence from a substantial fertilization and diseases treatments on the Sr isotopic composition of plants. A deviation observed between $^{87}\text{Sr}/^{86}\text{Sr}$ ratio in coffee trees and in the deep soil from their plantation was attributed to the use of fertilizers (Techer et al., 2011). White clay used to protect the trees from 'olive fly' disease induces an increase of the $^{87}\text{Sr}/^{86}\text{Sr}$ ratio of the mobile and exchangeable fractions of the soils. This imprint

was observed only under 'conventional agricultural modality' that implies high spreading of white clays on the trees, and it is not detectable in a 'biological agriculture' modality (Techer et al., 2017). Also, application of fertilizers were considered as a major source of diffusion of pollution in agricultural areas, which significantly modified the natural Sr isotopic signature of groundwater in the small agricultural area in France (Brenot et al., 2008). Disparities observed in this study were considered as significant despite the small catchment zone and predicted as most likely to occur on larger scales.

Apart from the described above agricultural practices, other activities such as mining, forest liming and soil acidification (Maurer et al., 2012), soil leaching (Song et al., 2014), and water irrigation strategies (Brenot et al., 2008; Hartman & Richards, 2014, Techer et al., 2017) have contributed to increase of Sr concentration in the environment, and thus, to change the natural Sr isotopic composition. Maurer et al. (2012) attempted to estimate the impact from ensemble of anthropogenic sources of Sr on the ecosystem by comparing the Sr IR of archeological faunal teeth (from pig, sheep/goat, and cattle) with deer teeth from present days. The results showed that modern samples are very likely to be anthropogenically influenced to some extent.

Summarizing, the type and age of bedrock predominantly define the actual strontium ratio in the system soil-water-plants. The features of regional climates, dust transportation may affect it and require careful consideration depending on the geographical region. The influence from human activity, for the current state of knowledge, is not considered as a significant factor for changing the Sr IR in the system soil-water-plants. However, all these factors are not constant from one year to another, and must to be taken into consideration for the most complete data interpretation.

A.1.4. Ratio $^{87}\text{Sr}/^{86}\text{Sr}$ as a food provenance tracer: experimental evidence

During last two decades the SR IR as an origin discriminating tool has demonstrated promising results for different food matrices. In this part an extended review of the published results concerning application of Sr isotope method to food traceability and authenticity is presented. The use of the Sr IR of a particular food product to determine its geographical origin has been presented in more than fifty papers, which cover more than twenty different food products from all around the world. The analytical methods, instrumentations, and precision of determination, can be found in the Table A.2 (at the end of this chapter). All recapitulative information about food products, its geographical origin, the range of observed Sr IR values, as well as the Sr IR values of reference samples, can be found in the Table A.3 (at the end of this chapter).

A.1.4.1. Beverages

Wine

The first attempt of application of the $^{87}\text{Sr}/^{86}\text{Sr}$ ratio for food authenticity and traceability was performed on wine in 1993 by (Horn et al., 1993). Since that time, wine is the most studied food product (Tables A.2 and A.3). The case of wine is particularly interesting due to its relation with a number of aspects: temporary constancy of Sr IR in the lithology of the geographical area of interest, biological assimilation of Sr in plants, effect of winemaking process, and long-term stability of Sr IR in wine during storage. The following scientific facts play most important roles in successful tracing of wine geographical origin:

1. Sr isotopic signature of plant is strongly related to the bioavailable fraction of the soil (Horn et al., 1993; Almeida & Vasconcelos, 2004; Vorster et al., 2010; Durante, et al., 2013; Mercurio et al., 2014; Durante et al., 2015; Petrini et al., 2015; Marchionni et al., 2016; Braschi et al., 2018), and can be transferred to organic material without any significant modification;
2. Sr isotope composition is a long-term stable parameter, it doesn't significantly depend on human activity, climate or season of production (Voerkelius et al., 2010; Marchionni et al., 2013; Petrini et al., 2015; Durante et al., 2015; Marchionni et al., 2016; Braschi et al., 2018);
3. No significant variations of strontium ratio were found during the winemaking procedure and wine ageing (Almeida & Vasconcelos, 2004; Durante et al., 2013; Petrini et al., 2015; Tescione et al., 2015; Catarino et al., 2016; Marchionni et al., 2016; Vinciguerra et al., 2016; Braschi et al., 2018).

The results of the first attempt of Sr IR application for wine traceability (Horn 1993) were considered to be promising and few years later the same group (Horn et al., 1998) successfully applied this approach to prove a wrong declaration of wine provenance. With this first wine authenticity case study, the great potential of the Sr IR method has become obvious: the ratio $^{87}\text{Sr}/^{86}\text{Sr}$ of false nominated wines did not correspond to those in the soil of the area of declared provenance. Then, Almeida and Vasconcelos (2001) registered by quadrupole-based ICP-MS significant differences in the $^{87}\text{Sr}/^{86}\text{Sr}$ ratio within a set of 8 wine samples originated from Portugal and France (Bordeaux). However, accuracy of quadrupole ICP-MS is generally accepted as being insufficiently precise for the routine use of the geographical origin assignment. Following that, the more sensitive and precise instrumental modification of ICP-MS with multi-detection system was successfully applied for the discrimination of geographic origin of 11 wines produced in geologically different regions (Barbaste et al., 2002). The similarity of Sr isotope composition in wine, grapes

and vineyard soil was the subject of several extensive researches (Green et al., 2004; Almeida & Vasconcelos, 2004; Vorster et al., 2010).

Recently, a series of studies addressing the Sr isotopic method for wine geographical origin determination has been performed on Italian's vineyards (Marchionni et al., 2013; Durante et al., 2013; Mercurio et al., 2014; Durante et al., 2015; Petrini et al., 2015; Tescione et al., 2015; Marchionni et al., 2016, Durante et al., 2016; Durante et al., 2018; Ghezzi et al., 2018) using high precision analytical instrumentations MC-ICP-MS and TIMS. The ratio $^{87}\text{Sr}/^{86}\text{Sr}$ of the 45 analyzed wines (Marchionni, et al., 2013) was found correlated with the isotopic values of the geological substratum of the studied four vineyards, showing little or no variation within the same vineyard, and among different vintages. In contrast, a large $^{87}\text{Sr}/^{86}\text{Sr}$ variation was observed among wines from the different geographical areas. Another group of researches (Durante et al., 2015) studied the case of Lambrusco PDO: 186 individual wines from four vintages (2009, 2010, 2011 and 2012) obtained by same grape variety, but cultivated in three different districts and, thus, different soils in the region of Modena. The obtained results showed a perfect agreement between the isotopic range of wines and the soils from corresponding districts. These two findings reinforce the hypothesis that the Sr isotopic signature of wines is strongly related to the strontium bioavailable fraction of the soil. Again, researches didn't find any significant variability among the different vintages of wines. The Sr-isotopic systematics was also applied to grape musts from different Glera vineyards in the Veneto Region (Northern Italy), the region producing Prosecco wines (Petrini et al., 2015). The analysis focused on musts from the 2010, 2011 and 2012 vintages, in order to avoid the possible influence of the vinification process and to verify the lack of Sr isotopic fractionation within the plant. Musts from the different vineyards were characterized by variable $^{87}\text{Sr}/^{86}\text{Sr}$ ratio, which remains reproducible in the different harvests. For each vineyard, the Sr-isotope ratio in the must and that of the labile fraction in the corresponding soil are correlated within experimental uncertainty, indicating that the isotopic composition in the must can be forecast on the basis of that of the soil.

An interdisciplinary study (Mercurio et al., 2014), involving geologists, chemists and pedologists, was performed on wines from vineyards of Piediroso, the Campi Flegrei volcanic area Naples, Italy. The obtained results definitely linked the wine to its origin by the ratio $^{87}\text{Sr}/^{86}\text{Sr}$: within the entire studied chain soil extract – plant – wine the ratio $^{87}\text{Sr}/^{86}\text{Sr}$ varied in a relatively small range from 0.7078 to 0.7084. This range was found to fit well with the typical range of $^{87}\text{Sr}/^{86}\text{Sr}$ for volcanites of Campi Flegrei (0.7065–0.7086). The results from this study (Mercurio et al., 2014) were in a good

agreement with those from the study of Marchionni et al., (2013) performed on the wine from the same region of Napoli.

For the provenance assessment of Italian wine 'Cesanese' from six selected vineyards in Lazio region, the ratio $^{87}\text{Sr}/^{86}\text{Sr}$ has been determined in wines, musts grape juices, soils and rocks (Marchionni et al., 2016). The data reveal that strontium isotope ratio remained constant for the wines from different vintage years and does not change through winemaking procedure, for this purpose the Sr ratio in musts was controlled as well. This results are especially meaningful due to taking into account the exceptional measurement accuracy and precision of their TIMS mass-spectrometer (the within-run precision of $^{87}\text{Sr}/^{86}\text{Sr}$ measurements has been typically below or equal to 10 ppm). An excellent correlation between Sr IR measured in geological substrata, vine branches and grape juices demonstrated by Durante, et al. (2013), Vinciguerra et al. (2016) and Braschi et al. (2018). More proof that neither winemaking nor aging are able to change the $^{87}\text{Sr}/^{86}\text{Sr}$ values through the processes, was presented in the study of Tescione et al. (2015) and Braschi et al. (2018) investigated oenological preparation chain in the laboratory conditions.

When looking at vineyards from around the world, the Sr IR method has been applied for the geographical origin classification of wines from South-Africa (Vorster et al., 2010), Argentina (Di Paola-Naranjo et al., 2011), Canada (Vinciguerra et al., 2016), Portugal (Martins et al., 2014; Fernandes et al., 2015; Catarino et al., 2016) and Romania (Geană et al., 2017). The quadrupole ICP-MS applied as of Sr isotopes ratio detection method (Martins et al., 2014; Fernandes et al., 2015; Catarino et al., 2016, Geană et al., 2017), is generally characterized by relatively lower analytical precision and accuracy in comparison with MC-ICP-MS or TIMS (Table A.2). For improving the regional discrimination of these wines, the additional parameters, such as physico-chemical characteristics (Catarino et al., 2016), trace elements (Di Paola-Naranjo et al., 2011; Geană et al., 2017, Fernandes, et al., 2015), organic components (Di Paola-Naranjo et al., 2011, Fernandes et al., 2015) and stable isotopes (Di Paola-Naranjo et al., 2011) were applied.

Orange juice

Within the EU-project "Pure Juice" approximately 150 authentic orange juice samples from several regions in North- and South-America, Africa and Europe were analysed in order to determine and/or verify their geographical origin (Rummel et al., 2010). It was found that orange juices from Cuba and Mexico show quite similar ratio $^{87}\text{Sr}/^{86}\text{Sr}$, ranged between 0.7056 and 0.7075. The samples from South Africa demonstrated the highest values of the ratio $^{87}\text{Sr}/^{86}\text{Sr}$ among all investigated samples, in the range of 0.7185–0.7224, which is in a good agreement with the data of Barbaste et al. (2002) obtained for South African wines. The range of the $^{87}\text{Sr}/^{86}\text{Sr}$ values

registered for jus from Florida (USA) and Spain partly overlapped: 0.7078-0.7083 and 0.7081 – 0.7091 respectively. A large variation of $^{87}\text{Sr}/^{86}\text{Sr}$ was noted for Italian samples (0.7073-0.7107), however, the largest span of the value $^{87}\text{Sr}/^{86}\text{Sr}$ was observed in Brasilein orange jus, from 0.7075 to 0.7188. This significant variability was explained by patchy sampling sites distribution in regions characterized by heterogeneous lithology. As result of this work, orange juices from South-Africa have been distinguished from almost all others by applying the Sr IR, while overlaps between others of single origins did not allow to distinguish them by means of Sr isotopes.

Mineral waters

The Sr IR method was applied to European mineral waters (Voerkelius et al., 2010; Brach-Papa et al., 2009; Montgomery et al., 2006). The series of mineral bottled waters from Britain shown a wide range of $^{87}\text{Sr}/^{86}\text{Sr}$ isotope compositions ranging between 0.7059 and 0.7207, the highest value was obtained from watercourse in the Dalradian aquifer of Aberdeenshire, Scotland (Montgomery et al., 2006). French mineral waters characterized also by a large variability of the Sr signatures: from 0.7082 for waters "Vauban" and "Amanda" from Northern France up to 0.7163 for mineral water "Arvie" from central part of France (Brach-Papa et al., 2009). Within the food traceability project "TRACE", an extensive investigation of Sr IR of about 650 different European natural mineral waters was performed (Voerkelius et al., 2010). Strontium isotope ratio in waters ranged from 0.7035 to 0.7777, and showed a strong correlation with a great diversity of European lithological settings. All authors mentioned the importance of the contribution of these data to authentication purposes of commercially available mineral waters.

A.1.4.2. Gramineae

Rice

Strontium isotope ratio method was used to characterize the origin of rice cultivated in Australia, California, China and Vietnam (Kawasaki et al., 2002). The value of $^{87}\text{Sr}/^{86}\text{Sr}$ of the Chinese and Vietnamese rice samples ranged from 0.710 to 0.711 were slightly higher than the majority of the Japanese samples. Australian rice showed the highest $^{87}\text{Sr}/^{86}\text{Sr}$ ratio of all the rice examined, ranging between 0.715 and 0.717. Conversely, the Californian rice had a value of $^{87}\text{Sr}/^{86}\text{Sr}$ around 0.706. More clear origin discrimination was observed through combining $^{87}\text{Sr}/^{86}\text{Sr}$ ratios of sixty-eight rice samples cultivated at different sites in Japan, California, China, Australia, Korea and Vietnam using only $^{87}\text{Sr}/^{86}\text{Sr}$ ratios or combination of it with cadmium concentrations and ratio $^{11}\text{B}/^{10}\text{B}$ (Oda et al. , 2002). The recent study (Ariyama et al., 2011) confirmed previous results (Kawasaki et al., 2002): Australian rice samples have higher mean value $^{87}\text{Sr}/^{86}\text{Sr}$ (0.7152) than that

in samples from USA (0.7058), China (0.7104) and Japan (0.7081), but they partly overlap with the rice samples from Thailand, also characterized relatively high Sr IR (0.7136). Improved geographical discrimination efficiency achieved for rice samples from Japan, Thailand, China and the USA by combination of Sr isotopic and elemental information (Ariyama et al., 2012), presented in the Fig. A.3. Recently, Lagad et al. (2017) observed the Sr IR in basmati rice varied within the interval from 0.7110 to 0.7340 depending on studied region in Northern India that allowed to discriminate the sample origin.

Barley, wheat

The ratio $^{87}\text{Sr}/^{86}\text{Sr}$ of barley and wheat of Australian origin demonstrated the same tendency like the rice from the same study (Ariyama et al., 2011), i.e., for both cereal crops from Australia, the Sr isotope ratio were significantly higher than those for the samples of other investigated origins. Australian barley (0.7145) and Australian wheat (0.7145) were found significantly distinct from Chinese barley (0.7104), Canadian barley (0.7109) and wheat (0.7080), from Californian barley (0.7087) and wheat (0.7080), and by a greater degree with Japanese barley (0.7073) and wheat (0.7062). Using the Sr elemental concentrations as an additional distinguishing parameter, Ariyama et al. (2011) have recognized Australian barley and wheat from the cereal corps of other origins. Recently, Liu et al. (2016; 2017) found the Sr isotopic signatures of wheat from six Chinese provinces to be statistically indistinguishable, however in good agreement with the ratio $^{87}\text{Sr}/^{86}\text{Sr}$ obtained for Chinese rice (Kawasaki et al., 2002; Ariyama et al. 2012). European cereals were also investigated for their Sr isotopic composition (Voerkelius et al., 2010; Asfaha et al. 2011). In combination with other stable isotope data and concentration of selected metals, a statistical approach allows to individualize 15 of the 17 sampling sites across Europe representing an extensive range of geographical and environmental characteristics was proposed.

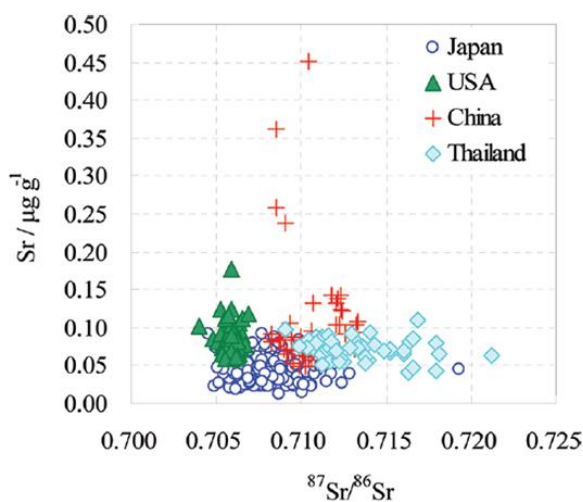


Fig. A.3. $^{87}\text{Sr}/^{86}\text{Sr}$ and Sr concentration in rice samples (from Ariyama et al., 2012).

A.1.4.3. Other food of vegetable origin

Asparagus

A large variety of European asparagus (more than 140 samples) were investigated in terms of their classification of geographical origin using Sr IR (Swoboda et al., 2008, Zannella et al., 2017). These studies present a great database for authentic Austrian Marchfeld asparagus and White Asparagus from Bassano del Grappa (PDO). A particularly important fact is that annual changes of Sr IR in asparagus are considered to be invariant. The asparagus samples from Marchfeld (0.7095 ± 0.0008) can be distinguished from asparagus from the neighboring countries only by value of $^{87}\text{Sr}/^{86}\text{Sr}$: with the probability of 100% from the Hungarian samples (0.7069 ± 0.0011), and with the probability more than 80% from the Slovakian asparagus (0.7079 ± 0.0014).

Cabbage

The Sr IR method was applied to distinguish the geographical origin of Chinese and Korean cabbage after a series of cases in Korea, when imported and less expensive cabbage from China was illegally sold as Korean product. The Sr IR analysis showed no distinct difference between fresh plants originated from China and South Korea (Bong et al., 2012b), nor in processed salad named “kimchi” (Bong et al., 2012a). On the contrary, a significant difference between the washed and unwashed “kimchi” samples was apparent, probably due to the presence/absence of salt with potentially relatively high Sr content. The authors suggested to apply an additional distinguishing parameter, such as concentrations of trace- or major elements.

Coffee

Coffee, along with wine and grains, has become one of the most studied food product in terms of using its Sr isotopic compositions to provenance purposes (Rodrigues et al., 2013). The ratio $^{87}\text{Sr}/^{86}\text{Sr}$ has been applied to coffee origin classification at regional level (Techer et al., 2011; Rodrigues et al., 2011a) and at an intercontinental scale (Liu et al., 2014; Rodrigues et al., 2011b). All performed studies have created a unique database of the ratio $^{87}\text{Sr}/^{86}\text{Sr}$ of coffee from worldwide origin: Africa (Ethiopia, Rwanda, Kenia, Tanzania, Malawi, Reunion, Uganda, Zambia, Zimbabwe), America (El Salvador, Guatemala, Jamaica, Mexico, Costa Rica, Nicaragua, Brazil, Colombia, Peru, Ecuador), South-East Asia et Pacific (Taiwan, Papua New Guinea, Indonesia, East Timor, Hawaii) (Appendix A, Table 2).

Africa: Green coffees from Zimbabwe (0.7169), Zambia (0.7121), Malawi (0.7131-0.7148), and Rwanda (0.7144) show the highest $^{87}\text{Sr}/^{86}\text{Sr}$ values among African samples, while coffee from Kenya (0.7069), Tanzania (0.7060), Ethiopia (0.7075) had the value significantly lower (Rodrigues et al., 2011b).

Central America: the results reported by (Rodrigues et al, 2011b) for coffee origin from El Salvador, Jamaica and Guatemala were in good agreement with the results obtained for coffee of the same origin (Liu et al., 2014), for coffee from Mexico (Rodrigues et al., 2011a), and for Mexican orange juice (Rummel et al., 2010).

South America: Brazilian coffee revealed a wide variation in Sr IR from 0.7068 to 0.7155, and was successfully distinguished from coffees origin Ecuador, Jamaica, Nicaragua and El Salvador (Rodrigues et al., 2011b). The similar large span was observed for Brazilian orange juices, had the values of $^{87}\text{Sr}/^{86}\text{Sr}$ ranging between 0.7075 and 0.7188 (Rummel et al., 2010).

South-Eastern Asia: Green coffee from East Timor was characterized by significantly higher values of the ratio $^{87}\text{Sr}/^{86}\text{Sr}$, ranging from 0.7159 to 0.7296 (Rodrigues et al., 2011b). These coffee samples have been distinguished from all other origins using only this criterion. The ratio $^{87}\text{Sr}/^{86}\text{Sr}$ reported by Rodrigues et al. (2011b) for coffee origin Papua New Guinea (0.7043) is in good agreement with those obtained by Liu et al. (2014) - 0.70472.

Summarizing, a successful discrimination of coffee geographical origin was obtained by using solely the ratio $^{87}\text{Sr}/^{86}\text{Sr}$, such as for coffees from different American countries (Ecuador, Jamaica, Nicaragua, El Salvador, Brazil and Hawaii), and for Asian coffee (Papua New Guinea and Indonesia). However, because of the large variability of Sr IR in coffee of different origins and existing overlapping between them, it has been proposed to apply additional isotopic systems, such as isotope ratios of light elements O, N, C, S, and concentrations of selected elements, to achieve more complete classifications of coffee (Rodrigues et al., 2013).

Olive Oil

The preliminary determination of Sr IR in olive oil faced the main complexities in relatively low concentrations of Sr in oil and the matrix rich of organic matters (Janin et al., 2014; Medini et al., 2015). Despite this, the feasibility of a discrimination based on the Sr isotopic tracer of such a complicated matrix was demonstrated: the $^{87}\text{Sr}/^{86}\text{Sr}$ ratios of the two studied Moroccan olive oils (the value is higher than 0.7089) appear to be significantly higher than the French samples from Nimes (the ratio $^{87}\text{Sr}/^{86}\text{Sr}$ varies around 0.7073–0.7088). The Sr isotopic compositions ($^{87}\text{Sr}/^{86}\text{Sr}$) of

varied organs (branches, leaves and olives) of olives trees and those of their growing environment (soils, waters, agricultural products) were discussed for two distinct agricultural fields in context of the geographical origin assignment (Techer et al. 2017).

Onion

Sr elemental and isotopic compositions were used to trace the geographical origin of onions from Japan, China, the USA, New Zealand, Australia, and Thailand (Hiraoka et al., 2017). The ratios of onions from different production regions of Japan were: 0.70395-0.70992 (n=128), China: 0.70974-0.71859 (n=100), USA: 0.70650-0.71324 (n=32), Australia: 0.70894-0.71056 (n=8), New Zealand: 0.70769-0.70883 (n=6) and Thailand: 0.70968-0.72099 (n=4). Sr content in onions from China, USA and Thailand were higher than the Sr content in Japanese. Using two parameters, Sr IR and Sr concentrations, onions from Japan were distinguished from onion from China. However, Sr content and $^{87}\text{Sr}/^{86}\text{Sr}$ ratios of Japanese onion were similar to those in samples from New Zealand and Australia. The classification of onions among main production regions within one country was possible for Japan and China.

Paprika

A comprehensive traceability study by Sr isotope composition of processed spice was performed on paprika (Brunner et al., 2010), especially aimed to establish a unique fingerprint of authentic product Szegedi Fűszerpaprika (PDO, Hungary) and its potential distinguishing from paprika of different origins. The Sr IR values in Szegedi paprika samples were ranged from 0.7076 to 0.7086. The paprika samples from China, Spain, Senegal and Italy can be clearly distinguished from each other by the Sr IR, only. The ratio $^{87}\text{Sr}/^{86}\text{Sr}$ and trace metals concentrations of authentic Szegedi Fűszerpaprika were proposed as sufficient criteria for fingerprinting this product with the goal to identify falsely declared samples. A considerable attention in this study has been given to possible alteration of the strontium isotopic composition during production process. The results confirmed that the Sr isotopic composition of paprika samples is not altered significantly through the food processing if no additional ingredients were added and if individual substances do not undergo a considerable mixing.

Potatoes

The discrimination of potato samples according to geological substrate has shown inconsistent results. For the potatoes grown in soils developed on alluvial sediments and volcanic substrates the successful discrimination of geographical origin by means of the ratio $^{87}\text{Sr}/^{86}\text{Sr}$ was obtained,

while the values of $^{87}\text{Sr}/^{86}\text{Sr}$ in potatoes grown in soils covering carbonate rocks partly overlapped both above mentioned groups (Zampella et al., 2011). Following these results, a model presupposed the multivariate treatment of the series of additional markers, such trace metals concentrations, secondary metabolites, and DNA, has been successfully applied for discriminating the origin of studied Italian potatoes (Adamo et al., 2012).

Sugar

Apart from olive oil, sugar is another complex food matrix for determining Sr IR primarily due to the low concentrations of Sr, but also because of the extremely high glucose content, which makes the sample preparation step a difficult task. The pilot measurements of Sr IS in sugar samples using different analytical methods (HR-ICP-MS, MC-ICP-MS and TIMS) were performed. In spite of differences in precision of HR-ICP-MS, all three techniques were suitable for the purpose of differentiating sugar samples on the basis of Sr isotopic compositions. The observed ratios $^{87}\text{Sr}/^{86}\text{Sr}$ of cane and beet sugar were within the range of 0.70810 – 0.71024. (Rodushkin, et al. 2011).

Tea

The Sr IR method was applied to determine the origin of tea leaf collected from four major plantation gardens in Taiwan (Chang et al., 2016). The tea leaf specimens in Taiwan display a wide variability of $^{87}\text{Sr}/^{86}\text{Sr}$ values, ranging from 0.70483 to 0.71454, and reflecting the large diversity in ambient soils and rocks. But only the tea samples from Taitung plantation (0.71379) was characterized by significantly different value of the ratio $^{87}\text{Sr}/^{86}\text{Sr}$ comparing to the others plantations - 0.70807 (Alishan), 0.70929 (Zhushan) and 0.70812 (Hualien).

Indian tea from geographically remote producing regions Assam, Darjeeling, Munnar and Kangra, showed even greater variability in the range of Sr IR than for tea from Taiwan (Lagad et al., 2013). On the basis of Sr IR data, Darjeeling tea samples were found to be more radiogenic than the other tea samples, the mean value of the ratio $^{87}\text{Sr}/^{86}\text{Sr}$ was 0.745 ± 0.029 , while this parameter for samples of other regions ranged between 0.711 and 0.732. Also, a strong correlation of the ratio $^{87}\text{Sr}/^{86}\text{Sr}$ in soil and plant was observed.

Vegetables (not specified)

Sr ratios of randomly selected samples of burdock, ginger, taro, garlic, podded pea, and other vegetables grown in Japan and China were examined for geographical provenance distinguishing (Aoyama et al., 2017). The $^{87}\text{Sr}/^{86}\text{Sr}$ ratios for most of the Chinese vegetables were higher than

those for the Japanese vegetables. Using the Sr concentrations, distinguishing between Japanese and Chinese vegetables has been reported for garlic and burdock.

A.1.4.4. Food products of animal origin

Livestock animals continuously consume a large variety of foods with associated elements and compounds that do not only originate from their natural surroundings. Supplementary nutrition can be industrially produced or brought from geographically distant sources. When animals are mainly feed by local produced feeds, the values of the ratio $^{87}\text{Sr}/^{86}\text{Sr}$ in their tissues will then reflect the local geological settings and could be used as a tracer for geographical origin. No fractionation of strontium isotopes is impervious to biological processes (Rossmann et al., 2000; Crittenden et al., 2007). For processed food, different preparation steps can slightly alter the original $^{87}\text{Sr}/^{86}\text{Sr}$ ratio of the raw material (Pillonel et al., 2003; Fortunato et al., 2004). Despite of these limitations, the discriminating potential of the $^{87}\text{Sr}/^{86}\text{Sr}$ ratio was confirmed on different types of prepared food matrices, which will be detailed further.

Dairy products

The first study performed on a food product of animal origin has demonstrated that the $^{87}\text{Sr}/^{86}\text{Sr}$ in butter of different European and non-European origin agreed with local geological structures (Rossmann et al., 2000). Accordingly this study, butter samples from Australia, Sweden, and Finland, showed the highest $^{87}\text{Sr}/^{86}\text{Sr}$ values among other samples: 0.71137, 0.71394, and 0.71292, respectively. Sr IR in butter samples from Germany varied in the significantly lower range: 0.70765-0.70895.

During examining of Emmental-type cheeses produced in Germany, France, Switzerland, Austria and Finland, the Sr isotope ratio data completed by light elements stable isotope ratios improved discriminating among origin of Finland and France (Pillonel et al., 2003). Next study (Fortunato et al., 2004) was focused more on confirming the authenticity and geographic traceability of cheese using specially the Sr IR. It has been found that the cheeses from St Gallen and Bern (Switzerland), Vorarlberg (Austria), and Savoy (France) showed the similar value of the ratio $^{87}\text{Sr}/^{86}\text{Sr}$ narrowly variable from 0.70812 to 0.70876, most likely that this regions belongs to the same geological sedimentary basin. However, that Finnish cheese showed significantly higher value - 0.71278, which is in good agreement with the results obtained for Finnish butter (Rossmann et al., 2000). Bontempo et al. (2011) measured the value $^{87}\text{Sr}/^{86}\text{Sr}$ in cheeses from different Italian regions, and

this parameter allows significantly distinguished cheeses from Asiago (0.70806) and Montasio (0.70773) in comparison with: Spressa (0.70981), Fontina (0.70970) and Toma (0.70963).

Milk from Australia and New Zealand was subjected for provenance study (Crittenden et al., 2007). Although no direct correlation of the Sr isotope ratios in the most of milk samples with anticipated geological values has not been found, the values of $^{87}\text{Sr}/^{86}\text{Sr}$ in the milk samples showed a large degree of variation indicating that stable strontium isotopes could prove useful in assessing geographic origin.

Meat and poultry

With reference to research studies aimed to origin differentiation of meat and poultry by means of Sr IR method (Franke et al., 2008; Baroni et al., 2011; Rummel et al., 2012; Rees et al., 2016), the following analytical challenges can be pointed out: 1) animal protein is known to be a difficult material to conduct Sr isotopic analysis; 2) higher ratio Rb/Sr in a raw material, typically more than 500; 3) low strontium concentration of meat and its small variation among samples. Other factors influencing on the Sr ratio in meat - intensive husbandry, type of feed and drinking water, possible contaminations with Sr of mineral supplements, contamination during food processing or influence from additives and preservatives - could mask country differences being present in the raw meat and poultry.

According Franke et al. (2008), the first data obtained for poultry showed the promising results: the samples origin of Germany (0.708) were significant by different from those of France and Hungary (0.711). However, the more recent study of Rees et al. (2016), performed on a large series of poultry worldwide, noted a relative homogeneity of the ratio $^{87}\text{Sr}/^{86}\text{Sr}$ among the samples origin Argentina (0.70785-0.70873), Brazil (0.70706-0.70905), and Europe (0.70861-0.70978) most likely due to intensive indoor farming methods applied on the majority of poultry factories. Only samples from Thailand had slightly more radiogenic Sr IR values (0.71034-0.71114). As a consequence, no clear discrimination has been reached among studied origins. Widely used practice of keeping commercially fattened poultry in cages with no access to free range and open environment, as well as feeding with industrial feed, resulting in the ratio $^{87}\text{Sr}/^{86}\text{Sr}$ reflects to a greater extent the feed components used in their diets than the local geological settings. Despite the expectations that beef should be in closer contact to their environment than poultry, the discriminative power of the Sr isotopes for countries of origin was even lower in the dried beef samples: the variations between investigated origin were within the range from 0.709 (USA, Canada) to 0.710 (Australia,

Switzerland), according Franke et al. (2008). For beef origin of Brazil and processed in Australia, the ratio $^{87}\text{Sr}/^{86}\text{Sr}$ was about 0.709, while the Brazil beef processed in Switzerland was 0.712. This fact illustrates that all details of meat preparation are extremely important and additional information about processing is needed, as well as more detailed specification concerning geographical placing of farms is request for successful distinguishing of origin.

However, beef samples origin from certain European regions have been distinguished only by means of the Sr IR within the TRACE project (Rummel et al., 2012; <http://www.trace.eu.org>). Discrimination of origin was consistent with the geological settings of the regions of beef provenance: samples from regions with acid magmatic rocks shown the consequently highest values of $^{86}\text{Sr}/^{87}\text{Sr}$ and those from limestone areas - the lowest strontium isotope ratio values (Fig. A.4). More clear classification of beef geographic origin was obtain on meat from three major cattle-producing regions of Argentina (Baroni et al., 2011). Samples from Cordoba presented the highest values of the ratio $^{87}\text{Sr}/^{86}\text{Sr}$, however, meat from Buenos Aires and Entre Ríos did not present significant differences although partly overlapping (Fig. A.5).

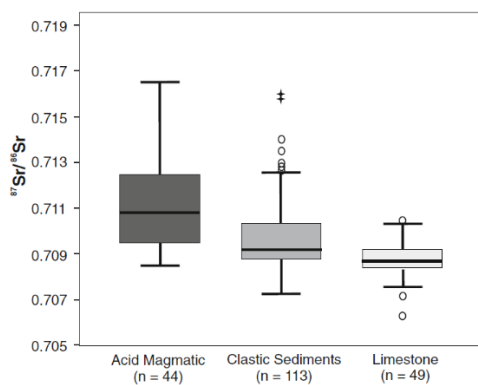


Fig. A.4. $^{87}\text{Sr}/^{86}\text{Sr}$ of authentic beef samples ordered by geological settings of the sampling sites). (Figure from Rummel et al., 2012).

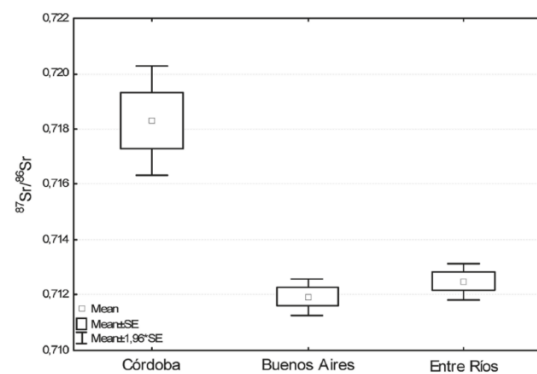


Fig. A.5. Box plot diagram displaying $^{87}\text{Sr}/^{86}\text{Sr}$ of beef origin of different Argentinean regions. (Figure from Baroni et al., 2011).

Caviar

Vendace and whitefish caviars from brackish- and freshwaters were tested for authentication and finding whether there are significant differences between the eggs from different sources (Rodushkin et al., 2007). Variations in the $^{87}\text{Sr}/^{86}\text{Sr}$ ratio for caviar from different harvests (on the

order of 0.05–0.1%) were found to be at least 10-fold less than differences between caviar processed from salt water and freshwater roe. Brackish water caviar origin from a sea bay shown the Sr ratio within a range from 0.71065 to 0.71099, while freshwater caviar samples had the values $^{87}\text{Sr}/^{86}\text{Sr}$ significantly higher: 0.72227 (Sweden), 0.72132 (Finland), and 0.71826 (USA). It has been assumed that the Sr IR of caviar origin of sea bay is a product of mixing Sr IR of seawater (0.70918) and Sr IR from northern Swedish rivers, where the ratio $^{87}\text{Sr}/^{86}\text{Sr}$ varied between 0.721 and 0.745.

A.1.5. Limitation of the method, problems in data interpretation and solutions

In order to identify geographic origins of a food sample on the basis of its Sr isotopic composition, the ratio $^{87}\text{Sr}/^{86}\text{Sr}$ of the sample must be compared to data of authentic samples from the region in question. This approach seems rather laborious technically and analytically because the creation of an authentic data base involves the development representative sampling strategy, complex sample-preparation procedures, precise and accurate isotopic analysis, and appropriate statistical data treatment and summarizing of results. A special concern is the assembling of an adequate number of authentic samples which can represent the maximally entire Sr isotopic variability of the area. It is challenging because of the large geological diversity and possible limited access to authentic reference samples in distant areas.

One of the most complete and successful studies was performed in the framework of the European project "TRACE" (Voerkelius et al., 2010). A geological map expressing a characteristic spatial distribution of $^{87}\text{Sr}/^{86}\text{Sr}$ across of Europe has been created and applied specially for food traceability and authenticity purposes. First, a large series of 650 different European natural mineral waters were analyzed for their Sr isotopic composition, and then, the results were used to elaborate a spatial prediction model for Sr IR by combining the measured data and the geological constitution of Europe available in Geographic Information System (GIS). The resulting map demonstrated a strong potential to predict the Sr isotopic composition of groundwater, honey and wheat samples. This study was one of the first experiences of establishing "isoscapes", or "isotope landscapes", - a new scientific concept, could be defined as spatially explicit predictions of elemental isotope ratios that are produced by executing process-level models of elemental isotope fractionation or distribution in a GIS (Bowen, 2010). Such landscapes have been established at first for light stable isotopes, (e.g., C, N, O and H) and have been addressed to scientific questions about terrestrial and aquatic ecosystems for climatic models application, Earth's element cycles, human

water use, and archaeological reconstructions. Recently, the applicability and significance of Sr isoscapes have been recognized in relation to various global environmental issues, such as an human/animal migration study (Frei & Frei, 2011; Frei & Frei, 2013; Kootker et al., 2016, Beard et al., 2000; Evans et al., 2010; Hobson et al., 2010), archeological artefacts (Kootker et al., 2016; Beard et al., 2000), and geological and/or hydrological study application (Bataille & Bowen, 2012; Bataille et al., 2014), and food origin determination and authenticity proof of regional food products (Evans et al., 2010; Frei & Frei, 2011; Frei & Frei, 2013). Such Sr isoscape maps were established for regions all over the world: Europe (Frei & Frei, 2011; Frei & Frei, 2013; Voerkelius et al., 2010; Kootker et al., 2016; Evans et al., 2010); Mediterranean (Hartman & Richards, 2014); North America: (Beard & Jonson, 2000; Bataille & Bowen, 2012; Bataille et al., 2014), and Asia (Asahara et al., 2006).

However, some geographic regions cannot be distinguished only using Sr isotope signatures because of the similarity of their geological settings. For this case another approach has been recognized as effective: combining of obtained information with the other analytical parameters, such as stable isotope ratios of light elements (Horn et al., 1998; Rodrigues et al., 2011a; Rodrigues et al., 2011b; Pillonel et al., 2003; Franke et al., 2008; Bontempo et al., 2011), multielemental data (Fortunato et al., 2004; Mercurio et al., 2014; Dehelean & Voica, 2012; Ariyama et al., 2012; Liu et al., 2014; Chang et al., 2016; Zampella et al., 2011; Adamo et al., 2012; Brunner et al., 2010; Bontempo et al., 2011), isotope ratio of boron (Vorster et al., 2010; Liu et al., 2014; Oda et al., 2002; Chang et al., 2016) and lead (Ariyama et al., 2012; Ariyama et al., 2011; Dehelean & Voica, 2011). The combination of the most discriminating parameters with Sr isotopes with following chemometrics data treatment highly increased the discrimination power of Sr isotope method for food provenance and origin determination.

A.2. Isotope ratios of Lead as tracers of environmental ambient pollution

A.2.1. Lead: general information and environmental impact

Lead (Pb) is a chemical element in the carbon group of periodic systems with atomic number 82 and atomic weight 207.2. Lead is nonessential, highly toxic heavy metal whose known effects on biological organisms are always deleterious. Lead is widely represented in the nature: it occurs as an important constituent of more than 200 minerals, but at the same time it is relatively rare metal with average concentration in the earth's crust is about 10 mg kg^{-1} . Apart from natural sources of the lead, there are many anthropogenic sources of lead exposure including emission from mining and metallurgy, additions of lead in paint, gasoline, water distribution systems. Lead is considered to be one of the most dangerous pollutants of the environment, because it easily moves into and throughout ecosystems and its compounds are readily absorbed and accumulated by plants.

A.2.1.1. Exposure pathways to the environment

Lead is naturally emitted to the environment predominantly by weathering rocks, soil particle flux, forest and brush fires, wind-blown suspension of dust and sea salt spray, volcanic eruption, radioactive decay, and, in minor proportions, meteoritic dust. The mean predicted natural emissions of lead to the global atmosphere is about $1.8 \times 10^9 \text{ kg}$ per year (Richardson et al., 2001). This value is two orders of magnitude higher than previous estimations made by Nriagu (1989) - about $1.2 \times 10^7 \text{ kg}$ per year. However, nowadays, anthropogenic emissions of lead is estimated much greater than natural rates and contributes up to 80-90 % from global lead emission (Komárek et al., 2008, Sen et al., 2012).

Historically, lead was one of the first metals to be exploited by humans due to its accessibility and ease of processing, it has been used extensively for weights and anchors, housewares, water piping, lead-based copper piping solder, and pottery glaze. In the period between the 18-th and 19-th centuries, the lead emission from human activity becomes more and more noticeable owing to greatly increased demand for this metal during the Industrial revolution. However, a long-term global accumulation of lead was occurred during XX-th century by impact from mining and mineral processing, utilization of automobile gasoline, waste incineration, coal and wood combustion, lead water pipes, Pb- containing fertilizers and pesticides in agriculture practices, production and use of ammunition and lead-acid batteries (Han et al., 2015). A special mention should be made about

vehicular emissions – a significant emission source of anthropogenic lead, which appeared with the adoption of organic lead compounds as an anti-knock additive in gasoline in the 1920's. During XX century alkyl-lead gasoline additives brought the largest contribution to world's metals pollution and became the most important sources of atmospheric lead pollution throughout the world in the 1960s and 1970s (Pacyna & Pacyna, 2001). Despite the fact that today more and more countries around the world are refusing the use of leaded gasoline, in 2011 the total population directly affected by tetraethyl lead from gasoline was estimated about 195 million people in the following countries: Afghanistan, Algeria, Iraq, North Korea, Burma, and Yemen (O'Brien, 2011) and much of this lead is still present in the environment as lead-contaminated dust, soil and sediments.

Today, much of Pb in production, such as industrial emissions, usage of Pb containing materials etc., are regulated by law or even have been banned, such as utilization of leaded automobile fuel, Pb-based paints and pipes. There are several remaining major sources of anthropogenic lead emission: production and utilization of aviation gasoline, metal industry, waste incinerators, fuel combustion, and weathering contaminated by burned leaded gasoline sides of roads, improper renovation of buildings and disposal of building materials.

A.2.1.2. Effects on terrestrial and aquatic systems

The main transport and distribution pathway for atmospherically emitted lead is the air. Some of lead can be transported through industrial wastes, sewage irrigation, the use of fertilizers and pesticides and their subsequent rainwater runoff from agricultural fields.

Air. Most of the lead in the air presents in the form of sub-micron-sized particles, which fall out near from the source. However, about 20 percent is widely dispersed (Rosman et al., 1994) and can be transferred over long distances. The surfaced ice at the North Pole has lead levels up to two orders of magnitude higher than in the in pre-historical era, at the less polluted South Pole this value is 3 to 5 times higher compared with the pre-technological period (Pattee & Pain, 2002). The atmospheric deposition is considered as a major process to remove Pb contained particles from the atmosphere (Pacyna & Pacyna, 2001). Most airborne lead eventually deposits on vegetation, soil- and water surfaces by dry deposition (gravitational settling of particles of all sizes) and/or wet deposition (the incorporation of particles into water drops).

Soils

Agricultural soils contaminated by Pb is one of the most serious ecological problems due to high lead toxicity for human health. Because of strong lead adsorption in soil, it is generally retained in the upper soil layers and can remain relatively immobile for up to 2000 years (Pattee & Pain, 2002). The world's average concentration of natural lead in sedimentary rocks and soils was estimated about 10 mg kg⁻¹, while world average Pb concentration in agricultural soils was assessed about 33.7 mg kg⁻¹ (Reimann et al., 2012). Naturally high soil lead concentrations exist in nature up to 1520 mg kg⁻¹, but in most cases elevated levels of lead in the soil are the result of human activities. In undisturbed ecosystems organic matter in the upper layer of soil surface retains atmospheric deposited lead with the tendency of migration through the soil profile towards deeper layers. In cultivated soils, this lead is mixed in the excavated zones with a tendency to penetrate within the plant root zone (Teutsch et al., 2001; Ettler et al., 2004).

Water

Lead released into aquatic systems can slowly dissolve and enter groundwater, making it potentially hazardous for plants and living organisms. But most of the lead and its compounds are deposited down to the bottom and accumulate in the sediments. They remain bioavailable far into the future due to their low solubility and relative stable from microbial degradation. Thus, soils as well as the ocean sediments become the most significant storage for anthropogenically emitted lead (Davies, 1995).

Plants

During development, plants are exposed to lead from the atmosphere through organic dust, toxic gases and chemicals. Lead dust deposition on the foliage reduces the light exposition, inhibit the respiration and photosynthesis, encouraging an elongation of plant, influencing root development, and might affect population genetics (Watmough, 1999; Pattee & Pain, 2002; Almeida & Vasconcelos, 2003a; Feng et al., 2011; Ndung'u et al., 2011). Lead-containing pesticides are of special concern: lead accumulation was observed in crops, leafy vegetables and fruits grown in orchard soils historically contaminated by lead arsenate (Codling et al., 2015; Codling et al., 2016). The pattern and degree of lead accumulation in vegetation are largely influenced by botanical species and the growth periods. Grazing animals are directly affected by the consumption of lead-contaminated forage (Feng et al., 2011).

A.2.2. Lead isotopes: systematics and applications

Lead has four stable, naturally occurring isotopes with atomic weights: ^{208}Pb , ^{206}Pb , ^{207}Pb and ^{204}Pb . The isotopes ^{206}Pb , ^{207}Pb and ^{208}Pb are the daughter products from the radioactive decay of ^{238}U and ^{235}U and ^{232}Th , respectively (Table A.4), their abundances co-vary strongly and depend on when minerals were formed. The isotope only ^{204}Pb is non-radiogenic and remains essentially constant at 1.4% in abundance. Small Pb isotope abundance variations occur in nature. The Pb isotopic composition of any mineral or material is the composite of the three independent decay chains. As a result, the specific isotopic compositions of different types of Pb-containing minerals are caused by the interplay of a number of processes, including radioactive decay of U and Th to Pb, the relative proportion of U–Th–Pb in the system, and mixing of Pb from different lead sources, natural or anthropogenic origin (Cheng & Hu, 2010). The ranges of isotopic ratios for most natural materials are within the intervals of: 14.0–30.0 for $^{206}\text{Pb}/^{204}\text{Pb}$; 15.0–17.0 for $^{207}\text{Pb}/^{204}\text{Pb}$ and 35.0–50.0 for $^{208}\text{Pb}/^{204}\text{Pb}$, although numerous examples outside these ranges are reported in literature (Bernat & Church, 1989). The fixed ratio of ^{204}Pb to the primordial amounts of the other lead isotopes may be used as a baseline to estimate the extra amounts of radiogenic lead present in rocks as a result of decay from uranium and thorium.

Lead isotopes are widely used in environmental studies to determine the source of lead pollution and to characterize their transport pathways because they are significantly more sensitive to trace than lead total concentrations. Pollution studies have taken advantage of the general association of pollution with lead, which displays a wide range of isotope abundance and can serve as a tracer (Rosman et al., 1998). The main advantages of the Pb isotope tracing method are: i) Pb isotope composition is not affected by any variations of multi-elements, isotopic fractionation, geological weathering and erosion; ii) Pb isotope systematics is extensively characterized, Pb isotopic variations are quite large and easily analyzed by several analytical methods (Vanhaecke & Degryse, 2012; Yip et al., 2012).

Table A.4. Relative isotopic abundances (IA) of Pb stable isotopes.

Isotope	IA, lower level, %	IA*, upper level, %	Parent isotope and	Half –life, years
^{204}Pb	1.4	1.65	Non-radiogenic	Non-radiogenic
^{206}Pb	20.84	27.48	^{238}U	4.468×10^9
^{207}Pb	17.62	23.65	^{235}U	7.038×10^8
^{208}Pb	51.28	56.21	^{232}Th	1.4008×10^{10}

The recent applications of lead isotope ratio measurements given below are not exhaustive and were summarized for illustrative purposes after a number of extensive reviews (Yip et al., 2008; Billström, 2008; Komárek et al., 2008; Cheng & Hu, 2010; Chang et al., 2011; Vanhaecke & Degryse, 2012; Irrgeher & Prohaska, 2016):

- Geochronological dating using U-Pb and U-Th-Pb systems;
- Lead tracing in material sources and exploration of metal deposits;
- Tracing Pb sources and monitoring historical and environmental changes using: human diet, bio tissues (animals and human origin), plants (e.g. tree rings, lichens), atmosphere aerosols and bulk deposit, soils, water, sediments, snow, ice cores, urban landfill;
- Forensic examination purposes using bio tissues (e.g. diet and human tissues); ammunition for identifying unknown corpses;
- Provenance of ancient materials and authentication of artifacts, paintings, statuettes;
- Traceability of food product origin (wines, rice, meat).

A.2.3. Principles of lead isotopic fingerprinting for food traceability

Pb isotopic fingerprinting is an individual characteristic which is based on the Pb ratios isotopes present in a sample, can be used to identify origins of this element in the sample, and to trace its geographical provenance under certain circumstances. The particular principle of traceability of food origin using Pb isotopic fingerprinting consists in the determination of isotope ratios of Pb in food or raw food material and their identification with those in sources of lead available in the region considered.

Lead emitted from natural and anthropogenic sources into the atmosphere, dispersed throughout it, deposited with dust and/or rain fall out on arable soil and absorbed by plants. Plants appropriate isotopic composition of the lead available for bio-accumulation. Recent studies stated that the uptaking of anthropogenic lead occurs primarily through the foliage and rather than the roots (Wathmont, 1999; Mihaljevic et al., 2006; Hu & Ding, 2009; Novak et al., 2010; Mihaljevic et al., 2015; Lim & McBride, 2015). Thus, plants represent the lead isotopic signature caused by mixing of anthropogenic and natural lead emissions with different apportioned contributions. The isotopic composition in plants from plantation close to urban areas will be close to those in corresponding sources of lead emissions (Marguá et al., 2006; Sracek et al., 2015). Conversely, the plants from environmentally clean areas will present lead isotopic composition shifted more to geogenic characteristics (Grousset et al., 1994).

Identification of Pb source is a challenge. Despite the fact that different types of ore deposits and anthropogenic sources have a specific and distinctive Pb-isotopic composition, the environment is influenced continuously by a combination of several substantial sources. To identify impacts from each of them, a different Pb isotope ratios are used, such $^{206}\text{Pb}/^{207}\text{Pb}$, $^{208}\text{Pb}/^{207}\text{Pb}$, $^{206}\text{Pb}/^{208}\text{Pb}$, $^{206}\text{Pb}/^{204}\text{Pb}$, $^{207}\text{Pb}/^{204}\text{Pb}$, $^{208}\text{Pb}/^{204}\text{Pb}$ (Ellam, 2010). By mapping the Pb isotopic compositions of the studied sample with references values, the major sources of the Pb presented can be identified (Komárek et al., 2008; Cheng & Hu, 2010; Mihaljevič et al., 2015). In cases when lead pollution is caused by multiple sources, the apportioned contributions of the major sources can also be determined (Cheng & Hu, 2010).

Nowadays, there are no more natural sites with pre-industrial lead background due to global anthropogenic influence (Pacyna & Pacyna, 2001). The pre-industrial, or geogenic, values of Pb isotope ratios can be obtained only by isotope analysis of deep ice- or sediments cores from remote regions and use as a reference value. (Brännvall et al., 2001; Han et al., 2015; Grousset et al., 1994).

A.2.4. Food origin by means of Pb isotopes

During last two decades the Pb IR as an origin discriminating tool has demonstrated promising results. An extended summary included instrumental supplies, food matrixes, analytical precision of Pb isotopic determination is presented in Table A.6 (at the end of this chapter).

The pioneering work concerning Pb isotope ratios application to food geographical origin assessment was published by Dean et al. (1987) described the difference between lead isotope compositions in European and Australian milk powder. The obtained $^{207}\text{Pb}/^{206}\text{Pb}$ ratio of Australian milk was consistent with a lead signature of domestic Broken Hill ore deposit. Later on, the comparison of Pb isotope composition of wine and milk from Australia and Italy revealed a significant difference between two origins (Crews et al., 1988; Dean et al., 1990). Relatively poor analytical accuracy and precision of quadrupole ICP-MS isotope determinations made the first source identification considerably complicated. In order to improve these parameters and to establish reliable sample preparation technics, wine samples were widely used as a studied matrix (Goossens et al., 1993; Goossens et al., 1994; Augagneur 1997; Almeida & Vasconcelos, 1999a; Almeida & Vasconcelos, 1999b; Rodushkin et al., 1999; Barbaste et al., 2001; Fortunato et al., 2003). As the result, the significant increase of accuracy of Pb isotope ratios determining by ICP-MS by one or two orders of magnitude using the new mass spectral instrumentation, such as high resolution (HR-ICP-MS) (Rodushkin et al., 1999), multicollection (MC-ICP-MS) (Barbaste et al., 2001; Fortunato et al., 2003) and time-of-flight (Tian et al., 2000). Recently, precision and accuracy

in Pb isotope ratios measurements by plasma source mass spectrometry were reviewed elsewhere (Irrgeher & Prohaska, 2016; Vanhaecke & Degryse, 2012).

The study of Rosman et al. (1998) could not identify clearly the dominant source of lead in French wine, apparently, because throughout that time, the complete elimination of lead from fuels in France was not achieved. However, examining Bordeaux wine produced much earlier, from 1895 till 1995 (Médina et al., 2000) made it possible to reconstruct the atmospheric lead fallout over the last century and reveal that chronological Pb signatures of wine reflect a regional western European imprint. Due to the difference of isotopic composition of lead ore used to produce the antiknock reagent from over the world, the Pb isotopic pattern of wine will differ from one origin to another. From the period when leaded gasoline was prohibited in Europe, this specific Pb isotopic composition was proposed to trace vintages of wine (Médina et al., 2000). Larcher et al. (2003) successfully applied the Pb isotope ratios to determine the origin of wines from different Italian regions.

Of special concern is the possibility of Pb contamination of wine during production and storage (Rosman et al., 1998; Médina et al., 2000). Indeed, some enological practices, such as the usage bentonites (Kment et al., 2005; Jakubowski et al., 1999), use of tin-lead capsules (Rosman et al., 1998), the brass alloys used for tubes and faucets in winery's equipment (Kaufmann, 1998; Rosman et al., 1998), were found to be potential sources of lead contaminations (Almeida & Vasconcelos, 2003a; Stockley et al., 2003). All these findings led to the legislated prohibition of tin-lead capsules in the European Union and the United States, and to substantial modernization of winery equipment by replacement of brass by stainless steel that resulted in a gradual decrease of lead levels in wine (Stockley et al., 1995; Kaufmann et al., 1998).

Apart from wines, the Pb isotopes traceability method has been applied also to rice, wheat, and barley samples (Ariyama et al., 2011; Ariyama et al., 2012). Despite the fact that a certain regional differentiation were reached by using only three Pb-isotopes diagrams, the best discrimination were obtained by applying multicomponent statistical analysis (Ariyama et al., 2012). Recently, two hundreds Spanish, French, Italian vinegars, and North American vinegars from California, US, were analyzed as part of an investigation into their Pb isotope ratio composition (Ndung'u et al., 2011). The presence of certain post-harvest Pb contamination has been reveal in most of the European origin samples, and none of them correlated with their presumed regional exposure to industrial lead aerosols by Pb-isotopic compositions (Fig. A.7), although their values were consistent with those observed in previous isotopic analyses of French wines (Augagneur et al., 1997; Rosman et al., 1998; Barbaste et al., 2001). In opposite, Pb isotope signatures of American vinegar were in a good correlation with regional exposure to local industrial lead aerosols (Fig. A.7). Consequently,

Californian vinegar was successfully distinguished from those of European origin, whereas it was not possible to distinguish vinegars among different European origin.

The recent study of Evans et al. (2015) demonstrated the new potential of the lead isotope tracing of food of animal origin. This study focused on Pb isotopic composition of farm livestock from three areas of Britain that have elevated natural Pb levels: Central Wales, the Mendips and the Derbyshire Peak District. The ratios $^{208}\text{Pb}/^{206}\text{Pb}$ and $^{207}\text{Pb}/^{206}\text{Pb}$ (consider as “environmental pollution tracer”) and the ratios $^{208}\text{Pb}/^{204}\text{Pb}$ and $^{206}\text{Pb}/^{204}\text{Pb}$ (“geogenic tracer”), both isotopic systems demonstrated the close association of values between biological samples and ore deposit. Meat from central Wales was distinguished from other origins. The main suggestion of authors seems to be very promising - the lead isotope traceability method might be used to determine the provenance of biological under favorable conditions.

A.2.5. Perspectives and limitation

Although the first studies considered the Pb isotope ratios as a promising tool to trace the food origin, the really impressive results were reported only for provenance discrimination on a large regional scale (Medina et al., 2000; Ndung'u et al., 2011). The global character of lead atmospheric pollution and simultaneous influences of a few substantial pollutant sources increase the complexity in more detailed classification. Indeed, according to above mentioned studies, the more successful distinguishing was reached for food products originating from geographical areas with one substantial Pb source, such as proxy ores mines (Mackay et al., 2013, Marguí et al., 2006; Hu et al., 2009; Evans et al., 2015).

Obviously, the Pb isotopic signatures of food products or food raw materials would reflect the plant's and/or animal's interaction with the environment (Marguí et al., 2006; Feng et al., 2011; Mackay et al., 2013; Evans et al., 2015). Thus, Pb isotope ratios could be useful criterions to distinguish food product from regions under different industrial load. However, It should be mentioned also that the Pb isotopic variation in food products may be affected by other Pb sources: i) any Pb-containing compounds in fertilizers and pesticides used during plant vegetation period; ii) and any food additives and substances used during food processing and technology. All these factors must be considered for the correct data interpretation.

A.3. Conclusion

In this review, a special interest has been focused on the mechanisms of forming of Sr and Pb stable isotope ratios in food and on their linkage to the environment of origin. The applications of Sr- and Pb- stable isotope ratios were successful for a large variety of matrices, from the most simple (e.g. water, beverages, vegetables) to the most complex (e.g. meat, fish, dairy products). The combination with other chemical characteristics (e.g. trace elements, stable isotope ratios of light elements, etc.) improved the discriminating power. By Sr- and Pb- isotope geochemical tracing of food products, it is possible to establish the characteristic values based on geological, geographical and geochemical specifications of production regions. Although that interpreting of geochemical trends for the aim of provenance remains a complex challenge, these markers are in the close relation with sourced areas and can help trace the food geographical origin. After examining the various food applications of Sr and Pb stable isotope ratios for food geographical assessment, it can be concluded that these approaches have a strong scientific potential for being involved in the future in modern legislative interactions aimed at guaranteeing food authenticity and geographical origin, and protecting customers and producers from possible frauds.

Table A.1. Concentrations of strontium in food and feed plants, mg kg⁻¹.

Plant	Tissue sample	Range	Mean	Reference
Apple	Fruits	0.5-1.7	0.9	Kabata-Pendias, 2010
Asparagus	Top	24-810	-	Swoboda et al., 2008
Barley	Grains	-	0.974	Ariyama et al., 2011
Bean	Pods	1.5-67	18	Kabata-Pendias, 2010
Blueberry	Berries	4.5-5.5	4.0	Kabata-Pendias, 2010
Cabbage	Leaves	1.2-150	45	Kabata-Pendias, 2010; Bong et al., 2012b
Carrot	Roots	1.5-131	25	Kabata-Pendias, 2010
Coffee	Beans	2.8-26.5	7.8	Rodrigues et al., 2011b; Techer et al., 2011
Corn	Grains	0.06-0.4	-	Kabata-Pendias, 2010
Dry-cured ham	Muscle	0.3-4.6	2.0	Epova et al., 2018a
Glover	Tops	95-850	219	Kabata-Pendias, 2010
Grass	Tops	6-37	24	Kabata-Pendias, 2010
Lettuce	Leaves	-	74	Kabata-Pendias, 2010
Lichens	Top	0.8-250	-	Kabata-Pendias, 2010
Lucerne	Tops	50-1500	662	Kabata-Pendias, 2010
Mousse	Top	2.8-51	15	Kabata-Pendias, 2010
Oats	Grains	1.8-3.2	2.5	Kabata-Pendias, 2010
Onion	Bulbs	1.1-88	50	Kabata-Pendias, 2010; Hiraoka et al., 2016
Orange	Fruits	-	0.5	Kabata-Pendias, 2010
Paper	Fruits	0.08-7.99	0.99	Song et al., 2014
Paprika	Fruits	1.2-45.8	17.1	Brunner et al., 2010
Potatoes	Tubers	-	2.6	Kabata-Pendias, 2010
Potatoes	Tubers	0.35-1.28	0.80	Zampella et al., 2011
Rice	Grains	0.04-3.9	0.070	Ariyama et al., 2012; Ariyama et al., 2011; Lagad et al., 2017
Salt, marine	Cristals	44-105	46	Epova et al., 2018a
Salt, mineral	Cristals	10-153	60	Epova et al., 2018a
Soybean	Leaves	58-89	-	Kabata-Pendias, 2010
Spinach	Leaves	45-70	-	Kabata-Pendias, 2010
Tea	Leafs	2.0-39	14.9	Chang et al., 2015, Epova et al., 2018d
Tomatoes	Fruits	0.4-91	9	Kabata-Pendias, 2010
Wheat	Grains	0.48-2.3	1.5	Kabata-Pendias, 2010; Ariyama et al., 2011
Wine	Wine	0.11-2.16	0.44	Epova et al., 2018b

Table A.2. Food product studied for authenticity, provenance and geographic origin using the strontium isotope ratio, analytical and statistical methods, precision of isotopic ratio determination.

Product	Country / Number of samples	Additional parameters	Instrumentation for $^{87}\text{Sr}/^{86}\text{Sr}$ detection	Precision RSD, %	Chemometric method	Reference
Food vegetable origin						
Asparagus	Austria /75; Slovakia /31; Germany /6; Hungary /24; Netherlands /14; Peru /5	non	ICP-MS-MC	0.02	Univariate	Swoboda et al., 2008
Asparagus	Italy /15	Multielements, REE	MC-ICP-MS	0.003	UPGMA	Zannella et al., 2017
Barley	Japan /221; Australia /50; USA /20; Canada /30	Pb Isotope ratios	HR-ICP-MS	0.055	Univariate	Ariyama et al., 2011
Cabbage	China /60; Korea /100	multielements	TIMS	0.001	MHC, LDA	Bong et al., 2012a,b
Cereal	Europe /557	$\delta^{13}\text{C}$, $\delta^{15}\text{N}$, $\delta^{18}\text{O}$, $\delta^{34}\text{S}$ multielements	TIMS, MC-ICP-MS	< 0.003	PCA, SIMCA PLS-DA	Asfaha et al., 2011
Coffee	Taiwan, Ethiopia, Tanzania, Malawi, Rwanda, Uganda, El Salvador, Guatemala, Puerto Rico, Jamaica, Colombia, Brazil, Indonesia, Papua New Guinea /21	B, Mn, Zn, Rb, Sr, Ba, Fe	MC-ICP-MS	0.0035	PCA	Liu et al., 2014
Coffee	Taiwan, Papua New Guinea; Sumatra; Indonesia; El Salvador; Guatemala, Puerto Rico; Jamaica; Colombia; Brazil; Ethiopia; Tanzania; Malawi; Rwanda; Uganda /21	$\delta^{11}\text{B}$, $\delta^{13}\text{C}$, $\delta^{15}\text{N}$, $\delta^{18}\text{O}$, multielements	MC-ICP-MS	0.0035	PCA	Liu et al., 2016
Coffee	Reunion Island, New Caledonia /26	non	TIMS	0.0003	Univariate	Techer et al., 2011
Coffee	Hawaii /47	$\delta^{13}\text{C}$, $\delta^{15}\text{N}$, $\delta^{18}\text{O}$, $\delta^{34}\text{S}$, multielements, REE	IRMS, ICP-MS	0.011	CDA	Rodrigues et al., 2011a
Coffee	Rwanda, Ephiopia, Kenia, UR Tansania, Malawi, Zambia, Zimbabwe, Hawaii, Mexico, Costa Rica, Guatemala, El Salvador, Nicaragua, Brasil, Peru, Jamaica, Indonesia, East Timor, Papua New Guinea /60	$\delta^{18}\text{O}$	MC-ICP-MS	0.0006 0.0012 0.0147	PCA	Rodrigues et al., 2011b
Grapes	Canada, Quebec / 16	non	TIMS	0.002	Univariate	Vinciguerra et al., 2016
Hot pepper	South Korea /31	non	MC-ICP-MS	0.001	Univariate	Song et al., 2014
Olive oils	Morocco /2; France /5	non	TIMS	0.003-0.02	Univariate	Medini et al., 2015
Onion	Japan /128; China /100; USA /32; Australia /8; New Zealand /6; Thailand /4	Sr	MC-ICP-MS	0.001-0.004	LDA	Hiraoka, et al., 2016
Orange juice	Mexico /9; Cuba /5; USA (Florida) /4; Uruguay /1; Paraguay /1; Israel /2; Italy /15; Spain /12; Greece /5; Morocco /2; Argentina /2; Brasil /13; Belize /1; South Africa (NE) /4; South Africa (Centre) /2	$\delta^{13}\text{C}$, $\delta^{15}\text{N}$, $\delta^2\text{H}$, $\delta^{34}\text{S}$	TIMS	< 0.003	LDA	Rummel et al., 2010
Pistachio	Italy /15	Multielements, REE	MC-ICP-MS	0.003	UPGMA	Zannella et al., 2017
Potatoes	Italy /38	multielements	MC-ICP-MS	0.020 – 0.100	PLS-DA, PCA	Zampella et al., 2011

Table A.2. (Continued)

Product	Country / Number of samples	Additional parameters	Instrumentation for $^{87}\text{Sr}/^{86}\text{Sr}$ detection	Precision RSD, %	Chemometric method	Reference
Potatoes	Italy /12	multielements	MC-ICP-MS	0.020 – 0.100	PLS-DA, PCA	Adamo et al., 2012
Paprika	Hungary /2; Spain /6; Germany /2; France /3; Italy /1; China /1; Romania /1; Sinegal /1; Unknown /5	Multielements, REE	MC-ICP-MS	0.001-0.003	PCA, CDA, ANOVA	Brunner et al., 2010
Rice	Japan /34; Australia /3; Vietnam /1; China /4; USA (California) /1	non	MC-ICP-MS	< 0.01	Univariate	Kawasaki et al., 2002
Rice	Japan /44; Australia /3; USA (California) /15; China /4; Korea /1; Vietnam /1	$\delta^{11}\text{B}$, Cd	MC-ICP-MS	< 0.01	Bivariate	Oda et al., 2002
Rice	Japan /58; Australia /4; USA /11; China /31; Thailand /7	Pb Isotope ratios	HR-ICP-MS	0.055	Univariate	Ariyama et al., 2011
Rice	Japan /200; China /50; Thailand /50; USA /50	Pb Isotope ratios, multielements	HR-ICP-MS	0.006	PCA, LDA, SIMCA, KNN	Ariyama et al., 2012
Rice	South Korea /46	non	MC-ICP-MS	0.001	Univariate	Song et al., 2014
Rice	India /84	REE, Sr, Rb	MC-ICP-MS	0.003	Bivariate	Lagad et al., 2017
Sugar	USA /1; Costa Rica /1; Argentina /1; Swaziland /1	Pb Isotope ratios, multielements	MC-ICP-MS, TIMS, HR-ICP-MS	0.003 < 0.002 0.05	PCA	Rodushkin et al., 2017
Tea	India /38	$\delta^{13}\text{C}$, Sr	MC-ICP-MS	0.004	PCA	Lagad et al., 2013
Tea	Taiwan /14	$\delta^{11}\text{B}$, multielements	MC-ICP-MS	0.003	PCA	Chang et al., 2016
Vegetables	Japan /300	Sr	MC-ICP-MS	0.002	LDA	Aoyama et al., 2017
Water	United Kingdom /32	non	TIMS	< 0.007	Univariate	Montgomery et al., 2006
Water	France /11	non	MC-ICP-MS	0.002-0.03	Univariate	Brach-Papa et al., 2009
Water	Europe /650	non	TIMS MC-ICP-MS	< 0.003	Univariate	Voerkelius et al., 2010
Wheat	Japan /44; Australia /16; USA /21; Canada /12	Pb Isotope ratios	HR-ICP-MS	0.055	Univariate	Ariyama et al., 2011
Wheat	China /54	$\delta^{13}\text{C}$, $\delta^{15}\text{N}$, δD	TIMS	0.007	CDA	Liu et al., 2016
Wine	Serbia, France, Italy /11	non	TIMS	0.02	Univariate	Horn et al., 1993
Wine	Germany	$\delta^{18}\text{O}$	TIMS	0.02	Univariate	Horn et al., 1998
Wine	Portugal, France /6	non	Q-ICP-MS	0.41	Univariate	Almeida et al., 2001
Wine	France, Chili, USA, Australia, Portugal, South Africa /11	non	MC-ICP-MS	0.0013-0.0165	Univariate	Barbaste et al., 2002
Wine	Portugal /18*	non	Q-ICP-MS	0.2 – 0.7	Univariate	Almeida et al., 2004
Wine	South-Africa /67	$\delta^{11}\text{B}$, Rb, Li, Sc, B	Q-ICP-MS	0.09	CDA	Vorster et al., 2010
Wine	Romania, Moldova /13	Pb Isotope ratios ; Ni, Hg, As, Cd, Cr, Pb	Q-ICP-MS	0.08	Univariate	Dehelean et al., 2012
Wine	Argentina /48	$\delta^{13}\text{C}$, multielements	TIMS	0.036	ANOVA, GPA	Di Paola-Naranjo et al., 2011
Wine	Italy /45	non	TIMS	< 0.001	Univariate	Marchionni et al., 2013

Table A.2. (Continued)

Product	Country / Number of samples	Additional parameters	Instrumentation for $^{87}\text{Sr}/^{86}\text{Sr}$ detection	Precision RSD, %	Chemometric	Reference
Wine	Italy	multielements (including REE)	MC-ICP-MS	0.005	HCA, FA	Mercurio et al., 2014
Wine	Italy /186	non	MC-ICP-MS	0.002	Univariate	Durante 2015
Wine	Italy /18*	non	TIMS	0.0023	Univariate	Tescione 2015
Wine	Italy /30*	non	TIMS	0.003	Univariate	Petrini et al., 2015
Wine	Portugal /22	non	Q-ICP-MS	No info	Univariate	Fernandes et al., 2015
Wine	Italy /42*	non	TIMS	< 0.001	ANOVA	Marchionni et al., 2016
Wine	Romania /21	multielements	Q-ICP-MS	0.0099 -0.5378	LDA	Geană et al., 2016
Wine	Portugal /12	physico-chemical parameters	Q-ICP-MS	No info	ANOVA	Catarino et al., 2016
Wine	Canada, Quebec /17	non	TIMS	0.002	Univariate	Vinciguerra et al., 2016
Wine	Italy /16*	multielements	TIMS	0.0045	Univariate	Ghezzi et al., 2018
Wine	Italy / 37	non	TIMS	< 0.002	Univariate	Braschi et al., 2018
Wine	France /43; China /3; unknown /14	multielements	MC-ICP-MS	< 0.002	Bivariate	Epova et al., 2018b
Food animal origin						
Cheese	Germany /3; France /6; Switzerland /6; Finland /2; Austria /3	$\delta^{13}\text{C}$, $\delta^{15}\text{N}$, $\delta^{2}\text{H}$, $\delta^{18}\text{O}$, multielements; selected radioactive elements	TIMS	0.003	PCA	Pillonel et al., 2003
Cheese	Germany /2; France /5; Switzerland /3; Finland /2; Austria /4; Australia /1 ; Canada /1	Selected multielements	TIMS	0.005	Univariate	Fortunato et al., 2004
Cheese	Italy /109	$\delta^{13}\text{C}$, $\delta^{15}\text{N}$, $\delta^{18}\text{O}$, $\delta^{34}\text{S}$, multielements	TIMS	0.005	CDA	Bontempo et al., 2011
Milk	Australia /5; New Zealand /1	$\delta^{13}\text{C}$, $\delta^{15}\text{N}$, $\delta^{18}\text{O}$, $\delta^{34}\text{S}$	TIMS	< 0.002	Univariate	Crittenden et al., 2007
Butter	Germany /11; Italy /4; Austria /3; Ireland /1; Finland /1; Norway /1; Sweden /1; Poland /1; Estonia /1; Lithuania /1; Australia /1, New Zealand /1; Argentina /1	$\delta^{13}\text{C}$, $\delta^{15}\text{N}$, $\delta^{18}\text{O}$, $\delta^{34}\text{S}$	TIMS	< 0.002	LDA	Rossmann et al., 2000
Beef	Argentina /83	$\delta^{13}\text{C}$, $\delta^{15}\text{N}$, Rb, Ca/Sr, K/Rb, multielements	TIMS	< 0.003	LDA, GPA, CCA	Baroni et al., 2011
Beef	Australia /8; Austria /5, Canada /8; USA /5; Switzerland /30; Brazil /16	$\delta^{18}\text{O}$	MC-ICP-MS		Univariate	Franke et al., 2008
Beef	Italy /65; Germany /56; UK /43; France /20; Spain /14; Greece /4; Ireland /4	non	MC-ICP-MS	0.04-0.4%	Univariate	Rummel et al., 2012
Poultry	Brazil, France, Germany, Hungary, Switzerland / 78	$\delta^{18}\text{O}$	MC-ICP-MS		Univariate	Franke et al., 2008
Poultry	Brazil /25; Europe /11; Chile /30; Thailand /33; Argentina /6	$\delta^{13}\text{C}$, $\delta^{15}\text{N}$, $\delta^{18}\text{O}$, $\delta^{34}\text{S}$, $\delta^{2}\text{H}$, multielements	TIMS	nd	CDA	Rees et al., 2016

* Number of samples includes wine, grape jus and must.

Table A.3. Strontium Isotope ratio in different food products reported from the region over the world.

Region	Country	Product / Number of samples	$^{87}\text{Sr}/^{86}\text{Sr}$ ratio interval	$^{87}\text{Sr}/^{86}\text{Sr}$ ratio mean	$^{87}\text{Sr}/^{86}\text{Sr}$ ratio in rock/soil	Reference
EUROPE		Mineral water /650	0.7035-0.7777	-	-	Voerkelius et al., 2010
		Poultry /11	0.70861-0.70978	0.70934	-	Rees et al., 2016
	Austria	Asparagus /68 (2006)	0.7083-0.7102	0.7095±0.0008	0.7083 (0.7083-0.7098) / soil extract	Swoboda et al., 2008
		Asparagus /14 (2005)	0.7081-0.7105	0.7094±0.0014	0.7146 (0.7137-0.7194) / soil	Swoboda et al., 2008
		Butter <i>Steiermark</i> /1	-	0.710180	-	Rossmann et al., 2000
		Butter <i>Lower Austria</i> /2	0.711978-0.712661	0.712320	-	Rossmann et al., 2000
		Cheese <i>Vorarlberg</i> /3	0.70805-0.70812	0.70817±0.00151	-	Fortunato et al., 2004; Pillonel et al., 2003
		Cheese <i>Salzburg</i> /1	-	0.70818±0.001	-	Fortunato et al., 2004; Pillonel et al., 2003
		Salt <i>Salzkammergut</i> /1	-	0.70712±0.00008	-	Epova et al., 2018a
		Cyprus	Salt <i>Pyramid</i> / 1	-	0.70904±0.00008	-
	Estonia	Butter /1	-	0.707042	-	Rossmann et al., 2000
	Germany	Asparagus /6	0.7081-0.7097	0.7086±0.0013	-	Swoboda et al., 2008
		Beef /56	0.70727-0.71594	0.70956±0.00185	-	Rummel et al., 2012 ABC
		Butter /11	0.707651-0.708995	-	-	Rossmann et al., 2000
		Cheese /2	0.70814-0.70833	0.70824±0.008	-	Fortunato et al., 2004
		Paprika /2	0.7078-0.7103	0.7091	-	Brunner et al., 2010
		Poultry /3	-	0.708±0.002	-	Franke et al., 2008
	Greece	Beef /4	0.70854-0.70887	0.70874±0.00015	-	Rummel et al., 2012
	Hungary	Asparagus /19	0.7056-0.7080	0.7069±0.0011	-	Swoboda et al., 2008
		Paprika /3	0.7076-0.7089	0.7083	0.7064-0.7091	Brunner et al., 2010
		Poultry /6	-	0.711±0.002	-	Franke et al., 2008
	Finland	Caviar	-	0.721315	-	Rodushkin et al., 2007
		Butter /1	-	0.712917	-	Rossmann et al., 2000
		Cheese /2	-	0.71293±0.01200	-	Fortunato et al., 2004; Pillonel et al., 2003
	France	Beef /20	0.71043-0.71347	0.71171±0.00107	-	Rummel et al., 2012

Table A.3 (Continued).

Region	Country	Product / Number of samples	⁸⁷ Sr/ ⁸⁶ Sr ratio interval	⁸⁷ Sr/ ⁸⁶ Sr ratio mean	⁸⁷ Sr/ ⁸⁶ Sr ratio in rock/soil	Reference	
EUROPE	France	Cheese <i>Savoie</i> /2	0.70827-0.70863	0.70845±0.005	-	Fortunato et al., 2004; Pillonel et al., 2003	
		Cheese <i>Bretagne</i> /2	0.70754-0.70755	-	-	Fortunato et al., 2004	
		Cheese <i>Bretagne</i> /3	-	0.70859±0.00184	-	Pillonel et al., 2003	
		Cheese <i>Jura</i> /1	-	0.70860±0.007	-	Fortunato et al., 2004	
		Dry-cured ham <i>Bayonne</i> /3	0.70854-0.70858	0.70855±0.00006	0.70840±0.00007 / rock salt		
		Mineral water /11	0.70822-0.71630	-	-	Brach-Papa et al., 2009	
		Olive oil /5	0.70727-0.70881	0.70808	-	Medini et al., 2015	
		Paprika /3	0.7083-0.7087	0.7085	-	Brunner et al., 2010	
		Poultry /2	-	0.711±0.002	-	Franke et al., 2008	
		Salt <i>Salies-de-Béarn</i> /4	0.70838-0.70842	0.70840±0.00007	-		
		Salt <i>Guérande</i> /2	0.70912. 0.70917	0.70915±0.00006	0.709176 ± 0.000003 / sea water	Epova et al., 2018a	
		Salt <i>Camargue</i> /2	0.70913. 0.70918	0.70916±0.00004	0.709176 ± 0.000003 / sea water	Epova et al., 2018a	
		Salt <i>Île de Ré</i> /1	-	0.70918±0.00005	0.709176 ± 0.000003 / sea water	Epova et al., 2018a	
		Wine <i>Muscadet</i> /2	0.70931-0.70996	0.70973	-	Horn et al., 1993	
		Wine <i>St Emilion</i> /4	0.70943-0.71005	0.70975	0.7085-0.7010	Barbaste et al., 2002	
		Wine <i>Chablis</i> /1	-	0.7086±0.0001	0.7085-0.7010	Barbaste et al., 2002	
		Wine <i>Saint-Émilion</i> /4	0.70829-0.70895	0.70864±0.00057	-	Epova et al., 2018b	
		Wine <i>Pauillac</i> /4	0.70906-0.70953	0.70930±0.00030	-	Epova et al., 2018b	
		Wine <i>Pomerol</i> /11	0.70968-0.71022	0.71001±0.00037	-	Epova et al., 2018b	
		Wine <i>Pessac-Léognan, red</i> /15	0.70910-0.70960	0.70939±0.00031	-	Epova et al., 2018b	
		Wine <i>Pessac-Léognan, white</i> /	0.70915-0.70980	0.70946±0.00058	-	Epova et al., 2018b	
		Wine <i>Immitated Bordeaux</i>	0.70523-0.71266	-	-	Epova et al., 2018b	
		Italy	Asparagus <i>Bassano del Grappa</i> /15	0.7078-0.7096	-	0.7064-0.7095 / soil extract	Zannella et al., 2017
			Beef /65	0.70628-0.71572	0.70905±0.00072	-	Rummel et al., 2012
			Butter /4	0.708818-0.712126	-	-	Rossmann et al., 2000
			Dry-cured ham <i>San Daniele</i> /1	-	0.70923 ± 0.00008	0.70913±0.00010 / sea salt	Epova et al., 2018a
			Dry-cured ham <i>Parma</i> /1	-	0.70925 ± 0.00008	0.70913±0.00010 / sea salt	Epova et al., 2018a
			Cheese /109	0.70773-0.70981	0.70897±0.00082	-	Bontempo et al., 2011
			Orange juices /15	0.7073-0.7107	-	-	Rummel et al., 2010
	Pistachio <i>Bronte</i> /15		0.7057-0.7072	-	0.7059–0.7071 / soil extract	Zannella et al., 2017	
	Potatoes /12	0.70474-0.78202	0.70690±0.00134	-	Adamo et al., 2012		
	Potatoes /19	0.70793-0.70878	0.70799±0.00068	/ Carbonate soil	Zampella et al., 2011		
	Potatoes /10	0.70793-0.70930	0.70879±0.00051	/ Alluvial sediments	Zampella et al., 2011		
	Potatoes /8	0.70448-0.70764	0.70552±0.00113	/ Volcanic substrate	Zampella et al., 2011		

Table A.3 (Continued).

Region	Country	Product / Number of samples	⁸⁷ Sr/ ⁸⁶ Sr ratio interval	⁸⁷ Sr/ ⁸⁶ Sr ratio mean	⁸⁷ Sr/ ⁸⁶ Sr ratio in rock/soil	Reference
EUROPE	Italy	Wine /6	0.70884-0.70943	0.70890	-	Horn et al., 1993
		Wine <i>Cesanese</i> /10	0.70898-0.71059	0.70951±0.00057	0.71036 (0.70944-0.71134) / rock	Marchionni et al., 2013
		Wine <i>Chianti Classico</i> /8	0.70877-0.71069	0.70958±0.00081	0.71474 (0.70746-0.72947) / rock	Marchionni et al., 2013
		Wine <i>Giglio Island</i> /3	0.70937-0.71131	0.71055±0.00103	0.71755 (0.71322-0.72071) / rock	Marchionni et al., 2013
		Wine <i>Aglianico del Vulture</i> /13	0.70679-0.70818	0.70771±0.00038	0.70695 (0.70522-0.70705) / rock	Marchionni et al., 2013
		Wine <i>Aglianico Compagno</i> /13	0.70822-0.70865	0.70840±0.00013	0.70820 (0.70656-0.71003) / rock	Marchionni et al., 2013
		Wine <i>Piedirosso</i> /3	0.70772-0.70799	0.70789±0.00015	0.70746 (0.70678-0.70860) / rock	Marchionni et al., 2013
		Wine <i>Aglianico</i> /29	0.70679-0.70865	0.70804±0.00043	0.70884 / limestone 0.70678-0.70797 / rock	Marchionni et al., 2013
		Wine <i>Cesanese</i> /42	0.70894-0.71062	0.70962±0.00043	0.71117 (0.70885-0.71796) / soil	Marchionni et al., 2016
		Wine <i>Piedirosso</i> /1	0.70816-0.70813	0.70831±0.00010	0.70804 (0.70788-0.70813) / soil	Mercurio et al., 2014
		Wine <i>Grasparossa</i> /68	0.70850-0.70964	-	-	Durante et al., 2015
		Wine <i>Salamino</i> /57	0.70862-0.70882	-	-	Durante et al., 2015
		Wine <i>di Sorbara</i> /61	0.70839-0.70885	-	-	Durante et al., 2015
		Wine <i>Prosecco</i> /30	0.70706-0.71266	0.70987±0.00131	0.70939 (0.70772-0.71097) / soil	Petrini et al., 2015
		Wine /18	0.70863-0.71002	-	0.71004-0.71023	Tescione et al., 2015
		Wine <i>musts Piedmont</i> /16	0.71161-0.71816	-	-	Ghezzi et al., 2018
		Wine mini-vinification /37	0.70816-0.70909	-	0.70805-0.70903 / soil	Branschi et al., 2018
			Ireland	Beef /4	0.70854-0.71033	0.70880±0.00130
	Butter /1	-		0.710234	-	Rossmann et al., 2000
	Kosovo	Wine /3	0.70981-0.71033	0.71007	-	Horn et al., 1993
	Lithuania	Butter /1	-	0.708137	-	Rossmann et al., 2000
	Norway	Butter /1	-	0.709497	-	Rossmann et al., 2000
	Poland	Butter /1	-	0.708806	-	Rossmann et al., 2000
		Salt <i>Wieliczka</i> /1	-	0.70839 ± 0.00010	-	Epova et al., 2018a
	Portugal	Wine /2	0.70660-0.71203	0.70931	0.712	Barbaste et al, 2002
		Wine /4	0.727-0.731	0.729	0.732	Ameida et al., 2004
		Vineyard soil /4	-	-	0.711-0.737 / soil	Martins et al., 2013
		Wine <i>Douro Wine Appellation</i> /22	0.7130-0.7175	-	-	Fernandes et al., 2015
		Wine <i>Palmela</i> /4	0.7075-0.709	-	-	Catarino et al., 2016

Table A.3 (Continued).

Region	Country	Product / Number of samples	⁸⁷ Sr/ ⁸⁶ Sr ratio interval	⁸⁷ Sr/ ⁸⁶ Sr ratio mean	⁸⁷ Sr/ ⁸⁶ Sr ratio in rock/soil	Reference
EUROPE	Portugal	Wine Óbidos /4	0.7080-0.7095	-	-	Catarino et al., 2016
		Wine Dão /4	0.713-0.715	-	-	Catarino et al., 2016
	Romania	Paprika /1	0.7085-0.7107	-	-	Brunner et al., 2010
		Wine Vrancea region /10	0.71310-0.72311	0.71679	-	Geană et al., 2016
		Wine Terasale region /11	0.71015-0.71296	0.71176	-	Geană et al., 2016
	Slovakia	Asparagus /28	0.7062-0.7093	0.7079±0.0014	-	Swoboda et al., 2008
	Spain	Beef /14	0.70897-0.71399	0.71076±0.00148	-	Rummel et al., 2012
		Dry-cured ham Iberian /11	0.70898-0.70956	0.70928 ± 0.00020	0.70913±0.00010 / sea salt	Epova et al., 2018a
		Orange juices /12	0.70809 -0.70913	-	-	Rummel et al., 2010
		Paprika /3	0.7137-0.7151	0.7154	-	Brunner et al., 2010
		Salt Andalusia /1	-	0.70835 ± 0.00010	-	Epova et al., 2018a
	Sweden	Butter /1	0.713943	-	-	Rossmann et al., 2000
		Caviar Kalix	0.71065-0.71099	-	-	Rodushkin et al., 2007
		Caviar Vänern	-	0.722270	-	Rodushkin et al., 2007
	Switzerland	Cheese /2	0.70788-0.70876	0.70832	-	Fortunato et al., 2004
		Cheese St Gallen /2	0.70827-0.70839	0.70833±0.004	-	Fortunato et al., 2004
		Cheese /6	-	0.70845±0.00113	-	Pillonel et al., 2004
		Poultry /7	-	0.709±0.001	-	Franke et al., 2008
		Beef Canton of Grisons /4	-	0.710±0.001	-	Franke et al., 2008
		Beef Canton of Valais /3	-	0.710±0.001	-	Franke et al., 2008
	The Netherlands	Asparagus /13	0.7096-0.7105	0.7098±0.0006	-	Swoboda et al., 2008
United Kingdom	Beef /43	0.70788-0.71649	0.71009±0.00209	-	Rummel et al., 2012	
	Mineral waters /32	0.70587-0.72065	-	-	Montgomery et al., 2006	
ASIA	China	Barley /31	0.7078-0.7134	0.7131±0.0016	-	Ariyama et al., 2011
		Cabbage /60	0.71059-0.71457	0.71156±0.00102	0.71529 (0.71827-0.71218) / soil	Bong et al., 2012b
		Cabbage /14	-	0.71100±0.00187	-	Bong et al., 2012a

Table A.3 (Continued).

Region	Country	Product / Number of samples	⁸⁷ Sr/ ⁸⁶ Sr ratio interval	⁸⁷ Sr/ ⁸⁶ Sr ratio mean	⁸⁷ Sr/ ⁸⁶ Sr ratio in rock/soil	Reference	
ASIA	China	Onion <i>Shandong</i> /36	0.71126-0.71478	0.71261	-	Hiraoka et al., 2016	
		Onion <i>Gansu</i> /42	0.70974-0.71449	0.71259	-	Hiraoka et al., 2016	
		Onion <i>Yunnan</i> /12	0.71032-0.71742	0.71222	-	Hiraoka et al., 2016	
		Onion <i>Jiangsu</i> /8	0.71125-0.71859	0.71314	-	Hiraoka et al., 2016	
		Onion <i>Henan</i> /2	0.71172-0.71149	0.71161	-	Hiraoka et al., 2016	
		Paprika /1	-	0.7171	-	Brunner et al., 2010	
		Rice /4	0.710-0.711	-	-	Kawasaki et al., 2002	
		Rice /50	0.708-0.713	0.7103	-	Ariyama et al., 2012	
		Rice /31	0.7078-0.7134	0.7104±0.0016	-	Ariyama et al., 2011	
		Tea	0.70532-0.74544	-	-	Epova et al., 2018d	
		Wheat <i>Xinxiang</i> /18	0.7105-0.7115	0.7110±0.0006	0.71188 (0.71169-0.71218) / soil extract	Liu et al., 2016	
		Wheat <i>Yangling</i> /18	0.7112-0.7116	0.7114±0.0005	0.71162 (0.71154-0.71175) / soil extract	Liu et al., 2016	
		Wheat <i>Shijiazhuang</i> /18	0.7119-0.7127	0.7122±0.0003	0.71296 (0.71277-0.71313) / soil extract	Liu et al., 2016	
		Wheat <i>Huixian</i> /9	0.71099-0.71148	0.71125±0.00061	0.71169±0.00012 / soil extract	Liu et al., 2017	
		Wheat <i>Yangling</i> /9	0.71135-0.71138	0.71136±0.00004	0.71160 / soil extract	Liu et al., 2017	
		Wheat <i>Huixian</i> /9	0.71190-0.71269	0.71226±0.00005	0.71281 / soil extract	Liu et al., 2017	
		Wine /3	0.70880-0.71036	-	-	Epova et al., 2018b	
			Japan	Barley /221	0.7026-0.7141	0.7073±0.0019	-
			Vegetables <i>Hokkaido</i> /44	0.70658-0.70810	0.70705	0.70776 (0.70713-0.70879) / soil extract	Aoyama et al., 2017
			Vegetables <i>Kanto region</i> /50	0.70641-0.70859	0.70742	0.70804 (0.70756-0.70840) / soil extract	Aoyama et al., 2017
			Vegetables <i>Chubu region</i> /30	0.70593-0.71301	0.70960	0.70839 (0.70621-0.71276) / soil extract	Aoyama et al., 2017
			Vegetables <i>Kinki region</i> /67	0.70880-0.70971	0.70937	0.70923 (0.70839-0.71159) / soil extract	Aoyama et al., 2017
			Vegetables <i>Chugoku-Shikoku</i> /50	0.70736-0.70964	0.70902	0.70926 (0.70836-0.71004) / soil extract	Aoyama et al., 2017
			Vegetables <i>Kyushu region</i> /51	0.70660-0.70926	0.70786	0.70821 (0.70785-0.70865) / soil extract	Aoyama et al., 2017
			Onion <i>Hokkaido</i> /60	0.70514-0.70875	0.70661	-	Hiraoka et al., 2016
		Onion <i>Saga</i> /24	0.70634-0.70946	0.70797	-	Hiraoka et al., 2016	
		Onion <i>Hyogo</i> /18	0.70877-0.70968	0.70919	-	Hiraoka et al., 2016	
		Onion <i>Aichi</i> /8	0.70577-0.70927	0.70739	-	Hiraoka et al., 2016	
		Onion <i>Nagasaki</i> /4	0.70860-0.70883	0.70869	-	Hiraoka et al., 2016	
		Onion <i>Gunma</i> /2	0.70838-0.70825	0.70831	-	Hiraoka et al., 2016	
		Onion <i>Tochigi</i> /2	0.70842-0.70844	0.70843	-	Hiraoka et al., 2016	
		Onion <i>Kanagawa</i> /2	0.70395-0.70396	0.70395	-	Hiraoka et al., 2016	
		Onion <i>Osaka</i> /2	0.70909-0.70909	0.70909	-	Hiraoka et al., 2016	
		Onion <i>Kagawa</i> /2	0.70858-0.70869	0.70863	-	Hiraoka et al., 2016	

Table A.3 (Continued).

Region	Country	Product / Number of samples	⁸⁷ Sr/ ⁸⁶ Sr ratio interval	⁸⁷ Sr/ ⁸⁶ Sr ratio mean	⁸⁷ Sr/ ⁸⁶ Sr ratio in rock/soil	Reference
ASIA	Japan	Onion <i>Ehime</i> /2	0.70909-0.70992	0.70950	-	Hiraoka et al., 2016
		Onion <i>Kumamoto</i> /2	0.70949-0.70955	0.70951	-	Hiraoka et al., 2016
		Rice /34	0.706-0.709	-	-	Kawasaki et al., 2002
		Rice /200	0.706-0.711	0.7079	-	Ariyama et al., 2012
		Rice /59	0.7049-0.7193	0.7081±0.0027	-	Ariyama et al., 2011
		Tea /13	0.70673-0.71070	-	-	Epova et al., 2018d
		Wheat /44	0.7026-0.7159	0.7062±0.0020	-	Ariyama et al., 2011
	India	Rice <i>Uttar Pradesh</i> /24	0.716049-0.734477	0.723996±0.005230	0.730560 (0.720215-0.740340) / soil	Lagad et al., 2017
		Rice <i>Uttarakhand</i> /7	0.711428-0.721605	0.715707±0.004725	0.717439 (0.711875-0.725890) / soil	Lagad et al., 2017
		Rice <i>Haryana</i> / 34	0.713535-0.733144	0.717898±0.004247	0.717022 (0.715761-0.719902) / soil	Lagad et al., 2017
		Rice <i>Punjab</i> /13	0.715031-0.721307	0.716932±0.001829	0.718575 (0.714866-0.721503) / soil	Lagad et al., 2017
		Rice <i>New Deli</i> /4	0.716736-0.718005	0.717492±0.000536	-	Lagad et al., 2017
		Tea <i>Assam</i> /16	0.711-0.732	0.717±0.006	0.720 (0.714-0.733) / soil	Lagad et al., 2013
		Tea <i>Darjeeling</i> /11	0.726-0.829	0.745±0.029	0.747 (0.726-0.797) / soil	Lagad et al., 2013
Tea <i>Kangra, Himachal Pradesh</i> /5		0.719-0.724	0.722±0.002	0.723 (0.719-0.728) / soil	Lagad et al., 2013	
Tea <i>Munnar</i> /6		0.714-0.723	0.718±0.003	-	Lagad et al., 2013	
Tea <i>Darjeeling</i> /1/		-	0.73640 ± 0.00016	-	Epova et al., 2018d	
Tea <i>Assam</i> /1		-	0.72082 ± 0.00023	-	Epova et al., 2018d	
Tea <i>unknown</i> /2	0.71155, 0.71324	-	-	Epova et al., 2018d		
Iran	Salt <i>Persian blue</i> /1	-	0.70790±0.00010	-	Epova et al., 2018a	
Nepal	Tea <i>White Shangri la</i> /1	-	0.73640±0.00040	-	Epova et al., 2018d	
Pakistan	Salt <i>Himalayan pink</i> /1	-	0.70794 ± 0.00010	-	Epova et al., 2018a	
South Korea	Hot paper, Rice /77	0.70803-0.73909	0.71712±0.00618	0.71566 (0.70485-0.76090) / rock 0.71910 (0.70646-0.76470) / soil	Song et al., 2014	
	Cabbage /100	0.70814-0.72018	0.71120±0.00193	0.71769 (0.70639-0.72836) / soil	Bong et al., 2012b	
	Cabbage /15	-	0.71097±0.00127	-	Bong et al., 2012	
	Tea <i>Hwagae Valley</i> / 5	0.71154-0.71632	-	-	Epova et al., 2018d	
	Vegetables <i>Yeungwol</i> /20	0.7125-0.7135	-	0.7127 / rock; 0.7125 / soil	Song et al., 2015	
	Vegetables <i>Gongju</i> /17	0.7148-0.7153	-	0.7158 / rock; 0.7145 / soil	Song et al., 2015	
	Vegetables <i>Jeju</i> /20	0.7078-0.7095	-	0.7060 / rock; 0.7077-0.7098 / soil	Song et al., 2015	

Table A.3 (Continued).

Region	Country	Product / Number of samples	⁸⁷ Sr/ ⁸⁶ Sr ratio interval	⁸⁷ Sr/ ⁸⁶ Sr ratio mean	⁸⁷ Sr/ ⁸⁶ Sr ratio in rock/soil	Reference
ASIA	Sri Lanka	Tea /5	0.71345-0.71996	0.71659	-	Epova et al., 2018d
	Taiwan	Coffee /3	0.70851-0.71012	0.70936	0.7158 (0.7134-0.7189) / rock	Liu et al., 2014
		Coffee /3	0.70851-0.70944	0.70937	0.71575 (0.71338-0.71894) / rock	Liu et al., 2016
		Tea /14	0.70482-0.71462	0.70982	0.70946 (0.70404-0.71262) / rock	Chang et al., 2016
	Thailand	Poultry /33	0.70826-0.71114	0.70935	-	Rees et al., 2016
		Rice /50	0.709-0.721	0.7129	-	Ariyama et al., 2012
		Rice /7	0.7096-0.7180	0.7136±0.0034	-	Ariyama et al., 2011
		Onion /4	0.70968-0.72099	0.71513	-	Hiraoka et al., 2016
	Turkey	Tea Rize /2	0.70662, 0.70671	-	-	Epova et al., 2018d
	Vietnam	Rice /1	-	0.711	-	Kawasaki et al., 2002
		Tea Suối Giàng /2	0.73617, 0.74035	-	-	Epova et al., 2018d
	PACIFIC	Australia	Barley /50	0.7090-0.7274	0.7145±0.0048	-
Beef /4			-	0.710±0.001	-	Franke et al., 2008
Butter /1			-	0.711367	-	Rossmann et al., 2000
Cheese /1			-	0.70950	-	Fortunato et al., 2004
Milk /5			0.7050-0.7155	-	-	Crittenden et al., 2007
Onion /8			0.70894-0.71056	0.70943	-	Hiraoka et al., 2016
Rice /3			0.715-0.717	-	-	Kawasaki et al., 2002
Rice /4			0.7144-0.7162	0.7152±0.0009	-	Ariyama et al., 2011
Wheat /16			0.7059-0.7245	0.7174±0.0073	-	Ariyama et al., 2011
Wine /1		-	0.70963±0.00001	-	Barbaste et al., 2002	
Hawaii		Coffee /3	0.7059-0.7067	0.7063	0.7041 (0.7038-0.7047) / rock	Rodrigues et al., 2011b
		Coffee /47	0.7050-0.7091	0.7066	-	Rodrigues et al., 2011a
		Salt Alaea red salt /1	-	0.70910	0.709176 ± 0.000003 / sea water	Epova et al., 2018a
Est Timor		Coffee /6	0.7159-0.7296	0.7249	0.70400 / rock	Rodrigues et al., 2011b
Indonesia	Coffee /1	-	0.7062	0.7047 (0.7045-0.7047) / rock	Rodrigues et al., 2011b	
	Coffee /1	-	0.70577	0.70400 / rock	Liu et al., 2014, 2016	

Table A.3 (Continued).

Region	Country	Product / Number of samples	⁸⁷ Sr/ ⁸⁶ Sr ratio interval	⁸⁷ Sr/ ⁸⁶ Sr ratio mean	⁸⁷ Sr/ ⁸⁶ Sr ratio in rock/soil	Reference
PACIFIC	New Caledonia	Coffee /6	0.706623-0.70808	0.7078	-	Techer et al., 2011
	New Zealand	Butter /1	-	0.709125	-	Rossmann et al., 2000
		Milk /1	-	0.7075	-	Crittenden et al., 2007
		Onion /6	0.70769-0.70883	0.70827	-	Hiraoka et al., 2016
	Papua New Guinea	Coffee /2	0.7042-0.7044	0.7043	0.7044 (0.7036-0.7054) /rock	Rodrigues et al., 2011b
Coffee /1		-	0.70472	-	Liu et al., 2014, 2016	
NORTH AMERICA	Canada	Barley /30	0.7089-0.7182	0.7109±0.0019	-	Ariyama et al., 2011
		Beef /2	-	0.709±0.001	-	Franke et al., 2008
		Cheese /1	-	0.70774	-	Fortunato et al., 2004
		Grapes Quebec / 16	0.70945-0.71522	-	0.70986-0.71546 / soil extract	Vinciguerra et al., 2016
		Wine Quebec / 17	0.70988-0.71546	-	0.70986-0.71546 / soil extract	Vinciguerra et al., 2016
	USA	Barley /20	0.7061-0.7127	0.7087±0.0020	-	Ariyama et al., 2011
		Beef /2	-	0.709±0.001	-	Franke et al., 2008
		Caviar	-	0.71826	-	Rodushkin et al., 2007
		Orange juices /4	0.7078-0.7083	-	-	Rummel et al., 2010
		Rice /15	0.703-0.707	0.706	-	Kawasaki et al., 2002
	Rice /50	0.704-0.707	0.7059	-	Ariyama et al., 2012	
	Rice /11	0.7040-0.7069	0.7058±0.0008	-	Ariyama et al., 2011	
	Wheat /21	0.7050-0.7103	0.7080±0.0012	-	Ariyama et al., 2011	
	Wine /1	-	0.70688±0.00001	-	Barbaste et al., 2002	
	Wheat /12	0.7064-0.7104	0.7080±0.0012	-	Ariyama et al., 2011	
	Onion /32	0.70650-0.71324	0.71110	-	Hiraoka et al., 2016	
CENTRAL AMERICA	Costa Rica	Coffee /2	0.7051-0.7064	0.7057	0.7039 (0.7035-0.7049) / rock	Rodrigues et al., 2011b
	Cuba	Orange juices /5	0.7056-0.7075	-	-	Rummel et al., 2010
El Salvador	Coffee /2	0.7041-0.7041	0.7041	0.7032	Rodrigues et al., 2011b	
	Coffee /1	-	0.70456	0.70320 / rock	Liu et al., 2014, 2016	

Table A.3 (Continued).

Region	Country	Product / Number of samples	⁸⁷ Sr/ ⁸⁶ Sr ratio interval	⁸⁷ Sr/ ⁸⁶ Sr ratio mean	⁸⁷ Sr/ ⁸⁶ Sr ratio in rock/soil	Reference	
CENTRAL AMERICA	Guatemala	Coffee /2	0.7045-0.7067	0.7056	0.7055 (0.7039-0.7066) / rock	Rodrigues et al., 2011b	
		Coffee /1	-	0.70509	0.70449 / rock	Liu et al., 2014, 2016	
	Jamaica	Coffee /3	0.7052-0.7057	0.7054	0.7055 (0.7035-0.7088)	Rodrigues et al., 2011b	
		Coffee /1	-	0.70625	0.70550 / rock	Liu et al., 2014, 2016	
	Mexico	Orange juices /9	0.7056-0.7075	-	-	Rummel et al., 2010	
		Coffee /2	0.7064-0.7076	0.7070	-	Rodrigues et al., 2011b	
	Nicaragua	Coffee /1	-	0.7047	0.7037	Rodrigues et al., 2011b	
	SOUTH AMERICA	Argentina	Beef /83	0.712-0.718	-	0.7066-0.7100 /soil	Baroni, et al., 2011
			Butter /1	-	0.707840	-	Rossmann et al., 2000
Poultry /6			0.70873-0.70875	0.70846	-	Rees et al., 2016	
Wine /48			0.7071-0.7092	-	-	Di Paola-Naranjo et al., 2011	
Brazil		Beef /4 **	-	0.712±0.002	-	Franke et al., 2008	
		Beef /2 ***	-	0.709±0.000	-	Franke et al., 2008	
		Coffee /7	0.7068-0.7155	0.7114	0.7060 (0.7059-0.7061) /rock	Rodrigues et al., 2011b	
		Orange juices /13	0.7075-0.7188	-	-	Rummel et al., 2010	
		Poultry /4	-	0.709±0.001	-	Franke et al., 2008	
		Poultry /25	0.70706-0.70905	0.70817	-	Rees et al., 2016	
Colombia		Coffee /1	-	0.70480	0.70530 / rock	Liu et al., 2014,2016	
Chile		Poultry /30	0.70721-0.70860	0.70793	-	Rees et al., 2016	
		Wine /1	-	0.70471±0.00001	-	Barbaste et al., 2002	
Ecuador		Coffee /1	-	0.7049	0.7030 (0.7024-0.7038) / rock	Rodrigues et al., 2011b	
Peru	Coffee /2	0.7112-0.7127	0.7120	-	Rodrigues et al., 2011b		
AFRICA	Ethiopia	Coffee /4	0.7073-0.7077	-	-	Rodrigues et al., 2011b	

Table A.3 (Continued).

Region	Country	Product / Number of samples	⁸⁷ Sr/ ⁸⁶ Sr ratio interval	⁸⁷ Sr/ ⁸⁶ Sr ratio mean	⁸⁷ Sr/ ⁸⁶ Sr ratio in rock/soil	Reference
AFRICA	Kenia	Coffee /12	0.7061-0.7075	0.7069	0.7068 (0.7061-0.7073) / rock	Rodrigues et al., 2011b
	Malawi	Coffee /2	0.7131-0.7148	0.7140	-	Rodrigues et al., 2011b
		Coffee /1	-	0.70597	0.70414 / rock	Liu et al., 2014, 2016
	Morocco	Olive Oil /2	0.70899-0.70914	0.70907	-	Medini et al., 2015
	Reunion	Coffee /20	0.70563-0.70577	0.70568	0.70426 / rock 0.70544 (0.70523-0.70563) / soil	Techer et al., 2011
	Rwanda	Coffee /1	-	0.7144	0.7067 (0.7054-0.7080) / rock	Rodrigues et al., 2011b
		Coffee /1	-	0.72027	0.71464±0.00141 / sedimentary rocks	Liu et al., 2014, 2016
		Tea <i>Kinihira</i> /2	0.71381, 0.71387	-	-	Epova et al., 2018d
	Senegal	Paprika /1	0.7197-0.7202	0.7200	-	Brunner et al., 2010
	South Africa	Orange juices /2	0.7185–0.7224			Rummel et al., 2010
		Wine /1	-	0.71255±0.00001	-	Barbaste et al., 2002
		Wine, Robertson /17	0.7113-0.7154	0.7134±0.0012	0.7142±0.0009	Vorster et al., 2010
		Wine, Stellenbosch /18	0.7070-0.7110	0.7100±0.0018	0.7120±0.0022	Vorster et al., 2010
		Wine, Swartland /20	0.7075-0.7141	0.7093±0.0014	0.7123±0.0023	Vorster et al., 2010
		Wine, Walker Bay /12	0.7078-0.7131	0.7100±0.0014	0.7121±0.0015	Vorster et al., 2010
Tanzania	Coffee /5	0.7047-0.7072	0.7060	0.7049 / rock	Rodrigues et al., 2011b	
	Coffee /1	-	0.71027	0.7063 / rock	Liu et al., 2014, 2016	
Uganda	Coffee /1	-	0.70579	0.70414 / rock	Liu et al., 2014, 2016	
Zambia	Coffee /1	-	0.7121	-	Rodrigues et al., 2011b	
Zimbabwe	Coffee /1	-	0.7169	-	Rodrigues et al., 2011b	

* Sr IR is reported as delta value ($\delta^{87}\text{Sr}$). Thus, the value of Sr IR for this table was recalculated using the formula: $^{87}\text{Sr}/^{86}\text{Sr}(\text{samples}) = (\delta^{87}\text{Sr} * 0.7093/1000) + 0.7093$.

** Country of processing – Switzerland.

*** Country of processing – Austria.

Table A.5. Lead isotope ratios in food product. Instrumentation, analytical methods, precision of isotope determination.

Product	Country / Number of samples	Purposes	Pb concentration, µg/L, Interval (Mean)	Instrumentation for isotope detection, analytical technique	RSD, % $^{206}\text{Pb}/^{207}\text{Pb}$, $^{208}\text{Pb}/^{206}\text{Pb}$	Reference
Milk powder	Europe, Australia /2	Identify possible lead sources	16-33	ICP-MS-Q	7-8	Dean et al., 1987
Milk powder	Europe, Australia /2	Improvement of analytical procedures *	16-21	ICP-MS-Q, stable isotope dilution	0,9-2,16	Crew et al., 1988
Wine	Italy /4 ; Australia /2	Improvement of analytical procedures *	30,8-143,4	ICP-MS-Q, stable isotope dilution	0,7-4	Crew et al., 1988
Wine	France /5 ; Germany 3 ; Spain /2	Improvement of analytical procedures *	1,63-58,8; (40)	ICP-MS-Q,	1,2 (0,2-3,4)	Goossens et al., 1993
Wine	France, Spain, Germany /3	Improvement of analytical procedures *	1,63-58,8 ; (40)	ICP-MS-Q, FI, stable isotope dilution	1,5-2,5	Goossens et al., 1994
Wine	Certified wine samples /3	Improvement of analytical procedures *	40-135	ICP-MS-Q, stable isotope dilution TIMS	0,05-0,3	Augagneur et al., 1997
Wine	France (vintages 1950-1991) /19	Identify possible lead sources, temporal variations of Pb IR	40-227	IRMS, stable isotope dilution	0,05	Rosman et al., 1998
Wine, Whisky	No information /2	Improvement of analytical procedures *	3,4-24	ICP-MS-HR	0,06	Rodushkin et al., 1999
Wine	Portugal /24	Improvement of analytical procedures, temporal variations of Pb IR	47-804	ICP-MS-Q	0,3	Almeida et al., 1999a
Wine	Portugal /8	Improvement of analytical procedures	47-290	ICP-MS-Q	0,3	Almeida et al., 1999b
Wine	France (vintages 1898-1995)	Identify possible lead sources, Discrimination of origin	50-2000	ICP-MS-Q	0,3-0,8	Medina et al., 2000
Wine	Uruguay /1 ; Australia /2 ; Canarias, Spain /5 ; California, USA /2; China /1; Italy /2; Canada /1; South Africa /2; Chile /2 ; France /2	Improvement of analytical procedures *, Lead source tracing; Discrimination of origin	5-150	ICP-TOF-MS	-	Tian et al., 2000
Wine	Uruguay /1 ; Australia /2 ; Canarias, Spain /5 ; California, USA /2; China /1; Italy /2; Canada /1; South Africa /2; Chile /2 ; France /2	Improvement of analytical procedures *, Lead source tracing	5-150	ICP-MS-Q, ICP-MS-MC, ICP-MS-TOF, stable isotope dilution	0,14-2,7 0,01-0,12 0,04-0,17	Barbaste et al., 2001
Wine	Italy /83	Discrimination of origin	10-149; (19**)	ICP-MS-Q	0,01-0,03	Larcher et al., 2003
Wine	Certified wine sample	Improvement of analytical procedures				Fortunato et al., 2003
Wine	Australia /2	Control vinification contamination	4-64	TIMS	Non reported	Stockley et al., 2003
Wine	Portugal /4	Control vinification contamination	4-50	ICP-MS-Q	0,85-1	Almeida et al., 2003

Table A.5 (Continued).

Product	Country / Number of samples	Purposes	Pb concentration, $\mu\text{g/L}$, Interval (Mean)	Instrumentation for isotope detection, analytical technique	RSD, % $^{206}\text{Pb}/^{207}\text{Pb}$, $^{208}\text{Pb}/^{206}\text{Pb}$	Reference
Vinegar	Italy, Spain, France, USA /205	Identify possible lead sources, Improvement of analytical procedures	15-307	ICP-MS-Q GFAAS	0,3	Ndung'u et al., 2004
Wine	Czech Republic /19	Identify possible lead sources	5,05-11,11	ICP-MS-Q	-	Mihaljevič et al., et al., 2006
Wine	Romania, Moldova /13	Identify possible lead sources	2-47	ICP-MS-Q	-	Dehelean et al., 2012
Wine	Brazil /94	Discrimination of origin				Almeida et al., 2016
Rice	Jiangsu Province, China	Air and soil pollution control	50-230	ICP-MS-Q	0,21-0,33	Feng et al., 2010
Rice	Japan /58; Australia /4; USA /11; China /31; Thailand /7	Discrimination of origin	-	ICP-MS-HR	0,17-0,21	Ariyama et al., 2011
Barley	Japan /221; Australia /50; USA /20; Canada /30	Discrimination of origin	-	ICP-MS-HR	0,11-0,34	Ariyama et al., 2011
Wheat	Japan /44; Australia /16; USA /21; Canada /12	Discrimination of origin	-	ICP-MS-HR	0,12-0,31	Ariyama et al., 2011
Rice	Japan /200; China /50; Thailand /50; USA /50	Discrimination of origin	-	ICP-MS-HR	0,11-0,34	Ariyama et al., 2012
Tea	China, Hangzhou /18	Lead contamination		ICP-MS-HR	0.05	Yuanfa et al., 2011

*- Improvement of analytical procedures were considered for further application to distinguish the source of lead origin in food.

** median values.

Chapter B

Analytical methods for determination of Sr and Pb isotopic compositions in food by MC-ICP-MS

Introduction

Consumers around the world are increasingly demanding reassurance regarding the quality of nutrition. Identification of food fraud, including altering, mislabeling, substituting or tampering with any food product is one of the most important and challenging issues facing the food industry. Tracing the geographical origin and authenticity of food can detect false description, substitution of cheaper ingredients, and adulteration, as well as incorrect origin labeling. The increasing interest in anti-fraud and consumer protection has led to the extension of scientific research and development of effective analytical methods for food authenticity control.

The determination of food geographical origin and its definitive authentication requires the use of highly sophisticated analytical techniques. The number of recognized analytical approaches based

on determination of elemental composition, organic components, stable isotopes configuration, and the genetic specifications have been successfully applied to provenance determinations of various food products (Reid et al., 2006; González et al., 2009; Drivelos & Georgiou, 2012). The natural variation of Sr- and Pb isotopic composition is a relatively new approach addressing to their geographical origin (Balcaen, et al., 2010; Resano & Vanhaecke, 2012; Zhao et al., 2014, Baffi & Trincherini, 2016; Coelho et al., 2017). Among the analytical methods traditionally used for the Sr and Pb isotopic analysis, the first reliable results were produced with thermal ionization mass spectrometry (TIMS). Recent instrumental developments made isotopic data obtained by multicollector inductively coupled plasma mass spectrometry (MC-ICP-MS) competitive with those obtained by TIMS, the reference technique in the field of isotopic analysis (Walczyk, 2004), what finally made MC-ICP-MS a confirmed technique used to provide highly precise and accurate detection of small isotopic variations (Meija et al., 2012; Irrgeher & Prohaska, 2016, Horsky et al., 2016).

With the main aim of this study to evaluate the applicability of Sr- and Pb isotope ratio methods for food geographic origin assessment, different food items were selected: wine, tea, dry-cured ham and salt; where, wine and tea are beverages made from vegetable origin raw materials, dry-cured ham is a food product derived from animals, and salt is the most famous food seasoning. Among selected products, tea undergoes a minimal industrial processing including harvesting, preliminary drying, twisting, enzymatic oxidation, final drying. Other operations are introduced into the process only for the production of certain species and varieties of tea (McKenzie et al., 2010). Winemaking implies more complex processing, starting with harvesting of grapes, destemming, crushing, pressing, alcoholic fermentation, racking, filtration, aging and bottling (Pohl, 2007). Most of these stages involve a direct contact with equipment and/or the addition of ingredients, which increases the risk of contamination and alteration of initial elemental concentrations, and consequently, their isotopic specifications. The dry-cured ham production includes a numbers of technological steps, such as trimming, salting, water rinsing, drying and ripening (Petrova et al., 2015), among which salting is the most affecting for elemental and isotopic composition of the final product due to the potential influence from salt.

This chapter aims to present an accurate and a high precise analytical approach for Sr- and Pb isotope determination in different food matrixes of vegetable and animal origin, which was necessary to achieve reliable experimental results and then, to interpret and discuss them on a competent way.

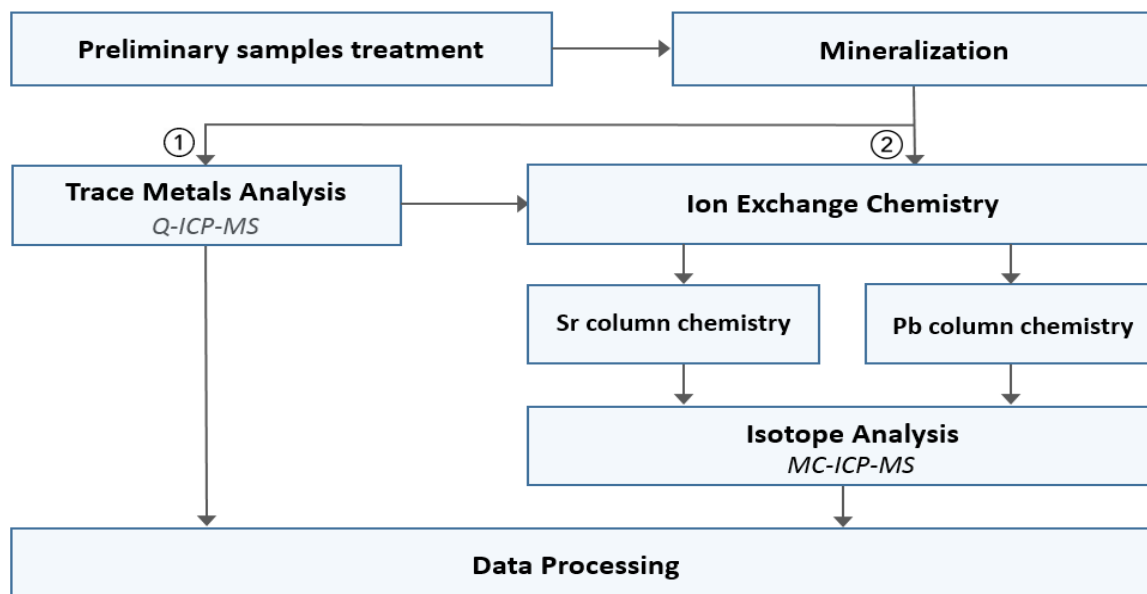


Fig. B.1. A schema of analytical approach applied in the study.

The analytical approach consists of the following stages: sample preparation (including stages of pretreatment, digestion, and matrix purification), elemental and isotopic analysis and statistical data treatment, a schema is presented on Fig. B.1.

B.1. A fit-for purpose procedure for sample preparation

The results of a chemical analysis can only be as good as the sampling and sample preparation; hence, it is important to ensure the quality of all performed operations. The choice of a sample preparation method is crucial in isotopic analysis, since it is one of the most difficult and time-consuming steps of the whole analytical process.

This approach was tested out on four series of samples - wine, tea, dry-cured ham and salt. The detailed description of the samples geographical origins can be found in the corresponding chapters: series of authentic and suspicious Bordeaux wines - in Chapter C, series of dry-cured hams and salt - in the Chapter D, and a large selection of teas of worldwide origin - in Chapter E.

All materials and chemical reagents used for sample preparation must be of the highest purity, as contamination during sample preparation is of greatest concern, especially for Pb. Thus, all reagents and vessels must be thoroughly cleaned, preparation blanks need to be controlled through all steps of sample preparation. In this study, sample handling was performed in a cleanroom class ISO 7. All polyethylene or Teflon vessels, tubes and vials were cleaned in 10% (v/v)

HNO₃, then in 10% (v/v) HCl, and rinsed with ultrapure water. Detailed information about materials, chemical reagents and apparatus used in this study is presented in Tables B.1, B.2, B.3, placed at the end of this Chapter.

B.1.1. Sample conditioning, sample pretreatment

After receiving the samples, a preliminary pretreatment was performed (if necessary), involving grinding, homogenization, and drying.

Wine. All wine samples were stored in glass bottles, without specifying the volumes and kept in a cold room prior analysis. No sample pre-treatment was applied.

Dry-cured ham. Samples were received packed in plastic bags. A slice of ham without visible fat was taken for each sample, lyophilized, homogenized and kept frozen at -18°C until analysis.

Salt. Samples of different salts were transferred from commercial packages to zipped plastic bags, large crystals were grounded. Samples were stored in a dry, dark place until analysis.

Tea. Tea leaves received for analysis were packed into commercial packages. From each package, an amount about 10 grams was dry-grinded using a mixer mill. The obtained powder was transferred to a zipped plastic bag and stored in a dry, dark place until analysis.

B.1.2. Sample digestion

First, a series of tests was carried out to determine the appropriate digestion method for each of studied matrix, including a hot plate, a microwave, and a high pressure archer. Here is presented the finally selected method by its efficiency of total mineralization of complex biological matrices and its productivity. However, some important observation in analytical procedures will be described in some detail to provide a sufficient information to evaluate and apply this method.

Each of the investigated food matrices contains various organic and inorganic components, which can cause potential problems during sample preparation. Tea is rich in polyphenols, enzymes, amino acids, the major organic components of wine are carbohydrates and polysaccharides while dry-cured ham is rich in proteins, lipids and salt.

A closed vessel microwave digestion, performed by an oven MARS 5 (CEM, Italy), has been chosen as a preferable method for isotopic analysis. A microwave was used. Each mineralization batch consisted of 11 samples and 1 blank. The standard microwave program for digestion provided

temperature 200°C and power 1600W, the stages included: ramping - 20 min, hitting - 20 min, and cooling - 20 min. Between each cycle of mineralization, a washing cycle (temperature 200°C, power 1600W, the stages included: ramping - 20 min, hitting - 20 min, and cooling - 20 min) with concentrated nitric acid was applied.

For a preliminary quantitative information on elemental composition, a digestion on DigiPREP hot block was performed, since it provided sufficient digestion of wine, tea and dry cured ham samples for trace and ultra-trace elemental analysis. The standard operating program for digestion was as follows: ramping from ambient temperature up to 45°C pendant 20 min, stabilizing of temperature at 45°C during 40 min, ramping from 45°C up to 90°C during 30 min, stabilizing of temperature at 90°C during 160 min.

Detailed sample preparation for each of sample matrixes is presented in the following sections.

B.1.2.1. Wine

Sample digestion for elemental analysis

For the elemental quantification analysis by Q-ICP-MS, to the volume of 0.5 mL of wine an amount 0.2 mL of HNO₃ was added followed by a 20 times dilution with ultrapure water.

Sample digestion for isotopic analysis

The sample digestion procedure for isotopic analysis involved a step of pre-concentrations due to a relatively low Sr and Pb concentrations, and it was as follows: at first, about of 10 mL of wine was evaporated in a Savillex vial until that the reduced volume was equivalent to approximately 1 mL. The complete evaporation of the sample should be avoided since it makes further manipulations more difficult. In a second step, 5 mL of HNO₃ were added gradually to the wine concentrate and left to react overnight at room temperature. Then 1 mL of H₂O₂ was added to the sample/acid solution. Finally, the resulting sample was microwaved under the conditions previously described (B.1.2.). After cooling, the solution was transferred into 50 mL polypropylene tubes and diluted with ultrapure water up to 30 mL.

Features that should be considered for wine preparation

The presented protocol is a modified version from the one proposed by Durante et al. (2015), where only 5 mL of wine was combined with 5 mL of HNO₃ and microwaved. The fact that some of Bordeaux wines had such low Sr and Pb concentrations, a larger volume is required to be

mineralized to ensure sufficient amounts of Sr and Pb for the isotopic analysis. Taking into account that the maximum volume allowing to be effectively digested in the microwave system is limited to 10 mL, a soft pre-concentration combined with the addition of H₂O₂ needs to be applied for efficiency reasons. When the concentration of Sr and Pb in a wine sample exceed 0.30 mg L⁻¹ and 0.01 µg L⁻¹ respectively, only 10 mL of digested wine is sufficient to perform both, Sr and Pb, isotopic analysis from the same mineralization. If a larger volume of wine (up to 20 mL) needs to be mineralized following the pre-concentration, it then requires the amounts of HNO₃ and H₂O₂ need to be increased up to 7 mL and up to 2 mL, respectively.

The low temperature mineralization without heating (Durante et al., 2015) was deemed to be ineffective for red wine samples. After reacting for 12 hours, the solutions containing 5 mL of wine and 5 mL of HNO₃, were still colored typically for the presence of non-destroyed organic matter (pale yellow color). When these samples were subjected to the subsequent Sr/matrix separation using Eichrom® resin, the fractionation of the solution on an ion-exchange column was observed due to the resin depletion by the presented organic matter. This fact was evident from a low recovery rate of the separation (lower than 50%, not acceptable for the isotopic determination), and, in particular, from a visible color changing of an ionic exchange resin (turned from white to yellow). In contrast, all samples passed the presented protocol of microwave digestion had a clear uncolored appearance and did not present any difficulties for the following matrix separation. Consequently, this method has been chosen as the preferable one.

B.1.2.2. Ham

Sample digestion for elemental analysis

For the total element concentration determination by ICP-MS about 0.2 g of lyophilized sample was combined with 5 mL HNO₃ and 1 mL of H₂O₂ and left for pre-digestion overnight at room temperature. The next day, the digestion was completed on the DigiPREP Block using the program described above (section B.1.2.) and at the end diluted with ultrapure water up to 50 mL. Based on this data, the mass of sample and preparation procedure was adapted to relatively low concentrations of Sr not exceeded 1 mg kg⁻¹ for certain samples. However, for the reason of a lower content of Pb in certain samples (about 5 µg kg⁻¹), the Pb isotopic analysis was not conducted.

Sample digestion for isotopic analysis

The sample digestion procedure for subsequent isotopic analysis was as follows: to the amount of 0.4-0.6 g of lyophilized sample were added 7 mL of HNO₃ and 1 mL of H₂O₂ and left for pre-digestion

overnight at room temperature. Next day the obtained substance was microwaved under the standard conditions, and then diluted with ultrapure water up to 30 mL.

Features that should be considered for ham preparation

Due to the low Sr concentration in some samples it was necessary to digest 3 or 4 aliquots of the same sample as described above and put digested solutions together in a Savillex vial to give in total 1.5-2 g of digested sample. Also it is necessary to use a sample with removed interlayers of fat, always presented in dry-cured ham. Fat content might rich up to 22% (Lucarini et al., 2013) and contains insignificant levels of metals (Ferrari et al., 2007), however, it is an interfering component for successful sample mineralization.

B.1.2.3. Tea

An amount of 0.2-0.4 g of tea was combined with 7 mL of HNO₃ (added gradually to prevent foam formation) and left to react overnight at room temperature. Then, 1 mL of H₂O₂ was added to the sample/acid solution. The resulted sample was microwaved under the standard conditions. After cooling, the solution was transferred into 50 mL polypropylene tubes and diluted with ultrapure water up to 30 mL. An aliquot of digested solution was taken to the elemental quantification analysis, the rest of it was used for further procedures of sample preparation for isotopic analysis.

B.1.2.4. Salt

About 0.3 g of salt was dissolved in 10 mL of ultrapure water to approach the salinity of the seawater. Then, samples were diluted 30 times with 2% HNO₃ (v/v). An aliquot of obtained solution was taken to the elemental quantification analysis, the rest of it was used for further procedures of sample preparation for isotopic analysis.

B.1.3. Multielemental analysis

Determination of total elemental concentrations is a necessary preliminary step in the isotopic analyses. For the elemental concentration detection and intermediate measurement control, a Q-ICP-MS NexION 300X was used according two modes of operation: 1) standard mode (no react gas supply into the cell); and 2) collision cell mode (with He as collision gas). The list of elements and instrumental operating modes applied are listed in Table B.4. The general operating conditions of the NexION 300X are presented in Table B.5. Multielemental calibration standards were made from

multi-element standards CCS-4 and CCS-6 (Inorganic Ventures, USA, 100 µg mL⁻¹, and reported uncertainties of preparation – 1.0026%) in the range of 0.01-200 µg kg⁻¹. A drift correction for ICP-MS data was controlled using the normalization to ¹⁰³Rh (an internal standard correction). All samples were prepared and analyzed in triplicates. For contamination control three replicates of the procedural blanks were prepared. Accuracy and precision of the measurements were verified by analyzing certified reference materials SLRS-5 “River water reference material for trace metals” (NRCC, Canada), CRM NIES 23 “Tea Leaves II” (NIES, Japan), and RM 8414 “Bovine Muscle Powder” (IRMM, Belgium). The recoveries were about 100 ± 11% depending on the element. The determined and the certified concentrations are presented in Table B.6. In the absence of certified reference material for trace elements in wine, the method of standard addition was applied for quality control, recoveries were within the acceptance maximal limits of ± 5%. For quality control of REE determination in ham samples, the standard addition method was also applied, in this case, recoveries were within the acceptance maximal limits of ± 25%.

Table B.4. Analyzed elements and operating detection modes.

Analyte	Mass (amu)	Mode	Analyte	Mass (amu)	Mode		
Al	Aluminum	27	Std	Ni	Nickel	58, 60	Collision
As	Arsenic	75	Collision	Pb	Lead	206, 207, 208	Std
Ba	Barium	137, 138	Std	Pr	Praseodymium	141	Std
Be	Beryllium	9	Std	Rb	Rubidium	85	Std
Cd	Cadmium	111	Std	Rh	Rhodium	105	Std, Collision
Co	Cobalt	59	Collision	Sc	Scandium	45	Collision
Cr	Chromium	52	Collision	Se	Selenium	78, 80	Collision
Cs	Cesium	133	Std	Sr	Strontium	86, 88	Std
Cu	Copper	63, 65	Collision	Sm	Samarium	147, 149	Std
Dy	Dysprosium	161, 163	Std	Tb	Terbium	159	Std
Eu	Europium	151, 153	Std	Tl	Tallium	205	Std
Fe	Iron	56	Collision	Tm	Thulium	169	Std
Ga	Gallium	69	Std	U	Uranium	238	Std
Gd	Gadolinium	155, 157	Std	V	Vanadium	51	Collision
Ho	Holmium	165	Std	Y	Yttrium	89	Std
Li	Lithium	7	Std	Yb	Ytterbium	172	Std
Mn	Manganese	55	Collision	Zn	Zinc	66	Collision
Nd	Neodimium	142	Std				

Std – standard operating mode (without collision/reaction gas).

Table B.5. Instrumental settings and data acquisition parameters of the NexION-300S.

Component / Parameter	Type / Value / Mode
Nebulizer	Meinhard® glass microconcentric
Spray Chamber	Glass cyclonic
Triple Cone Interface	Nickel / Aluminum
RF Power	1600 W
Operating mode	Standard / Collision
Collision Gas	He
Plasma Gas Flow	15.0 L/min
Auxiliary Gas Flow	1.00 – 1.20 L/min
Nebulizer Gas Flow	1.00 – 1.05 L/min
Collision Gas Flow	3.4 L/min
Sample Uptake Rate	230 µL/min
Integration Time	500 – 1500 ms
Replicates per Sample	5
Washing time	240 s

Table B.6.

Certified and determined concentrations of elements in reference materials SLRS-5, RM 8414 and NIES 23.

Element	SLRS-5 - River Water		RM 8414 - Bovine Muscle Powder		NIES 23 - Tea Leaves II	
	Measured	Certified	Measured	Certified	Measured	Certified
Be	0,006 ± 0,002	0,005*	-	-	-	-
Al	46,7 ± 1,9	49,5 ± 5,0	1,7 ± 0,4	1,7 ± 1,4	368 ± 26	540*
V	0,315 ± 0,052	0,317 ± 0,033	4,6 ± 0,2	5,0*	-	-
Cr	0,214 ± 0,021	0,208 ± 0,023	0,066 ± 0,003	0,071 ± 0,038	-	-
Mn	0,075 ± 0,015	0,081 ± 0,006	0,36 ± 0,2	0,37 ± 0,09	706 ± 43	704 ± 52
Fe	90,25 ± 0,08	91,2 ± 5,8	65,9 ± 2,5	71,2 ± 9,2	-	-
Co	0,05 ± 0,02	0,05*	0,0063 ± 0,0003	0,007 ± 0,003	-	-
Ni	0,444 ± 0,161	0,476 ± 0,064	0,041 ± 0,002	0,05 ± 0,04	7,44 ± 0,32	7,89 ± 0,57
Cu	17,1 ± 0,2	17,4 ± 1,3	2,54 ± 0,10	2,84 ± 0,45	8,05 ± 0,45	9,48 ± 0,76
Zn	0,83 ± 0,09	0,845 ± 0,095	144 ± 4	142 ± 14	33,9 ± 2,9	31,9 ± 2,2
As	0,48 ± 0,13	0,413 ± 0,039	0,010 ± 0,001	0,009 ± 0,003	-	-
Se	-	-	0,070 ± 0,004	0,076 ± 0,010	-	-
Sr	51,3 ± 1,8	53,6 ± 1,3	0,065 ± 0,003	0,052 ± 0,015	3,39 ± 0,19	3,93 ± 0,25
Rb	-	-	26,1 ± 0,9	28,7 ± 3,5	-	-
Cd	0,0083 ± 0,0026	0,0060 ± 0,0014	0,012 ± 0,002	0,013 ± 0,011	-	-
Cs	-	-	0,029 ± 0,002	0,05*	0,081	0,0932*
Ba	14,3 ± 0,9	14,0 ± 0,5	0,047 ± 0,003	0,05*	-	5,43*
Pb	0,087 ± 0,033	0,081 ± 0,006	0,25 ± 0,03	0,38 ± 0,24	-	-
U	0,088 ± 0,008	0,093 ± 0,006	-	-	-	-

*- Concentration estimates are provided.

B.1.4. Ion exchange chemistry

The sample matrix exerts a quite pronounced influence on the extent of mass discrimination during isotopic analysis. To obtain reliable results of the highest quality, the target element needs to be isolated from the matrix. In the context of the presented study, for the precise and accurate determination of Sr isotope ratios, an effective elimination of rubidium (Rb) is necessary to avoid the isobaric interference from ^{87}Rb on ^{87}Sr , which cannot be resolved even by high resolution isotope ratio measurements. In order to obtain reliable results of Pb isotopic analysis, a substantial pre-concentration with the simultaneous removal of matrix elements is needed due to commonly low Pb concentrations in the samples.

B.1.4.1. Sr column chemistry

A chromatographic Sr-selective resin Eichrom[®] consisting of an octanol solution of 4,4'(5')-bis(*t*-butyl-cyclohexano)-18-crown-6 sorbed on an inert polymeric support was used for Sr/matrix separation (Horwitz et al., 1992). The analytical protocol for Sr matrix separation was adapted from Martin et al. (2013). The following procedure was applied (Table B.7):

1. **Columns preparation.** An amount of 100 mg of the Eichrom[®] Sr-selective resin was put into a 2 mL column fitted with appropriate filters to fix the resin inside of the column to ensure a slow constant flow rate of about 0.5 mL min⁻¹ required to obtain a reliable recovery rate. At first, to avoid any contaminations, the packed resin was prewashed by 5 mL of 3 mol L⁻¹ HNO₃ and rinsed with 20 mL of ultrapure water. Then, the resin was conditioned with 2 mL of 3 mol L⁻¹ HNO₃ to ensure the sufficient activation of the binding groups.
2. **Sample preparation.** Aliquots of a digested samples with an approximate content of 2-2.5 µg of Sr (necessary amount for reliable isotopic ratio determination) were evaporated in Savillex vials using a hot block at 80°C close to dryness and then re-dissolved in 4 mL of 3 mol L⁻¹ HNO₃. For the better dissolution of the residue, vials were agitated with ultrasound for 1 hour. Then, re-dissolved samples were loaded into the columns.
3. **Matrix removal.** The matrix removal was accomplished by flushing the column twice with 4 mL of 3 mol L⁻¹ HNO₃.
4. **Sr elution.** The Sr elution from columns was obtained by rinsing the columns with 10 mL of ultrapure water. This fraction was collected for following isotopic analysis. The resulted solutions contained about 200 µg L⁻¹ of Sr, and were ready to be analyzed by MC-ICP-MS.

Table B.7. The procedure for the sample matrix removal for Sr isotopic analysis.

Eichrom SR-B50-S	Step
0,100 g of Eichrom resin	Preparation
2 x 5 mL 3 mol L ⁻¹ HNO ₃ , 4 x 5 mL UPW*	Clean
2 mL 3 mol L ⁻¹ HNO ₃	Condition
Sample in 4 mL 3 mol L ⁻¹ HNO ₃	Sample Load
2 x 4 mL 3 mol L ⁻¹ HNO ₃	Rinse
2 x 5 mL UPW*	Elute

*-UPW – ultrapure water

The concentrations of Sr and Rb were controlled using a Q-ICP-MS before and after Sr/matrix separation. The obtained recoveries for Sr were in the range of 90 – 105%. The procedural blanks (including all stages of digestion and matrix separation) were control with every batch of 25 samples, the levels of Sr were below 0.3 µg L⁻¹ and the levels of Rb were below the detection limit of 0.005 µg L⁻¹.

The presented protocol implies the use of a smaller amount of ion-selective resin than the procedure previously described (Durante et al., 2015; Vinciguerra et al., 2017). The theoretical binding capacity of the Eichrom® Sr Spec resin is approximately 10 mg mL⁻¹ and the bed density is 0.35 g mL⁻¹ (Horwitz et al., 1992). According to recommendations (Horwitz et al., 1992), the resin should be loaded with only 10–20% of its maximum capacity which results in a practical binding capacity of 1-2 mg mL⁻¹. Therefore, an amount of 100 mg of resin has the ability to retain 0.286 mg of Sr. With the present protocol, the solutions obtained after the Sr/matrix separation step have an average content of 2 µg of Sr, thus there is no reason to use a larger amount of resin than 100 mg. For the Sr/Rb separation procedure, 3 mol L⁻¹ concentration of HNO₃ was found to be sufficient for matrix removal, as it was previously shown for water samples (Martin et al., 2013) and wine samples (Marchionni et al., 2016; Vinciguerra et al., 2017) in comparison with 8 mol L⁻¹ used by Durante et al. (2015).

After using for one separation cycle, the Eichrom® Sr Spec resin was tested in terms of their multiple usage after cleaning by flushing through it 10 mL of 3 mol L⁻¹ HNO₃ followed by 20 mL of ultrapure water. The amount of Sr retained by the cleaned resin after the washing cycle was below 0.5 µg L⁻¹ (0.25%), and Rb was removed quantitatively. The re-used columns were tested by SRM 987 solution in concentration of 200 µg L⁻¹, the ratio ⁸⁷Sr/⁸⁶Sr was not significantly different from

those in single-used columns ($p > 0.5$). The results show that resin can be re-washed and re-used, at least, up to three times. The only limitation factor is possible depletion of resin, to avoid this it is necessary to obtain a loaded sample after complete digestion excluding the presence of any non-destroyed organic matter.

B.1.4.2. Pb column chemistry

A precise and accurate determination of Pb isotope ratios by MC-ICP-MS requires isolation of Pb from the sample matrix. For this purposes, an ion-exchange resin Dowex AG1-X8 was used, according to Ortega et al. (2012) and Barre et al. (2018). The Dowex AG1-X8 resin is composed of strongly basic anion exchangers with quaternary ammonium functional groups attached to the styrene divinylbenzene copolymer lattice. From the digests, further Pb was extracted using the Dowex[®] resin following the procedure Ortega et al. (2012) adapted for biological matrices (Barre, 2018). The Pb matrix separation procedure consists of several stages (Table B.8):

1. **Columns preparation.** An amount of 0.5 mL of Dowex[®] ion exchange resin, previously activated with HCl Ultrex[®] in proportions 1:1 (v/v) was put into a 2 mL pre-cleaned column fitted with appropriate filters. To avoid any contaminations, the packed resin and filters were prewashed with 1 mL of 0.5 mol L⁻¹ HBr and 1 mL of 6 mol L⁻¹ HCl, completed by rinsing with 0.5 mL of ultrapure water between each step. Then, the resin was conditioned with 0.5 mL of 0.5 HBr to ensure the sufficient activation of the binding groups.
2. **Sample preparation.** The aliquots of digested wine samples with an approximate content of 0.2 µg of Pb were evaporated in 30 mL Savillex vials using a hot block at 80°C close to dryness and then the residue was re-dissolved in 0.6 mL of 0.5 mol L⁻¹ HBr. For better re-dissolution, the solutions were processed in ultrasonic bath for 1 hour, then the supernatant was taken out by a micropipette and passed through the column. The remaining deposit is re-suspended in 0.6 mL of 0.5 mol L⁻¹ HBr, agitated as mentioned above. The second supernatant passed through the column.
3. **Matrix removal.** The removal of the sample matrix was accomplished by flushing the column twice with 1 mL of 0.5 mol L⁻¹ HBr.
4. **Pb elution.** Pb elution was obtained by triple rinsing of the column with 1 mL of 6 mol L⁻¹ HCl. The resulting solutions were evaporated on a hotplate until dry and re-dissolved in 3 mL 2% HNO₃. To obtain a quantitative recuperation of Pb from the residue, the vials were agitated by ultrasound for 1 hour.

Table B.8. The procedure for the sample matrix removal for Pb isotopic analysis.

Dowex AG1-X8	Step
0,5 mL of activated* Dowex resin	Preparation
0.5 mL UPW**, 2 x 0.5 mL 0,5 mol L ⁻¹ HBr, 0.5 mL UPW, 2 x 0.5 mL 6 mol L ⁻¹ HNO ₃ , 0.5 mL UPW	Clean
0,5 mL 0,5 mol L ⁻¹ HBr	Condition
sample dissolved in 1,2 mL 0.5 mol L ⁻¹ HBr	Sample Load
2 x 1 mL 0.5 mol L ⁻¹ HBr	Rinse
3 x 1 mL of 6 mol L ⁻¹ HCl	Elute

*-UPW – ultrapure water

Following this matrix purification procedure, solutions in the amount of 3 mL with Pb concentrations of 30 µg L⁻¹, ready to be analyzed by MC-ICP-MS were obtained. The concentrations of Pb were controlled using a Q-ICP-MS before and after Pb matrix separation. The recoveries for Pb were in the range of 85-110%.

B.2. Isotopic analysis

Isotopic analysis is the determination of isotopic signatures or the distribution of stable isotopes within chemical compounds. Isotopes of a chemical element tend to participate in many physical processes and bio-, geo-, chemical reactions. Isotopic analysis plays an important role in geochemistry because the isotopic variations of elements provide information about age of rocks, the sources of origin, and other processes that have affected on the geological evolution (Vanhaecke, F. & Kuzer, 2012).

B.2.1. Instrumentation, method description and operating parameters

Isotopes of a given element are atoms with the same chemical properties, but with different nuclear constitutions: while the nucleus contains always the same number of proton, the number of neutrons can vary. Due to different numbers of neutrons, isotopes of a given element will be characterized with different masses. This feature underlies isotope analysis, which allows to characterize the isotopic configuration of an element. For the determination of Sr and Pb isotopic compositions a high resolution MC-ICP-MS Nu Plasma-HR was used. A schema of a multi-collector mass spectrometer Nu Plasma 2 is presented on Fig. B.2.

The mass-spectrometer combines an ICP plasma source, a high resolution double-focusing system (electrostatic and magnetic), an energy filter, the zoom lens system and multiple collectors for the detection of ions. The ions are produced by introducing a sample into an inductively coupled Ar plasma, which creates positively charged ions by stripping off electrons. These ions are accelerated across the high electrical potential gradient (up to 10 kV) and focused into a beam by an electrostatic zoom lens system (a series of slits and charged plates). The ion beam then passes through an energy filter where it is consistently sorting with respect to the ion energy, and then passing through the magnetic field where the ions are separated on the basis of their mass to charge ratio. These mass-resolved beams are then directed into a system of collectors where the ions are converted into voltage. Isotope ratios are calculated by comparing voltages from the different collectors (Wieser et al., 2012).

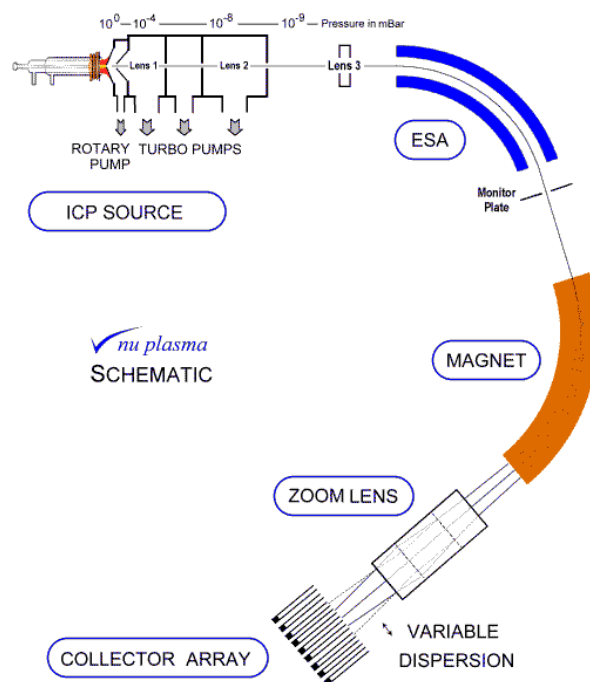


Fig. B.2. A schema of a multi-collector mass spectrometer Nu Plasma 2.

B.2.2. Isotope ratio measurements and precision

Highly precise and accurate isotope ratio measurements are crucial in terms of correct interpretation of results, when very slight variations in the isotopic compositions need to be quantified. Usually, the isotope ratio precision attainable is reported as the within-run precision – 2SD% or RSD expressed as parts per million (ppm) for number of replicate measurements

obtained under favorable experimental conditions. The analytical precision of Sr isotope ratio determination on MC-ICP-MS instruments have been reported on the level of 0,002% RSD or 18 ppm (Balcaen et al., 2005; Weis et al., 2006). For Pb isotope ratios measurements, the analytical precision could achieve the best level of 0,005% (RSD) or 121 ppm for ratios $^{208}\text{Pb}/^{204}\text{Pb}$ (Weis et al., 2006; Irrgeher et al., 2015). To obtain an accurate value it is necessary to correct in for possible mass discrimination effects.

B.2.2.1. Mass discrimination and mass bias correction

Isotopic measurements in ICP-MS may show significant bias with respect to the corresponding true value because ion registration is susceptible to an effect of mass discrimination and it may amount to several percent per mass unit (Meija et al., 2012). This effect occurs because the differences in the efficiency of extraction and transmission of ions as a function of target mass.

Bracketing - an external standard correction

A consistent repeating of external standard measurements after several samples in the sequence allows to correct to a certain degree the mass discrimination effect. In the presented study, a solution containing an isotopic standard of the target element (certified isotopic composition, or at least known isotope ratio) was measured before and after two (Pb isotope analysis) or four (Sr isotope analysis) sample. A correction factor was calculated on the basis of the observed bias between the measured value and the true value of the isotope ratio of interest. The best results can be obtained if the concentration of the target element in the samples matches with the standards within maximal deviation of 20%.

Internal correction for elements with one (or more) radiogenic isotopes

During Sr isotopic determination, to obtain a correct isotope value of the $^{87}\text{Sr}/^{86}\text{Sr}$ ratio, a normalizing against the non-radiogenic $^{86}\text{Sr}/^{88}\text{Sr}$ ratio with value of 0.1194 is needed (Faure, 1986; Vanhaecke et al., 2009).

Internal standard correction

An element of similar mass to target elements, can be used to correct the mass bias. During Pb isotopes determination, all samples were spiked by thallium (Tl) standard solution prepared from NIST SRM 997. The bias between the measured $^{203}\text{Tl}/^{205}\text{Tl}$ isotope ratio and the corresponding true value of an reference material was then used to determine the mass discrimination per mass unit

for the analyte. Several approaches are discussed in the review (Vanhaecke et al., 2009) depending on type of mass discrimination function. In this study, an exponential law according to Albarède et al. (2004) was used for internal standard correction.

Isotopic reference materials

To ensure that the obtained isotopic data are reliable and accurate, they should be traceable to the same reference. In practice, it can be realized by applying isotopic reference materials (IRMs) for correction for bias and for validation of the analytical procedure (Vogl & Pritzkow, 2012).

The choice of IRMs is limited. The most important requirement is a special rate of purity of IRMs. In this study, the Sr isotopic standard NIST SRM 987 (pure SrCO₃) and the Pb isotopic standard SRM 981 (high purity Pb metal) were used. In addition, to control the sample preparation procedure, a non-isotopic reference material BCR 482 (trace metals in lichen), with known values of Pb isotope ratios from previous studies (Cloquet et al., 2006, Barre et al., 2018) was used. All reference materials used in the study are presented in Table B.3.

B.2.2.2. Sr isotope ratio measurement

The collectors of the Nu-Plasma HR were configured for better detection of Sr isotopes (Table B.9). The general operating parameters of the mass spectrometer were optimized daily to achieve the maximum ion intensity for Sr using standard solution NIST SRM 987 with a concentration of 100-200 ng mL⁻¹ (Table B.10). The measurements followed a conventional “sample standard bracketing” calibration sequence with the NIST SRM 987 standard. After blank subtraction, the ratio ⁸⁷Sr/⁸⁶Sr was corrected for mass bias using the constant ⁸⁸Sr/⁸⁶Sr ratio of 0.1194 and potential remaining interferences from ⁸⁷Rb. A second correction was applied relatively to the bracketing standard following Albarède et al. (2004) with the ⁸⁷Sr/⁸⁶Sr value for NIST SRM 987 of 0.710255. The precision and accuracy of the Sr isotopes measurement were controlled using NIST SRM 987, the measured value was 0.710247 ± 0.000039 (the uncertainty expressed as two standard deviation, 2SD), the recommended reference value of NIST SRM 987 is 0.710255 ± 0.000023 (Waight et al. 2002). The external reproducibility of the isotope ratio measurement was equal to 49 ppm (RSD) from total almost two hundreds measurements of NIST SRM 987 performed during analysis (Table B.11). Also, Table B.11 reports the reproducibility for NIST 987 in solutions of 60, 100 and 200 µg L⁻¹ (concentrations were adjusted depending on the Sr content in samples), for NIST 987 proceeded through the column preparation step, and values of ⁸⁷Sr/⁸⁶Sr ratio obtained for CRM NIES 23. The reproducibility for SRM NIST 987 obtained during one measurement session

of 5 days is presented in Table B.12, and graphically presents in Fig. B.3. For samples, an Individual $^{87}\text{Sr}/^{86}\text{Sr}$ ratios and measurement uncertainties were calculated from independently digested triplicates. Instrumental blanks and blanks related to sample preparation procedure were controlled daily, the typical levels are reported in Table B.10.

Table B.9.

Mass assignment to Faraday cup detectors of Nu-Plasma HR for Sr and Pb isotopic determination.

Cup	H7	H6	H5	H4	H3	H2	H1	Ax	L1	L2	IC0	L3	IC1	IC2	L4
Mass						88Sr	87Sr			86Sr		85Rb			83Kr
				208Pb	207Pb	206Pb	205Tl	204Hg	203Tl	202Hg					

Table B.10.

Instrument settings, data acquisition parameters for wet plasma operating conditions of Nu-Plasma HR and typical sensitivity for Sr isotopic analysis.

Parameter	Type / Value
RF Power	1300 W
Acceleration voltage	6000 V
Instrument Resolution	Low resolution (~ 400)
Nebulizer	200 $\mu\text{L}/\text{min}$ micro-concentric
Spray Chamber	Cinnabar cyclonic 20 mL
Sample Uptake Rate	230 $\mu\text{L}/\text{min}$
Interface Cones	Nickel Wet plasma cones, Type A
Gas parameters (Ar):	
Plasma Gas Flow	13.0 L/min
Auxiliary Gas Flow	0.8 L/min
Nebulizer Gas Flow	1.00 – 1.05 L/min
Acquisition parameters:	
Number of blocks	3
Number of measurements/block	20
Integration time (s)	10 s
Total acquisition time (s)	600 s
Replicates per sample	5
Wash time	240 s
Uptake time	240 s
Zero	OPZ
Typical sensitivity, 88-Sr (100 ppb)	7 V
Blank control, 85-Rb (standard)	< 0.00001 V
Blank control 85-Rb (sample preparation)	< 0.015 V

Table B.11. Summarized precision of Sr isotope measurements.

	NIST 987 reference value	NIST 987 Total 194**	NIST 987 200 ppb 98**	NIST 987 100 ppb 69**	NIST 987 60 ppb 27**	NIST 987 preparation* 10**	NIES 23 tea leaves 5**
$^{87}\text{Sr}/^{86}\text{Sr}$	0,710255	0,710266	0,710277	0,710248	0,710245	0,710266	0,708666
2SD	0,000023	0,000035	0,000029	0,000015	0,000027	0,000017***	0,000031***
RSD, ppm		49	41	21	39	24	43

* - Solution of NIST 987 ($200\mu\text{g kg}^{-1}$) proceeded through the column preparation step.

** - number of measurements.

*** - standard deviation from the mean.

Table B.12. Precision of Sr isotope measurements during a typical session of 5 days*.

NIST 987	n	$^{87}\text{Sr}/^{86}\text{Sr}$	2SD	RSD, ppm
1 day	5	0,710262	0,000025	36
2 day	15	0,710272	0,000018	25
3 day	22	0,710286	0,000024	34
4 day	22	0,710278	0,000024	33
5 day	10	0,710291	0,000033	46

* - The presented results were obtained during a measurement session of 5 days: 24-25 March 2014, carried on wine and tea samples.

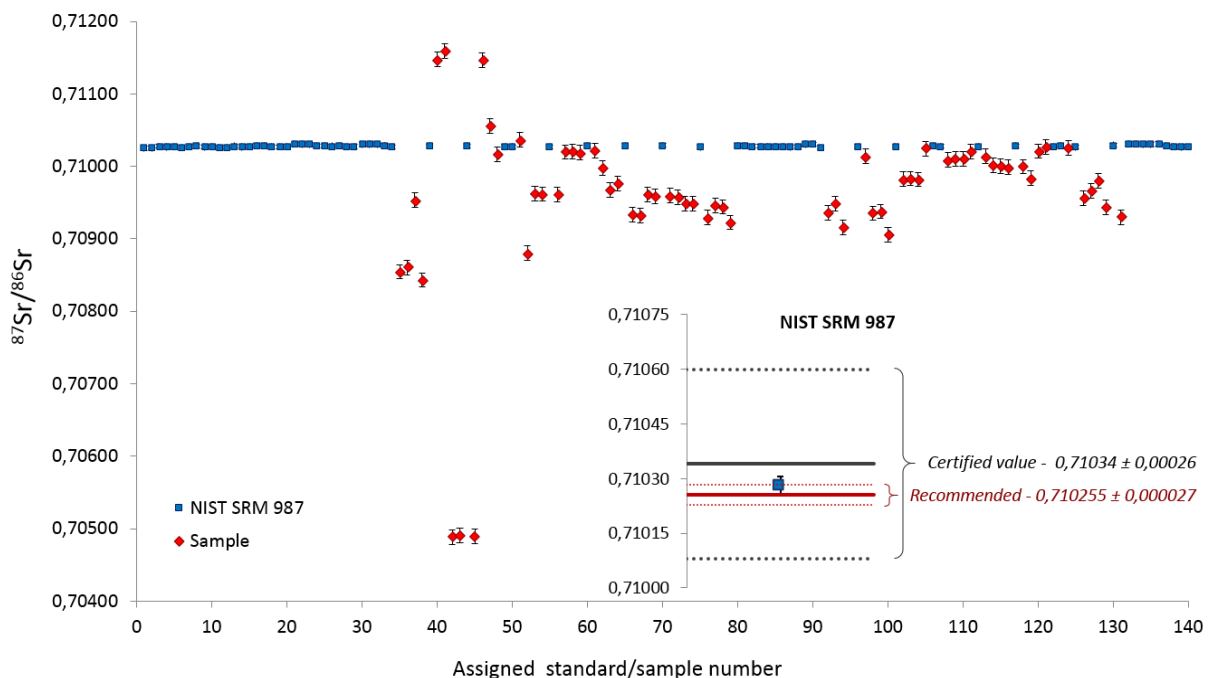


Fig. B.3. The reproducibility, accuracy and precision of measurement on example of 2 days measurement sequence.

B.2.2.3. Pb isotope ratio measurement

The collectors of the Nu-Plasma HR were configured for a better detection of Pb isotopes (Table B.9.). The operating parameters of the mass-spectrometer were optimized daily using the standard solution SRM NIST 981 (Table B.13). Two types of sample introduction systems were used depending on Pb concentration in the samples. For samples with Pb concentrations adjusted to between 100-200 ng mL⁻¹, a micro-concentric nebulizer with flow rate of 200 µL min⁻¹, a cyclonic spray chamber, and nickel plasma cones (wet plasma conditions) were used. For samples with a relatively lower Pb concentrations, adjusted to between 20 and 30 ng mL⁻¹, the sample introduction was achieved through the use of the desolvating nebulizer DSN-100 combined with appropriate nickel cones (dry plasma conditions). The use of the desolvating nebulizer allows to concentrate the analyte in the aerosol and simultaneously reduce the solvent load during the MC-ICP-MS measurements, thus, significantly increase the sensitivity of Pb isotope determination.

Measurements were performed using a conventional “sample standard bracketing” calibration sequence with the NIST SRM 981 as described in Ortega et al. (2012). After blank subtraction, the correction for the isobaric interference from ²⁰⁴Hg on the mass $m/z = 204$ was made by monitoring the isotope ²⁰²Hg following the subtraction of the ²⁰⁴Hg contribution on this mass: $^{204}\text{Hg} = ^{202}\text{Hg} \times 0.229$. Afterwards, the normalization of the signal was made by using standard solution of SRM 981 according Albarède et al. (2004) and mass bias correction by using the SRM 997 according Ortega et al. (2012).

The combination of the different methodological approaches mentioned above resulted in accurate and precise Pb isotope ratios determinations by MC-ICP-MS. The measured Pb ratios of NIST SRM 981 were as followed (certified values are in brackets): $^{208}\text{Pb}/^{204}\text{Pb} = 36.724 \pm 0.006$ (36.722 ± 0.037); $^{207}\text{Pb}/^{204}\text{Pb} = 15.500 \pm 0.002$ (15.492 ± 0.015); $^{206}\text{Pb}/^{204}\text{Pb} = 16.9417 \pm 0.0014$ (16.937 ± 0.018); $^{208}\text{Pb}/^{206}\text{Pb} = 2.1677 \pm 0.0002$ (2.1681 ± 0.0009); $^{206}\text{Pb}/^{207}\text{Pb} = 1.09300 \pm 0.00005$ (1.09332 ± 0.00039). An external reproducibility was equivalent to 157 ppm ($^{208}\text{Pb}/^{204}\text{Pb}$), 131 ppm ($^{207}\text{Pb}/^{204}\text{Pb}$), 81 ppm ($^{206}\text{Pb}/^{204}\text{Pb}$), 72 ppm ($^{208}\text{Pb}/^{206}\text{Pb}$), 50 ppm ($^{207}\text{Pb}/^{206}\text{Pb}$) for RSD (relative standard deviation) for the NIST SRM 981 solution analyzed (n=15) during a typical 1-day session. The obtained results for reference materials used to quality control are presented in Table B.14 (NIST SRM 981), Table B.15 (BCR 482) and Table B.16 (NIES 23). A special attention during Pb isotope analysis was paid on the instrumental and procedure blanks, since external contaminations is always possible and critical for the quality of data. The instrumental blank and the preparation blank (related to all stages of sample preparation) were controlled daily. The typical values are presented in Table B.13.

Table B.13. Instrument settings, data acquisition parameters for dry plasma operating conditions of Nu-Plasma HR and typical sensitivity for Pb isotopic analysis.

Parameter	Type / Value
RF Power	1300 W
Acceleration voltage	6000 V
Instrument Resolution	Low resolution (~ 400)
Desolvator	DSN100
Sample Uptake Rate	230 µL/min
Interface Cones	Nickel Dry plasma cones, Type B
Gas parameters:	
Plasma Gas Flow	13.0 L/min
Auxiliary Gas Flow	0.8 L/min
Nebulizer Gas Flow	1.00 – 1.05 L/min
Acquisition parameters:	
Number of blocks	3
Number of measurements/block	20
Integration time (s)	10 s
Total acquisition time (s)	600 s
Replicates per Sample	5
Wash time	600 s
Uptake time	180 s
Zero	ESA
Typical sensitivity, total Pb (15 ppb)	
	8-9 V
Typical sensitivity, total TI (1,5 ppb)	
	0,8-0,9 V
Instrumental blank	
	0,005 V
Sample preparation blank	
	0,02-0,03 V

Table B.14. Comparison of the obtained and certified values of NIST 981.

SRM	$^{208}\text{Pb}/^{204}\text{Pb}$	$^{207}\text{Pb}/^{204}\text{Pb}$	$^{206}\text{Pb}/^{204}\text{Pb}$	$^{208}\text{Pb}/^{206}\text{Pb}$	$^{207}\text{Pb}/^{206}\text{Pb}$	$^{206}\text{Pb}/^{207}\text{Pb}$
NIST 981 certified	36,7219	15,4916	16,9374	2,16810	0,91464	1,09332
uncertainties	0,0369	0,0149	0,0183	0,00087	0,00033	0,00039
NIST 981 - 1 day typical session, n=13	36,7237	15,4995	16,9417	2,16769	0,91488	1,09300
2SD	0,0058	0,0020	0,0014	0,00016	0,00005	0,00005
RSD (ppm)	157	131	81	72	50	50
NIST 981 - 3 day sessions, n=50	36,7238	15,4996	16,9417	2,16769	0,91488	1,09300
2SD	0,0124	0,0040	0,0033	0,00033	0,00007	0,00009
RSD (ppm)	338	259	193	153	81	81
NIST 981, column, recovery 97%, n=4	36,72437	15,48712	16,95212	2,16636	0,91358	1,09457
2 SD	0,00748	0,00394	0,00329	0,00076	0,00036	0,00044
RSD (ppm)	204	255	194	349	399	399

Table B.15. Comparison of the Pb isotope ratios obtained in this study and previously reported values for BCR 482.

Source	Parameter	$^{208}\text{Pb}/^{204}\text{Pb}$	$^{207}\text{Pb}/^{204}\text{Pb}$	$^{206}\text{Pb}/^{204}\text{Pb}$	$^{208}\text{Pb}/^{206}\text{Pb}$	$^{207}\text{Pb}/^{206}\text{Pb}$
Measured BCR 482	Mean (n=4)	37,474	15,5629	17,60448	2,12773	0,88404
	2SD	0,023	0,0074	0,00540	0,00071	0,00015
	RSD (ppm)	620	475	307	336	175
Cloquet et al., 2006 BCR 482	Mean (n=4)	37,49	15,5701	17,6111	2,12879	0,88411
	2SD	0,02	0,0070	0,0073	0,00030	0,00010
	RSD (ppm)	528	450	415	143	115
Barre et al., 2013 BCR 482	Mean (n=5)	37,4986	15,56660	17,61490	2,12880	0,88370
	2SD	0,0025	0,00088	0,00096	0,00008	0,00001
	RSD (ppm)	136	113	109	72	19

Table B.16. The values of Pb isotope ratios of NIES 23 obtained in this study.

NIES 23	$^{208}\text{Pb}/^{204}\text{Pb}$	$^{207}\text{Pb}/^{204}\text{Pb}$	$^{206}\text{Pb}/^{204}\text{Pb}$	$^{208}\text{Pb}/^{206}\text{Pb}$	$^{207}\text{Pb}/^{206}\text{Pb}$	$^{206}\text{Pb}/^{207}\text{Pb}$
Mean (n=3)	38,1520	15,6092	18,0619	2,1123	0,8642	1,1571
2SD	0,0080	0,0028	0,0056	0,0004	0,0002	0,0003
RSD (ppm)	210	182	309	199	230	230

B.4. Chemometric technics for assessing food authenticity and traceability

In the present work the Principal Component Analysis (PCA) was used for data treatment due to the simplicity of use and a reliable interpretation of the results. PCA was found to be a useful technique for the classification of different origins of dry-cured ham and Asian teas using either multielemental or Sr- and/or Pb isotopic compositions, the latter providing a better discrimination. Results are presented in Chapters D and E, respectively.

B.5. Conclusion

In the present Chapter, the analytical methods used for the Sr and Pb isotopic composition of food determination are described. The importance of an integrated analytical approach is highlighted: it allows better understanding of the potential issues that may arise during sample preparation and analysis, including samples selection, sampling, sample pre-treatment, mineralization, trace element and isotopic analysis. Using this approaches, Sr and Pb isotopic compositions in studied samples were determined with the high level of accuracy and precision. The situation is somewhat more delicate for Pb isotopic ratios where a potential contamination may be introduced during the original preparation of the samples. The Pb isotope ratios of BCR 482 (Tables B.15) and CRM NIES 23 (Table B.16), as well as Sr isotope ratio of CRM NIES 23 (Table B.16) can be used as comparative values for further studies.

Table B.1. Materials used in the experiment.

Name	Additional information	Purpose
Savillex vials	30 mL, PFA, Savillex Corporation, USA	Sample pre-concentration; sample evaporation
Ion-separation columns	2 mL, Triskem International, France	Matrix purification
Tubes 3-15	3-15 mL	Elemental / Isotopic analysis

Table B.2. Apparatus used in the experiment.

Name	Additional information	Purpose
Milli-Q system	Resistivity of 18.2 MΩ cm, Millipore USA, Molsheim, France).	Sample preparation / Isotope analysis
Mixer mill	Retsch MM200; accomplished by Teflon jars and balls	Sample pretreatment (tea)
Lyophilisateur	Freeze Dryer Alpha 1-4 LSC Martin Christ Gefriertrocknungsanlagen GmbH; Germany	Sample pretreatment (dry-cured ham)
Acid distillation system	Acid Distillation system Savillex, USA	Acid purification
Microwave	MARS 5, CEM Corporation, Milan, Italy accomplished by 12 position carousel, 12 Teflon XP-1500 Plus high pressure vessels, temperature probe RTP-300 Plus, pressure sensor ESP-1500 Plus	Sample digestion for isotopic / multielemental analysis
DigiPREP	Block Digestion Systems, SCP Science, Canada	Sample digestion for multielemental analysis
Centrifuge	4/8 positions; Hettich, Germany	Sample preparation
Ultrasonic cleaner	Branson 8510MT, Branson, USA	Cleaning protocol, sample preparation

Table B.3. Reagents used in the experiment.

Name	Additional information	Purpose
Nitric acid, HNO ₃	high purity subboiled in the laboratory	Sample digestion
Nitric acid, HNO ₃	reagent grade, 69.0-70.0%, Instra Analysed Reagent, J.T.Baker®, Fisher Scientific	Acid to be purified by subboiling
Nitric acid, HNO ₃	10% v/v, 69.0-70.0%, Instra Analysed Reagent, J.T.Baker®, Fisher Scientific	Cleaning protocol
Nitric acid, HNO ₃	67-70%, ULTREX® II Ultrapure Reagent, J.T.Baker, Fisher Scientific	Preparation of standards, samples and reagents for elemental // isotopic analysis / Sr - Matrix purification
Hydrochloric acid HCl	10% v/v, 36.5-38.0%, Instra Analysed Reagent, J.T.Baker®, Fisher Scientific	Cleaning protocol
Hydrochloric acid HCl	33-36%, ULTREX, J.T.Baker™, Fisher Scientific	Pb - Matrix purification
Hydrobromic acid HBr	44-49%, Optima™, Fisher Scientific	Pb - Matrix purification
Hydrogen peroxide H ₂ O ₂	30%, ULTREX® II Ultrapure Reagent, J.T.Baker®, Fisher Scientific, France	Sample digestion
CCS-4, CCS-6	Multielemental standards, Inorganic Ventures, USA	Quality control / Elemental analysis
Sr-selective ion exchange resin	Eichrom® SR-B50-S, Triskem International, France	Sr / Matrix purification
Pb-selective ion exchange resin	Dowex®, AG1-X8 (1X8 100-200 mesh), Acros Organics, France	Pb / Matrix purification
CRM SLRS-5	River water, NRCC, Ottawa, Canada	Quality control / Elemental analysis
RM 8414	Bovine Muscle Powder, NRCC, Canada	Quality control / Elemental analysis
CRM NIES 23	Tea Leaves II, NIES, Japan	Quality control / Elemental analysis
SRM NIST 997	Tl, isotopic standard, high-purity thallium metal, NIST, USA	Quality control / Pb Isotopic analysis
SRM NIST 981	Pb, isotopic standard, high-purity lead metal, NIST, USA	Quality control / Pb Isotopic analysis
SRM NIST 987	Pure SrCO ₃ , isotopic standard, strontium carbonate, NIST, USA	Quality control / Sr Isotopic analysis
BCR 482	Lichen, IRMM, Belgium	Quality control / Pb Isotopic analysis

Chapter C

Authentic and regional discrimination of Bordeaux wines using elemental and non-traditional isotopic fingerprinting

Abstract

The elemental and isotopic compositions of Sr and Pb of 43 authentic Bordeaux wines from the world prestigious châteaux are presented in the context of geographical origin and authenticity. The results demonstrate a relatively small variability of both isotopic systems in studied Bordeaux wines with a strong relation to the environment of vine's growth. Particularly, a clearly defined correlation of Pb isotopic compositions in Bordeaux wines with European atmospheric Pb signatures was observed. The Sr isotope ratio of wine was recognized as a specific descriptor for viticultural sub-regions. In the contrary, Sr- and Pb- isotopic compositions of suspicious wines bought in the China market and labeled Bordeaux, significantly exceed the narrow spans observed in the authentic samples. The unique Sr binary signature may trace individual wineries and imitated wines. A significant discrepancy between the Pb isotopic patterns of suspicious and authentic Bordeaux wines evidences the incorrect indication of origin.

C.1. Relevance of the issue

Bordeaux, a territory in southwestern France, is one of the most famous and largest world's wine producing region. The Bordeaux vineyards constitute a conglomerate of vineyards "terroirs" extending over 112 000 ha. Its production represents almost half of all wines produced in France. It represents a global bulk volume of about 6.5 million hectoliters and more than 850 million bottles of wine that are produced and delivered every year with wine qualities ranging from everyday table wines to some of the most expensive and prestigious wines in the world (Lecat et al., 2016). To foster its quality, the concept named "appellation" ("Appellation d'Origine Contrôlée", AOC) has been developed, which takes into account the great care of the grape varieties selected and the approved winemaking practices for each of Bordeaux's 57 appellations. The appellations are geographically localized and cover sub-regions, individual villages or even specific vineyards. Bordeaux wines are known by their "*terroir*" – the combination of various environmental factors that have an impact on the wine taste and link the style of the wines to the specific locations (Médoc, Gravé, etc.) (Wilson, 1999; Bourrouilh, 2006). The prestigious wineries or "*châteaux*" – are most of the time a traditional term to name a winemaking estate.

Wine traceability and authenticity are extremely important issues for the wine production and distribution sector due to the enormous economic damage caused by frauds. Despite of the fact that frauds have always existed, today the damage from counterfeited wine evaluated only for French wine market is around 36 million euros (Lecat et al., 2016). The traceability of prestigious Bordeaux wines is becoming crucial, since the French wines are among the most copied. A number of new approaches aimed at reducing the sales of counterfeited wines, such as serial and individual numbers, laser ablation and engraving of the glass of the bottle, variety of stickers, etc., have been introduced recently. All these actions are targeted to the expertise of recognition on the wine bottle. But despite of all initiatives, falsified wine is still a serious problem, since the wine itself contained in the bottle can be falsified. This leads not only to commercial losses, but also sometime results in important health risk in case if the counterfeited wine could present some compounds and contaminants affecting the health of the customers and hence damaging eventually the image of the brand.

The determination of the geographical provenance and definitive authentication of wine requires the use of highly sophisticated analytical techniques. The number of recognized analytical

approaches based on determination of elemental composition, organic components, stable light isotopes configuration, and the genetic specifications of wine have been successfully applied to provenance determinations of wines (Médina et al., 2013; Cozzolino & Smyth, 2013; Camin et al., 2017). Among these methods, the natural variation of stable isotope ratios of heavy elements, so-called “non-traditional” – strontium and lead, is a relatively new approach addressing to its geographical origin (Balcaen et al., 2010). The theoretical basis and application of Sr- and Pb isotope ratios methods are described in Chapter A.

To our knowledge, the data available in literature concerning Sr and Pb isotopic characteristics and elemental profiles of Bordeaux wines is limited. More often the Bordeaux wines were used as comparative samples in studies devoted to wines from other regions, as in the study of Koreňovská & Suhaj (2005), where one sample of white Bordeaux wine was used in the context of classification among Slovakian wines. Recently, 4 red and 3 white wines from Bordeaux were included in a study aimed to the geographical origin classification of 29 French wines (Tian et al., 2017). However, no individual elemental concentrations were presented in the paper, and finally, an adequate and successful discrimination of Bordeaux wines has not been achieved. Only four samples of Bordeaux wine from Saint-Émilion were examined for the Sr isotopic composition (Barbaste et al., 2002). The Pb isotopic composition of Bordeaux wines was described only once (Médina et al., 2000).

When all wines produced in France, the general lack of objective studies of elemental and stable isotopic compositions of French wines can be stated. France is one of the largest wine producers in the world (Lecat et al., 2016), however, there are only a few studies dedicated to elemental composition of certain individual French wines (Tian et al., 2017), and to their Sr-, Pb- isotopic signatures (Horn et al., 1993; Rosman et al., 1998). Such uncomplete and fragmented information does not allow to propose a justified and reinforced hypothesis about a specified trace elemental patterns and isotopic fingerprints of French, and particularly, of Bordeaux wines.

Therefore, the objectives of this work were to study Sr-, Pb- isotopic compositions and multielemental profiles of a large selection of prestigious Bordeaux wines and to assess to their authentic signatures and discriminate different Bordeaux wines by means of these parameters. Another special objective was addressing to wine authenticity issue: could these parameters be a useful tool to confirm or disprove the declared origin of some suspicious wines labeled “Bordeaux” purchased in China.

C.1.1. Sample description

The region of Bordeaux represent an exceptional environment, which was formed as results of superimposition of paleogeographical, structural and climatic events. Its geological formation occurred during the Tertiary period by the upwarping of the area and the offset of the Bordeaux faults and the delivery of a huge amount of detrital sediments. The whole yield the famous gravels, modeling the morphology, and originating complex soils were effected by large climatic events (such as alternating marine transgressions and regressions on a very flat area) and a number of small-scale climatic events, (such alternating glacial-interglacial periods), reworked detrital sediments in a network of imbricated fluvial terraces (Wilson, 1999; Bourrouilh, 2012).

Authentic Bordeaux wine. In this study, a series of 43 authentic Bordeaux wines from prestigious AOC, produced between 1969 and 2012 (most of them after 2000), classified as First Growth (*French - "Grand Cru"*) or not, were provided by winemaking estates, territorially located on a restricted area of about 50 km radius, encompassing the famous Bordeaux viticultural lands of Médoc, Graves and Libourne. These wineries belong to the following appellations: Pomerol (11 red wines, vintages 1969-2010), Saint-Émilion (4 red wines, vintage 2011), Pessac-Léognan (15 red wines and 9 white wines, vintages 2009-2012), and Pauillac (4 red wines, vintages 2004-2007).

The geographical location of the studied vineyards can be seen on Fig. C.1. Pomerol and Saint-Émilion represent the famous appellations of Bordeaux from right bank of the Dordogne River. The vineyards of Saint-Émilion are planted on soils formed from the erosion of several types of source rocks (mostly clays and sands) and are located on the slope of the large calcareous plateau. The vineyards of Pomerol are traditionally grown on soils containing some deep fine clays with a mixture of sand resting on a calcareous molasses. Geographically, these two estates are very close, with the distance not exceeding 5 km, but with very distinctive soil compositions (Wilson, 1999; Bourrouilh, 2006). Pessac-Léognan and Pauillac represent two winemaking sub-regions of the left bank of the Garonne River – Haut-Graves and Haut-Médoc, respectively. The vineyards of Pessac-Léognan are located within the Bordeaux urban activity zone on a typical soil constituted of several ridges which contain gravel, pebbles and stone, overlaying a complex basement of sand and limestones. The vineyards of Pauillac are situated in the northern section of the viticultural strip along the Médoc peninsula on the crest of low gravely terrace mounds and consists the soil derived from ferruginous climatic residual crust, resting on a marly calcareous basement with inclusions of varying proportions of sand, gravel and clay in layers of varying depth (Wilson, 1999; Bourrouilh, 2006).

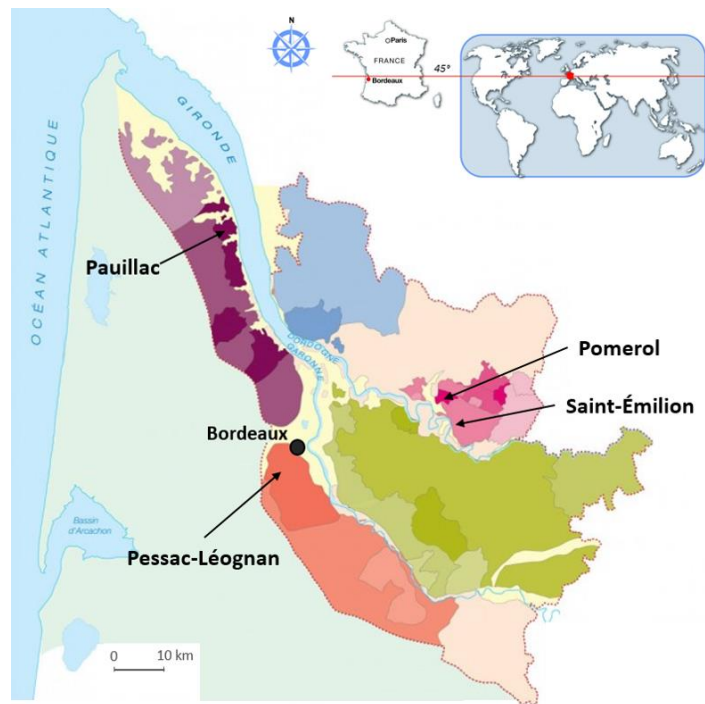


Fig. C.1. Geographical map of the origin of the Bordeaux wines

“Other wines” purchased in China. The discriminative capability of Sr isotope marker was also tested on a set of 17 red wines, purchased in the China market, produced in 1998-2009. This group included 14 samples of wine labeled “Bordeaux” and 3 samples of wine of Chinese production. For some bottles, the indicated “Bordeaux” origin caused mistrust due to incorrect labels containing spelling mistakes in the names of the known wineries, or even not-existing winery’s names. The real geographical origin for these wines was unknown. Exact names of production regions of original Chinese wines were also not specified. The complete list of samples can be seen on the Table C.1.

C.2. Strontium elemental and isotopic compositions of Bordeaux wines

C.2.1. Introduction

Historically, the first application of Sr isotope ratio method for food provenance assessment was performed on wine (Horn et al., 1993). Since then, the implementation of the method has been actively developing and currently its practical relevance for the geographical origin identification is proved for various of food products (Baffi & Trincherini, 2016; Coelho et al., 2017).

Strontium is neither essential nor nutritional element for vine. However, the presence of this element in the soils and hence in the grapes and, later consequently, in the wine, is a direct signature of the soil on which the plant is grown. (Horn et al., 1993; Horn et al., 1998). The grape plant uptakes Sr from the water-soluble fraction of soil (Green et al., 2004), is then assimilated in all parts of plant (Mercurio et al., 2014), and transferred into wine without being altered during the winemaking (Almeida & Vasconcelos, 2004). Following first promising results, a series of studies have been performed aiming at investigating the correlation between $^{87}\text{Sr}/^{86}\text{Sr}$ ratios in the system soil-water-grapes-wine (Almeida & Vasconcelos, 2001; Barbaste et al., 2002; Almeida & Vasconcelos, 2004; Vorster et al., 2010; Di Paola-Naranjo et al., 2011, Vinciguerra et al., 2016). When looking at vineyards from around the world, the Sr isotope ratio method has been applied for the geographical origin classification of wines from South-Africa (Vorster et al., 2010), Argentina (Di Paola-Naranjo et al., 2011), Canada (Vinciguerra et al., 2016), Portugal (Fernandes et al., 2015; Martins et al., 2014; Catarino et al., 2016) and Romania (Geană et al., 2017).

Recently, some new information and interests have been raised on this topic following the publication of a series of studies performed on Italian wines. Using large sample selection of authentic samples it was confirmed that: i) Sr isotope composition of wine remained constant for different vintage years (Mercurio et al., 2014; Durante et al., 2015; Petrini et al., 2015; Marchionni et al., 2013; Marchionni et al., 2016), ii) the ratio $^{87}\text{Sr}/^{86}\text{Sr}$ was not affected by winemaking process (Petrini et al., 2015; Tescione et al., 2015; Marchionni et al., 2016; Durante et al., 2016), and iii) the ratio $^{87}\text{Sr}/^{86}\text{Sr}$ in wine can be forecasted on the basis of that of local pedological settings (Durante et al., 2013; Mercurio et al., 2014; Durante et al., 2015, Marchionni et al., 2013; Petrini et al., 2015; Marchionni et al., 2016; Durante et al., 2018). These studies are of great interest because an extensive database of Sr isotope variations in Italian wines has been created, a wide range of methodological questions have been discussed, and finally, obtained data were used to build strontium isotopic maps able to objectively support the Lambrusco PDO wines origin (Durante et al., 2018).

In this study, an analytical approach for geographical origin specification of Bordeaux wines by means of Sr elemental / isotopic compositions is presented. This approach is developed and adapted for the accurate and high precise determination of $^{87}\text{Sr}/^{86}\text{Sr}$ ratio using MC-ICP-MS, and has been applied to a wide variety of authentic samples of prestigious wineries with specific aims at identification of their Sr signatures with respect of individual wineries (geographic origin discrimination on a small scale) and examining wines with suspicious declaration of origin from viticultural region of Bordeaux.

C.2.2. Strontium elemental concentrations

The Sr elemental concentration in wine can already be an important criterion addressed to the geographical origin since its concentration in vine is strongly regulated by the vineyard's soil composition. The box plots on Fig. C.2 graphically display the mean values and the variation of Sr elemental content across the studied wine samples. In authentic Bordeaux wines, the Sr concentrations do not exceed the level of 0.52 mg kg^{-1} . A comparative analysis of the concentration's variability shows a high level of consistency of the results between studied wines from Saint-Émilion, Pessac-Léognan (white, red wines), and Pauillac, meaning that the Sr concentrations remain relatively constant with a low inter variability within the same winery. However, it is worth mentioning that among the studied authentic Bordeaux wines, the wine from Pomerol are characterized by higher Sr concentrations ranging heterogeneously between $0.33 - 0.52 \text{ mg kg}^{-1}$, which is significantly different from the wine samples produced on the nearby winery in Saint-Émilion, where the concentration was detected at the level of $0.16 - 0.19 \text{ mg kg}^{-1}$.

When comparing the average Sr concentrations of the authentic Bordeaux wines to the suspicious "Bordeaux" purchased in China, we can immediately observe an obvious difference between the authentic samples and the set of wines with unclear provenance (Fig. 2). Further, the individual boxes allocated the samples "suspicious Bordeaux" and "suspicious Pauillac" display also a much higher degree of dispersion and evident skewness. In terms of concentrations, the Sr levels vary in the suspicious samples from 0.29 to 2.16 mg kg^{-1} with the mean value significantly higher than that for authentic Bordeaux, and seem to be more similar to those in wine from the group "China". As mentioned previously, the Sr in wine is mostly originated from grapes, which, in its turn, obtained this element from the labile fraction of soil (Petrini et al., 2015; Vinciguerra et al. 2016). Hence, the large variability of Sr concentration in wine reflects the wide diversity of underlying geological bedrocks and soils formed on them. Therefore, the results of Sr concentrations in suspicious wines reflect the substantial heterogeneity of geological setting on which grapes for these wines were grown, which is not consistent with the rather homogeneous sedimentary basin of Bordeaux (Wilson, 1999; Bourrouilh, 2006). Thus, examining the Sr concentrations in wine, it can be already stated that this parameter can reveal some significant differences and already highlight the alien geographical provenance of the samples.

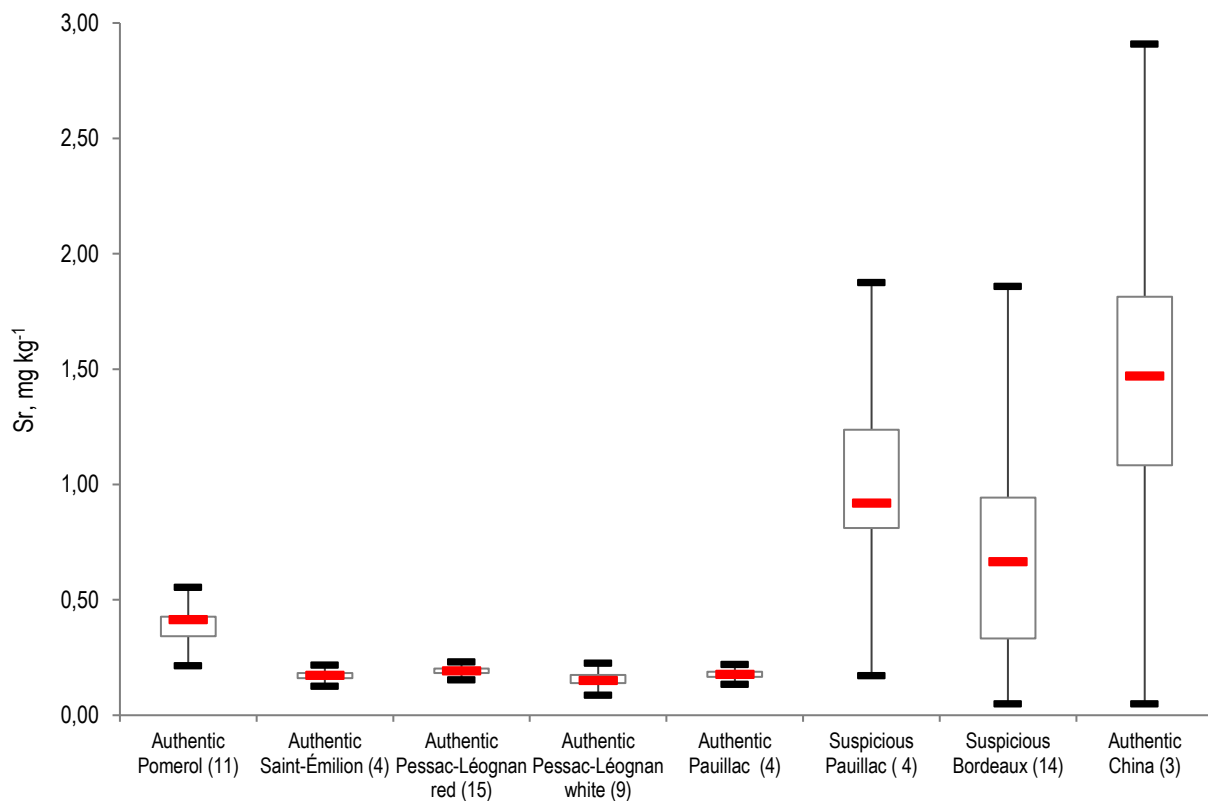


Fig. C.2. Sr concentrations in wines.

Table C.1. Studied wines, Sr elemental concentrations and Sr isotope ratios.

Origin / country of purchase	Appellation / type of wine	Year	Sr, mg kg ⁻¹	⁸⁷ Sr/ ⁸⁶ Sr
Authentic Bordeaux / France	Pomerol / red	1969	0,429 ± 0,011	0,71010 ± 0,00008
	Pomerol / red	1973	0,315 ± 0,009	0,71020 ± 0,00005
	Pomerol / red	1978	0,337 ± 0,010	0,71020 ± 0,00006
	Pomerol / red	1979	0,361 ± 0,008	0,71014 ± 0,00006
	Pomerol / red	1989	0,347 ± 0,009	0,71022 ± 0,00004
	Pomerol / red	1992	0,319 ± 0,008	0,70998 ± 0,00008
	Pomerol / red	2002	0,422 ± 0,013	0,71002 ± 0,00008
	Pomerol / red	2003	0,458 ± 0,008	0,71000 ± 0,00008
	Pomerol / red	2004	0,414 ± 0,012	0,70984 ± 0,00004
	Pomerol / red	2009	0,425 ± 0,012	0,70968 ± 0,00004
	Pomerol / red	2010	0,516 ± 0,011	0,70976 ± 0,00005
Authentic Bordeaux / France	Saint Emilion / red	2011	0,157 ± 0,005	0,70895 ± 0,00009
	Saint Emilion / red	2011	0,163 ± 0,005	0,70877 ± 0,00005
	Saint Emilion / red	2011	0,180 ± 0,005	0,70855 ± 0,00004
	Saint Emilion / red	2011	0,185 ± 0,006	0,70829 ± 0,00009

Table C.1. Studied wines, Sr elemental concentrations and Sr isotope ratios (Continued).

Origin / country of purchase	Appellation / type of wine	Year	Sr, mg kg ⁻¹	⁸⁷ Sr/ ⁸⁶ Sr	
Authentic Bordeaux / France	Pessac-Léognan / red	2009	0,197 ± 0,006	0,70910 ± 0,00006	
	Pessac-Léognan / red	2009	0,180 ± 0,005	0,70934 ± 0,00008	
	Pessac-Léognan / red	2009	0,221 ± 0,007	0,70957 ± 0,00004	
	Pessac-Léognan / red	2009	0,209 ± 0,006	0,70949 ± 0,00008	
	Pessac-Léognan / red	2009	0,191 ± 0,006	0,70936 ± 0,00007	
	Pessac-Léognan / red	2010	0,185 ± 0,006	0,70938 ± 0,00010	
	Pessac-Léognan / red	2010	0,175 ± 0,005	0,70915 ± 0,00009	
	Pessac-Léognan / red	2010	0,185 ± 0,006	0,70959 ± 0,00008	
	Pessac-Léognan / red	2010	0,180 ± 0,005	0,70960 ± 0,00010	
	Pessac-Léognan / red	2011	0,202 ± 0,006	0,70930 ± 0,00008	
	Pessac-Léognan / red	2011	0,186 ± 0,006	0,70946 ± 0,00010	
	Pessac-Léognan / red	2011	0,198 ± 0,006	0,70944 ± 0,00011	
	Pessac-Léognan / red	2011	0,202 ± 0,006	0,70923 ± 0,00004	
	Pessac-Léognan / red	2011	0,176 ± 0,005	0,70932 ± 0,00008	
	Pessac-Léognan / red	2011	0,208 ± 0,006	0,70949 ± 0,00010	
Authentic Bordeaux / France	Pessac-Léognan / blanc	2010	0,150 ± 0,004	0,70956 ± 0,00008	
	Pessac-Léognan / blanc	2010	0,174 ± 0,005	0,70949 ± 0,00008	
	Pessac-Léognan / blanc	2010	0,139 ± 0,004	0,70970 ± 0,00010	
	Pessac-Léognan / blanc	2011	0,122 ± 0,004	0,70980 ± 0,00004	
	Pessac-Léognan / blanc	2011	0,193 ± 0,006	0,70915 ± 0,00009	
	Pessac-Léognan / blanc	2012	0,160 ± 0,005	0,70920 ± 0,00007	
	Pessac-Léognan / blanc	2012	0,145 ± 0,004	0,70967 ± 0,00006	
	Pessac-Léognan / blanc	2012	0,111 ± 0,003	0,70962 ± 0,00008	
	Pessac-Léognan / blanc	2012	0,199 ± 0,006	0,70915 ± 0,00008	
Authentic Bordeaux / France	Pauillac / red	2004	0,167 ± 0,005	0,70944 ± 0,00006	
	Pauillac / red	2005	0,167 ± 0,005	0,70930 ± 0,00006	
	Pauillac / red	2006	0,192 ± 0,006	0,70953 ± 0,00005	
	Pauillac / red	2007	0,185 ± 0,006	0,70906 ± 0,00004	
Bordeaux ? / China	suspicious Pauillac / red	2004	1,52 ± 0,05	0,71266 ± 0,00004	
	suspicious Pauillac / red	2005	0,74 ± 0,02	0,71014 ± 0,00009	
	suspicious Pauillac / red	2006	0,89 ± 0,04	0,70523 ± 0,00007	
	suspicious Pauillac / red	2007	0,95 ± 0,03	0,70861 ± 0,00004	
Bordeaux ? / China	suspicious Bordeaux / red	1998	0,533 ± 0,015	0,71148 ± 0,00010	
	suspicious Bordeaux / red	2005	0,291 ± 0,009	0,71147 ± 0,00009	
	suspicious Bordeaux / red	2006	0,81 ± 0,02	0,70953 ± 0,00005	
	suspicious Bordeaux / red	2007	0,368 ± 0,010	0,70863 ± 0,00006	
	suspicious Bordeaux / red	2007	0,332 ± 0,010	0,71017 ± 0,00006	
	suspicious Bordeaux / red	2008	1,45 ± 0,04	0,70843 ± 0,00006	
	suspicious Bordeaux / red	2009	0,326 ± 0,010	0,71021 ± 0,00008	
	suspicious Bordeaux / red	2009	0,312 ± 0,009	0,71056 ± 0,00005	
	suspicious Bordeaux / red	-	0,94 ± 0,03	0,70991 ± 0,00008	
	suspicious Bordeaux / red	-	0,59 ± 0,02	0,71159 ± 0,00006	
	Authentic China / China	red wine	-	0,70 ± 0,02	0,71036 ± 0,00005
		red wine	-	2,16 ± 0,06	0,70880 ± 0,00007
red wine		-	1,47 ± 0,05	0,70970 ± 0,00006	

C.2.3. Strontium isotope ratios

Following the Sr elemental analysis, the Sr isotopic ratios of studied wines were determined for further evaluation of their discriminating potential regarding the geographic origin. The Sr concentrations and $^{87}\text{Sr}/^{86}\text{Sr}$ ratios obtained for both groups of wines, authentic and suspicious, are listed in Table C.1 and graphically presented on Fig. C.3.

C.2.3.1. Authentic Bordeaux wine

The results displayed on Fig. C.3 clearly indicate that the $^{87}\text{Sr}/^{86}\text{Sr}$ ratios in authentic Bordeaux wines vary within a relatively narrow range, between 0.70829 and 0.71022. When considering in detail the series of samples originating from the individual wineries, the $^{87}\text{Sr}/^{86}\text{Sr}$ ratio measured for wines from Pomerol lies in the range of 0.70968 – 0.71022. This data set is significantly higher than that for the wines from Saint-Émilion (0.70829 – 0.70895), and moderately overlapped with the global span of analytical measurement the wine from Pauillac (0.70906 – 0.70953) and Pessac-Léognan (0.70900 – 0.70980). Indeed, the wine from Saint-Émilion has a tendency of expressing a lower $^{87}\text{Sr}/^{86}\text{Sr}$ values resulted by a slight depletion in radiogenic isotope ^{87}Sr . Wines of Grand Cru of Saint-Émilion are cultivated on soils developed on a large limestone plateau formed during Oligocene (about of 32 million years ago) and preserved the value of the $^{87}\text{Sr}/^{86}\text{Sr}$ ratio of seawater of the period of formation. At that time, the ratio $^{87}\text{Sr}/^{86}\text{Sr}$ was in the range of 0.7079-0.7082 (Koepnick et al., 1985; Jones et al., 1994), and it has been printed out in these limestones, and therefore continue to be a major contributing factor to the low values of $^{87}\text{Sr}/^{86}\text{Sr}$ ratios in plants that grow on it, and ultimately become apparent in wine. It is noticeably for wines from Pauillac and Pessac-Léognan, but yet, to a greater extent with respect to samples from Pomerol. In Pomerol, vines are cultivated on more recent alluvial terraces relating to the period of Pleistocene (< 2 million years ago) formed of sands, pebbles and clays from the glacial erosion of the Central Massif and the Pyrenees. The slow and continuous dissolution of these siliceous elements of earth's crust (the $^{87}\text{Sr}/^{86}\text{Sr}$ ratios ranged from 0.715 to 0.730) can only raise up the $^{87}\text{Sr}/^{86}\text{Sr}$ ratio of seawater of Pleistocene (about 0.7090-0.7091), what can be observed in Pomerol wine: 0.7098 - 0.7102 (Fig. C.4).

When examining the largest group of red and white wines originated from Pessac-Léognan appellation and produced during years 2009-2012, the $^{87}\text{Sr}/^{86}\text{Sr}$ ratios obtained ranged from 0.70910 to 0.70960 with mean of 0.70939 ± 0.00031 for 15 samples of red wines, and from 0.70900 to 0.70980, with mean of 0.70935 ± 0.00058 for 9 samples of white wines.

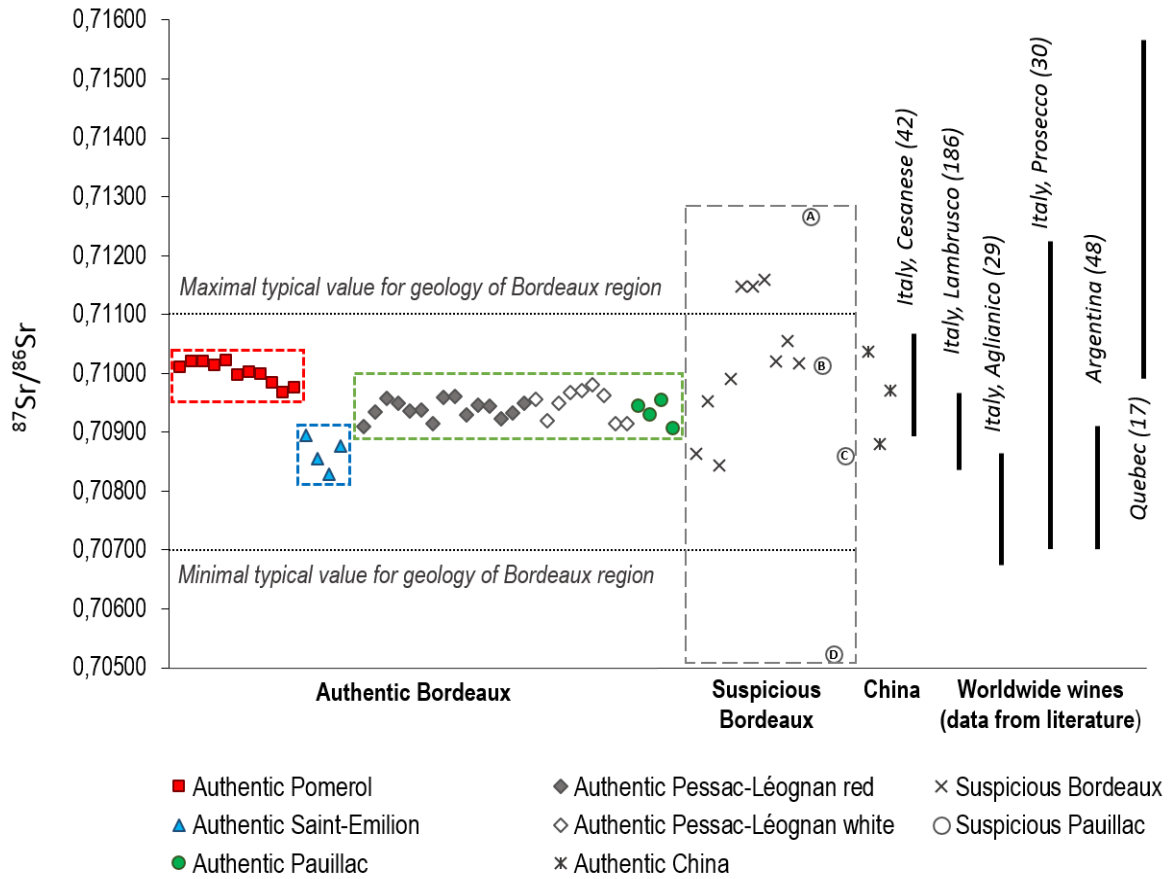


Fig. C.3. $^{87}\text{Sr}/^{86}\text{Sr}$ in the wines and comparison with wines from different world origin, as reported in the literature. Legend: the error bars are smaller than the marks; references: Di Paola-Naranjo et al., 2011; Marchionni et al., 2013; Durante et al., 2015; Marchionni et al., 2016; Petrini et al., 2015; Vinciguerra et al., 2016; number of samples is presented in the in brackets. Samples of suspicious Pauillac are marked as A, B, C and D as described in the text.

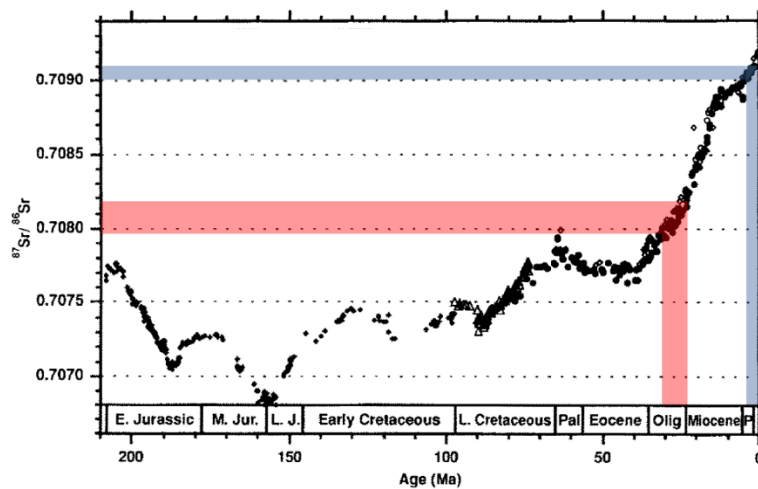


Fig. C.4. Evolution of $^{87}\text{Sr}/^{86}\text{Sr}$ ratios in Jurassic and Cretaceous sea water with respect of the period of geological formation of Saint-Émilion limestone plateau (red bound) and alluvial terraces of Pomerol (blue bound). Modified after: Jones et al., 1994.

This finding is consistent with the recent observations. First, different grape varieties equally accumulate Sr from the labile fraction of soil within the same geological substrata (Di Paola Naranjo, et al. 2011; Vinciguerra et al., 2016). With regards to Bordeaux wines, these facts are extremely important since the winemaking traditions in Bordeaux integrate the practice of wine varietal blending (*fr. "l'assemblage des cépages"*), when wine is produced from different grape's varieties (i.e., Cabernet Sauvignon, Merlot, Cabernet Franc etc. - for red wines, and Sauvignon blanc, Semillon, Muscadelle, etc. – for white wines), and then assembled with the proportions which may vary according to the vintage. Further, the $^{87}\text{Sr}/^{86}\text{Sr}$ ratio in wine from a definite vineyard is generally stable from one vintage to another (Durante et al., 2015; Petrini et al., 2015; Marchionni et al., 2013; Marchionni et al., 2016). Indeed, a certain variability observed in the samples of Pessac-Léognan (0.071% for red wines and 0.092% for white wines) represents a variability not depending on the year of production (Fig. C.3), and it is not likely due to the practice of vine varietal blending, because such differences have been already observed for Italian Cesanese mono-varietal wine, produced during the period of 7 years by the same winery (Marchionni et al., 2016). However, additional contribution to the Sr isotopic compositions of a wine from the winemaking processes and agricultural practices are possible and will be detailed later in the text.

The studied authentic Bordeaux wines characterized by a relatively narrow range of variations of Sr isotope ratios can be explained by the overall homogeneous geological and pedological settings. Indeed, the geology for region of Bordeaux is very well described with the specific consideration of regional viticulture (Wilson, 1999; Bourrouilh, 2006). This territory is a part of Gironde-Aquitaine sedimentary basin formed by erosion of the Pyrenees and the Massif Central between the end of the Tertiary and the beginning of the Quaternary periods (Wilson, 1999). The soils are formed on limestone bedrock originated from expanses of alluvial sediments deposited by the Garonne and Dordogne rivers with gravel inclusions. According to Voerkelius et al. (2010), the anticipated values of the $^{87}\text{Sr}/^{86}\text{Sr}$ ratio in environmental samples from this region are between 0.70701 and 0.71100. All ratios $^{87}\text{Sr}/^{86}\text{Sr}$ obtained in this study for authentic Bordeaux wines are within the predicted limits (Fig. C.3).

When comparing the average of Sr isotope ratios obtained for authentic Bordeaux wine and those from other wines worldwide, it is notable that they have some important overlaps which certainly highlight the similarity of geological and pedological settings of such territories (Fig. C.3). In order to achieve a reliable qualitative comparison, we used only data obtained by MC-ICP-MS and TIMS. Indeed, a series of papers recently published on Italian wines reports Sr isotopic ratios that display a similar range in Cesanese wines: 0.70894 – 0.71062 (Marchionni et al., 2016), as well as from

Lambrusco products: 0.70840 – 0.70964 (Durante et al., 2015). The whole interval of the ratios $^{87}\text{Sr}/^{86}\text{Sr}$ which can be potentially found in Bordeaux wine has been recorded in Prosecco wine (Petrini et al., 2015), while a significant overlap with Aglianico wine (0.70679 – 0.70865) is unlikely (Marchionni et al., 2013). When examining the Sr isotopic ratios in wine originated from other continents, the span of the $^{87}\text{Sr}/^{86}\text{Sr}$ expressed in lower values (0.7071 – 0.7093) has been recorded for wine from Argentina (Di-Paola Naranjo et al., 2011). On the contrary to studied Bordeaux samples, wines from Quebec displays a dispersion between 0.70988 and 0.71546 (Vinciguerra et al., 2016) with relative enrichment of radiogenic isotope ^{87}Sr . This is certainly related to the general differences of metamorphic and geological settings of Quebec compared to the sedimentary basin of the Aquitaine region.

C.2.3.2. “Other wines” purchased in China

The $^{87}\text{Sr}/^{86}\text{Sr}$ ratios recorded in wines from the group with mislabeled declaration of origin presented a very wide dispersion encompassing and significantly exceeding the narrow range observed in the authentic Bordeaux wine samples and ranging from 0.70523 to 0.71266. From 17 samples included in this series, only 12 (9 suspicious “Bordeaux” and 3 original wines from China) were within the reference interval of typical Bordeaux $^{87}\text{Sr}/^{86}\text{Sr}$ values, according the spatial prediction map (Voerkelius et al., 2010). The $^{87}\text{Sr}/^{86}\text{Sr}$ values for remaining 5 samples are outlier of these limits. According Voerkelius et al. (2010) and Marchionni et al. (2013), the wine with measured $^{87}\text{Sr}/^{86}\text{Sr}$ value of 0.70523 could be produced, most likely, from grapes planted on soils developed on volcanic, ophiolites or intrusive rocks. On the contrary, more radiogenic values of $^{87}\text{Sr}/^{86}\text{Sr}$ (0.711 – 0.713) can be caused by soils of vineyards developed on igneous or metamorphic, granitoidic rocks. These types of geological settings are very different from the typical geological structure of the area of Bordeaux, which is a large sedimentary basin (Wilson, 1999; Bourrouilh, 2006). Such wide amplitude of $^{87}\text{Sr}/^{86}\text{Sr}$ variability was observed also for Italian Prosecco wines 0.70706-0.71215 (Petrini et al., 2015) and wines from Quebec (Vinciguerra et al., 2016). In both cited studies, the vineyards of interest were planted on territories of a wide geological and pedological diversity.

These overall results are important since they demonstrate that studied wines represent a certain specification of Sr isotopic composition when considering their geographical origin. However, when the ratio $^{87}\text{Sr}/^{86}\text{Sr}$ is used as the only criterion, it is not a sufficiently discriminating tool neither for the wine origin of same region (Bordeaux), nor for wine origin of geographically distinct regions but having similar geology and soil substrates. Obviously, only five suspicious wines with

outliers of $^{87}\text{Sr}/^{86}\text{Sr}$ cannot be attributed to Bordeaux origin. The geographical provenance of the remaining 9 wines labeled “Bordeaux” and purchased in China cannot be contested on the basis of their Sr isotope signatures, because they have the values $^{87}\text{Sr}/^{86}\text{Sr}$ within the permissible interval for authentic samples from region of Bordeaux. Moreover, $^{87}\text{Sr}/^{86}\text{Sr}$ ratio of some Italian wines, such as previously mentioned Cesanese, Lambrusco, Prosecco and Chinese wines from this study have the ratio $^{87}\text{Sr}/^{86}\text{Sr}$ also disposed in the same range. Thus, it is important to state that the Sr isotope ratio cannot be the distinctive criterion singularly applied for geographical origin assignment due to specificity of world lithological diversity.

C.2.4. Combination of $^{87}\text{Sr}/^{86}\text{Sr}$ and Sr concentrations

In geosciences, the enhanced discriminating potential of strontium lies in the interaction of its two characteristics - elemental concentration and isotopic composition (Green, et al. 2004). We attempted to find this interaction on example of the studied set of authentic Bordeaux samples, and then use to discriminate between Bordeaux’s wine production sub-regions and sign out the geographical origin of authentic and suspicious Bordeaux wines.

C.2.4.1. The case of Pomerol wine

At first, the correlation of these two parameters depending on vintage was appraised using the exceptional long-time series of wines produced in a winery of Pomerol during the period of 1969-2010. It is a small winemaking estate which keeps the process uniform for many decades. For these samples, the significant mirrored dependency of Sr concentration versus the ratio $^{87}\text{Sr}/^{86}\text{Sr}$ from the years of wine production is presented in Fig. C.5. Indeed, despite of the overall rather narrow span in terms of both Sr concentrations and Sr isotopic ratio comparison, we can still observe a significant difference due to the high precision of the isotopic measurements. Over the studied vintages, for the first 20 years we can note a slight enrichment in radiogenic isotope ^{87}Sr , then followed by a slight depletion in ^{87}Sr for the most recent 20 years. Such variation would be expected to be depended on quality of vintage, since the excellence or poorness of vintage directly lies to annual meteorological conditions. However, the wine made in the poor year 1969 (*French - “Millésime médiocre”*) and in the best year 2009 (*French - “Millésime exceptionnel”*) have the same Sr concentration $0.429 \pm 0.011 \text{ mg kg}^{-1}$ and $0.425 \pm 0.012 \text{ mg kg}^{-1}$, while the values of $^{87}\text{Sr}/^{86}\text{Sr}$ differ: 0.71010 ± 0.00002 and 0.70976 ± 0.00005 , for 1969 and 2009 respectively.

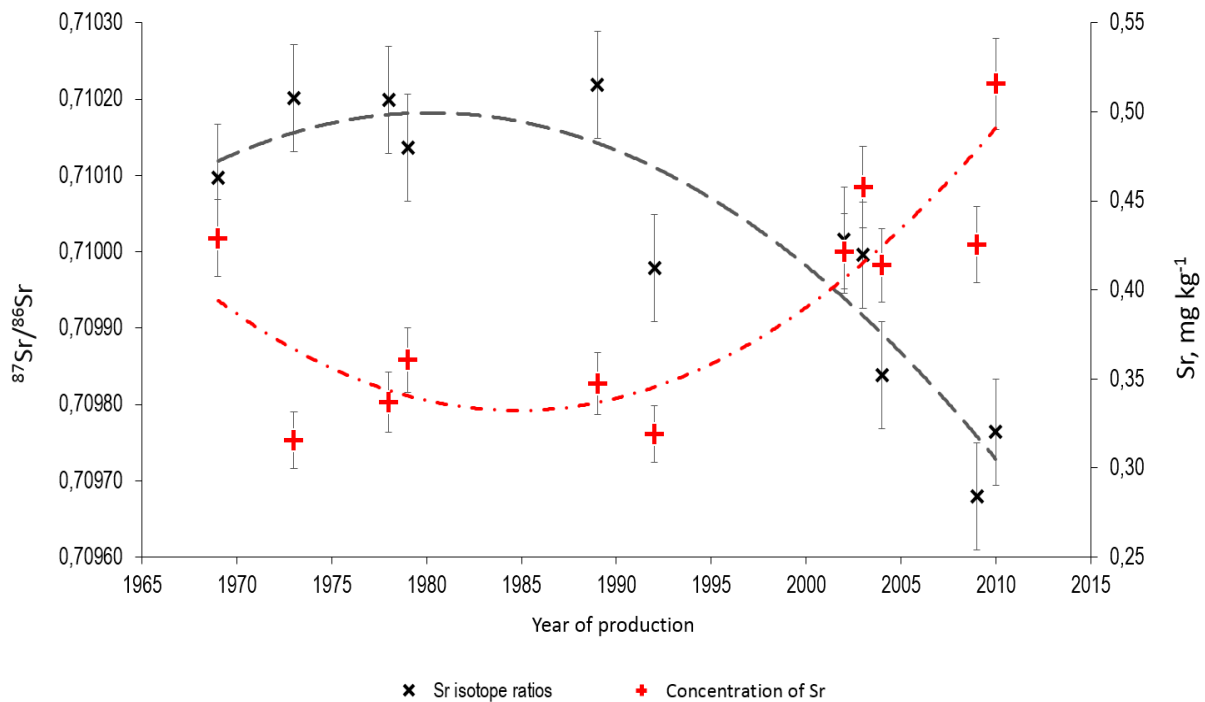


Fig. C.5. Time dependent changes of Sr concentrations and $^{87}\text{Sr}/^{86}\text{Sr}$ ratios in wines from Pomerol.

Such interesting opposite relationship of these two parameters can most likely be explained by changing the source of available Sr either during vine growing or wine making. Indeed, viticulture and winemaking included various activities that can potentially change the Sr elemental content and, therefore, the Sr isotopic composition of wine (Pohl, 2007). In the absence of detailed information of vineyard- and winemaking management due to the commercial confidentiality, only hypothesis of what caused such behavior can be made. Some agricultural practices, such addition of certain substances to regulate the pH of vineyard soil such as calcium carbonate, could have been actively applied in 1990's. If these substances rich in strontium of marine origin with characteristic $^{87}\text{Sr}/^{86}\text{Sr}$ of sea water - 0.70918 (Allègre, et al. 2010), this could explain the simultaneous increase in concentrations with the shift of the $^{87}\text{Sr}/^{86}\text{Sr}$ ratio toward this value. Other substances added during winemaking, such bentonite, can also affected on the Sr isotopic composition of wine. These observations clearly underline that even within a narrow range of the $^{87}\text{Sr}/^{86}\text{Sr}$ ratio variability within a specific set of samples, slight significant differences may help to unravel the viticultural and winemaking features.

C.2.4.2. Variability of Sr isotope and Sr elemental content and its application to discriminate between Bordeaux's wine production sub-regions

With the goal to trace the regional dependence of Sr elemental and isotopic signatures from the studied wines, and examining the possible discrimination on the basis of geochemical settings, we plotted the ratios $^{87}\text{Sr}/^{86}\text{Sr}$ versus inverse Sr concentration (Fig. C.6). Such diagrams are primarily used to trace the geochemical evolution of the soils horizons and can then allow to relate the evolution of the data with processes of evaporation/sedimentation. In the case of wine samples, this allows to assess their potential origin from the same or different geological regions. It can be clearly seen that this graph groups together most of the authentic Bordeaux wine samples with a slight distinction for the Pomerol wines. All the genuine Bordeaux wines form an elongated cloud of points, bounded by limits of anticipated values $^{87}\text{Sr}/^{86}\text{Sr}$ (Voerkelius et al., 2010) with, however, a large span of Sr concentrations. This clearly reflects that all the authentic Bordeaux wine samples could belong to a single overall geochemical and pedological system (Fig. C.6A). On the contrary, the suspicious "Bordeaux" wines are remarkable by the extreme diversity of Sr isotope ratio and Sr concentrations, which is explained by their dubious origin from certainly very distinctive geological background. However, three suspicious samples from this group were located in close proximity to the wine from Pomerol. From their disposition on the scatter plot, the origin of these three wines appears to be from Bordeaux. However, these wines have been identified as not complying with the labeling rules of AOC (grape varieties, production sites).

From the closer examining of the series of Bordeaux wine (Fig. C.6B), it can be observed that the wines from Pomerol, Saint-Émilion, and Pessac-Léognan (white wine) are characterized by a significant variabilities in Sr concentrations as well as in Sr isotopic composition, which exceed by several times the measurement uncertainties of analytical determination. Furthermore, a typical trend applicable to most of the samples and expressed in an inverse relationship between total Sr concentrations and Sr isotopic compositions can be highlighted (Fig. C.6B): a lesser value of the $^{87}\text{Sr}/^{86}\text{Sr}$ ratio corresponds to its higher elemental content without direct correlation with year of wine production. Indeed, wine from Pomerol represent the period of 40 years, samples of white wine from Pessac-Léognan – 4 years, and wine from Saint-Émilion were produced from the same vintage. This trend is most likely due to geochemical processes in soils, the similar behavior has been observed previously on example of solid soils from two vineyards, irrigated and not irrigated (Green et al., 2004). Apart from the reason of the mixing of two soil's horizons with distinct Sr isotope ratios, the difference in mobility of Sr isotopes in soil might take a place, because the radiogenic isotope ^{87}Sr is present in a larger proportion at lower Sr total concentrations in wine.

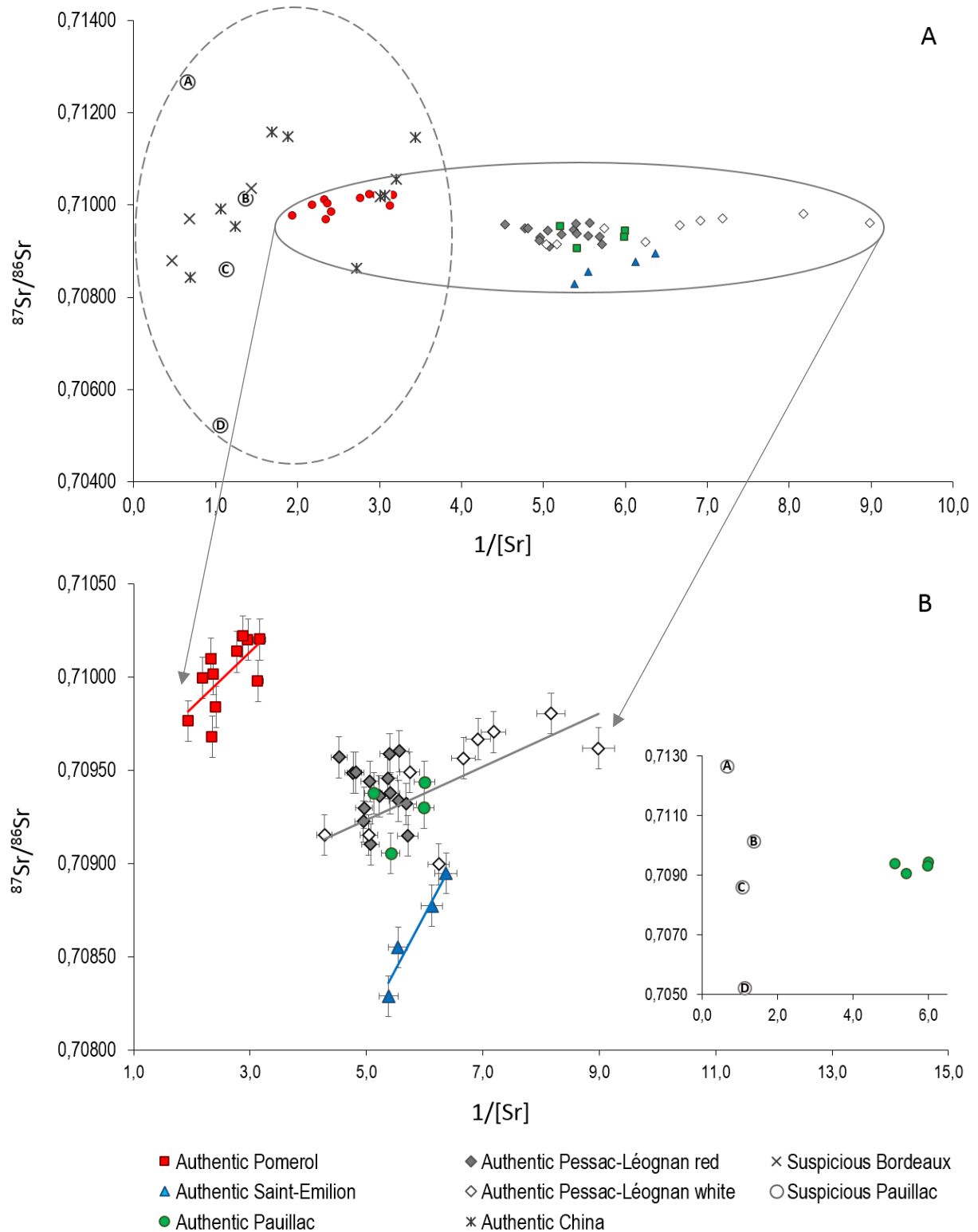


Fig. 6. Ratios of $^{87}\text{Sr}/^{86}\text{Sr}$ as a function of $1/\text{[Sr]}$ concentrations the wines studied: (A) – wines of authentic and suspicious Bordeaux origins; (B) – wines of Bordeaux origin. The error bars are smaller than the marks when are not indicated. Samples of suspicious Pauillac are marked as A, B, C, and D, as described in the text.

This hypothesis gives an additional explanation for the previously discussed case of mirrored variability between $^{87}\text{Sr}/^{86}\text{Sr}$ and Sr concentrations in wine from Pomerol. The interaction of these two parameters gives means to discriminate between Bordeaux's viticultural sub-regions. For the studied set of Bordeaux wines, we can clearly evidence their differences when plotting again specifically the evolution of the Sr isotopic ratio against the $1/[\text{Sr}]$ (Fig. C.6B). We can see at first that the groups of wines originating from Pomerol and Saint-Émilion plotted very differently with respect to other samples. On the contrary, there is a significant overlap for the samples originating from Pessac-Léognan (red wine), Pessac-Léognan (white wine) and Pauillac. Without special consideration of four samples from Saint-Émilion, it can be noted that the complete discrimination of a single winery by means of Sr specifications was achieved for the wine from Pomerol. Such particularity is primarily resulted by vineyard's soils of this Château possesses unique clay-rich soil that differs even from neighboring vineyards of the same appellation where the soil is a mixture of gravel-sand or clay-sand (Wilson, 1999; Bourrouilh, 2006).

C.2.4.3. Testing of wine authenticity by means of $^{87}\text{Sr}/^{86}\text{Sr}$ and Sr concentrations

Most of the studies dedicated to investigation of the Sr isotopic compositions of wines are aimed to authenticity tracing (Durante et al., 2015; Geană et al. 2017). The approach based on authentic specification of Sr elemental and isotopic composition has been applied on suspicious "Bordeaux" wines purchased in China. Four bottles from this series were labeled as a wine of high commercial value from a prestigious château from Pauillac appellation. By a visual examination, these bottles were indistinguishable from the authentic ones. In order to evaluate their authenticity, we have compared their Sr isotopic and elemental signatures with those of authentic samples from the same winery and the same years of production. Regarding Sr concentrations in two comparative groups "suspicious Pauillac" and "authentic Pauillac", a significant discrepancy can be observed immediately (Fig. C.2). The suspicious wines contained 1.52, 0.74, 0.95, and 0.89 mg kg^{-1} , while the concentrations for authentic wines were 0.17, 0.17, 0.19, and 0.18 mg kg^{-1} , respectively for corresponding years of production. Further, the $^{87}\text{Sr}/^{86}\text{Sr}$ ratios in suspicious wines varied largely from 0.70523 to 0.71266 (uncolored circles marked by letters A, B, C and D on the Fig. C.3) and $^{87}\text{Sr}/^{86}\text{Sr}$ for two samples (uncolored circles marked by B and C on the Fig. C.3) are within the range of anticipated values for Bordeaux region, but differ from the values of the corresponding authentic wine (green circles), 0.71031 and 0.70878. The combination of two criterions, $^{87}\text{Sr}/^{86}\text{Sr}$ and Sr concentration immediately clearly indicates that 2 comparing groups do not belong to the same set of samples, and the actual geographical origin of suspicious wines does not correspond

to the declared one (the insertion chart on the Fig. 6B). Therefore, the binary Sr signature, isotopic and elemental, can help to characterize wine for authentic purposes.

C.2.5. Factors of influence on variability of Sr isotope and Sr elemental content

As presented above, the use of the combined information of Sr elemental concentrations and Sr isotopic composition of wine can give an evidence on its geographic origin. In this context it is important to estimate the allowable fluctuation range of both parameters and factors affecting them. Apart the crucial role of soil, there are several important factors that influence on Sr elemental and isotopic variability in wine: climatic conditions, agricultural practices, management of wineries, winemaking techniques may be considered as the most significant.

Climatic conditions. The region of Bordeaux is influenced by atmospheric precipitations forming under the Atlantic Ocean, which can bring significant wet dissolved Sr elemental flux with a strong dependency on seasonal to inter-annual scales (Maneux et al., 1999). In case of high rainfall year, two effects are theoretically possible: 1) the flux of marine Sr with sea water isotopic signature $^{87}\text{Sr}/^{86}\text{Sr} = 0.70918$ (Allègre et al., 2010) can result the slight shift of the ratio $^{87}\text{Sr}/^{86}\text{Sr}$ in wine to the value of sea water; 2) considerable precipitations can change the hydrochemical dynamics in soil horizons resulting in the release of extra-amount of bioavailable Sr sourced from soil or sub-soil substrata (Nakano et al., 1993). The climatic influence on the ratio $^{87}\text{Sr}/^{86}\text{Sr}$ in wine is a global factor and should be traced to a certain extent in all wines produced in the region. The global changing of environmental climatic conditions, such as an increasing of ambient air temperature and variation of humidity can potentially lead to changing of Sr elemental and isotopic composition in labile soil fraction and, consequently, the $^{87}\text{Sr}/^{86}\text{Sr}$ ratio in wine.

Managing of vineyards. The roots system of vines from not irrigated Bordeaux's vineyards develops over the years and can reach 20 meters deep. In search of water, the vine roots intersect the different layers of soil and sub-soil and uptake the bioavailable Sr. Therefore, wine produced from a young vines with still evolving roots system and wine from a mature vineyard can slightly differ in $^{87}\text{Sr}/^{86}\text{Sr}$ due to geological heterogeneity of vineyard's soil profiles. Another factor affected directly on Sr quantitative and qualitative content in wine is the application of fertilizers on vineyard soil. For example, some lime and clay added for pH regulation purposes, have their individual $^{87}\text{Sr}/^{86}\text{Sr}$ ratio. The Bordeaux mixture, commonly used fertilizer on grape vines to control fungal infection, is a chemical containing a substantial amount of Sr at the level about of 100 mg kg^{-1} with the $^{87}\text{Sr}/^{86}\text{Sr}$ ratio 0.708095 (Techer et al., 2017). The dissolution of the Bordeaux mixture

by rainfall can obviously augment the flux of bioavailable Sr, however, can only raise down the $^{87}\text{Sr}/^{86}\text{Sr}$ ratio observed in wine.

Managing of wineries. The increasing/decreasing of vineyards through the purchase/sale of neighboring sites differed by pedological settings, as well as wine-making estate mergers may lead to one-off changes the $^{87}\text{Sr}/^{86}\text{Sr}$ ratio in the period considered. Modification and renovation of winemaking facilities (tanks, reservoirs, etc.), composition of the glass and possible migration of Sr from it should be also taken into account.

Features of production process. The particular features of winemaking within an individual winery, such as the longtime usage of special equipment, adding of special yeasts, bentonite during vinification could cause the specification in both, Sr elemental and isotopic composition of wine, with a certain regularity. Bottling and storage the wine is also an important stage for Sr specification due to possible migration of Sr from the glass (Chesson et al., 2012). It might be the most difficult changes to correct, because of the commercial confidentiality of process. Potentially, this features can be used to specify the Sr elemental and/or isotopic signatures of the final product (Epova et al., 2018).

Analyzing all these factors, a hypothesis can be made: the internal variability of $^{87}\text{Sr}/^{86}\text{Sr}$ within the studied wineries can be caused by different reasons. For the winery from Pomerol there is a visible continuous influence from a new source of Sr starting around the late 1990's, that might be due to application of fertilizers or modification of the winemaking process. For other winemaking estates in Pessac-Léognan and Saint-Émilion it is a difficult to single out a specific idea from the number of those available, thus, further studies are required.

This is the first study concerns the Sr isotopic and Sr elemental compositions of a large selection of authentic Bordeaux wines. Results demonstrate a moderate variability of $^{87}\text{Sr}/^{86}\text{Sr}$ ratio and Sr concentrations with a strong possibility to assigned the Sr specification for individual wineries. The $^{87}\text{Sr}/^{86}\text{Sr}$ ratio found to be relatively stable in varietal blended wine and wine from different vintages. Consequently, both characteristics may be use as distinctive criterions for Bordeaux wine due to direct link to soil's specificity. The combination of both parameters creates the terroir-inherent and winemaking-related tracer for authenticity and geographical origin assessment. The uniqueness of this binary signature may trace even individual wineries and its applicability has been proved on example of four imitated wines.

However, it is important to note the limitation of Sr isotopic approach, which solely cannot be relied upon to definitely identify the geographical origin due to wide world geological and pedological diversity and numerous factors masking the geological signature of wine. Nevertheless, the suspicious wines of declared Bordeaux origin presented radically different values from those of the authentic Sr isotopic and elemental characteristics. They may be considered most likely as an imitation or mislabeling.

C.3. Lead elemental and isotopic compositions of Bordeaux wines

C.3.1. Introduction

Natural variation of lead isotopic ratios in food and beverage is a relatively new approach for addressing the geographical origin of wines (Médina et al., 2013; Resano & Vanhaecke, 2012). Pb isotopic fingerprinting is an individual characteristic which is based on the Pb isotopic specification, and can be used to identify the origins of this element in a sample, and to trace the sample's geographical provenance under certain circumstances (Chapter A, section A.2.3). The particular principle of traceability of food origin using Pb isotopic fingerprinting consists in the determination of Pb isotope ratios in a sample followed by their identification and referencing to those in Pb sources available in the region considered.

One of the first applications of Pb isotope ratios for the source identification purposes in food products was performed on milk powder and wine and have shown the possibility to distinguish the geographical origin of samples due to specificity of Australian regional Pb isotopic composition (Crews et al., 1988). Indeed, the $^{207}\text{Pb}/^{206}\text{Pb}$ ratio recorded in Australian samples was similar to those of lead mined from the local ore deposit named Broken Hill. Soon after, the analysis of Pb isotope ratios revealed the occurrence of significant differences between Australian and European wines, confirming the specific isotopic composition of Pb found in Australian product (Dean et al., 1990). Examination of an exceptional series of Bordeaux wine produced in 1895-1995 made it possible to reconstruct the atmospheric lead fallout over the last century and reveal that chronological Pb signatures of wine reflected a specific regional western European imprint (Medina et al., 2000). Since then, several studies on tracing wine's geographical origin using Pb isotopic specification were conducted (Larcher et al., 2003; Mihaljevič et al., 2006; Ndung'u et al., 2011). Lead isotopic compositions were determined in wines originated from European countries (France, Germany, Italy, Spain, Portugal, Czech Republic, Romania, Moldova, America (USA, Canada, Brazil, Uruguay, Chili), from Asia (China, Japan), from South Africa and Australia, and the results obtained were used for assessing the origin and classification purposes as well as for identifying of Pb emission sources (all references can be seen from Chapter A, Table A.5).

The main goal of this experiment is addressed to the application of Pb isotopes for geographic provenance assignment of wines. To achieve this objective, the Pb isotope ratios of authentic and that of suspicious Bordeaux wines were determined according to the analytical procedure described in Chapter B, and then, together with Pb concentrations, were investigated with a specific attention to the regional environmental lead composition. With these results, it is expected to clarify the question if these suspicious wines originated from the region of Bordeaux.

C.3.2. Results

The mean values (\pm standard deviation, SD) and ranges of variability of obtained of Pb concentrations and Pb isotope ratios in authentic and suspicious Bordeaux wines and wines originated from China, are summarized in Table C.2. All results of individual samples can be seen in Table C.3 placed at the end of the chapter.

C.3.2.1 Lead concentrations

Box plots on Fig. C.7 displays the variability of Pb elemental concentrations in the studied wine samples. In authentic Bordeaux wines, lead content is ranging from $4.4 \mu\text{g kg}^{-1}$ to $161 \mu\text{g kg}^{-1}$ (Table C.2). The lowest Pb concentrations were observed in the wine produced in a winery that belongs to Saint-Émilion AOC, vintage 2011 (mean is $4.9 \pm 0.4 \mu\text{g kg}^{-1}$), the highest values are referred to the wine from a winery associated to Pomerol AOC, vintage of 1969 ($163.1 \pm 0.8 \mu\text{g kg}^{-1}$) and 1973 ($161.2 \pm 0.9 \mu\text{g kg}^{-1}$). Such elevated Pb content in wines of old vintages was observed previously by Medina et al. (2000) and Rosman et al. (1998). Regardless these relatively high Pb concentrations, all the wines analyzed are within the health safety standards: the permissible limit of Pb in food and beverage is $200 \mu\text{g L}^{-1}$ (European Commission Regulation Ce 466/2001). This limit was recently updated and decreased with now a maximum content of only $150 \mu\text{g L}^{-1}$ in wines produced after 2007 (International Organization of Vine and Wine, OIV code). The Pb concentrations in suspicious Bordeaux are generally within the range observed for authentic Bordeaux, however, with a higher dispersion. The lead in wines of Chinese origin are generally slightly higher and ranged in the span of 28.2 - $54.6 \mu\text{g kg}^{-1}$. No statistically significant difference was observed between authentic and imitated Bordeaux wine (Table C.4) based on the Pb concentration alone.

Table C.4. *P*- values and significance of the differences between the Pb concentrations and Pb isotope ratios for authentic and imitated Bordeaux wines.

Parameter	Pb ($\mu\text{g/L}$)	$^{208}\text{Pb}/^{204}\text{Pb}$	$^{207}\text{Pb}/^{204}\text{Pb}$	$^{206}\text{Pb}/^{204}\text{Pb}$	$^{208}\text{Pb}/^{206}\text{Pb}$	$^{206}\text{Pb}/^{207}\text{Pb}$
<i>p-values</i>	0,801	0,023	0,00001	0,003	0,0008	0,011
<i>Level of significance</i>	*	*	***	**	**	**

* - not statistically significant

** - statistically significant

*** - highly statistically significant

Table C.2. Interval and means of Pb isotopic ratios and Pb concentrations determined in wines.

Origin	Appellation / type of wine, number of samples	Vintage	Criterion	Pb, $\mu\text{g kg}^{-1}$ *	$^{208}\text{Pb}/^{204}\text{Pb}$ **	$^{207}\text{Pb}/^{204}\text{Pb}$ **	$^{206}\text{Pb}/^{204}\text{Pb}$ **	$^{208}\text{Pb}/^{206}\text{Pb}$ **	$^{206}\text{Pb}/^{207}\text{Pb}$ **
All authentic Bordeaux	red, white, n=43	1969-2012	<i>interval</i>	4,39—163,1	37,938—38,672	15,594—15,659	17,964—18,657	2,0726—2,1120	1,1516—1,1914
			<i>mean</i>	24,1 \pm 33,1	38,207 \pm 0,156	15,621 \pm 0,014	18,191\pm0,146	2,1003 \pm 0,0086	1,1644 \pm 0,0084
France, Bordeaux	Pomerol, Ch. #1* / red, n=11	1969 - 2010	<i>interval</i>	16,7—163,1	37,938—38,201	15,594—15,619	17,964—18,194	2,0997—2,1120	1,1518—0,1648
			<i>mean</i>	57,2 \pm 55,0	38,073 \pm 0,091	15,609 \pm 0,008	18,088 \pm 0,067	2,1048 \pm 0,0035	1,1589 \pm 0,0038
France, Bordeaux	Saint Emilion / red, n=4	2011	<i>interval</i>	4,39—5,30	38,297—38,368	15,629—15,644	18,234—18,358	2,0883—2,1003	1,1654—1,1746
			<i>mean</i>	4,94 \pm 0,40	38,326 \pm 0,033	15,636 \pm 0,006	18,304 \pm 0,053	2,0939 \pm 0,0049	1,1704 \pm 0,0038
France, Bordeaux	Pessac-Léognan / red, n=15	2009 - 2011	<i>interval</i>	10,1—17,7	38,047—38,267	15,614—15,626	18,024—18,227	2,0980—2,1108	1,1544—1,1667
			<i>mean</i>	12,7 \pm 2,2	38,200 \pm 0,058	15,620 \pm 0,004	18,169 \pm 0,052	2,1025 \pm 0,0030	1,1631 \pm 0,0031
France, Bordeaux	Pessac-Léognan / blanc , n=9	2010 - 2012	<i>interval</i>	9,4—16,2	38,160—38,672	15,616—15,659	18,138—18,657	2,0726—2,1039	1,1614—1,1914
			<i>mean</i>	12,8 \pm 2,5	38,354 \pm 0,231	15,633 \pm 0,019	18,335 \pm 0,235	2,0920 \pm 0,0143	1,1728 \pm 0,0136
France, Bordeaux	Pauillac authentic / red, n=4	2004 - 2007	<i>interval</i>	16,8—27,8	38,091—38,281	15,609—15,624	18,104—18,175	2,1003—2,1117	1,1577—1,1632
			<i>mean</i>	21,6 \pm 4,3	38,160 \pm 0,074	15,617 \pm 0,007	18,137 \pm 0,026	2,1040 \pm 0,0045	1,1608 \pm 0,0021
Unknown	Suspicious "Bordeaux" / red, n=14	1998-2009	<i>interval</i>	8,60—44,5	37,723—38,310	15,519—15,636	17,724—18,336	2,0894—2,1366	1,1404—1,1726
			<i>mean</i>	18,5 \pm 8,9	38,071 \pm 0,172	15,587 \pm 0,035	18,033 \pm 0,206	2,1113 \pm 0,0155	1,1569 \pm 0,0109
China	Authentic China origin / red, n=3	1998 - 2009	<i>interval</i>	28,2—54,6	38,156—38,307	15,598—15,621	18,089—18,187	2,1029—2,1138	1,1597—1,1653
			<i>mean</i>	38,9 \pm 13,9	38,236 \pm 0,076	15,609 \pm 0,012	18,133 \pm 0,050	2,1087 \pm 0,0055	1,1617 \pm 0,031

*- In this table the concentrations corresponding to a mass fraction in weighted unit is used. Indeed, the wine has a slightly lower density 0.99 kg L^{-1} (Somers & Evans, 1974), this fact makes it possible to compare the concentrations expressed in mass and volume equivalent with an insignificant approximation lesser than the analytical uncertainties of the ICP-MS determination. The concentrations are accurate to 3%.

** - Presented uncertainties related to complete process of sample preparation including digestion and column separation were estimated on independently prepared triplicates of samples RSD): 503 ppm ($^{208}\text{Pb}/^{204}\text{Pb}$), 246 ppm ($^{207}\text{Pb}/^{204}\text{Pb}$), 556 ppm ($^{206}\text{Pb}/^{204}\text{Pb}$), 560 ppm ($^{208}\text{Pb}/^{206}\text{Pb}$), 450 ppm ($^{207}\text{Pb}/^{206}\text{Pb}$).

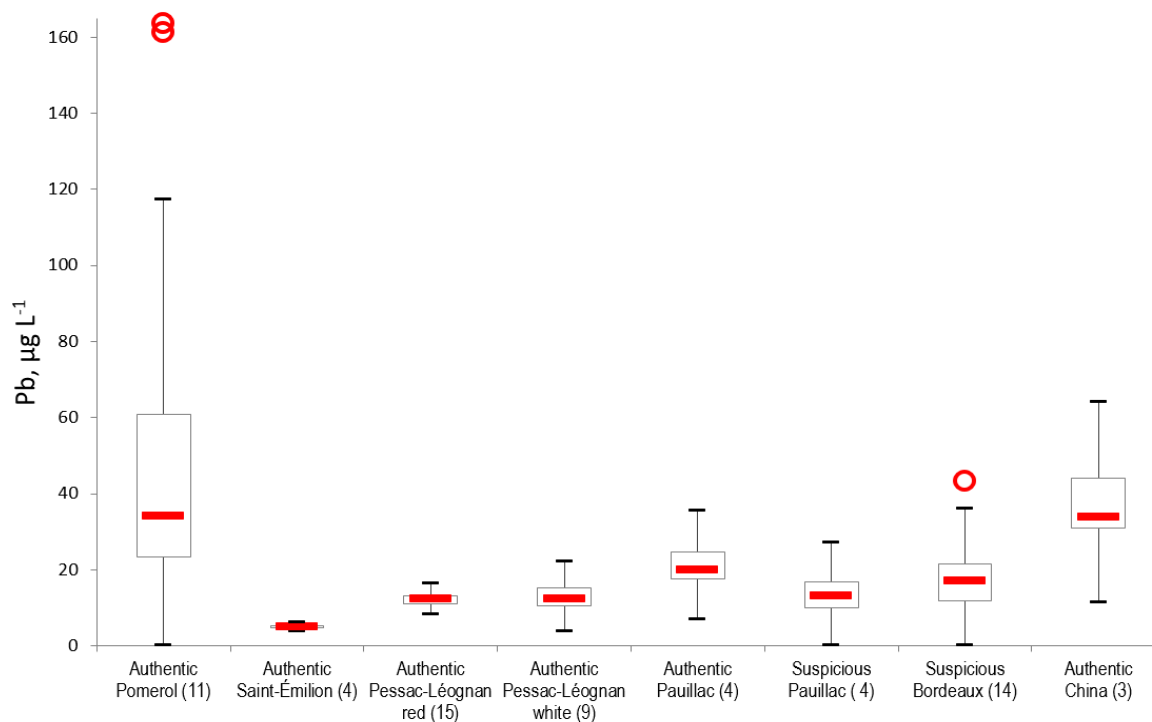


Fig. C.7. Box plots of the Pb concentrations determined in studied wine samples. Legend: number of samples between brackets. Outliers are higher than the 75th percentile of 1.5 times the interval between the 25th and 75th percentile.

C.3.2.2. Lead isotope ratios

The mean values of lead isotope ratios in authentic wines are as follows: $^{208}\text{Pb}/^{204}\text{Pb}$ - 38.207 ± 0.156 ; $^{207}\text{Pb}/^{204}\text{Pb}$ - 15.621 ± 0.014 ; $^{206}\text{Pb}/^{204}\text{Pb}$ - 18.191 ± 0.146 ; $^{208}\text{Pb}/^{206}\text{Pb}$ - 2.1003 ± 0.0086 ; $^{206}\text{Pb}/^{207}\text{Pb}$ - 1.1644 ± 0.0084 ; whereas such values for suspicious Bordeaux wines were 38.271 ± 0.172 , 15.587 ± 0.035 , 18.033 ± 0.206 , 2.1113 ± 0.0155 , and 1.1569 ± 0.0109 , respectively. When examining these results using the t-test (Table C.4), for the $^{207}\text{Pb}/^{204}\text{Pb}$ ratio, a high level of significance of difference could be estimated (p -value = 0.00001), also, some other significant differences were found for ratios $^{208}\text{Pb}/^{206}\text{Pb}$ and $^{206}\text{Pb}/^{204}\text{Pb}$, (p -values are 0.0008 and 0.003, respectively).

Comparing Pb isotope ratios obtained in the present study to the bibliographic data (Fig. C.8), the authentic French Bordeaux wines cover the central part of the range of the $^{206}\text{Pb}/^{207}\text{Pb}$, $^{208}\text{Pb}/^{206}\text{Pb}$, ratios and are consistent with the values of other European wines, including wines from Bordeaux (Médina et al., 2000) and south-east of France (Rosman et al., 1998). A few bibliographic references reported the $^{208}\text{Pb}/^{204}\text{Pb}$, $^{207}\text{Pb}/^{204}\text{Pb}$, and $^{206}\text{Pb}/^{204}\text{Pb}$ ratios in wine from over the world. However, the intervals of variability are definitely larger due to some analytical complexity of the

determination of the low-abundance isotope ^{204}Pb . The Pb isotope ratios observed for wines of suspicious Bordeaux origin and wines from China generally present the same span of values as that have been registered for authentic Bordeaux wines. However, on a closer look, it can be seen that their compositions are slightly depleted on radiogenic isotopes ^{206}Pb , ^{207}Pb , and ^{208}Pb , which is certainly related to the different vine growing environment.

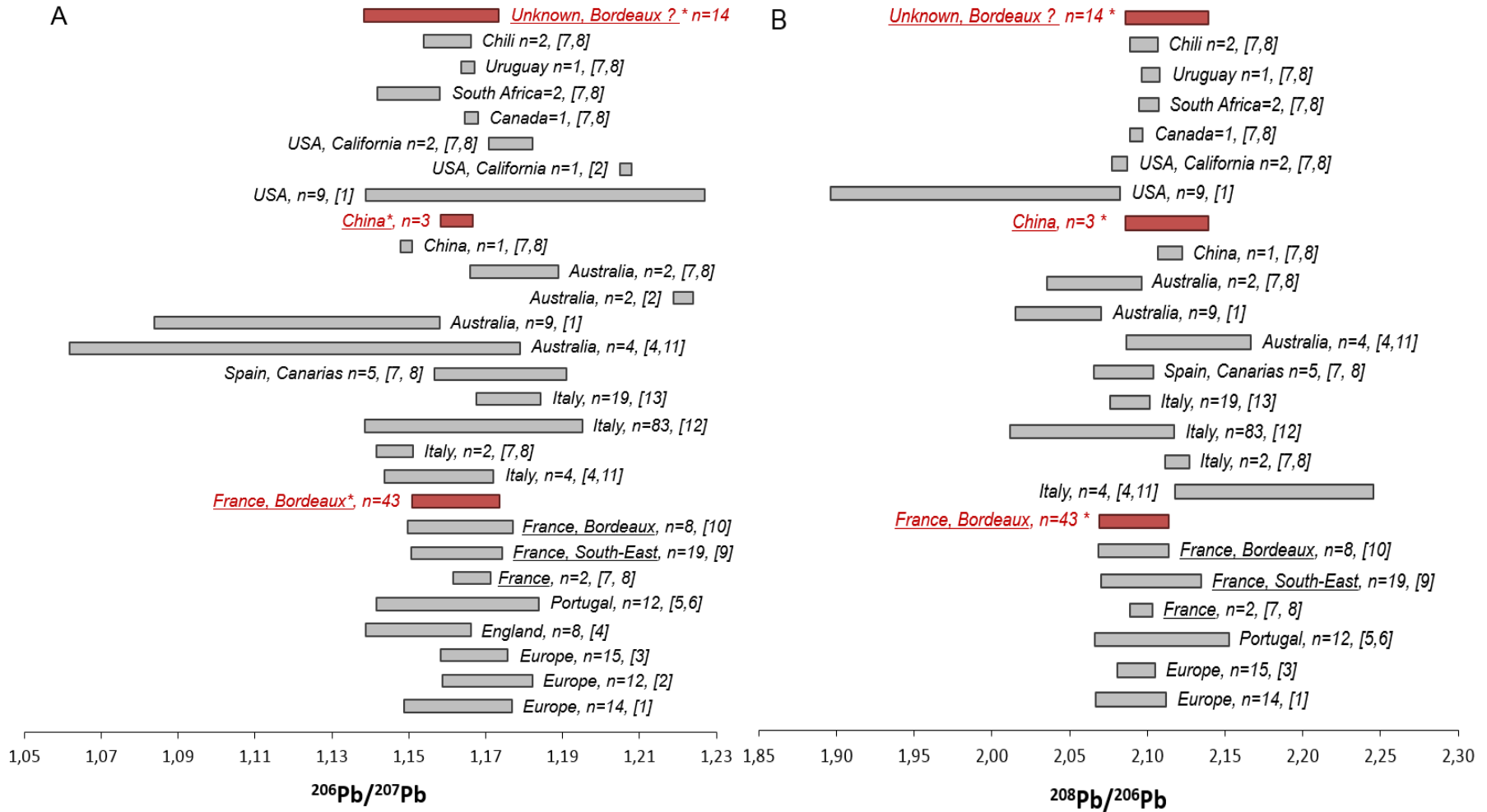
When examining individually the $^{208}\text{Pb}/^{204}\text{Pb}$, $^{207}\text{Pb}/^{204}\text{Pb}$, $^{206}\text{Pb}/^{204}\text{Pb}$, $^{208}\text{Pb}/^{206}\text{Pb}$, $^{206}\text{Pb}/^{207}\text{Pb}$ ratios, and the Pb elemental concentrations, none of these parameters individually allow to emphasize a confidence in the declaration of origin of suspicious wines in comparison to authentic ones. This is primarily due to the fact that the averaged values and ranges of variability used for such comparison do not consider the likely changing of Pb concentration in the sources of constituent.

C.3.3. Temporal evolution of lead content in wines during the period of 1962-2012

Gradual significant changes in Pb elemental content and Pb isotopic composition in wines over the past decades are of considerable research interest and reflect to a greater extent the global changes in European atmosphere (Rosman et al., 1998; Médina et al. 2000; Larcher et al., 2003; Mihaljevič et al., 2006). In order to better assess to temporal variability of the Pb elemental and isotopic composition in the studied wines, the data from the Bordeaux wines were combined with the results previously obtained for 18 red wines produced by a winery in the south-east of France in the period of 1962 – 1991 (Rosman, et al., 1998).

C.3.3.1. Changes of Pb concentrations

The results of the Pb concentrations in Bordeaux wines are consistent with the previous study of wines from the south-east of France, where a noticeable decrease of Pb concentrations was observed during 1950 – 1991 (Rosman et al., 1998): the total Pb concentrations detected in wines produces before 1980 fluctuate widely from 78 to 227 $\mu\text{g kg}^{-1}$, with most of the values were higher than 110 $\mu\text{g kg}^{-1}$. Similarly, the Pb concentrations of the Bordeaux wines produced in 1969 were 163 and 161 $\mu\text{g kg}^{-1}$, respectively (Table C.3). However, in years 1978-1979, the Pb content dropped from 85 $\mu\text{g kg}^{-1}$ down to 37 $\mu\text{g kg}^{-1}$. When taking into account the data of Rosman et al. (1998), the resulting downward trend began around 1980s and since then, a gradual and consistent decrease in Pb concentrations in French wines can be observed (Fig. C.9A). Since 2009, all measured overall concentrations Pb concentrations within this period of 50 years, decreased of about 15 fold, and been depleted from 163 $\mu\text{g kg}^{-1}$ down about 10 $\mu\text{g kg}^{-1}$ now. This decline can be unambiguously attributed to the phasing out of leaded gasoline.



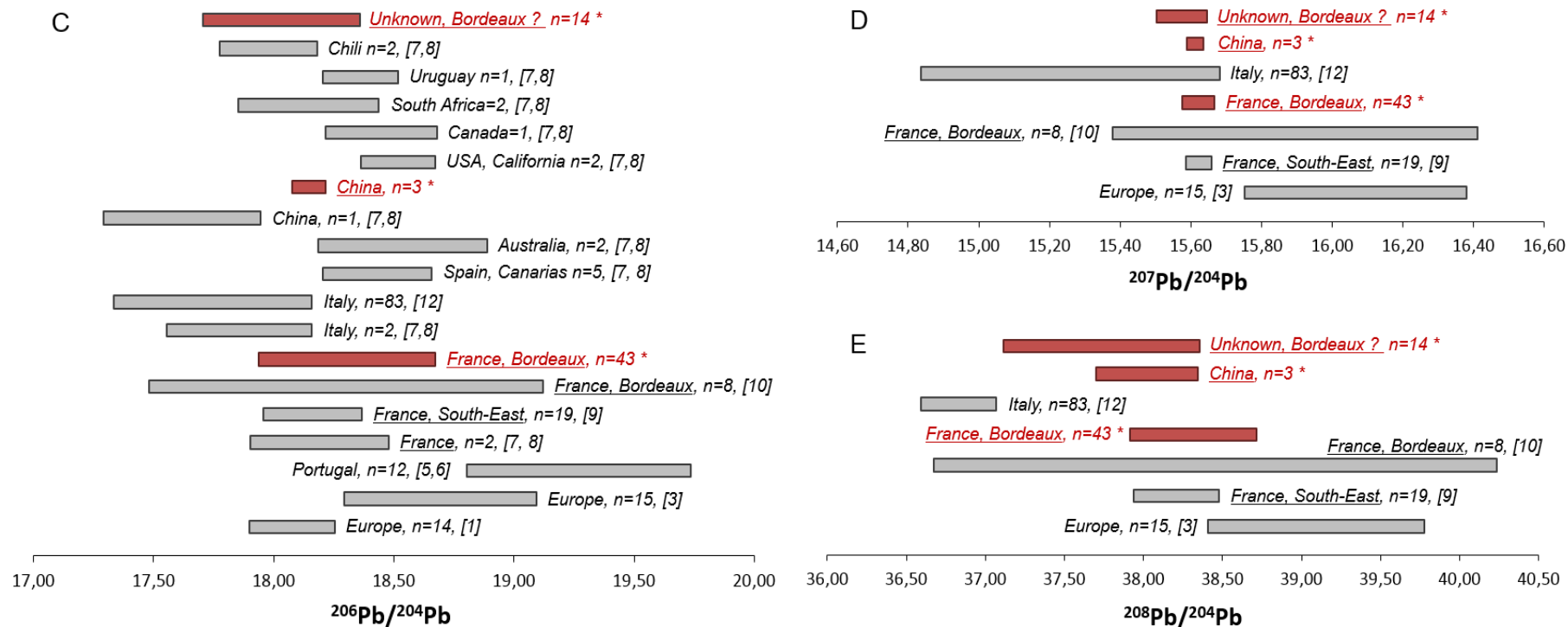


Fig. C.8. Ranges of values of lead isotope ratios: (A) – $^{206}\text{Pb}/^{207}\text{Pb}$, (B) – $^{208}\text{Pb}/^{206}\text{Pb}$, (C) – $^{206}\text{Pb}/^{204}\text{Pb}$, (D) – $^{208}\text{Pb}/^{204}\text{Pb}$, and (E) – $^{206}\text{Pb}/^{204}\text{Pb}$ for wines from different geographical origin world over, as reported in literature. Legend: *n*, number of samples; * - wines from this study. References: [1] – Augagneur et al., 1997; [2] – Rodushkin et al., 1999; [3] – Goossens et al., 1994; [4] – Dean et al., 1990; [5] – Almeida et al., 1999; [6] – Almeida et al., 2003; [7] – Tian et al., 2000; [8] – Barbaste et al., 2001; [9] Rosman et al., 1998; [10] – Médina et al., 2000; [11] – Crews et al., 1988; [12] – Larcher et al., 2003; [13] – Mihaljevič et al., 2006. Figure modified after Larcher et al., 2003.

C.3.3.2. Changes of the $^{208}\text{Pb}/^{204}\text{Pb}$ ratio

Despite of the fact that the concentrations give a direct first quantitative information about Pb content in wines, introducing the Pb isotopic signatures allows to reveal its qualitative characteristics and inform us on the nature and origin of the lead taken up by vines. Rosman et al. (1998) could not identify clearly the dominant Pb source in examined wines, apparently, because at that time, the complete elimination of lead from fuels in France was not achieved. With the consideration of the Bordeaux wine series, the evolution of the Pb isotopic composition can be further clarified, because the temporal span is extended over more than two decades and covered 12 years of lead-free gasoline usage up to 2012. The temporal changes in the $^{208}\text{Pb}/^{204}\text{Pb}$ ratio reproduces an obvious V-shaped trend (Fig. C.9B). This curve decreased continuously from 1960 to sometime in the mid 1980's and has been increasing steadily ever since. Such trend indicates the binary mixing of two major lead sources with changing proportions. The increase of the $^{208}\text{Pb}/^{204}\text{Pb}$ ratio with the simultaneous decline of Pb concentration observed around 1985 for Bordeaux wines, is similar to those reported in European aerosols (Grousset et al., 1994) and is associated with beginning of the phasing out of leaded gasoline in the early 1980's. The aerosol lead signatures recorded in the European atmosphere in 1960's and 1970's, were mainly originated from alkyl-lead compounds added to petrol for their antiknock properties (Elbaz-Poulichet et al., 1984; Monna et al., 1997).

When examining the trend on Fig. C.9B, we can clearly identify two main Pb sources in wine. One end member is the natural (or geogenic) lead contained in crust-derived dust particles or in soil whose geogenic $^{208}\text{Pb}/^{204}\text{Pb}$ ratio was reported for the region of Bordeaux as 38.721 ± 0.006 (Elbaz-Poulichet et al. 1984). The other end member represents the global anthropogenic overall industrial European lead formed by mixing of multiplicity of existing emissions, predominantly from leaded gasoline consumption (Grousset et al., 1994). The average value of the $^{208}\text{Pb}/^{204}\text{Pb}$ ratio in leaded gasoline in France was reported to be 36.71 ± 0.21 (Monna et al., 1997). These two end members form a mixing line on which spread the variability of $^{208}\text{Pb}/^{204}\text{Pb}$ ratio in wines. The downward trend of the ratio $^{208}\text{Pb}/^{204}\text{Pb}$ in 1960's-1970's was caused by steadily increasing fraction of anthropogenic lead (Fig. C.9A). Since the early 1980's, the fraction of natural lead becomes equivalent and begins to gradually prevail over the anthropogenic fraction due to phasing out of leaded gasoline. This fact is reflected in the upward trend of the ratio $^{208}\text{Pb}/^{204}\text{Pb}$.

When comparing the $^{208}\text{Pb}/^{204}\text{Pb}$ ratio in two wine series in 1960-1990: from southwestern France (Bordeaux, this study) and from southeastern France (Rosman et al., 1998), the greater impact of natural lead on wines from southeastern more than for wines from southwestern can be suggested according to their more geogenic values of the $^{208}\text{Pb}/^{204}\text{Pb}$ ratios. (Fig. C.9B).

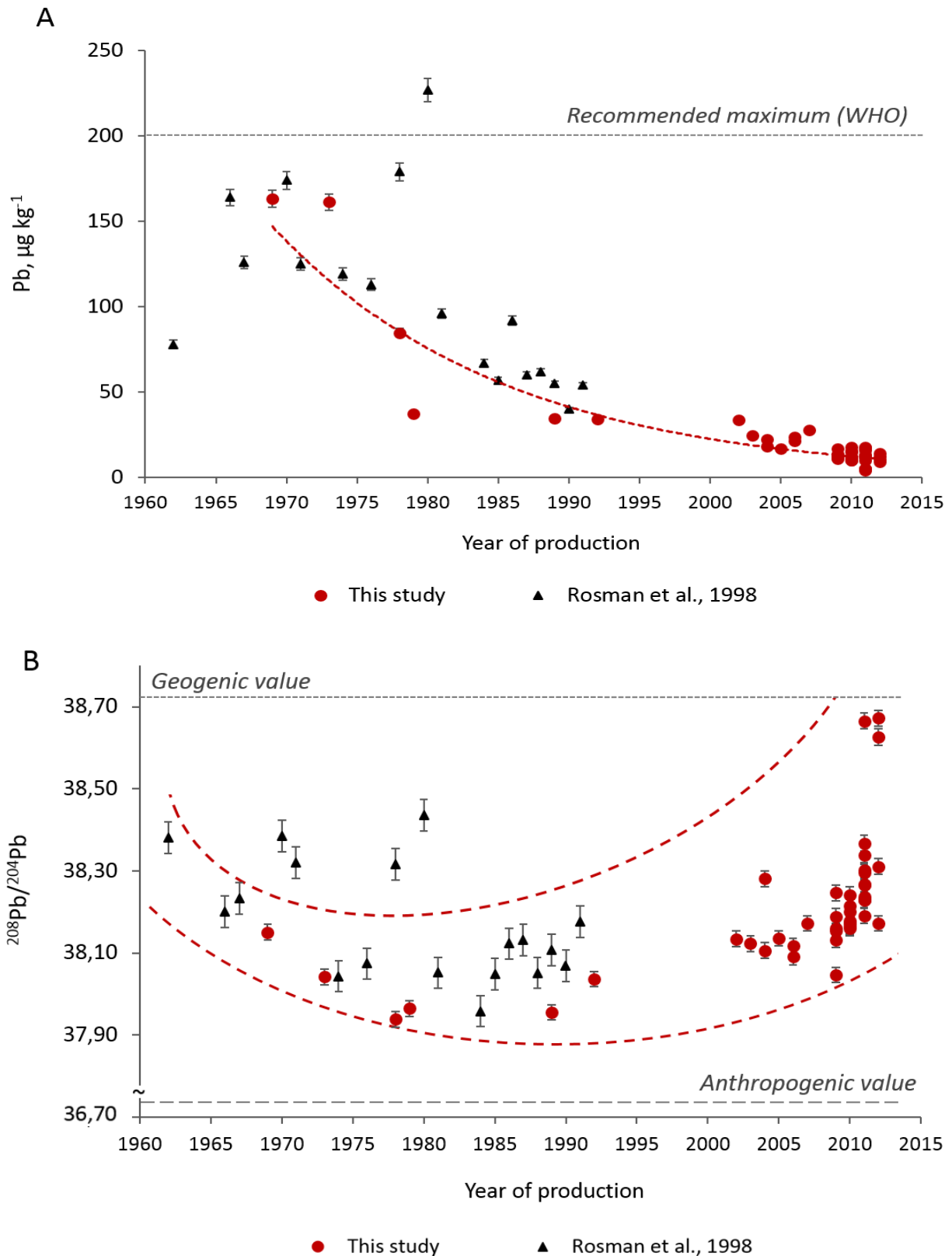


Fig. C.9. Evolution of Pb concentration (A) and $^{208}\text{Pb}/^{204}\text{Pb}$ ratio in French wines during period of 1965-2012, observed in the wine from south-east (Rosman et al., 1998) and wine from Bordeaux (this study). The error bars are smaller than the marks when are not indicated.

A fraction of natural lead contained in dust particles originated mostly from the Sahara Desert was found in aerosols over southern Europe (Grousset et al., 1994). This fact explains the larger variability in Pb isotopic composition of wines from one year to another observed for the series of wine from southeastern France (Rosman et al., 1998). Four wine samples from this series of vintages 1970, 1971, 1978, 1981 have the more “geogenic” values of $^{208}\text{Pb}/^{204}\text{Pb}$ ratio comparing to others. Furthermore, these wines are characterized by a relatively high total Pb content as well (Fig. C.9A). Such Pb specification may be the result of the influence of Sahara dust. The intensity of such periodic meteorological event differs from one year to another. Hence, changing of proportions of transported minerogenic dust in the atmosphere can explain the observed variability in the Pb isotopic composition of wines. In opposite, the French south-west (Bordeaux) is influenced predominantly by atmospheric precipitations formed under the Atlantic Ocean, which can bring significant wet dissolved Pb elemental flux with a strong dependency on seasonal to inter-annual scales (Maneux et al., 1999). This fact explains a smooth changes without extremes nor in the concentrations, neither in the $^{208}\text{Pb}/^{204}\text{Pb}$ ratio, observed in Bordeaux wine.

C.3.4. Geographic provenance of wines by means of $^{208}\text{Pb}/^{206}\text{Pb}$ and $^{206}\text{Pb}/^{207}\text{Pb}$

The differentiation of authentic Bordeaux wines and wines of suspicious Bordeaux origin purchased in China can be illustrated by Fig. C.10, where these two groups are plotted on the three-isotope diagram $^{208}\text{Pb}/^{206}\text{Pb}$ versus $^{206}\text{Pb}/^{207}\text{Pb}$. This is the most used diagram in environmental studies for the assessment of the contribution from major Pb emission sources, such natural processes of rock weathering and vehicular / industrial emissions (Ellam, 2010).

C.3.4.1. Bordeaux wines of vintages of 1969-2012

In the region of Bordeaux, the historical record of Pb signatures have been extensively studied and described (Elbaz-Poulichet et al., 1984; Grousset et al., 1994; Monna et al., 1995; Monna et al., 1997). According to Monna et al. (1997), Pb derived from leaded gasoline contributed between 40% and 80% to total airborne load of particulate lead in France during the years of its implementation. The total contribution from vehicle exhaust to the atmosphere significantly declined after 1980 due to phasing out of leaded gasoline (Grousset et al., 1994). In order to compare the Pb isotope ratios in Bordeaux wines with those in the environment of vine’s growth, the references of two main end-members in the binary mixing system were plotted on Fig. C.10: pre-industrial sediments from Gironde River in the region of Bordeaux (Grousset et al., 1994; Elbaz-Poulichet et al., 1984) and French leaded gasoline as the predominant anthropogenic Pb source

(Monna et al., 1995; Monna et al., 1997). To better illustrate the temporal changes in the $^{208}\text{Pb}/^{206}\text{Pb}$ and $^{206}\text{Pb}/^{207}\text{Pb}$ ratios, the samples of Bordeaux wines were divided into two groups according to the year of production: one group is represented by wines produced in 1969-2005 (uncolored circles with red border) and the another group integrates the wines produced in 2006-2012 (red circles).

The Pb isotopic composition of Bordeaux wines reveals that observed ratios do match perfectly the line of the binary mixing, confirming by the closeness of two linear regressions. The Pb signatures of Bordeaux wines fell into the respective range of aerosols registered in Europe in the period of 1987-1992. Generally, the Bordeaux wines produced in 1969-2005 (uncolored circles), display lead signatures that are more anthropogenic than the wines produced in the later period of 2006-2012 (red colored circles).

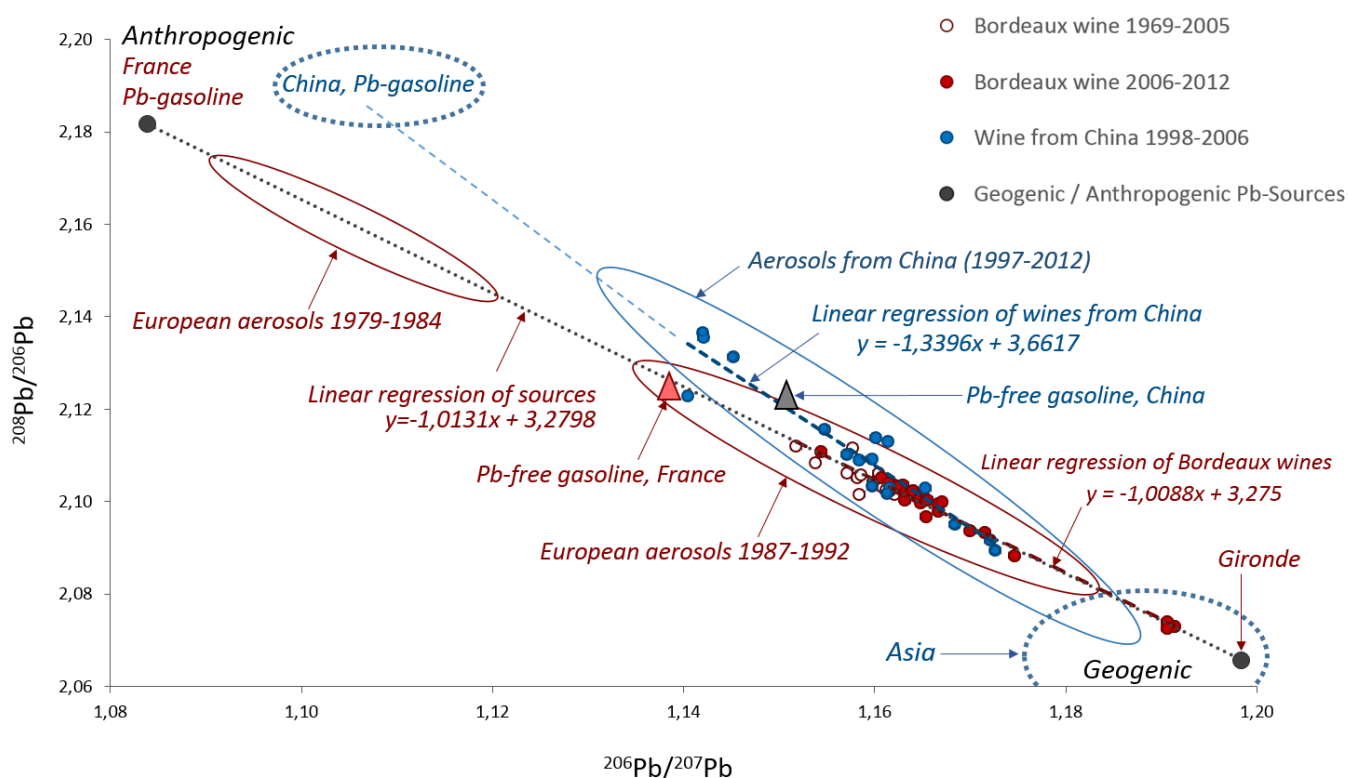


Fig. C.10. Ratios $^{208}\text{Pb}/^{204}\text{Pb}$ and $^{207}\text{Pb}/^{204}\text{Pb}$ in authentic Bordeaux wines and wines with suspicious Bordeaux origin (purchased in China) in comparison with the predominant anthropogenic lead sources: Pb-containing gasoline from France (Monna et al., 1997) and Asia (Chen et al., 2005), Pb free gasoline from Asia (Chen et al., 2005) and France (Veyseyre A. et al., 2001), unpolluted sediments from Gironde, France (Grousset et al., 1994; Elbaz-Poulichet et al., 1984), unpolluted subsoil from China (Li et al., 2012; Bi et al., 2017), the record of European aerosols (Grousset et al., 1994), and Chinese aerosols (Mukai et al., 1993; Bi et al., 2017). Error bars are smaller than the marks.

The points corresponding to the wines produced earlier are scattered widely around the line connecting two end-members, indicating a direct impact from other anthropogenic sources, such as industrial and urbanistic exhaust, coal burning, etc. For the first years following the removal of leaded gasoline, a secondary contamination from the resuspension of road surface dust could maintain signatures of leaded gasoline in the atmosphere. However, the general shift of Bordeaux wines produced in 2006-2012 towards the natural geogenic signature evidences that in the last decade, the relative contribution of natural Pb into the atmosphere has increased.

C.3.4.2. Wines with the suspicious Bordeaux provenance, vintages 1998-2009

The wines from the group of suspicious Bordeaux origin overlap somewhat with authentic Bordeaux samples with a tendency to be shifted upwards and towards anthropogenic references (Fig. C.10). Such a trend indicates that Pb preserved in these wines was derived from sources substantially different from those available in the region of Bordeaux.

Objective evidence and experimental observations concerning this group of wines:

- the veritable origins of wines labeled “Bordeaux” and purchased in China from were unknown;
- some bottles caused mistrust due to incorrect labels;
- the provenance other than from Bordeaux for certain wines was confirmed by Sr isotopic compositions of wine.

Based on these facts, a hypothesis on their presumable Asiatic provenance was made. According to the results of Sr isotopic analysis (Chapter C, section C.2), some wines from this series presented some Sr isotopic signatures that could refer to these of the Bordeaux region, and could be mislabeled Bordeaux wines. Such a hypothesis does not completely reflect the real origins of these wines, but this approximation is necessary to compare the Pb signatures of wines with those of originating from the environment of vine growth. Based on these observations, the signatures of Pb isotopes ratios of leaded gasoline and unpolluted sediments from Asia were therefore used as references for dominant end-members in the plot of $^{208}\text{Pb}/^{206}\text{Pb}$ versus $^{206}\text{Pb}/^{207}\text{Pb}$.

Most of Asian countries have regulated leaded gasoline since 2000. However, some of the wine that were produced before this event, could thus be influenced from the signature of the leaded gasoline. Apart from this fact, unleaded gasoline, despite its name, contains lead in the proportions ranging from tens to hundreds of parts per billion and displayed a relatively consistent isotopic composition (Chen et al., 2005). As mentioned before road dust resuspension is also possible (Sun et al., 2006).

Wines of this series were not divided into different temporal groups because of a relatively small number of samples covered only 10 year's period of wine production, from 1998 to 2009. As it can be seen in Fig. C.10, these points (blue circles) form a cloud with the resulted line slightly shifted upward from the Bordeaux wines, and this disposition is consistent with Chinese aerosols 2.07 – 2.15 for $^{208}\text{Pb}/^{206}\text{Pb}$, and 1.13 – 1.19 for $^{206}\text{Pb}/^{207}\text{Pb}$ (Bi et al., 2017). Mukai et al. (2001) noted this trend as common for Chinese lead which were influenced by continental thorium-rich crust. A few samples are located closely to signatures of Chinese unleaded gasoline $^{208}\text{Pb}/^{206}\text{Pb} = 2.125$ and $^{206}\text{Pb}/^{207}\text{Pb} = 1.145$, respectively (Chen et al., 2005; Cheng & Hu, 2010). The linear regression of the suspicious wine series is different from this of authentic Bordeaux, and seems to be more oriented towards the signatures of Chinese leaded gasoline, $^{208}\text{Pb}/^{206}\text{Pb} = 2.18 - 2.204$ and $^{206}\text{Pb}/^{207}\text{Pb} = 1.098 - 1.117$ (Chen et al., 2005; Li et al., 2012). These observations can be served as an indirect evidence that some these wines could have been produced in Asia. Further, Pb isotope compositions of suspicious wines are extensively scattered around the resulting line indicating the presence of others important end-members mixed with the natural lead and lead derived from gasoline, such combustion of local coils which contributes up to 70% in total airborne particulate Pb in certain Chinese provinces (Li et al., 2012; Xu et al., 2012). For a more detailed discussion about the origin of lead affecting these suspicious wines, it is of full relevance to have the detailed information about their geographical origin.

C.3.5. Geographic provenance of wines by means of non-radiogenic isotope ^{204}Pb

A more reliable differentiation of wines of European and non-European origin can be obtained from the plot $^{208}\text{Pb}/^{204}\text{Pb}$ and $^{207}\text{Pb}/^{204}\text{Pb}$ presented on Fig. C.11. The introducing of geogenic isotope ^{204}Pb data in environmental studies reflects the contribution from natural Pb-sources to the atmosphere. By combining with radiogenic isotopes ^{208}Pb and ^{207}Pb , the multiplicity of existing Pb emissions may be considered simultaneously (Ellam, 2010). Reimann et al. (2012) highlighted the predominance of lead of geogenic origin in European agricultural sites, therefore, $^{208}\text{Pb}/^{204}\text{Pb}$ and $^{207}\text{Pb}/^{204}\text{Pb}$ ratios can bring a meaningful outcome for the regional specification of plants and food products of vegetable origin. Detection of minor ^{204}Pb isotope required the ultimate instrumental precision because its abundance is only 1% of total lead. The use of MC-ICP-MS provides the required level of accuracy and precision. The plot on Fig. C.11 identifies two wine series by distinctive linear regression. Whilst authentic Bordeaux samples are closely grouped around the line within the intervals of 15.60-15.66 for the $^{207}\text{Pb}/^{204}\text{Pb}$ ratio and 37.94-38.67 for the $^{208}\text{Pb}/^{204}\text{Pb}$ ratio, the suspicious Bordeaux are extensively scattered around the resulting curve with

the tendency to present the lower radiogenic values for both isotopic systems. Such distinguishable radiogenicity does not contradict with assumed Asiatic origin of wines. It reflects in a greater extent the lead from low radiogenic, geologically ancient mines that are common in Asia (Bingquan, 1995; Bi et al. 2017). The large dispersion of the points, both along the length of the line and around it, may be a consequence of the influence from multiplicity of lead sources. The point of intersection of two regression lines is a controversial zone for reliable determination of wine origin by Pb isotopes, because samples can be attributed to both groups. On the contrary, the suspicious wines placed distantly from the point intersection, can be assigned with a high probability of not being originating from Bordeaux.

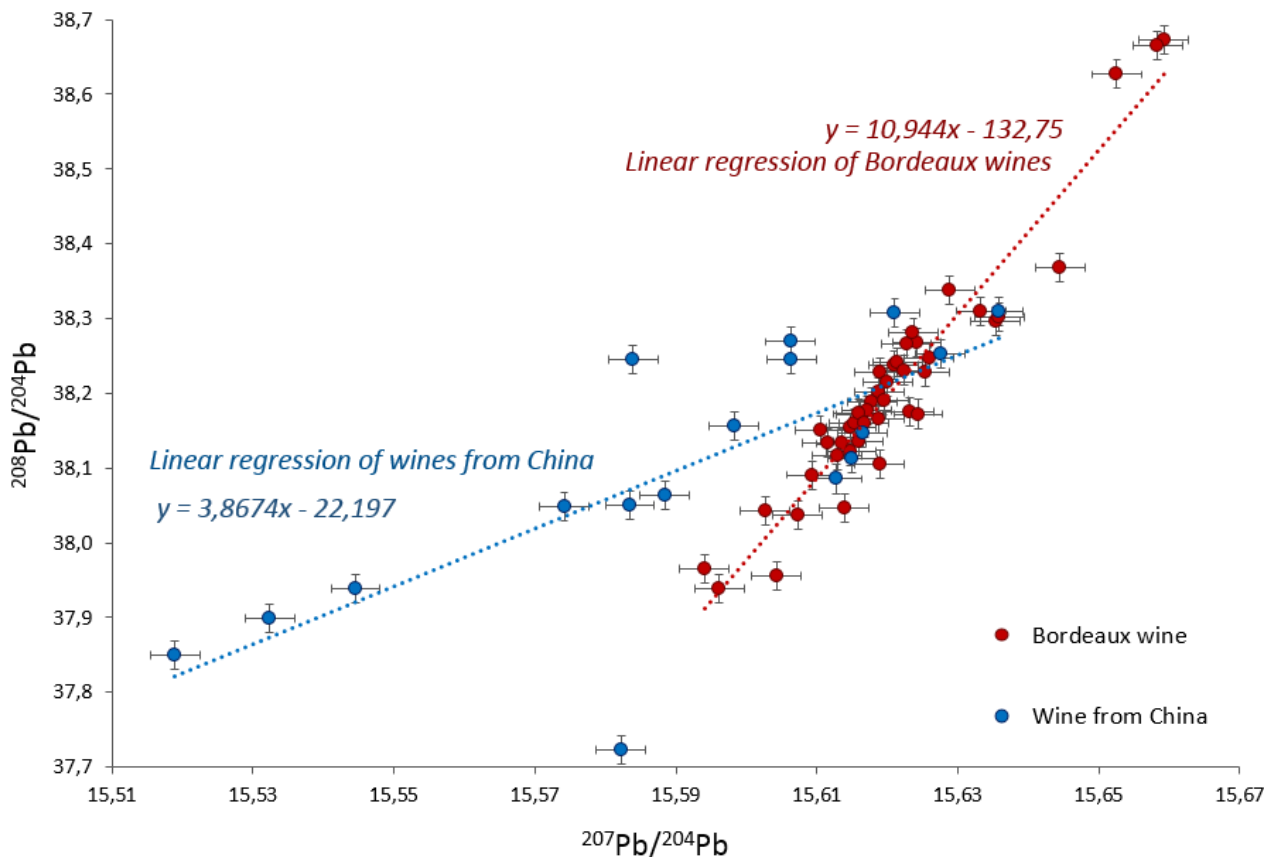


Fig. C.11. Comparison of linear regressions of ratios $^{208}\text{Pb}/^{204}\text{Pb}$ and $^{207}\text{Pb}/^{204}\text{Pb}$ in authentic Bordeaux wines and “wines from China”- wines with suspicious Bordeaux origin being purchased in China. Parameters of the “Bordeaux” linear regression: $y = 4.5651x - 33.012$; $R = 0.918$. Parameters of the linear regression of the series “wines from China”: $y = 3.6058x - 18.099$; $R = 0.7431$.

C.3.6. Wine dating

The preserved chronological specification suggests to apply the Pb isotopic fingerprint to trace years of wine production. Relative dates of vintage can be traced considering the dates of substantial industrial or meteorological events, such as years of phasing out of the leaded gasoline or long-distance influences from dust storms. As it has been shown in section C.3.3, the gradual withdrawal of lead from gasoline and increased rates of other Pb contributors in the European atmosphere caused a change in the Pb signatures of wines. The combination of total Pb content with the $^{208}\text{Pb}/^{204}\text{Pb}$ ratio provide a tool to distinguish different vintages with a relatively high degree of confidence over the different decades.

The isotopic composition of Pb in Bordeaux wine reflects the atmosphere of the region and thus can provide a useful information addressing its geographical origin. This study highlights following important observations which could be key questions and can benefit the food provenance and authenticity assessments:

- i) a direct positive consequence of the leaded gasoline's ban: a drastic decrease of total lead concentrations in authentic Bordeaux within a period of 50 years and the substantial predominance of lead of natural origin in recently produced wines;
- ii) the generally excellent match between the Pb isotopic signatures in Bordeaux wine ($^{206}\text{Pb}/^{207}\text{Pb}$ and $^{208}\text{Pb}/^{206}\text{Pb}$) and those of the European atmosphere;
- iii) the wines of suspicious Bordeaux origin would follow more the trend from the Asiatic atmospheric Pb regression. Compared to the European signatures, it is evidentially more impacted by the residual contribution from tetraethyl anthropogenic Pb;
- iv) $^{208}\text{Pb}/^{204}\text{Pb}$ and $^{207}\text{Pb}/^{204}\text{Pb}$ ratios are recognized as reliable criterions for origin discrimination due to simultaneous contributions from anthropogenic and natural sources, particularly for distinguishing of the origins with elevated and/or specified natural Pb levels.

Determination of Pb in vintage wines can be a method for reconstructing a sequential history of atmospheric evolution and reflect relative dates, or the order in which one event occurred relative to another.

C.4. Elemental composition of Bordeaux wine for classification purposes

The elemental composition of wine is widely applied for discrimination according to geographical origin (Médina et al., 2013; Cozzolino & Smyth, 2013). In studied wines, elemental concentrations were determined according to analytical procedures previously mentioned in Chapter B, section B.1.3. A short discussion about the trace elemental compositions of authentic and suspicious Bordeaux wines is presented in Appendix 1, elemental data is presented in Table 1.1 (Appendix 1).

The elemental concentrations of studied Bordeaux wines were evaluated for the potential application of geographical origin classification:

- Revealing of elemental fingerprinting of authentic Bordeaux wines;
- Comparison of different wineries within the region of Bordeaux;
- Approbation of an authentic elemental fingerprint.

C.4.1. Authentic Bordeaux versus imitated Bordeaux and Chinese wines

When addressing the trace elemental profiles of authentic Bordeaux wines, some notable particularities can be attributed to this group in comparison to the group of “Bordeaux imitation” and wine originating from China. First, the concentrations of Li, Sr, Fe, Mn, Ni, differ significantly in these groups, with the lowest concentrations always attributed to the group of authentic Bordeaux wines. A similar trend can be seen also for Al, V, Cd, Cs, and Ba; however, to a lesser extent. Also, it is notable that the concentrations of Mn, Co, Ni, Pb, Cd, Cr, and Sr varied in a relatively narrow span for authentic Bordeaux, while the samples of imitated Bordeaux have higher concentrations and larger variability for the most of analyzed elements. This observation is not unexpected, since this group includes samples with unknown geographical origins, as well as the precise geographical origins of Chinese wines is still unknown. However, some samples from the group of imitated Bordeaux demonstrated anomalously high concentrations of Li, Mn, Ni, Sr, Rb, Cs, Pb, which are not typical for Bordeaux, but were observed in the series of Chinese wines (Table 1.1 from Appendix 1; Zou et al., 2012).

In general view, the profiles of mislabeled Bordeaux provided a sense of the variability of elements similar to those in Chinese wines. Nonetheless, the exact decision about their exact provenance cannot be made based on the available information. If it could be assumed that some of these mislabeled Bordeaux wines, which were sold on the Chinese market, were also produced in China, this large variability of concentrations could be explained by a great diversity of geological settings, agricultural practices and winemaking traditions across the country (Zou et al., 2012).

C.4.2. Differences in elemental content in red and white wines

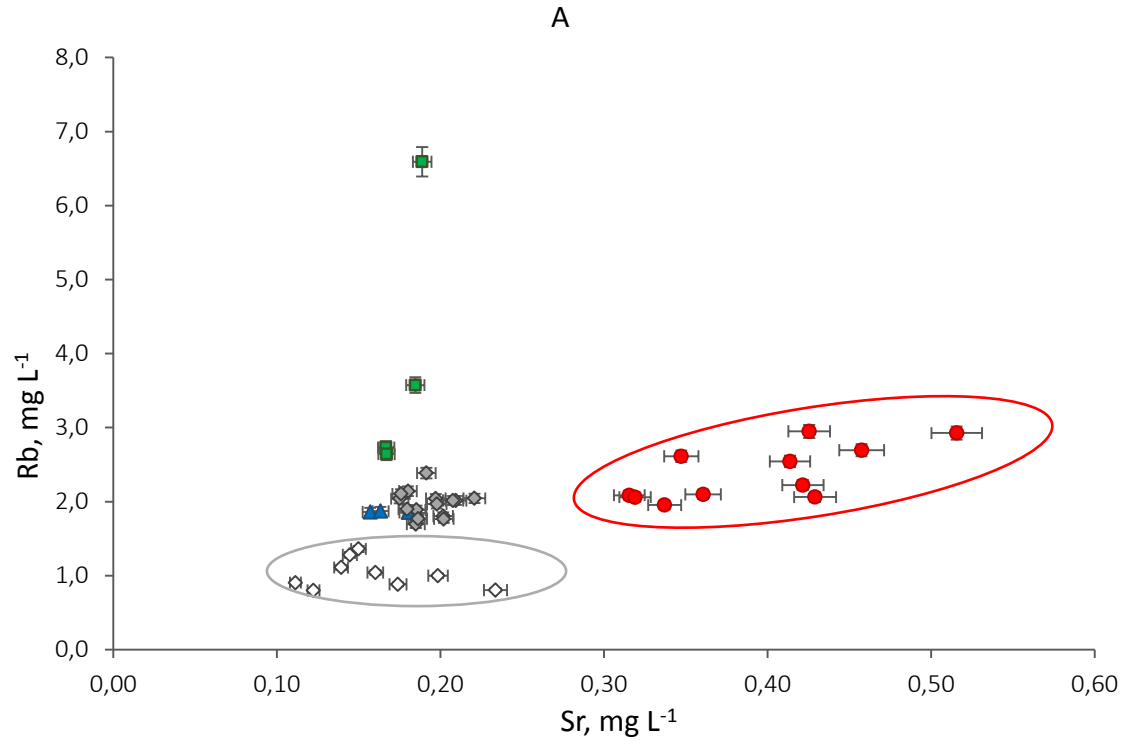
The variation in inorganic compositions of two types of wine, red and white, was one of the points of interest and has been evaluated on wines from Pessac-Léognan. Red wines from Pessac-Léognan presents higher concentrations of following elements: V, Rb, Cs, Ba, B, Al, Co and Ni. The levels of Li, Mn, Fe, Cu, Zn, Sr, Cd, and Pb do not differ significantly among red and white wines within the same winery. Previous studies also found higher elemental concentrations of Rb and Sr (Geană et al., 2013) and Rb, Cs, Sr, Ba (Greenough et al., 2005) in red wines in comparison to white ones.

The most significant difference in elemental content has been attributed to vanadium, whose mean concentrations were $0.85 \pm 0.65 \mu\text{g L}^{-1}$ for white wines, and $48.5 \pm 29.1 \mu\text{g L}^{-1}$ for red wines. However, Geană et al. (2013) did not reveal any significant differences in levels of this element. Therefore, the observed contrast in its content can be a consequence of winemaking process, such as the use of special types of reservoirs and tanks containing vanadium alloys.

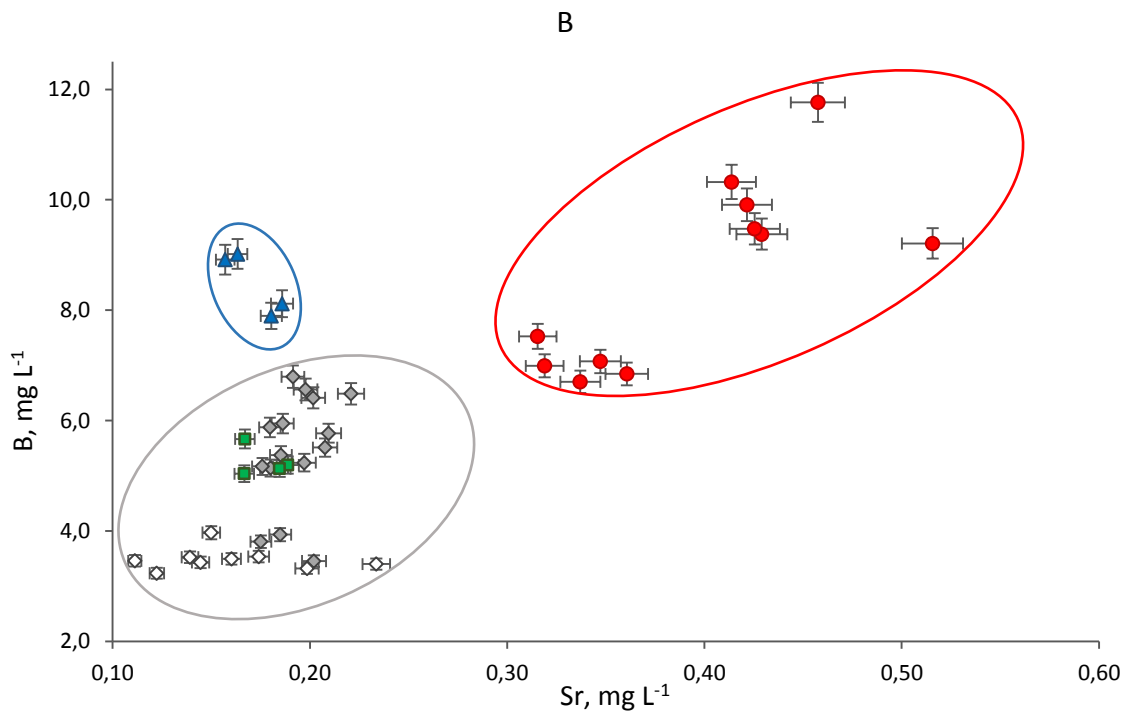
C.4.3. Is it possible to identify one Bordeaux winery from others?

The combination of trace-elements concentrations could be used for identifying an elemental signature of an individual winery. Despite the limited number of samples, some preliminary regularities can be highlighted.

Wines from Pomerol and white wine from Pessac-Léognan can be distinguished with respect to other wines when using only the elemental concentrations of Sr and Rb (Fig. C.12A). Among these two elements, Sr has a higher discrimination potential. Despite of a grouping tendency of four Pauillac wines over the remaining samples, the distinctive differentiation for other wineries is inconclusive due to observed overlapping. The next diagram (Fig. C.12B) considers the impact of boron, whose compounds are included in vineyard's fertilizers. The combination of Sr and B strengthens the discrimination of Pomerol and allocates four samples of Saint-Émilion to an individual separate group on the scatter plot. However, white and red wine from Pessac-Léognan and Pauillac are somewhat overlapping. In order to obtain a better discriminating sign attributed to the origins of wines, the weight of vanadium in form of its invers concentrations ($1/V$) has been applied on the Fig. C.12C. This elemental combination (B and V) clearly shows the better discrimination: white wines Pessac-Léognan, Pomerol, are distinctly separated. Despite of the limited number of samples, here also, the grouping tendency can be seen for the Saint-Émilion and Pauillac wines.



● Pomerol ▲ Saint-Emilion ◆ Pessac-Léognan red ◇ Pessac-Léognan white ■ Pauillac authentic



● Pomerol ▲ Saint-Emilion ◆ Pessac-Léognan red ◇ Pessac-Léognan white ■ Pauillac authentic

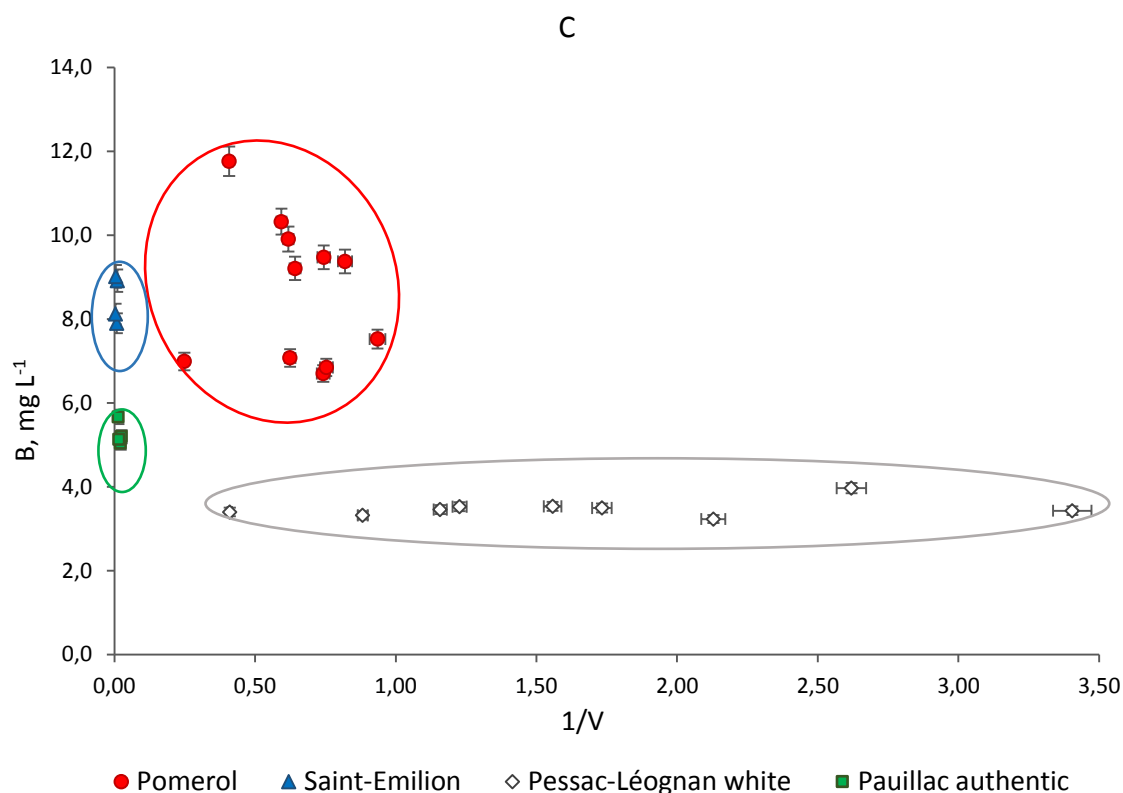


Fig. C.12. Classification of different Bordeaux wineries by means of selected elemental concentrations: A) Sr and Li; B) Sr and B; C) B and V.

The distinctive potential of trace elements fingerprint is evident for the origin classification of Bordeaux wines on a small geographical scale. Trace elements such as Sr, Rb, B and V are considered as the most distinctive constituents. Using them, the classification of wine from Pomerol, Saint-Émilion, Pessac-Léognan and Pauillac was possible with only the function of two variables. The most distinctive elemental composition was observed for wines from Pomerol. The study on application of elemental concentrations to Bordeaux wine geographical origin discrimination needs to be continued by using multivariate data analysis to ensure the more reliable differentiation of the provenance.

C.5. Wine authenticity by means of trace elements and Sr- Pb- isotopic signatures

The trace elemental- and isotopic approach for authenticity approving was tested on adulterated wines, included in the group of wines with misstated "Bordeaux" origin. Their labels indicated that it was a high value wine from the exact named Châteaux from Pauillac appellation. The perfect external presentation of the bottles, corks, labels and capsules were consistent with the norms applied in this winery. By a visual examination, these bottles were indistinguishable from the authentic exemplars; however, the fact of adulteration was previously confirmed (personal communication). In order to evaluate the efficiency of multi-elemental and isotopic approach, a set of authentic wines from the same winery and the same years of production was included in the study (figure in the list as Chateau #4, Pauillac).

As regard to comparison of trace elemental composition of the authentic and imitated samples, a significant dissimilarities were observed for the concentrations of Sr, B, Fe, Ni, Ba, Li, Mn (Table 1.1 from Appendix I). Suspicious samples contained elements Sr, B, Fe, Ba, Li, Mn in concentrations greater than authentic samples, while level of Ni was lower. Figures C.13A and C.13B present the comparison of elemental concentrations in two survey groups: A) Sr and Li, B) Fe and Mn. The concentrations of two "geo"-markers, Sr and Li, are regulated in wine by vineyard's soil, while Fe and Mn, can be additionally transferred to wine from fertilizers. Both scatter plots indicate that authentic and imitated wines can be distinguished by using the selected elements. The close patterns of Sr, Li, Mn and Fe for 4 authentic wines reflect the similarity on soil composition and agricultural practices within a vineyard. An obviously large span of concentrations of elements in question indicates the contrary.

Using Sr isotopic signatures on the scatter plot increases the confidence in precision of determination: a better re-grouping of genuine samples in comparison to previous elemental diagrams can be achieved (Fig. C.13C). When applying Pb isotope ratios, a striking analogy of the atmospheric environment of wine's origin is pointed out (Fig. C.13D). Like in the previous example from Fig. C.13 A and B, it is obvious that four suspicious wines are certainly not from Bordeaux, moreover, it can be specified that all the four samples are from geographically remote places.

As it can be seen, both, elemental and isotopic analysis indicate an apparent authentic specification of genuine product comparing to suspicious one. However, the definition obtained by isotopic patterns is unquestionably more precise. Therefore is suggested to perform a study using a larger series of genuine and suspicious samples. We believe that Sr- and Pb- isotopic patterns may be a promising criterions for authentic Bordeaux wine.

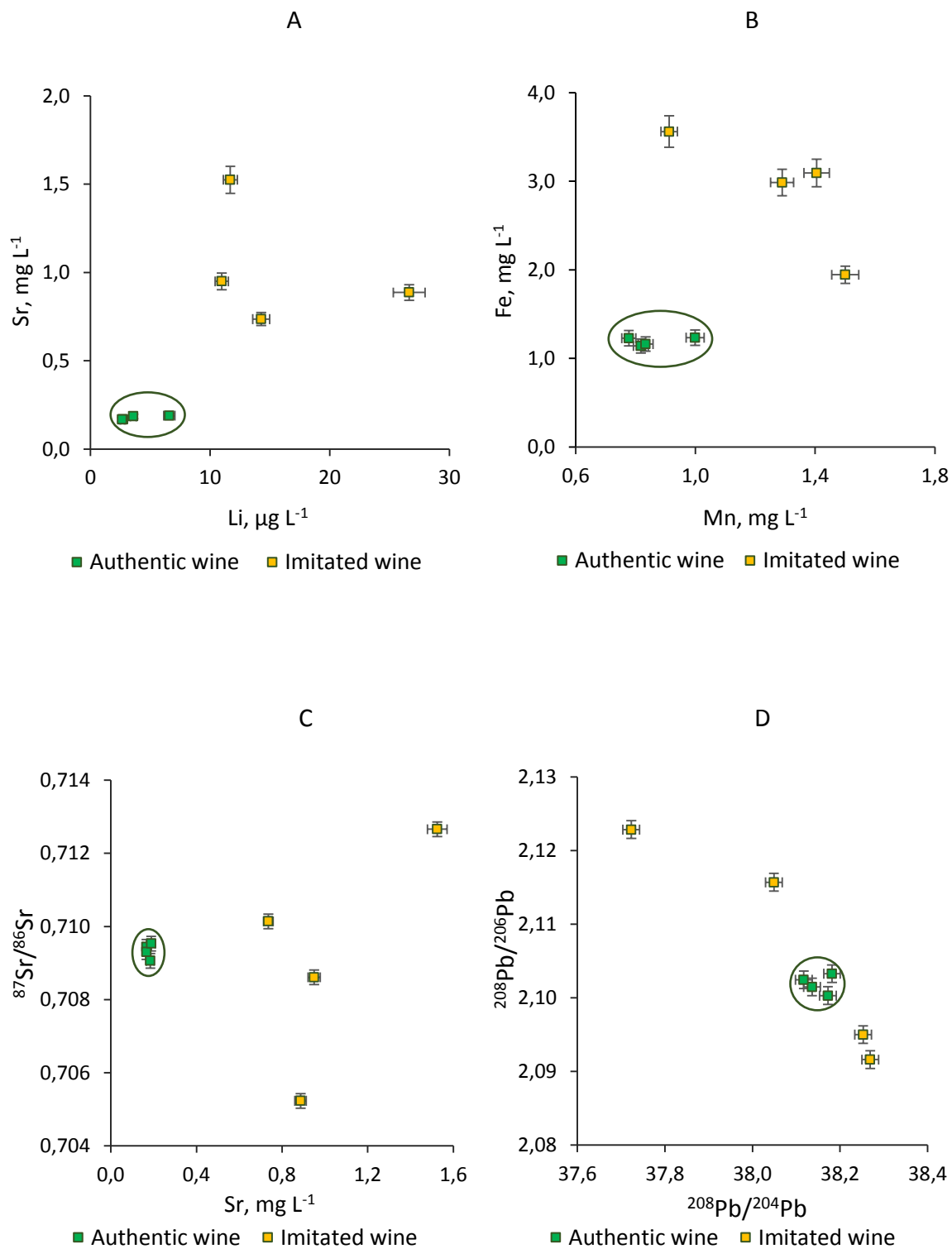


Fig. C.13. Comparison of elemental and isotopic compositions in authentic and adulterated wines from Pauillac: (A) - of Sr vs Li; (B) - Fe vs Mn; (C) - ⁸⁷Sr/⁸⁶Sr vs Sr elemental concentrations; (D) - ²⁰⁸Pb/²⁰⁶Pb vs ²⁰⁸Pb/²⁰⁴Pb.

C.6. Conclusion

Elemental and isotopic compositional similarity of Bordeaux wines is due to environmental factors (geology, soil, climate, low levels of atmospheric pollution), norms and regulations of agricultural practices (interdiction of irrigation, application of fertilizers), and national traditions of winemaking.

Bordeaux is characterized by relatively similar geological settings, however, there are a slight diversity among its sub-regions. Due to new instrumental analytical developments, such MC-ICP-MS, it is became possible to detect a small variations in Sr isotopic composition of wine and then to discriminate their geographical origin. While Sr isotopic signatures can help to distinguish Bordeaux wines on a small regional scale, the Pb isotopes are fairly homogeneous within the region of Bordeaux and are influenced primarily by the atmosphere. Taking into account the compositional difference of lead isotopic signatures on a continental scale, this tracer can be a useful tool to detect counterfeited "Bordeaux" wines produced outside of the homonymous territory.

The Sr- and Pb- isotopic signatures of genuine regional wine can be reinforced by trace elemental patterns and together can become an accurate, precise, multi-level fingerprint of Bordeaux wines and can be used when considering possible fraud involving branded wines. For more reliable classification of the studied wines, the application of statistical methods for data treatment will be made.

Table C.3. Pb isotope ratios and Pb concentrations determined in wines.

Vinery / Type of wine Appellation / Provenance	Year	Pb, µg L ⁻¹	²⁰⁶ Pb/ ²⁰⁴ Pb	²⁰⁷ Pb/ ²⁰⁴ Pb	²⁰⁶ Pb/ ²⁰⁴ Pb	²⁰⁸ Pb/ ²⁰⁶ Pb	²⁰⁷ Pb/ ²⁰⁶ Pb	²⁰⁶ Pb/ ²⁰⁷ Pb
Pomerol (Chât. 1) red wine Bordeaux France	1969	163	38,150	15,610	18,114	2,1061	0,8618	1,1604
	1973	161	38,042	15,603	18,071	2,1052	0,8634	1,1581
	1978	84,7	37,938	15,596	17,964	2,1120	0,8682	1,1518
	1979	37,1	37,965	15,594	18,064	2,1016	0,8632	1,1584
	1989	34,6	37,955	15,604	18,002	2,1084	0,8667	1,1538
	1992	34,0	38,037	15,607	18,060	2,1062	0,8642	1,1571
	2002	29,5	38,134	15,611	18,121	2,1044	0,8615	1,1607
	2003	24,4	38,123	15,615	18,127	2,1031	0,8614	1,1608
	2004	22,1	38,106	15,619	18,095	2,1058	0,8632	1,1585
	2009	16,7	38,154	15,615	18,162	2,1007	0,8597	1,1631
	2010	18,0	38,201	15,619	18,194	2,0997	0,8585	1,1648
Pessac-Léognan (Chât. 3), red wine Bordeaux France	2009	12,9	38,247	15,626	18,205	2,1009	0,8574	1,1650
	2009	13,2	38,189	15,618	18,165	2,1023	0,8598	1,1631
	2009	13,8	38,133	15,614	18,137	2,1025	0,8609	1,1616
	2009	11,1	38,160	15,615	18,138	2,1039	0,8609	1,1615
	2009	11,5	38,047	15,614	18,025	2,1108	0,8662	1,1544
	2010	12,4	38,215	15,620	18,187	2,1012	0,8588	1,1643
	2010	11,0	38,242	15,621	18,207	2,1004	0,8580	1,1655
	2010	10,1	38,171	15,616	18,144	2,1038	0,8607	1,1618
	2010	11,2	38,175	15,623	18,134	2,1052	0,8615	1,1607
	2011	17,5	38,267	15,624	18,222	2,1009	0,8574	1,1650
	2011	12,4	38,228	15,619	18,193	2,1013	0,8586	1,1647
	2011	13,2	38,238	15,621	18,226	2,0980	0,8571	1,1667
	2011	17,7	38,267	15,623	18,227	2,0995	0,8571	1,1666
	2011	12,4	38,191	15,619	18,158	2,1033	0,8602	1,1625
2011	10,3	38,228	15,625	18,172	2,1036	0,8598	1,1630	
Pessac-Léognan (Chât. 3), white wine Bordeaux France	2010	10,1	38,178	15,617	18,157	2,1027	0,8601	1,1626
	2010	15,7	38,165	15,619	18,201	2,0968	0,8581	1,1653
	2010	15,1	38,160	15,617	18,138	2,1039	0,8610	1,1614
	2011	12,3	38,231	15,622	18,184	2,1024	0,8591	1,1640
	2011	16,2	38,666	15,658	18,644	2,0740	0,8399	1,1906
	2012	12,3	38,672	15,659	18,657	2,0729	0,8393	1,1914
	2012	9,37	38,172	15,616	18,151	2,1031	0,8604	1,1623
	2012	10,5	38,310	15,633	18,244	2,0999	0,8569	1,1670
2012	14,0	38,627	15,653	18,636	2,0726	0,8399	1,1906	

The concentrations are accurate to 3%. The analytical precision of isotopic measurements achieved: 503 ppm (²⁰⁸Pb/²⁰⁴Pb), 246 ppm (²⁰⁷Pb/²⁰⁴Pb), 556 ppm (²⁰⁶Pb/²⁰⁴Pb), 560 ppm (²⁰⁸Pb/²⁰⁶Pb), 450 ppm (²⁰⁷Pb/²⁰⁶Pb), 450 ppm (²⁰⁶Pb/²⁰⁷Pb) related to complete process of sample preparation including digestion and column separation were estimated on independently prepared triplicates of samples (RSD).

Table C.3. Pb isotope ratios and Pb concentrations determined in wines (Continuation).

Vinery / Type of wine								
Appellation / Provenance	Years	Pb, µg L ⁻¹	²⁰⁸ Pb/ ²⁰⁴ Pb	²⁰⁷ Pb/ ²⁰⁴ Pb	²⁰⁶ Pb/ ²⁰⁴ Pb	²⁰⁸ Pb/ ²⁰⁶ Pb	²⁰⁷ Pb/ ²⁰⁶ Pb	²⁰⁶ Pb/ ²⁰⁷ Pb
Saint-Emilion (Chât. 2)	2011	5,2	38,297	15,635	18,234	2,1003	0,8580	1,1654
red wine	2011	4,9	38,368	15,644	18,329	2,0932	0,8536	1,1715
Bordeaux	2011	4,4	38,302	15,636	18,294	2,0937	0,8547	1,1700
France	2011	5,3	38,338	15,629	18,358	2,0883	0,8513	1,1746
Pauillac (Chât. 4)	2004	18,3	38,182	15,624	18,127	2,1033	0,8618	1,1577
red wine	2005	16,8	38,136	15,616	18,147	2,1015	0,8605	1,1620
Bordeaux	2006	21,5	38,117	15,613	18,130	2,1025	0,8612	1,1612
France	2007	27,8	38,172	15,624	18,175	2,1003	0,8597	1,1632
Mislabeled	2004	11,6	37,723	15,582	17,770	2,1229	0,8769	1,1404
Pauillac	2005	14,6	38,253	15,628	18,259	2,0950	0,8559	1,1684
Unknown	2006	19,1	38,049	15,574	17,985	2,1157	0,8660	1,1548
	2007	8,60	38,269	15,606	18,296	2,0916	0,8532	1,1721
Bordeaux	1998	23,1	37,849	15,519	17,724	2,1355	0,8756	1,1421
Mislabeled	2005	10,3	38,310	15,636	18,336	2,0894	0,8528	1,1726
red wine	2006	25,4	37,939	15,545	17,801	2,1313	0,8732	1,1452
Unknown	2007	16,3	38,085	15,613	18,107	2,1033	0,8622	1,1597
	2007	17,9	38,050	15,583	18,031	2,1102	0,8642	1,1570
	2008	11,9	37,899	15,532	17,738	2,1366	0,8756	1,1420
	2009	18,7	38,147	15,616	18,140	2,1030	0,8609	1,1616
	2009	15,3	38,113	15,615	18,134	2,1018	0,8611	1,1613
	-	44,4	38,064	15,588	18,033	2,1090	0,8644	1,1584
	-	21,5	38,245	15,584	18,099	2,1130	0,8610	1,1614
China	-	33,7	38,156	15,598	18,089	2,1092	0,8623	1,1597
red wine	-	54,6	38,307	15,621	18,122	2,1138	0,8620	1,1601
	-	28,2	38,245	15,606	18,187	2,1029	0,8581	1,1653

The concentrations are accurate to 3%. The analytical precision of isotopic measurements achieved: 503 ppm (²⁰⁸Pb/²⁰⁴Pb), 246 ppm (²⁰⁷Pb/²⁰⁴Pb), 556 ppm (²⁰⁶Pb/²⁰⁴Pb), 560 ppm (²⁰⁸Pb/²⁰⁶Pb), 450 ppm (²⁰⁷Pb/²⁰⁶Pb), 450 ppm (²⁰⁶Pb/²⁰⁷Pb) related to complete process of sample preparation including digestion and column separation were estimated on independently prepared triplicates of samples (RSD).

Chapter D

$^{87}\text{Sr}/^{86}\text{Sr}$ isotope ratio and multielemental signatures as indicators of origin of European cured hams: The role of salt

Abstract

We have examined the potential of discriminant inorganic constituents (trace-, ultra-trace elements and Sr isotope ratios) to assess the origin of world famous brands of European dry-cured hams. The variation of the multielemental composition with principal component analysis allowed to discriminate Bayonne hams. Determined ratio $^{87}\text{Sr}/^{86}\text{Sr}$ was recognized as a strong additional distinctive parameter. The ratio $^{87}\text{Sr}/^{86}\text{Sr}$ allowed to better separate all the different categories of hams in addition to the multi-elemental detection. The major contribution of the value $^{87}\text{Sr}/^{86}\text{Sr}$ for the Bayonne ham is directly related to its curing due to the salt used in process coming from the nearby salt mine Salies-de-Béarn. Since the salt represents around 4% of the final product, it will therefore strongly influence the elemental and isotopic composition of hams. The overall discrimination potential of strontium isotope ratio is evidenced in the final statistical discrimination of the origin of hams.

D.1. Introduction

Dry-cured ham is a traditional meat product originating from southern European countries. Today the production is mainly carried out in Spain, France and Italy. Different types of dry-cured ham can be found depending on the origin of raw material and techniques of curing. All these dry-cured hams bring a significant economic importance for the national meat industries and potentially can become an object of forgery or mislabeling. European Union schemes of geographical indications, known as Protected Designation of Origin (PDO) and Protected Geographical Indications (PGI), distinguished them on the basis of their genotypes, regional origins and the features of curing processes, and hence have the motivation to guarantee the authenticity and quality of products. The requirements of various regulatory authorities for chemical analysis applied in food control domain are becoming more sophisticated every day (De La Guardia & González, 2013c). Various analytical methods, such as spectroscopy, genetic analysis, metabolomics- and proteomics technologies, are widely applied to determinate the geographical origin and authenticity of meat products (Franke et al., 2005). Among them, inductively coupled plasma mass-spectrometry (ICP-MS) implies a quadrupole-based mass analyzer system (Q-ICP-MS) is the fastest growing multi-element trace element analysis technique, while the multicollection ICP-MS (MC-ICP-MS) allows the determination of isotopic composition of elements with exceptional precision. Both techniques are widely used in last decade in studies of geographical origin determination (De La Guardia et al., 2013).

Multielemental fingerprinting achieves a certain success in geographical provenance determination of meat. It reflects the mineral composition of surrounding environment (soil, water, and litter) but also includes the incoming contribution of elements associated with the feeding and supplementation of animals, and finally the anthropogenic pollutions (Franke et al., 2005). Recent studies evidenced the relevance of use the multi-elemental composition for the geographic authentication of pork (Kreitels et al., 2017) and its potential to differentiate between conventional and organic pork (Zhao et al., 2016). However, some of agricultural practices, such as controlled feeding and intensive rearing, can minimize the chemical variation and will then interfere with geographic origin determination based on multi-discriminant statistics (Kreitels et al., 2014). The application of the precise and accurate specification of isotopic compositions of elements can reinforce the discrimination potential (Franke et al., 2005; Balcaen et al., 2010; Zhao et al., 2014; Camin et al., 2016). Stable isotope ratio determination is one of the robust and most discriminant methods with traditional approach based on ratios of light bio elements such as

hydrogen, nitrogen, oxygen, carbon and sulfur, determined often by methods isotope ratio mass spectrometry (IRMS) and nuclear magnetic resonance (NMR). The ratios of $^2\text{H}/^1\text{H}$, and $^{18}\text{O}/^{16}\text{O}$ are strongly latitude dependent, while local agricultural practices and animal diet will rather affect the ratios $^{15}\text{N}/^{14}\text{N}$, and $^{13}\text{C}/^{12}\text{C}$, respectively. Stable isotope ratios of light elements have been recently successfully applied to identify authenticity of food of animal origin (Camin et al., 2016), and, especially, for the dry-cured ham differentiation (Perini et al., 2013). The recent instrumental development of MC-ICP-MS have expanded the potential of isotope analysis by adding the so-called “non-traditional” elements – strontium, lead (Balcaen et al., 2010). This innovation has improved the information related with the provenance studies due to the outstanding precision and accuracy of simultaneous multi-isotopes detection.

Dealing with non-traditional isotopes, Sr isotope ratios are routinely used in geosciences for dating and origin determination of minerals and for tracing the temporal changes in the hydrologic and sedimentary cycles. Over the last decade there has been an increasing interest in the Sr isotopes application as a sensitive geochemical tracer in paleontology, archeology and food sciences (Balcaen et al., 2010; Coelho et al., 2017). The geochemical basis for application of Sr isotope ratio to food’s geographical origin has been recently reviewed (Baffi & Trincherini, 2016). In summary, the ratio $^{87}\text{Sr}/^{86}\text{Sr}$ is a long-term stable parameter, which does not significantly depend on human activity, climate or season of production, but is regulated by local geological environment. The ratio $^{87}\text{Sr}/^{86}\text{Sr}$ appears to be an encouraging provenance tracer and has already demonstrated its great discriminating potential for geographical origin differentiation of various types of food matrices (e.g. Zhao et al., 2014).

Food of animal origin is of special concern. Animals continuously consume a large variety of foods with associated elements and compounds that do not only originate from their natural surroundings. Supplementary nutrition can be industrially produced or brought from geographically distant sources. When animals are mainly feed by local produced feeds, the values of the ratio $^{87}\text{Sr}/^{86}\text{Sr}$ in their tissues will then reflect the local geological settings and could be used as a tracer for geographical origin. This was demonstrated on various types of meats and poultry (Franke et al., 2008; Rees et al., 2016; Baroni et al., 2011; Rummel et al., 2012). For processed food, different preparation steps can alter the original $^{87}\text{Sr}/^{86}\text{Sr}$ ratio of the raw material. Despite of these limitations, the discriminating potential of the $^{87}\text{Sr}/^{86}\text{Sr}$ ratio was confirmed on different types of prepared food matrices, such cheese (Pillonel et al., 2003; Fortunato et al., 2004; Bontempo et al., 2011) and butter (Rossmann et al., 2000).

Raw meat used in dry-cured ham production varies largely by the mode of farming. While black Iberian pigs are free-range-reared race, the white genotypes used for Parma, San Daniele, and Bayonne hams are intensively reared (Ordóñez & De La Noz, 2007). The main ingredient generally added during production is salt (Jiménez-Colmenero et al., 2010). This addition will modify the taste of cured ham and will add the presence of trace elements associated in the salt matrix.

For this study, we have selected some of the most representative European cured hams: Iberian Ham (Jamón ibérico, Spain, Portugal), Bayonne Ham (Jambon de Bayonne, France), Parma (Prosciutto di Parme, Italy), San Daniele Ham (Prosciutto San Daniele, Italy). The objective of this study was to investigate their elemental and Sr isotopic compositions and use them to address the potential discriminant power of combination of multi-elemental, isotopic and statistical analysis to discriminate the ham's geographical origin.

A flow chart (Fig. D.1) provided below shows the procedure for analytical determination of elemental content and Sr isotope ratio completed with the follow-up statistical data treatment. Details concerning sample preparation, elemental and isotopic analysis can be found in Chapter B.

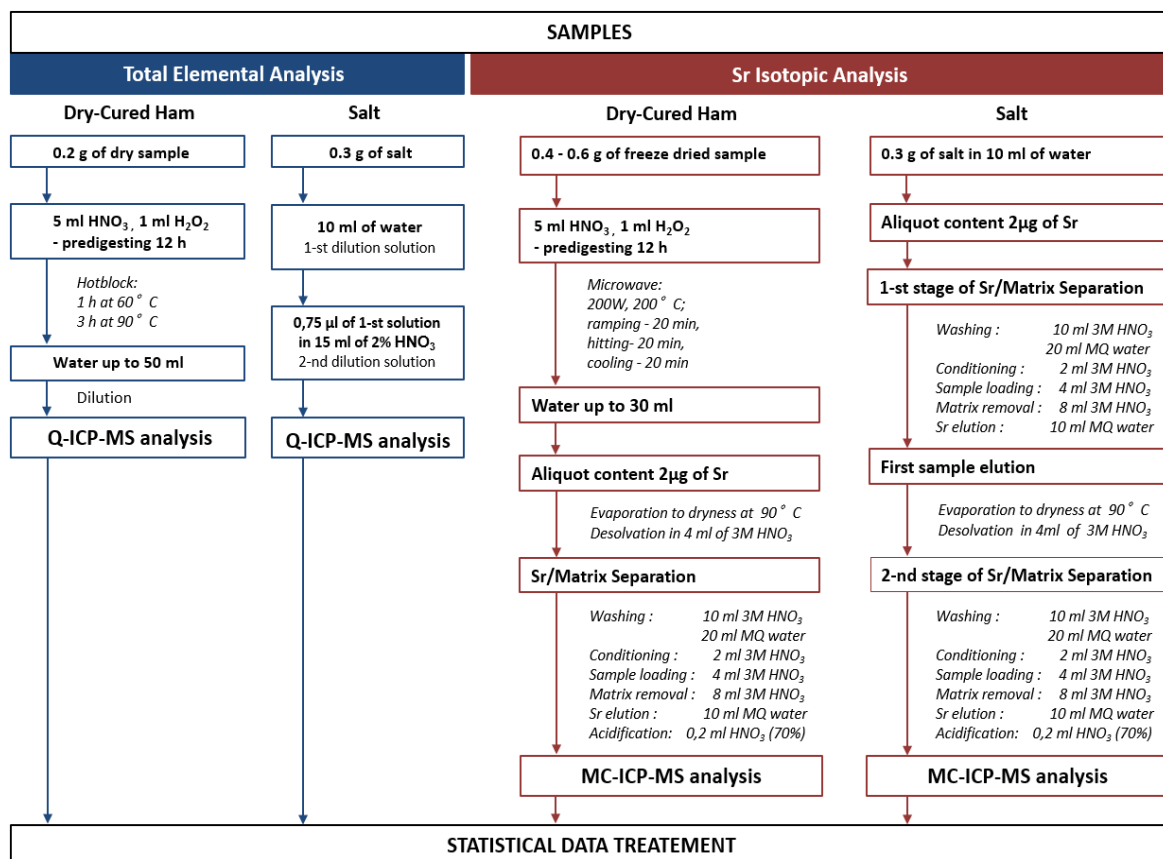


Fig. D.1. Analytical protocol.

D.1.1. Samples

Eleven Iberian hams originating from various provenances were collected from local producers from southwestern regions of the Iberian Peninsula, which are the principal production areas of Iberian ham, including Huelva, Seville, Avila, Badajoz and Estremadura in Spain, and Alentejo in Portugal. Two sample of Parma and San Daniele ham were purchased in local Spanish markets. Finally, three samples of Bayonne ham from different producers were purchased on local French supermarkets. From each packet a slice of ham without visible fat was taken, lyophilized, homogenized and kept frozen until analysis.

In order to assess the influence on Sr isotope ratios of ham, several natural salts have been purchased on local supermarkets and specialized bio-stores. The different salts used in this study were coming from seawater production plants from the French Atlantic coast (“Noirmoutier”, “Guérande”, “Île de Ré”), from the Mediterranean Sea (“Camargue”, Cypriot “Pyramid salt”), and from the Pacific Ocean (Hawaiian “Alaea salt”). Other types of salt originated from salts mines were from France (Saline “Salies-de-Béarn”), Pakistan (mine Khewra, “Himalayan pink salt”), Poland (mine “Wieliczka”), Austria (Salzkammergut, table salt “Alpine”), Iran (“Persian blue salt”), and finally, from Spain (“Andalusia”). Table D.1 presents the list of ham and salt samples, detailed information about origins, provenance, preparations and conditioning.

D.2. Elemental composition

Table D.2 reports the mean concentrations (on a dry weight basis) with the minimum and maximum limits, and analytical uncertainties, expressed as the maximal RSD value of individual triplicates for thirty-four trace and ultra-trace elements in the studied ham samples. Data is arranged in order of decreasing concentrations. The elemental concentrations obtain for individual samples of Iberian and Bayonne ham can be viewable in Table D.3 placed at the end of the Chapter.

D.2.1. Selected trace and ultra-trace elements in cured hams

In this study we have referred as traces elements the elements presenting in the hams with concentrations ranging from about 100 mg kg⁻¹ down to 1 mg kg⁻¹.

Table D.1. Dry-cured ham and salt: geographical provenance of studied samples.

Sample	Type / curing time / months	Geographical provenance	Source / Conditionnement / Appearance
Dry-cured hams			
IS1	Iberian Ham / 22	Spain, Seville	Prepared and packed by A* (Spain)
IA	Iberian Ham / 22	Spain, Avila	Prepared and packed by A* (Spain)
IB	Iberian Ham / 21	Spain, Badajoz	Prepared and packed by A* (Spain)
IS2	Iberian Ham / 18	Spain, Seville	Prepared and packed by B* (Spain)
IE	Iberian Ham / 22	Spain, Extremadura	Prepared and packed by B* (Spain)
IAJ	Iberian Ham / 22	Portugal, Alentejo	Prepared and packed by B* (Spain)
IH1	Iberian Ham / 22	Spain, Huelva	Prepared and packed by B* (Spain)
IH2	Iberian Ham / 03	Spain, Huelva	Prepared and packed by C* (Spain)
IH3	Iberian Ham / 14	Spain, Huelva	Prepared and packed by C* (Spain)
IH4	Iberian Ham / 26	Spain, Huelva	Prepared and packed by C* (Spain)
IH5	Iberian Ham / 40	Spain, Huelva	Prepared and packed by C* (Spain)
SD	Italian Ham / 12	Italy, San Danielle	Packed in supermarket (Spain)
PM	Italian Ham / 12	Italy, Parma	Packed in supermarket (Spain)
B1	Bayonne Ham	France, South-West	Prepared and packed by D* (France)
B2	Bayonne Ham	France, South-West	Prepared and packed by E* (France)
B3	Bayonne Ham	France, South-West	Prepared and packed by G* (France)
Salts			
SB1	Gross salt Salies-de-Béarn	France, South-West	Mineral deposit, Extra large white crystals, 5-10 mm
SB2	Gross salt Salies-de-Béarn	France, South-West	Mineral deposit, Extra large white crystals, 5-10 mm
SB3	Gross salt Salies-de-Béarn	France, South-West	Mineral deposit, Extra large white crystals, 5-10 mm
SB4	Flake salt de Salies-de-Béarn	France, South-West	Mineral deposit, Small damp flakes, < 2 mm
AN	Rock salt Andalusia	Spain, Andalusia	Mineral deposit, Large light grey crystals, 2-5 mm
AL	Alpine rock salt	Austria, Salzkammergut	Mineral deposit, Large light pink/grey crystals, 2-5 mm
PB	Persian Blue rock salt	Iran, Semnan	Mineral deposit, Large light blue/beige crystals, 2-5 mm
K	Rock salt Khewra Salt Mine	Himalayas, Pakistan	Mineral deposit, Large light pink/white crystals, 2-5 mm
W	Rock salt Wieliczka	Poland, Cracow	Mineral deposit, Large grey/dark grey crystals, 2-5 mm
G1	Flake salt Guérande	France, Atlantic coast	Sea salt, Small white damp flakes, < 2 mm
G2	Salt fine Guérande	France, Atlantic coast	Sea salt, Very fine white crystals, < 1 mm
C1	Flake salt Camargue	France, Mediterranean coast	Sea salt, Small white damp flakes, < 2 mm
C2	Salt fine Camargue	France, Mediterranean coast	Sea salt, Very fine white crystals, < 1 mm
N	Flake salt Noirmoutier	France, Atlantic coast	Sea salt, Small white damp flakes, < 2 mm
IR	Flake salt Île de Ré	France, Atlantic coast	Sea salt, Small white damp flakes, < 2 mm
CY	Pyramid salt	Chypre, Mediterranean sea	Sea salt, Pyramid-shaped flakes, 2-5 mm
HW	Alaea salt	Hawaii, Pacific ocean	Sea salt, Red/brown large damp crystals, 2-5 mm

Trace elements in cured hams

Among all the studied samples, the trace elemental concentrations varied within large intervals for following metals: Zn ($56.4 - 143 \text{ mg kg}^{-1}$), Fe ($24.6 - 75.9 \text{ mg kg}^{-1}$), Rb ($5.77 - 23.1 \text{ mg kg}^{-1}$), Cu ($1.79 - 4.99 \text{ mg kg}^{-1}$), Sr ($0.27 - 4.58 \text{ mg kg}^{-1}$), and Al ($0.26 - 2.61 \text{ mg kg}^{-1}$). The most significant variances were attributed to Iberian ham, since samples from different localities were assigned in this group. In contrast, Italian hams demonstrate similar values between the two brands studied: Zn - 83.3 mg kg^{-1} and 74.5 mg kg^{-1} ; Fe - 31.5 mg kg^{-1} and 31.3 mg kg^{-1} ; Rb - 18.3 mg kg^{-1} and 17.9 mg kg^{-1} ; and Cu - 2.44 mg kg^{-1} and 2.07 mg kg^{-1} , respectively for the Parma and San Daniele hams.

To the best of our knowledge, the data available in literature for trace elements composition of dry-cured hams is very limited, and only several essential metals in Italian hams have already been considered, such as Zn, Fe, Se, Cu, Mn (Lucarini et al., 2013; Jiménez-Colmenero et al., 2010; Adamsen et al., 2006B). The concentrations of Fe and Zn found in our study are in good agreement with the results published by Jiménez-Colmenero et al. (2010), where Fe was reported in interval of $34.0 - 62.3 \text{ mg kg}^{-1}$; and Zn in the interval of $41.5 - 56.6 \text{ mg kg}^{-1}$. In contrary, the levels of Fe and Zn, reported by Lucarini et al. (2013) are slightly lower than those in the same brand of hams in this work: in Parma ham the concentrations of Fe were found - 17.0 mg kg^{-1} and these of Zn - 43.4 mg kg^{-1} , for San Daniele ham the concentrations of Fe were 17.4 mg kg^{-1} and these of Zn - 44.9 mg kg^{-1} . Unfortunately, the authors do not give any details specifying if the given concentrations referred to defatted ham or not. Indeed, the total fat content might reach up to 22% (Lucarini et al., 2013) and this generally results in significantly lower metal content (Ferrari et al., 2007). However, concentrations of these metals published by Adamsen et al. (2006B) for Parma ham (Fe - 31.0 mg kg^{-1} and Zn - 78.0 mg kg^{-1}) are in good agreement with the results for the same brand of ham in the presented study.

Ultra-trace elements in dry-cured hams

The ultra-trace elements, as we have considered concentrations below 1 mg kg^{-1} , varied in the studied samples with a very wide spread, achieving the differences of 30-40 times between maximal and minimal concentrations for some elements, such as Cs, Pb, Cd and Tl (Table D.2).

The elemental contents of Mn and Se in this study varied between the range (with mean value in parentheses): $224 - 881 \text{ } \mu\text{g kg}^{-1}$ ($424 \text{ } \mu\text{g kg}^{-1}$), and $177 - 441 \text{ } \mu\text{g kg}^{-1}$ ($310 \text{ } \mu\text{g kg}^{-1}$) respectively. These levels are consistent to those reported by Lucarini et al. (2013): $200 \text{ } \mu\text{g kg}^{-1}$ and $280 \text{ } \mu\text{g kg}^{-1}$ for Mn and Se respectively, and to concentrations of Se measured at $500 \text{ } \mu\text{g kg}^{-1}$ by Jiménez-Colmenero et al. (2010).

Table D.2. Concentrations of selected elements (on dry weight basis) and values of the ratio $^{87}\text{Sr}/^{86}\text{Sr}$ in dry cured hams

Element/ Parameter	All hams			Iberian ham			Bayonne ham			Parma ham	San Daniele ham	RSD*/2SD**
	mean, n = 16	minimum	maximum	mean, n = 11	minimum	maximum	mean, n = 3	minimum	maximum			
Trace elements, mg kg ⁻¹												
Zn	93,0	56,4	143	96,1	56,4	143	91,0	83,2	97,5	83,3	74,5	2,8
Fe	41,0	24,6	75,9	45,9	24,6	75,9	29,7	26,8	34,9	31,5	31,3	2,5
Rb	13,8	5,77	23,1	12,0	5,77	17,9	17,6	14,6	23,1	18,3	17,9	3,2
Cu	2,92	1,79	4,99	3,26	1,88	4,99	2,14	1,79	2,63	2,44	2,07	2,4
Sr	1,96	0,27	4,58	1,29	0,27	3,97	3,75	2,93	4,58	1,52	4,48	3,1
Al	1,40	0,26	2,61	1,55	1,11	2,61	0,36	0,26	0,53	1,79	2,53	6,8
Ultra-trace elements, µg kg ⁻¹												
Mn	424	224	881	408	224	784	611	365	881	338	304	2,9
Se	310	177	441	308	177	441	314	295	336	361	377	5,8
Ni	273	31,1	2314	116	56,2	198	32,3	31,1	33,7	736	2314	6,0
Cs	176	17,2	574	185	17,2	574	106	89,6	124	88,8	440	3,7
Cr	101	83,7	141	102	83,7	141	89,6	86,1	92,4	94,7	118	3,8
Ba	76,1	13,8	175	96,7	56,5	175	17,4	13,8	21,3	87,0	79,8	5,9
Li	50,6	15,7	211	30,6	15,7	72,6	142	66,4	211	19,8	39,1	4,6
As	48,7	6,92	114	65,0	21,9	114	8,52	6,92	9,88	16,0	30,0	7,1
Pb	42,5	4,17	125	51,2	14,5	125	5,62	4,17	6,78	74,4	61,1	6,3
V	32,5	15,3	44,6	31,3	15,3	39,7	35,1	27,7	39,8	44,6	39,0	2,7
Cd	21,3	1,34	59,3	22,4	5,42	59,3	2,05	1,34	2,55	43,8	55,1	5,2
Sc	14,6	12,0	18,4	15,0	12,3	16,5	12,3	12,0	12,7	13,7	18,4	10,6
Co	6,54	1,33	20,6	7,41	3,79	20,6	1,68	1,33	2,10	7,54	13,3	4,1
Ga	6,08	4,48	10,4	6,65	5,18	10,4	4,80	4,48	5,23	5,43	6,38	6,7
Tl	1,39	0,089	3,85	0,79	0,089	2,05	3,41	2,72	3,85	1,79	1,05	4,0

* - Analytical uncertainties for trace metal analysis represent the maximal RSD (%) value of individual triplicates.

** - Analytical uncertainties for isotopic analysis represent the maximal 2SD value of individual triplicates.

Table D.2. Concentrations of selected elements (on dry weight basis) and values of the ratio $^{87}\text{Sr}/^{86}\text{Sr}$ in dry cured hams (Continued).

Element/ Parameter	All hams			Iberian ham			Bayonne ham			Parma ham	San Daniele ham	RSD*/2SD**
	mean, n = 16	minimum	maximum	mean, n = 11	minimum	maximum	mean, n = 3	minimum	maximum			
Ultra-trace elements, $\mu\text{g kg}^{-1}$												
Y	1,44	0,64	2,74	1,52	0,80	2,74	0,75	0,64	0,89	1,89	1,46	5,2
Nd	0,82	0,40	1,25	0,88	0,51	1,25	0,47	0,40	0,61	1,14	1,02	8,7
Gd	0,52	0,12	1,43	0,50	0,24	1,43	0,48	0,12	1,17	0,55	0,31	10,6
Pr	0,22	0,11	0,33	0,23	0,15	0,33	0,13	0,11	0,15	0,31	0,27	7,3
Be	0,21	0,066	0,32	0,22	0,11	0,32	0,12	0,066	0,16	0,28	0,32	13,2
U	0,20	0,059	0,30	0,23	0,14	0,30	0,087	0,059	0,10	0,22	0,24	12,2
Sm	0,15	0,077	0,31	0,17	0,10	0,31	0,087	0,077	0,10	0,18	0,17	12,8
Dy	0,15	0,071	0,25	0,16	0,12	0,25	0,096	0,071	0,13	0,15	0,18	13,2
Yb	0,10	0,045	0,240	0,11	0,059	0,24	0,062	0,045	0,086	0,11	0,10	14,5
Eu	0,070	0,029	0,13	0,075	0,046	0,12	0,037	0,029	0,042	0,062	0,065	15,0
Ho	0,044	0,019	0,074	0,041	0,025	0,066	0,043	0,019	0,058	0,051	0,041	9,3
Tb	0,040	0,017	0,059	0,041	0,029	0,059	0,030	0,017	0,036	0,047	0,038	13,7
Tm	0,024	0,012	0,045	0,023	0,012	0,040	0,022	0,019	0,025	0,020	0,019	23,8
Rb/Sr	10,5	3,27	33,6	12,6	3,27	33,6	4,14	3,28	6,19	12,0	4,00	-
$^{87}\text{Sr}/^{86}\text{Sr}$	0,70911	0,70854	0,70956	0,70928	0,70898	0,70956	0,70855	0,70854	0,70858	0,70925	0,70923	0,00010**

* - Analytical uncertainties for trace metal analysis represent the maximal RSD (%) value of individual triplicates.

** - Analytical uncertainties for isotopic analysis represent the maximal 2SD value of individual triplicates.

Unfortunately, the lack of published information regarding the other metals content in dry-cured ham does not allow any comparative consideration of the rest of data. The minimal content of Ni were detected in the Bayonne ham – $32.3 \mu\text{g kg}^{-1}$, while in Iberian ham Ni was observed in a larger range of concentrations $56.2 - 198 \mu\text{g kg}^{-1}$, with mean value – $116 \mu\text{g kg}^{-1}$. It is worth mentioning that the Ni concentrations in both Italian samples have been found to be extremely high, at the level of one order of magnitude higher than those in other samples: for the Parma ham Ni was measured at the level of $736 \mu\text{g kg}^{-1}$ and for San Daniele ham - $2314 \mu\text{g kg}^{-1}$. These values have been confirmed by repeating the analysis of these samples with the same preparation steps and ICP-MS determination. It is therefore possible that Ni migrates from stainless steel ware during the slicing for pre-packing in a store.

An important variability was observed for the content of Cs among the studied samples: $17.2 - 574 \mu\text{g kg}^{-1}$ for Iberian hams, $89.6 - 124 \mu\text{g kg}^{-1}$ for Bayonne hams, $88.8 \mu\text{g kg}^{-1}$ for Parma ham, $440 \mu\text{g kg}^{-1}$ for San Daniele. In contrast, the variabilities of Cr and V were relatively minor: $83.7 - 141 \mu\text{g kg}^{-1}$ ($101 \mu\text{g kg}^{-1}$), and $15.3 - 44.6 \mu\text{g kg}^{-1}$ ($32.5 \mu\text{g kg}^{-1}$) respectively, with mean value in parentheses. The same slight variations of Sc and Ga concentrations were also noted: $12.0 - 18.4 \mu\text{g kg}^{-1}$ ($14.6 \mu\text{g kg}^{-1}$) and $4.48 - 10.4 \mu\text{g kg}^{-1}$ ($6.1 \mu\text{g kg}^{-1}$), respectively.

The content of Ba and Li varied within considerable intervals: $13.8 - 175 \mu\text{g kg}^{-1}$ and $15.7 - 211 \mu\text{g kg}^{-1}$ respectively, with minimal value of Ba ($17.4 \mu\text{g kg}^{-1}$) and maximal value of Li ($142 \mu\text{g kg}^{-1}$) referred to the Bayonne ham.

For elements such as Pb, Cd, and As whose elevated content in food can lead to intoxication, the reported concentrations were characterized by maximal amplitudes: Pb - $4.17 - 125 \mu\text{g kg}^{-1}$, Cd - $1.34 - 59.3 \mu\text{g kg}^{-1}$, and As - $6.92 - 114 \mu\text{g kg}^{-1}$ on dry weight basis. The minimal concentrations of Pb ($5.62 \mu\text{g kg}^{-1}$), Cd ($2.05 \mu\text{g kg}^{-1}$), and As ($8.52 \mu\text{g kg}^{-1}$) were observed in the Bayonne ham. All the concentrations reported here for all individual hams did not exceed the safety levels suggested by WHO/FAO (2012) mentioned as: Pb - 0.20 mg kg^{-1} ; As - 0.50 mg kg^{-1} , and Cd - 0.40 mg kg^{-1} in most frequently consumed food products (expressed on wet weight).

The maximal range of Co concentration was evidenced in Iberian ham samples $3.8 - 20.6 \mu\text{g kg}^{-1}$, following the decreasing order of concentration: San Daniele - $13.3 \mu\text{g kg}^{-1}$, Parma - $7.5 \mu\text{g kg}^{-1}$, and Bayonne ham - $1.68 \mu\text{g kg}^{-1}$.

Thallium was detected in cured hams within the range of concentrations $0.089 - 3.85 \mu\text{g kg}^{-1}$ with maximal content in the Bayonne ham. Thallium, together with Cd, has the largest amplitude of variations. Concentrations of Y, on the contrary, do not display any notable variations among different cured-ham brands: $0.64 - 2.74 \mu\text{g kg}^{-1}$.

The minimal levels of Be and U were attributed to the Bayonne ham: $0.066 - 0.16 \mu\text{g kg}^{-1}$ and $0.059 - 0.10 \mu\text{g kg}^{-1}$, while in other samples the intervals were shifted toward higher concentrations: $0.11 - 0.32 \mu\text{g kg}^{-1}$ and $0.14 - 0.30 \mu\text{g kg}^{-1}$ for Be and U respectively.

The following REE were quantified in dry-cured ham samples: Nd ($0.40 - 1.25 \mu\text{g kg}^{-1}$), Gd ($0.12 - 1.43 \mu\text{g kg}^{-1}$), Pr ($0.11 - 0.33 \mu\text{g kg}^{-1}$), Sm ($0.077 - 0.31 \mu\text{g kg}^{-1}$), Dy ($0.071 - 0.25 \mu\text{g kg}^{-1}$), Yb ($0.45 - 0.24 \mu\text{g kg}^{-1}$), Eu ($0.029 - 0.13 \mu\text{g kg}^{-1}$), Ho ($0.019 - 0.074 \mu\text{g kg}^{-1}$), Tb ($0.017 - 0.059 \mu\text{g kg}^{-1}$), and Tm ($0.012 - 0.045 \mu\text{g kg}^{-1}$). The measurement uncertainties of analytical determination of these elements were in the relatively higher range of 10-23% (RSD) due to low concentrations. The lowest content of detected REE (except Gd, Ho, Tm) were observed in the Bayonne ham.

D.2.2. Variability of elements composition of dry-cured ham

The studied Iberian ham was characterized by the largest variability in concentrations of most analyzed elements. This could be caused by following reasons: a) it is the largest group of samples, b) considerable territorial distribution of production zones; c) differences in animal's nutrition and ham preparation process. However, some observations can be made. The Zn concentration in samples produced in Huelva were higher and varies within the interval $97.2 - 143 \text{ mg kg}^{-1}$ with mean value of 122 mg kg^{-1} , while for other Iberian hams the span of Zn concentration was $56.4 - 78.1 \text{ mg kg}^{-1}$ (Table D.3, with the exception of samples from Avilla, also evaluated for Zn at the level of 127 mg kg^{-1}). It has been previously noted for the Parma dry-cured ham, that some trace elements like Zn and Fe seemed to be associated with the protein content of meat, such as Zn-porphyrin - a protein, have been founded formed gradually during the whole processing period of the ham, but most importantly increases during maturation (Adamsen, et al., 2006A). Except for Zn, no any other geographical origin depending patterns in the elemental distribution among studied Iberian hams were revealed. Five samples from Huelva were characterized by a large variation of elemental content (Table D.3, at the end of the Chapter).

As regard to trace elements composition for regional classification purposes, some notable particularities can be attributed to the French Bayonne ham. First, these ham samples are characterized by a minimal concentrations of numbers of elements, such as Be, Al, Sc, Co, Ni, As, Y, Cd, Ba, Pb, U, Pr, Nd, Eu, Sm. The lower contents of following elements - Pb, U, Cd, Ni and As can be interpreted as a possible result of a lesser anthropogenic (or industrial) impact on animals during their growth and nutrition. Earlier, REE have been considered as promising natural feed additive for maintaining and improving performance levels in animal husbandry in certain

countries (He et al., 2010), and, from the other hand, REE have been advised as powerful discriminant characteristics for the geographical discrimination of vegetable samples (Brunner et al., 2010). Despite of the fact that three studied samples of Bayonne ham were produced independently and geographically distant from each other, the concentrations of determined REE (except Gd) were characterized by very close values, which can be the result of applying the same norms to the animals feeding within the same consortia of production.

The elements such as Li, Mn, Sr, Rb, Tl are presented in the Bayonne ham in concentrations notably higher than in other investigated hams, that may be related to animal husbandry, but also to features of dry-curing process, and especially, salting. The exact reason of elevated concentrations of above-mentioned elements can be found only through determination of trace elemental content of raw meat source. This distinguishing elemental composition of Bayonne ham has a great potential to be further studied in terms of its application to authenticity of this brand cured hams.

The use of ratio Rb/Sr as a parameter depended on the geochemical composition of soil has been found useful to geographical origin discrimination among vegetable samples (Brunner et al., 2010). Obviously, for food products of animal origin the ratio Rb/Sr reflects to a greater extent the geographical provenance of feed and could be useful in case of strong nutrition control applied. For studied Iberian hams this ratio varies to a large extent, from 3.3 to 33.6, for two Italian hams the values were - 4 and 12, and the narrower spread of the Rb/Sr for the French Bayonne ham - 3.3, 6.2, and 5.0 (Table D.3).

D.2.3. Elemental content of salt samples

As mentioned previously, salt is the main and often the only ingredient added in dry-curing, what evidently exerts an influence on the formation of trace elemental signatures in ham. According to features of dry-cured ham production, San Daniele, Parma and Iberian hams are salted with natural humid and/or dry sea salts (Ordóñez et al., 2007; Consorzio del Prosciutto di San Daniele; Consorzio del Prosciutto di Parma; Denominación de Origen Jamón de Huelva), while Bayonne ham is exclusively salted with mine salt from the local salt mine Salies-de-Béarn (South-West France) naturally crystallized in the basement of the basin of the Adour river approximately 200-100 million years ago (Consortium du Jambon de Bayonne). In this context, it seemed to be interesting to consider trace elemental compositions of different salts used in ham production.

In order to assess the potential link between the elemental content and the salting procedure associated with the production of ham, we present in Table D.4 the ranges of elemental concentrations in various types of salts and measurement uncertainties (RSD), arranged in order of decreasing mean concentrations. The highest elemental content were found in large colored crystal salts originated from mines Wieliczka, Salzkammergut (Alpine salt) and Semnan (Persian Blue). In studied salts, the iron levels ranged from 2.0 to 874 mg kg⁻¹ with the highest content dedicated to the salt from Wieliczka mine. The next highest iron concentration (403 mg kg⁻¹) was found in “Alaea” sea salt from Hawaii. Salt from Salies-de-Béarn present the lowest content of Fe in comparison with the other salt samples. The Sr concentrations in all salt samples ranged from 12.2 to 153 mg kg⁻¹, with maximal value found in Alpine salt. The salt from Salies-de-Béarn has a level of Sr comparable with other mining salt originating from Wieliczka, Andalusia, and sea salts from Camargue and Noirmoutier – about 80 mg kg⁻¹. Concentrations of Mn varied in the range of 0.21 – 9.43 mg kg⁻¹ for sea salts, and 0.27 – 37.2 mg kg⁻¹ for mining salts. Barium in sea salt samples ranged between 0.065 mg kg⁻¹ and 0.51 mg kg⁻¹, while for mining salts the minimal detected content was attributed to the flake salt Salies-de-Béarn - 0.015 mg kg⁻¹, and the maximal level of Ba reached 15 mg kg⁻¹ has been found in the salt from Wieliczka.

While all studied sea salt samples were characterized by the absence of detectable Tl, the mineral salts samples found to be significantly more enriched with this element, the maximal values were attributed to Persian blue salt (14.6 mg kg⁻¹) and for Alpine salt (14.2 mg kg⁻¹). In mining salts from Salies-de-Béarn and Wieliczka, Tl was found in concentrations about 6.5 mg kg⁻¹.

Another element that is very distinctive in the Bayonne ham is lithium. Except for the gray mining salt Wieliczka, the salt from Salies-de-Béarn presented the highest content of Li compared to all other samples – 0,99 – 1,37 mg kg⁻¹. Both these elements Tl and Li were also found to have the highest concentration in Bayonne ham compared to all other elements.

Concentrations of Zn varied from 0.31 mg kg⁻¹ (Persian Blue) to 3.40 mg kg⁻¹ (Cyprus). Concentrations of Rb were lower than limit of detection (LOD) for samples from Andalusia and Camargue, and maximal values found for Persian blue salt (1.59 mg kg⁻¹).

Small concentrations of several trace elements (<2 mg kg⁻¹) were found in the studied salts. Levels of Cu and V in the most of the samples ranged around 0.5-0.7 mg kg⁻¹, and 0.2-0.6 mg kg⁻¹ respectively, only Hawaiian “Alaea” salt contained 0.99 mg kg⁻¹ and 0.95 mg kg⁻¹, and “Wieliczka”

Table D.4. Elemental content and ratios $^{87}\text{Sr}/^{86}\text{Sr}$ in salt samples (mg kg^{-1}).

Element/ Parameter	Rock salt		Sea salt		Salt with highest content	Salt with lowest content
	maximum	minimum	maximum	minimum		
Fe	874	< 1,0	403	2,0	W, HW	SB, SB4
Sr	153	9,9	105	12,2	AL, N	SB4, C2
Mn	37,2	0,27	9,43	0,21	W, SB, SB4, G2	C2, PB, C1
Ba	15,0	0,015	0,51	0,065	W, AL	PB, SB4, CY, IR
Tl	14,6	< 2,5	< 2,5	< 2,5	PB, AL	K, AN and sea salts
Zn	3,78	0,31	3,40	1,03	SB, SB4, CY, HW	PB
Rb	1,59	0,063	0,81	0,041	PB, W, G1	C2, AN
Li	1,55	< 0,15	0,77	< 0,15	W, SB4, SB, G1	AN, PB, C2, N
Cu	1,53	0,46	0,99	0,47	W, HW	PB, G2
V	1,44	0,23	0,95	0,22	W, HW	SB, SB4, N, CY
Ni	1,08	< 0,05	0,96	< 0,05	W, CY	SB, SB4, PB, G2, C1, C2, IR
As	0,78	0,046	0,17	0,069	AL, W	SB, SB4, N
Pb	0,64	0,052	0,83	< 0,03	CY, W, AN	HW, PB
Co	0,32	< 0,01	0,14	< 0,01	W, HW	SB, SB4, PB, G2, C1, C2, N, IR, CY
Cs	0,13	< 0,02	0,056	< 0,02	W	K, AN, PB, most of sea salts
Cd	0,063	< 0,01	< 0,01	< 0,01	AN	most of rock- and sea salts
$^{87}\text{Sr}/^{86}\text{Sr}$	0,70839	0,70712	0,70918	0,70904	AL	C2, G2

AL - Alpine rock salt, AN - Andalusian rock salt, SB – gross salt Salies-de-Béarn (average), SB4 – flake salt Salies-de-Béarn, C1 – gross salt Camargue, C2 – flake salt Camargue, CY - Cyprus, G1 – gross salt Guérande, G2 – flake salt Guérande, HW – Alaea salt, IR – flake salt Île de Ré, K – gross salt Khewra, N – flake salt Noirmoutier, PB – gross salt Persian Blue, W – gross salt Wieliczka.

1.53 mg kg^{-1} and 1.44 mg kg^{-1} , respectively for Cu and V. The maximum levels of Ni were found to be around 1 mg kg^{-1} for both types of salt. Arsenic was detected at the concentrations below 0.2 mg kg^{-1} , with the exception of two mining salts: “Alpine” (0.78 mg kg^{-1}) and “Wieliczka” (0.62 mg kg^{-1}). Most of the studied salts contained Pb at the level lower than 0.3 mg kg^{-1} . In two mining salts Pb levels were detected around 0.64 mg kg^{-1} (Wieliczka, Andalusia), and maximal concentration was attributed to Cyprus sea salt (0.83 mg kg^{-1}). Negligible amounts of Co and Cs were detected in sea salt from Guérande and in some of mining salts, for the rest, the concentrations of these elements were reported below the LOD. Concentrations of Cd were detected only for Andalusia salt (0.063 mg kg^{-1}). Concentrations of Cd, Pb, Cu and As in the studied sea salt samples are consistent with those described in Galvis-Sánchez et al. (2013). All individual elemental concentrations of salts can be seen in Table D.5 and D.6, at the end of this Chapter.

D.3. Strontium isotopic signatures

D.3.1. $^{87}\text{Sr}/^{86}\text{Sr}$ in dry-cured hams

The ratios $^{87}\text{Sr}/^{86}\text{Sr}$ in dry-cured hams were determined by MC-ICP-MS and is presented in Table D.2. The variation range of $^{87}\text{Sr}/^{86}\text{Sr}$ for all the samples changed between 0.70854 and 0.70956. The individual mean values attributed to different brands of dry cured ham were respectively: 0.70855 ± 0.00006 – Bayonne ham; 0.70928 ± 0.00020 – Iberian ham; 0.70925 ± 0.00008 – Parma ham, and 0.70923 ± 0.00008 – San Daniele ham (measurement uncertainties presented as 2SD from triplicates). We can immediately notice that the Bayonne ham has the Sr isotope signature highly significantly distinctive from the other studied dry-cured hams (p -value < 0.001), whereas between Italian and Iberian ham no significant differences were observed (p -value > 0.5).

In the absence of published data for $^{87}\text{Sr}/^{86}\text{Sr}$ ratios in any pork, we have compared the obtained results with those available for European raw beef. According to Rummel et al. (2012), the $^{87}\text{Sr}/^{86}\text{Sr}$ ratios in raw non-processed meat varied to a large extent. For sample originating from Limousin, France, the interval of values was 0.71043 – 0.71347, from Trentino, Italy: 0.70628 – 0.71042, from Tuscany, Italy: 0.70877-0.71572, and from Barcelona, Spain: 0.70897-0.71399. These large spread of $^{87}\text{Sr}/^{86}\text{Sr}$ ratios in animal tissues reflect the variation of Sr in the aggregate of surrounding things were the animals were raised, including feeding, nutrition, and water in the course of husbandry as essential factors for Sr isotope ratios formation in the raw material, although also atmospheric and/or agricultural impact can be expected (Rummel et al., 2012; Franke et al., 2008). In the case of pig farming sector designated for food production labeled by PDO/PGI, the feeding regimes are strictly controlled within consortia regulations. For the PGI dry-cured ham production, the quality of ham is related with famous free-range-reared Iberian pigs fed on acorns found on selected and limited pasturelands, while the intensively-reared white Bayonne pigs are fed mostly on corn exclusively from South-West of France. These differences will therefore be reflected in the Sr isotopic signatures in their tissues and will represent both the origin and the feeding habits. In the case of the Iberian pigs it will be closely matching the local geological settings since the pigs feed on selected food coming from specific areas.

The fact that we have found a relatively narrow variation of $^{87}\text{Sr}/^{86}\text{Sr}$ in studied dry-cured hams compared to the data of Rummel et al. (2012), raised the question about potential influence from ingredients added during preparation process.

D.3.2. $^{87}\text{Sr}/^{86}\text{Sr}$ in salts

In order to assess the potential link between the ratio $^{87}\text{Sr}/^{86}\text{Sr}$ in cured hams and this in salts, we have closely examined the Sr isotopic composition of studied salts. Indeed, Sr is one of the major constituents of the salts (Table D.4). The salting may alter the Sr isotope ratio of the initial food product, as it has been shown on example of kimchi salad (Bong et al., 2012) and sturgeon caviar (Tchaikovsky et al., 2015). Indeed, it is worthwhile mentioning that origin of salt used in dry-curing is important for certain PDO/PGI (Consortium du Jambon de Bayonne). Iberian, San-Daniele and Parma hams are salted with sea salts, while the Bayonne ham is salted exclusively with mining salt from Salies-de-Béarn. These facts make the ratio $^{87}\text{Sr}/^{86}\text{Sr}$ in different salts and its contribution to the Sr isotopic composition in cured hams an interesting case study.

The results of Sr isotopic analysis of salt samples can be seen in Table D.4 (minimal and maximal values for sea and rock salts), all individual data is presented in Table D.5 (rock salts), D.6 (sea salts). All sea salt samples showed no significant variations in Sr isotope ratios among different origins (p -value = 0.98). The mean of $^{87}\text{Sr}/^{86}\text{Sr}$ in sea salts is 0.70913 ± 0.00010 , which is expectedly close to those for actual seawater - 0.709176 ± 0.000003 (Allègre et al., 2010). However, the $^{87}\text{Sr}/^{86}\text{Sr}$ ratio in rock salt samples largely varied, and moreover, all individual values were significantly lower compared to those of sea salt samples. The minimal value was obtained for Alpine salt from Salzkammergut - 0.70712 ± 0.00008 . Himalayan salt and Persian blue salt have close values: 0.70794 ± 0.00010 and 0.70790 ± 0.00010 , respectively. Three salt samples present similar values of $^{87}\text{Sr}/^{86}\text{Sr}$: Andalusian rock salt, salt from Wieliczka and from Salies-de-Béarn, their values are respectively - 0.70835 ± 0.00010 ; 0.70839 ± 0.00010 ; and 0.70840 ± 0.00007 . The reason for difference in Sr isotopic compositions between mineral and sea salts is closely related to the origins. The rock salt, known also as halite, is traditionally mined from abundant salt caves that were formed millions years ago as ocean salt settled in certain geologic pockets during substantial transformations in the geological structure of the Earth's crust. Obviously, mineral rock salt preserved the elemental and isotopic compositions of sea water of the period of its formation. Many studies have been dedicated to the determination of Sr isotopic compositions of pre-historical sea water and they have noted that the value $^{87}\text{Sr}/^{86}\text{Sr}$ varied to a large extent from 0.7068 up to 0.7091 (e.g., Jones et al., 1994; Koepnick et al., 1985). The geological formation of the salt deposit Salies-de-Béarn relates to the ages of Jurassic and Trias Period of Mesozoic Era, according to Curnelle (1983). At that time, the Sr isotope ratio in sea water changed in the range of 0.7070 – 0.7080 (Jones et al., 1994; Koepnick et al., 1985). This is in good agreement with Sr isotope ratio measured in the salt samples from Salies-de-Bearn, which is 0.70838 ± 0.00012 .

D.4. Is strontium in ham mostly sourced from salt?

The small spread of $^{87}\text{Sr}/^{86}\text{Sr}$ values of dry-cured hams and corresponding salt could be evidenced in Fig. D.2A and D.2B. From Fig. D.2A, it can be clearly seen that four groups of hams can be distinguished by their respective increasing $^{87}\text{Sr}/^{86}\text{Sr}$ ratios. The first group of ham with the lowest values is represented by the Bayonne ham samples B1, B2, B3 (0.70854 - 0.70858). Next to it is the group contained Iberian hams origin Seville (IS1), Avila (IA) and Badajoz (IB) with the values of $^{87}\text{Sr}/^{86}\text{Sr}$ ratios between 0.70898 and 0.70903. The third group includes Iberian hams origins Seville (IS2), Huelva (IH2, IH3, IH5), and Italian hams San Daniele (SD), and Parma (PM), they have the $^{87}\text{Sr}/^{86}\text{Sr}$ values in the range of 0.70923 – 0.70928. The highest values of $^{87}\text{Sr}/^{86}\text{Sr}$ (0.70947 – 0.70956) were obtained in the fourth group assigned Iberian hams origins Estremadura (IE), Huelva (IH1, IH4) and Alentejo (IAJ). Three comparative lines have been also plotted on Fig. D.2A and D.2B representing the ratio $^{87}\text{Sr}/^{86}\text{Sr}$ in modern seawater (Allègre et al., 2010), pre-historical ocean (Koepnick et al., 1985), and water catchment in area close to the mine Salies-de-Béarn (Martin et al., 2013).

Despite of the small variability between the samples from groups #2 (IS1, IA, IB), #3 (IS2, IH2, IH3, IH5, SD, PM), and #4 (IE, IH1, IH4, IAJ), which are almost limited by the measurement uncertainties, the mean value of the ratio $^{87}\text{Sr}/^{86}\text{Sr}$ of all Iberian and Italian ham samples (0.70928) is centered around to the mean ratio $^{87}\text{Sr}/^{86}\text{Sr}$ of studied sea salts samples (0.70913) and those of actual sea water (0.70918) (Fig. D.2A and D.2B). On the contrary, we can see the mean value of the ratio $^{87}\text{Sr}/^{86}\text{Sr}$ of the Bayonne hams correlates with those in the salt from Salies-de-Béarn and those in stream waters originating from the water catchment of Salies-de-Béarn (0.70855, 0.70840, and 0.70850, respectively). These results clearly highlight that: 1) the Sr isotope ratio in ham is mainly controlled by the curing process; and 2) the signature of the Sr isotope ratio is closely linked to the type of and origin of salt used in the curing process.

However, for Iberian hams a slight positive shift of the ratio $^{87}\text{Sr}/^{86}\text{Sr}$ (samples IE, IH1, IH4, IAJ), or a slight negative shift of the ratio $^{87}\text{Sr}/^{86}\text{Sr}$ (samples IS1, IA1, IB) can be observed with regards to the $^{87}\text{Sr}/^{86}\text{Sr}$ in sea salt. These slight Sr isotopic differences could reflect the individual variabilities of $^{87}\text{Sr}/^{86}\text{Sr}$ ratios in the raw material from the different origins.

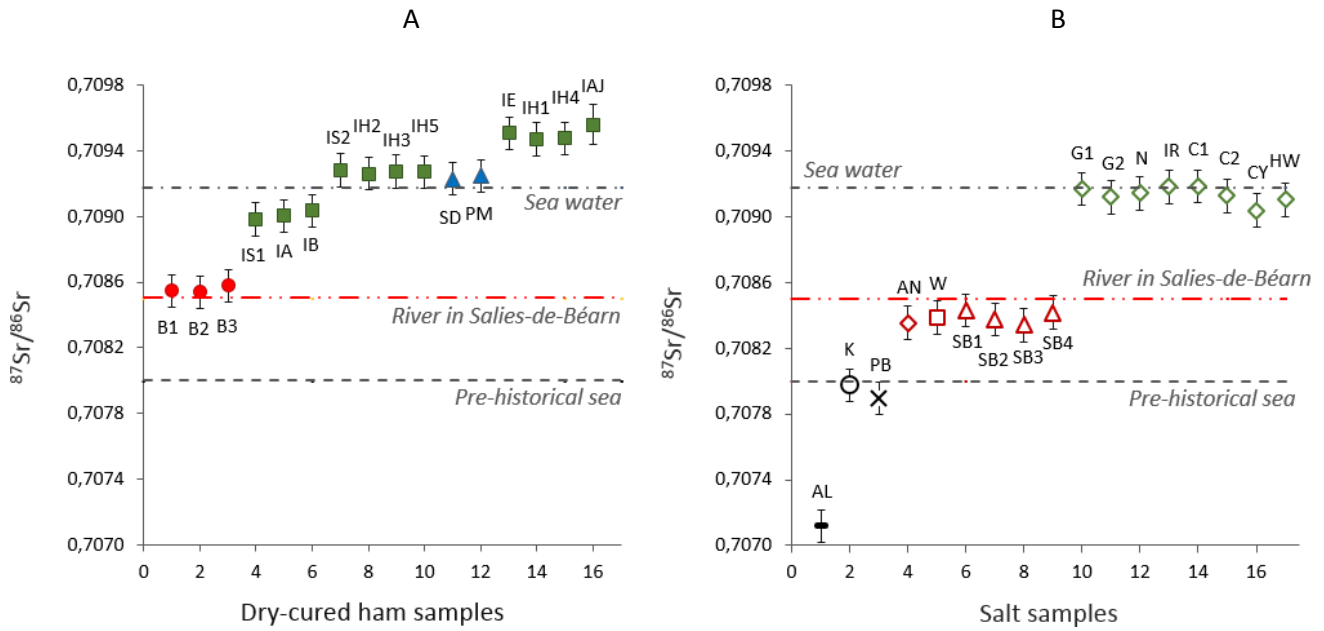


Fig. D.2. Sr isotope ratios in dry-cured ham and salt samples. (A) - $^{87}\text{Sr}/^{86}\text{Sr}$ in dry-cured ham samples; (B) - $^{87}\text{Sr}/^{86}\text{Sr}$ in salt samples. ● - Bayonne ham (B1, B2, B3); ■ - Iberian ham origin Seville (IS1, IS2), Avila (IA), Badajoz (IB), Huelva (IH1, IH2, IH3, IH4, IH5), Alentejo (IAJ); ▲ - Italian ham San Daniele (SD), Parma (PM); line “Sea water” - $^{87}\text{Sr}/^{86}\text{Sr}$ in actual sea water 0.709176 (Allègre et al., 2010); line “Pre-historical sea” - the upper limit of ratio $^{87}\text{Sr}/^{86}\text{Sr}$ in the Jurassic-Trias period - 0.7080 (Koepnick et al., 1984); line “River in Salies-de-Béarn” - ratio $^{87}\text{Sr}/^{86}\text{Sr}$ in water catchment in area of salt mine Salies-de-Béarn - 0.70850 (Martin et al., 2013); (■) - rock salt from Alps (AL), (○) - rock salt from Khewra, Himalaya (K), (×) - Persian blue salt (PB), (◇) - Andalusian rock salt (AN), (□) - salt from Wieliczka salt mine (W), (△) - salt Salies-de-Béarn (SB1, SB2, SB3, SB4), (◇) - sea salts in order on the graph: flake salt Guérande (G1), gross salt Guérande (G2), flake salt Noirmoutier (N), flake salt Île de Ré (IR), flake salt Camargue (C1), salt fine Camargue (C2), sea salt Chypre (CY), sea salt Hawaii (HW). The errors bars present the maximal measured uncertainties of individual triplicates (2SD).

The hypothesis that the Sr isotopic composition of salt do the major contribution to the $^{87}\text{Sr}/^{86}\text{Sr}$ ratio of dry-cured ham can be evident from the scatter plot (Fig. D.3) with strong positive correlation between $^{87}\text{Sr}/^{86}\text{Sr}$ ratios in dry-cured hams and those from the salt samples, showing that the ratio in different type of salt used for curing substantially defines this parameters in cured ham. In this respect, the Bayonne ham clearly stands out with a distinct signature with respect to all other hams.

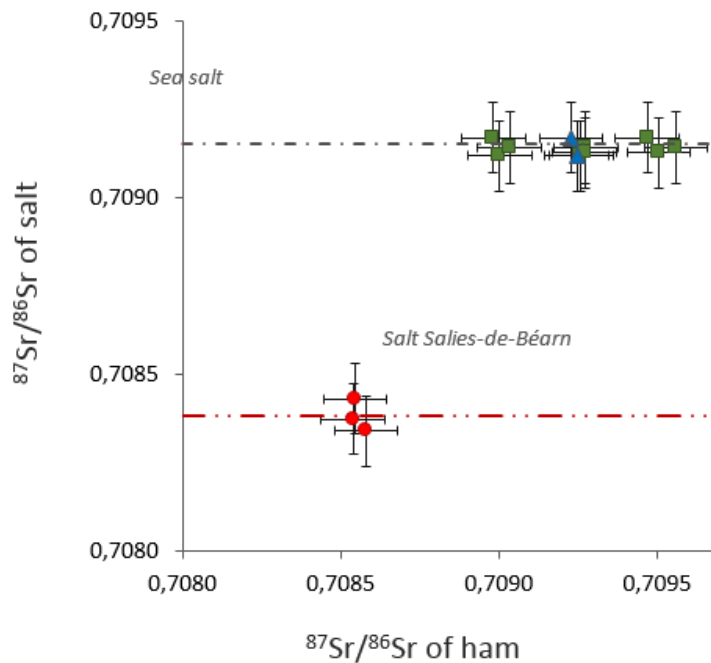


Fig. D.3. Correlation of Sr isotope ratios in dry-cured ham and salt samples. ● - Bayonne ham; ■ - Iberian ham; ▲ - Italian ham; line “Sea salt” - mean value of the ratio $^{87}\text{Sr}/^{86}\text{Sr}$ in the studied sea salt samples - 0.70913 ± 0.00010 (this study); line “Salt Salies-de-Béarn” - mean value of the ratio $^{87}\text{Sr}/^{86}\text{Sr}$ in studied salt from Salies-de-Béarn - 0.70840 ± 0.00007 (this study). Values of $^{87}\text{Sr}/^{86}\text{Sr}$ of salts are randomly distributed between ham samples. The errors bars represent the maximal measured uncertainties of individual triplicates (2SD).

D.5. Statistical approach

Multivariate data analysis applied to elemental and isotope data treatment of raw meat has allowed to solve a variety of questions regarding authenticity and geographical origin determination (e.g. González & De La Guardia, 2013a; Kreitals et al., 2014; Kim et al., 2017). Different objectives of food control analysis define the specific strategy of statistical data treatment and generally required a large selection of studied samples and authentic reference materials. In considering limited number of samples in this study, we examined only discrimination of hams by its geographical provenance. We have treated all elemental and Sr isotope information by principal component analysis (PCA) using the freeware Excel add-in PopTools v 3.2 with the goal to evaluate discriminating potential of trace elemental and Sr isotopic compositions of hams. These results are presented on Fig. D.4A and D.4B.

In figure 4A, the scatter PCA plot which with two components (PC1, PC4) indicates that the Bayonne ham can already be distinctively identified with respect to other hams when using only the elemental concentrations displayed in Table D.3. The variables PC1 and PC4 represents 39% and 10% respectively of the total variance and were chosen because they enabled a better discrimination between the different ham origins. The Iberian and Italian hams are somewhat overlapping. Also the discrimination between Italian and Iberian ham is not clear. In order to obtain better discriminating impact on the origin of the ham, we have added the statistical weight of the $^{87}\text{Sr}/^{86}\text{Sr}$ values and the occurrence of selected trace elements with higher discriminating potential such as Li, Cu, Ni, Sr, Cd, Pb. The results are presented in Fig. D.4B with two components PC1 (34%) and PC4 (13%). It clearly shows the better discrimination: the origin of the Bayonne ham is distinctly separated and fully identified. Despite of the limited number of samples, here also, the grouping tendency can be seen for the Iberian hams of Huelva origin and Italian hams.

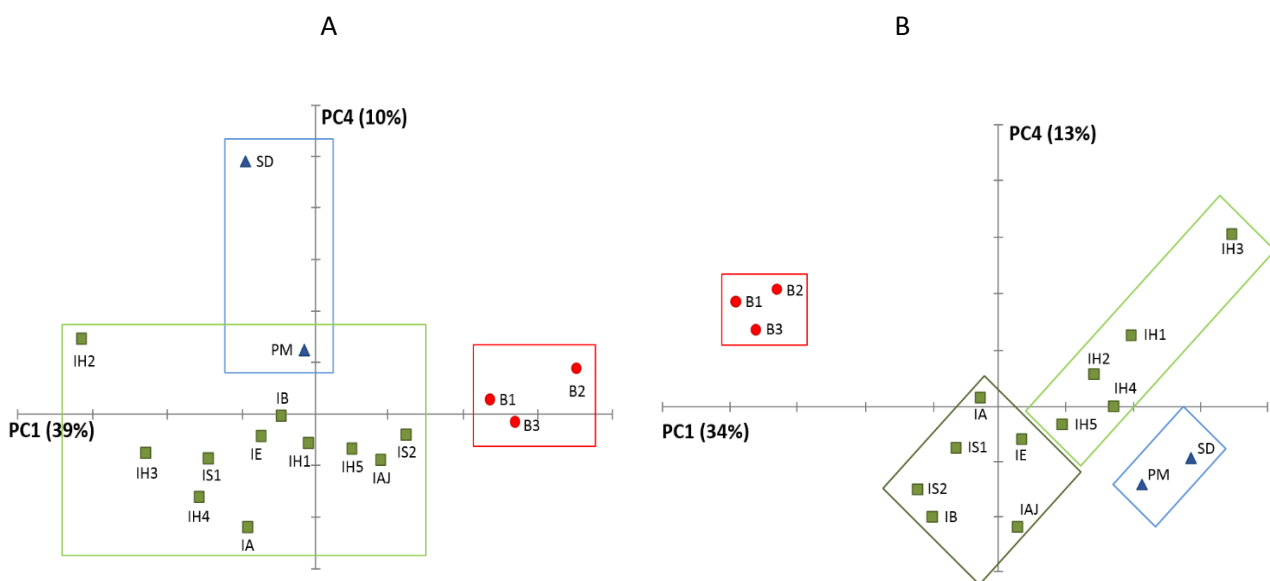


Fig. D.4. PCA for discrimination of dry-cured ham's geographic origin: (A) - Only multielemental data of Cu, Ni, Cd, Pb; (B) - $^{87}\text{Sr}/^{86}\text{Sr}$ and concentrations of Sr, Li. ● - Bayonne ham (B1, B2, B3); ■ - Iberian ham origin Seville (IS1, IS2), Avila (IA), Badajoz (IB), Huelva (IH1, IH2, IH3, IH4, IH5), Alentejo (IAJ); ▲ - Italian ham San Daniele (SD), Parma (PM).

D.6. Conclusion

Multi-elemental and Sr isotopic composition of some of most renowned European cured hams, such as Iberian, Bayonne, Parma and San Daniele, were investigated. The main objective was to find the most discriminant parameters for their geographic origin determination. As in cured ham production, the only additive ingredient is salt, the elemental and Sr isotopic composition of salts of different geographic origin (France, Austria, Poland, Spain, Pakistan, Iran, Chypre) and way of production (sea and mine salts) were also analyzed. The 34 trace and ultra-trace elements were determined by Q-ICP-MS. A total of 19 trace and ultra-trace elements differed significantly among the studied hams. The most significant deviation was observed for the Bayonne ham. Trace elements such as Sr, Tl, Li were considered as the most distinctive constituents of hams, originated mostly from salt used in dry-cured process. The following Sr isotope analysis by MC-ICP-MS determined the $^{87}\text{Sr}/^{86}\text{Sr}$ ratios in the studied hams ranged from 0.70854 to 0.70858 for Bayonne ham and 0.70898 – 0.70956 for Iberian, San Daniele and Parma hams. It was found out that Bayonne ham has a characteristic elemental and Sr isotopic fingerprint due to the salt used for its production.

The distinctive potential of the $^{87}\text{Sr}/^{86}\text{Sr}$ ratio testifies the considerable improvement for fingerprinting proposes of Bayonne ham and it can be also a useful parameter for distinguishing the cured hams origins Spain and Italy. However, for better representativeness of the data, a large homogeneous sample selection is required. Based on the obtained results, we can conclude that the discrimination among the different origin for dry-cured ham is the result of both raw meat elemental/isotopic content and processing practices. Further research is needed to study authentic dry-cured hams, as well as raw meat and salt to evaluate salt contribution to the elemental and Sr isotopic composition of dry-cured ham. Such study can help to establish specific characteristics of cured meat products for authenticity tracing purposes, provenance confirmation and/or counterfeit detection.

Food Chemistry 246 (2018) 313–322



$^{87}\text{Sr}/^{86}\text{Sr}$ isotope ratio and multielemental signatures as indicators of origin of European cured hams: The role of salt

Ekaterina N. Epova^{a,b,*}, Sylvain Bérail^a, Tea Zuliani^c, Julien Malherbe^a, Laurence Sarthou^b, Manuel Valiente^d, Olivier F.X. Donard^a

^a LCABIE, UMR UPPA-CNRS 5254 IPREM, Hélioparc, 2 avenue Président P. Angot, 64053 Pau, France

^b Laboratoires des Pyrénées et des Landes, rue des Écoles, 64150 Lagor, France

^c Jozef Štefan Institute, Jamova cesta 39, 1000 Ljubljana, Slovenia

^d The Autonomous University of Barcelona, Chemistry department, Centre GTS, Campus de la UAB, Edifici CN, 08193 Bellaterra, Barcelona, Spain

Table D.3. Elemental content and Sr isotope ratio in individual dry-cured ham samples.

Element/ Parameter	Iberian ham								RSD*/2SD**
	IS1	IA	IB	IS2	IE	IH1	IH2	IH3	
Trace elements, mg/kg									
Zn	78,1	127	56,4	59,1	65,7	129	123	143	2,8
Fe	33,7	61,1	24,6	30,0	38,6	59,1	57,7	75,9	2,5
Rb	10,0	9,20	5,77	10,8	13,2	17,9	13,0	15,0	3,2
Cu	2,44	3,47	1,88	1,88	4,90	4,42	3,39	4,99	2,4
Sr	0,86	0,27	0,72	0,83	1,27	1,31	3,97	1,75	3,1
Al	1,80	1,65	1,33	1,69	1,11	1,46	2,61	1,60	6,8
Ultra-trace elements, µg/kg									
Mn	449	334	228	224	372	563	470	784	2,9
Se	271	378	228	227	177	441	357	437	5,8
Ni	198	99,0	100	110	120	136	124	141	6,0
Cs	33,5	17,2	18,2	386	264	574	48,2	163	3,7
Cr	97,5	101	85,5	116	108	141	109	86,1	3,8
Ba	103	56,5	71,9	130	56,9	61,1	175	149	5,9
Li	30,1	16,6	15,7	21,5	26,3	29,5	72,6	33,6	4,6
As	35,6	21,9	26,2	90,9	109	41,2	114	93,4	7,1
Pb	49,2	14,5	44,6	23,0	125	88,6	82,9	44,5	6,3
V	39,7	36,2	15,3	24,2	27,7	31,4	32,0	36,3	2,7
Cd	18,2	8,20	37,2	8,28	5,42	11,4	59,3	31,3	5,2
Sc	14,5	16,3	16,5	14,7	14,8	14,8	15,4	15,8	10,6
Co	3,79	5,62	8,18	4,54	4,19	9,75	20,6	7,32	4,1
Ga	5,90	6,70	5,18	6,14	5,53	6,34	10,38	7,89	6,7
Tl	0,26	0,12	1,10	1,65	0,69	2,05	0,32	1,27	4,0
Y	2,74	1,14	1,24	1,08	0,80	1,28	2,27	1,85	5,2
Nd	1,25	0,71	0,75	0,82	0,51	0,87	1,19	1,12	8,7
Gd	0,43	0,33	0,28	0,49	0,25	0,24	0,93	0,36	10,6
Pr	0,28	0,18	0,20	0,18	0,15	0,24	0,33	0,31	7,3
Be	0,29	0,17	0,18	0,11	0,32	0,16	0,26	0,20	13,2
U	0,27	0,14	0,27	0,20	0,28	0,23	0,30	0,23	12,2
Sm	0,28	0,11	0,10	0,13	0,10	0,15	0,22	0,31	12,8
Dy	0,25	0,12	0,13	0,15	0,12	0,18	0,19	0,20	13,2
Yb	0,12	0,082	0,070	0,11	0,075	0,11	0,13	0,11	14,5
Eu	0,078	0,046	0,060	0,082	0,056	0,085	0,12	0,098	15,0
Ho	0,052	0,028	0,025	0,034	0,041	0,066	0,045	0,049	9,3
Tb	0,042	0,033	0,029	0,033	0,038	0,059	0,052	0,045	13,7
Tm	0,026	0,015	0,012	0,024	0,023	0,040	0,018	0,026	23,8
Rb/Sr	11,7	33,6	8,0	13,0	10,4	13,7	3,3	8,5	-
⁸⁷ Sr/ ⁸⁶ Sr	0,70898	0,70900	0,70903	0,70928	0,70951	0,70947	0,70926	0,70927	0,0001**

* - Analytical uncertainties for trace metal analysis are presented as the maximal RSD (%) value of individual triplicates.

** - Analytical uncertainties for isotopic analysis are presented as the maximal SD value of individual triplicates.

Table D.3. Elemental content and Sr isotope ratio in individual dry-cured ham samples (Continued).

Element/ Parameter	Iberian ham			Bayonne ham			San Daniele	Parma	RSD*
	IH4	IH5	IAJ	B1	B2	B3	SD	PM	2SD**
Trace elements, mg/kg									
Zn	118	97,2	62,1	92,3	97,5	83,2	74,5	83,3	2,8
Fe	53,5	40,8	29,7	34,9	27,2	26,8	31,3	31,5	2,5
Rb	11,4	15,8	10,2	15,0	23,1	14,6	17,9	18,3	3,2
Cu	3,13	3,41	1,96	2,63	1,79	2,01	2,07	2,44	2,4
Sr	0,88	1,08	1,24	4,58	3,73	2,93	4,48	1,52	3,1
Al	1,27	1,11	1,37	0,29	0,53	0,26	2,53	1,79	6,8
Ultra-trace elements, µg/kg									
Mn	328	324	235	881	365	586	304	338	2,9
Se	221	346	194	295	336	312	377	361	5,8
Ni	65,1	72,1	56,2	33,7	31,1	32,0	2314	736	6,0
Cs	115	229	125	105	124	89,6	440	88,8	3,7
Cr	83,7	93,0	114	90,2	86,1	92,4	118	94,7	3,8
Ba	71,7	92,2	31,5	17,2	13,8	21,3	79,8	87,0	5,9
Li	31,3	28,5	19,7	148,7	210,8	66,4	39,1	19,8	4,6
As	53,0	65,5	57,9	9,9	8,8	6,9	30,0	16,0	7,1
Pb	20,4	19,3	15,2	5,9	4,2	6,8	61,1	74,4	6,3
V	32,5	37,2	18,1	39,8	37,8	27,7	39,0	44,6	2,7
Cd	16,0	28,7	11,5	1,3	2,6	2,3	55,1	43,8	5,2
Sc	15,2	12,3	15,1	12,3	12,0	12,7	18,4	13,7	10,6
Co	4,88	5,15	4,59	1,33	2,10	1,59	13,3	7,54	4,1
Ga	6,30	6,11	4,61	4,67	4,48	5,23	6,38	5,43	6,7
Tl	0,089	0,37	1,29	3,66	2,72	3,85	1,05	1,79	4,0
Y	1,48	1,28	2,23	0,70	0,89	0,64	1,46	1,89	5,2
Nd	0,73	0,85	0,79	0,40	0,61	0,41	1,02	1,14	8,7
Gd	0,26	1,43	0,96	0,14	1,17	0,12	0,31	0,55	10,6
Pr	0,18	0,24	0,25	0,12	0,15	0,11	0,27	0,31	7,3
Be	0,22	0,28	0,20	0,14	0,16	0,07	0,32	0,28	13,2
U	0,18	0,20	0,17	0,10	0,10	0,06	0,24	0,22	12,2
Sm	0,10	0,18	0,17	0,08	0,10	0,08	0,17	0,18	12,8
Dy	0,14	0,16	0,19	0,09	0,13	0,07	0,18	0,15	13,2
Yb	0,059	0,24	0,13	0,06	0,09	0,04	0,10	0,11	14,5
Eu	0,048	0,074	0,134	0,042	0,041	0,029	0,065	0,062	15,0
Ho	0,031	0,041	0,074	0,053	0,058	0,019	0,041	0,051	9,3
Tb	0,037	0,041	0,056	0,036	0,036	0,017	0,038	0,047	13,7
Tm	0,020	0,027	0,045	0,025	0,022	0,019	0,019	0,020	23,8
Rb/Sr	13,0	14,6	8,2	3,3	6,2	5,0	4,0	12,0	-
$^{87}\text{Sr}/^{86}\text{Sr}$	0,70947	0,70927	0,70956	0,70855	0,70854	0,70858	0,70923	0,70925	0,0001**

* - Analytical uncertainties for trace metal analysis are presented as the maximal RSD (%) value of individual triplicates.

** - Analytical uncertainties for isotopic analysis are presented as the maximal SD value of individual triplicates.

Table D.5. Elemental content and Sr isotope ratio in individual rock salts

Elements	Rock salt							RSD*/2SD**
	Salies-de-Béarn B1, B2, B3	Salies-de-Béarn B4	Khewra K	Wieliczka W	Andalusia AN	Alpine AL	Persian Blue PB	
As	0,050	0,046	0,075	0,62	0,072	0,78	0,060	11,1 - 25,1
Ba	0,046	0,015	0,48	15,0	0,150	1,79	0,025	1,3 - 12,0
Cd	0,009	0,007	< 0,006	0,007	0,063	< 0,006	< 0,006	12,3 - 14,3
Co	< 0,010	< 0,010	0,018	0,32	0,012	0,047	< 0,010	3,1 - 13,4
Cs	0,050	0,070	< 0,008	0,132	< 0,008	0,055	< 0,008	3,7 - 10,5
Cu	0,62	0,68	0,67	1,53	0,72	0,70	0,46	2,5 - 12,0
Fe	< 1,0	< 1,0	25,7	874	7,96	144	3,37	3,8 - 11,8
Li	0,99	1,37	0,48	1,55	< 0,15	0,34	< 0,15	2,5 - 20,2
Mn	10,9	10,8	1,20	37,2	3,80	4,65	0,27	2,0 - 10,3
Ni	0,038	0,020	0,073	1,08	0,079	0,14	0,028	5,3 - 20,6
Pb	0,08	0,084	0,093	0,64	0,63	0,24	0,052	1,4 - 13,0
Rb	0,44	0,60	0,16	1,10	0,063	0,53	1,59	3,1 - 8,9
Sr	72,8	9,9	19,5	77,9	69,4	153	15,8	1,8 - 5,6
Tl	5,73	6,60	< 2,5	6,53	< 2,5	14,2	14,6	4,6 - 10,0
V	0,23	0,27	0,35	1,44	0,33	0,42	0,29	1,5 - 20,7
Zn	3,78	3,36	2,14	2,41	1,88	1,40	0,31	4,8 - 12,8
87Sr/86Sr	0,70838	0,70842	0,70800	0,70839	0,70835	0,70712	0,70790	0,00009**

* - Analytical uncertainties for trace metal analysis are presented as the maximal RSD (%) value of individual triplicates.

** - Analytical uncertainties for isotopic analysis are presented as the maximal SD value of individual triplicates.

Table D.6. Elemental content and Sr isotope ratio in individual sea salts.

Elements	Sea salt								RSD*/2SD**
	Guérande G1	Guérande Fds G2	Camargue C1	Camargue FdS C2	Noirmoutier N	Île de Ré IR	Cyprus CY	Alaea HW	
As	0,17	0,10	0,075	0,077	0,069	0,11	0,083	0,080	11,1 - 25,1
Ba	0,47	0,080	0,19	0,10	0,26	0,071	0,065	0,51	1,3 - 12,0
Cd	< 0,006	< 0,006	< 0,006	< 0,006	< 0,006	< 0,006	< 0,006	< 0,006	12,3 - 14,3
Co	0,054	< 0,010	< 0,010	< 0,010	< 0,010	< 0,010	< 0,010	0,14	3,1 - 13,4
Cs	0,056	< 0,008	< 0,008	< 0,008	< 0,008	< 0,008	< 0,008	< 0,008	3,7 - 10,5
Cu	0,59	0,47	0,53	0,68	0,60	0,56	0,50	0,99	2,5 - 12,0
Fe	149	15,0	1,98	2,72	2,43	14,8	11,4	403	3,8 - 11,8
Li	0,77	0,49	0,17	< 0,15	< 0,15	0,58	0,58	0,23	2,5 - 20,2
Mn	5,87	9,43	0,33	0,21	3,06	5,12	4,76	4,81	2,0 - 10,3
Ni	0,53	0,050	0,053	0,051	0,096	0,052	0,96	0,57	5,3 - 20,6
Pb	0,56	0,22	< 0,02	0,13	0,070	0,26	0,83	< 0,03	1,4 - 13,0
Rb	0,81	0,27	0,11	0,041	0,11	0,36	0,35	0,16	3,1 - 8,9
Sr	44,1	43,5	72,0	12,2	105	41,8	33,0	13,7	1,8 - 5,6
Tl	< 2,5	< 2,5	< 2,5	< 2,5	< 2,5	< 2,5	< 2,5	< 2,5	4,6 - 10,0
V	0,58	0,26	0,30	0,31	0,22	0,31	0,23	0,95	1,5 - 20,7
Zn	1,79	1,63	1,03	2,23	1,75	1,26	3,40	3,09	4,8 - 12,8
87Sr/86Sr	0,70912	0,70917	0,70913	0,70918	0,70914	0,70918	0,70904	0,70910	0,00009**

* - Analytical uncertainties for trace metal analysis are presented as the maximal RSD (%) value of individual triplicates.

** - Analytical uncertainties for isotopic analysis are presented as the maximal SD value of individual triplicates

Chapter E

Geographic origin classification of tea by means of Sr-, Pb- isotopic and elemental compositions

E.1. Relevance of the issue

Tea is one the most recognized aromatic beverage in the world, historically originating from China, and mostly produced in Asia. Tea has well-known beneficial effects on health which are affected by many specific factors relating its growing and processing, such as varieties of the tea plant, soil, climate, altitude and type of fermentation. For this reason, one of the main questions of customers concerns its geographical origin and authenticity. Unfortunately, tea is one of those products that are subject to mislabeling, imitation and substitution. Differentiation of tea according to its origin can be achieved using several chemical parameters, such as elemental composition, amino acid contents, volatile components, catechins and purine alkaloids (McKenzie et al., 2010). Among

different methods commonly used to identify food geographical origin, the natural variations of Sr and Pb stable isotopes are relatively new analytical approaches (Balcaen et al., 2010). In a plant, both parameters are related to the environment of the place of growth: Sr isotopic composition reflects the soil and the general geological structure, the Pb isotopes trace environmental ambient pollutions in the region.

Stable isotope ratios of Sr have already been applied to classify Indian tea among different producing regions (Lagad et al., 2013). Apart from Indian tea, a large number of Japanese cereals and vegetables was examined for Sr isotopic compositions and a strong correlation of these values in plants and soil was reported (Ariyama et al., 2011; Ariyama et al., 2012; Hiraoka, 2016; Aoyama et al., 2017). With this respect, a successful assignment of vegetable's provenance was obtained (Aoyama et al., 2017). Detailed geochemical maps expressing areal distributions of $^{87}\text{Sr}/^{86}\text{Sr}$ ratio in the land surface have been published for several Japanese provinces (Asahara et al., 2006). Although the Sr isotopic specification of Chinese plants and vegetables is not described as extensively as for Japanese agricultural products, some studies reported a variability of $^{87}\text{Sr}/^{86}\text{Sr}$ values with a much larger span than those in Japan (Liu et al. 2016; Liu et al., 2017; Hiraoka, 2016).

In contrary to Sr isotope ratio method, there is no reliable results in food geographical origin classification by Pb isotopes in Asian products. However, namely the Pb isotopes approach has a greater distinctive potential for food provenance tracing in Asia. Although natural sources continuously release considerable amounts of Pb and in spite the phasing out of tetra-alkyl Pb in gasoline, Pb anthropogenic inputs are still much greater than natural sources and can contribute up to 80-90% from global Pb emissions (Komárek et al., 2008, Sen et al., 2012). Korea, China, and Japan are the most fastest-growing economies in East Asia, where most of the Pb in the atmosphere is derived from industrial and urban activities, such as mining, vehicular exhaust, fossil fuels, and combustion of Pb-containing coal (e.g., Mukai et al., 2001; Chen et al., 2005; Cheng & Hu, 2010). The Pb isotopic composition of a plant is sensitive to the local anthropogenic Pb inputs, and then can help to assign its geographical origin (Médina et al., 2000; Larcher et al., 2003; Mihaljevič et al., 2006; Ariyama et al. 2011; Mihaljevič et al., 2015). With this respect, the Pb isotope ratios in wines originating from Asia were found to be different from those in French wines (section C.3).

A particular interest on tea was deemed important because during growth it acquires an appropriate ensemble of geogenic and anthropogenic signatures of the environment of its origin, and, therefore, tea leaves may serve as an example of vegetable matrix for assessing the geographic provenance using regional environmental signatures of Pb and Sr.



Fig. E.1. Known geographical origins of Chinese teas including provinces: Yunnan (south west of China); Guangxi, Guangdong (south of China) and Fujian, Zhejiang, Anhui, Hubei, Jiangxi (east of China).

E.1.1. Geographical origins of tea samples

A total of sixty teas were obtained from specialized tea stores with exact provenance information, and from supermarkets with a clear indications of the country and/or the region of production. Detailed description of studied tea samples is presented in Table E.1, placed at the end of this chapter.

China and Taiwan

China is the biggest world producer and exporter of tea. Most of the studied teas were originated from following Chinese provinces: Fujian (n=6); Yunnan (n=4), Zhejiang (n=3), Anhui (n=2), Guangdong (n=2), Guangxi (n=2), Jiangxi (n=1), Hubei (n=1) and three samples of unknown origin, in total – 24 involved samples (Fig. E.1). From all Chinese teas concerned: one was a red tea, two were black teas, two teas were blue/green teas; two teas were semi-fermented, one tea was post-fermented Pu-Erh tea; one tea was certified as “organic” tea, and three tea samples contained aromatic additives (jasmin, bergamot, orange) at levels less than 0,5%. One sample of green tea from Taiwan was also involved in the study (Fig. E.1).

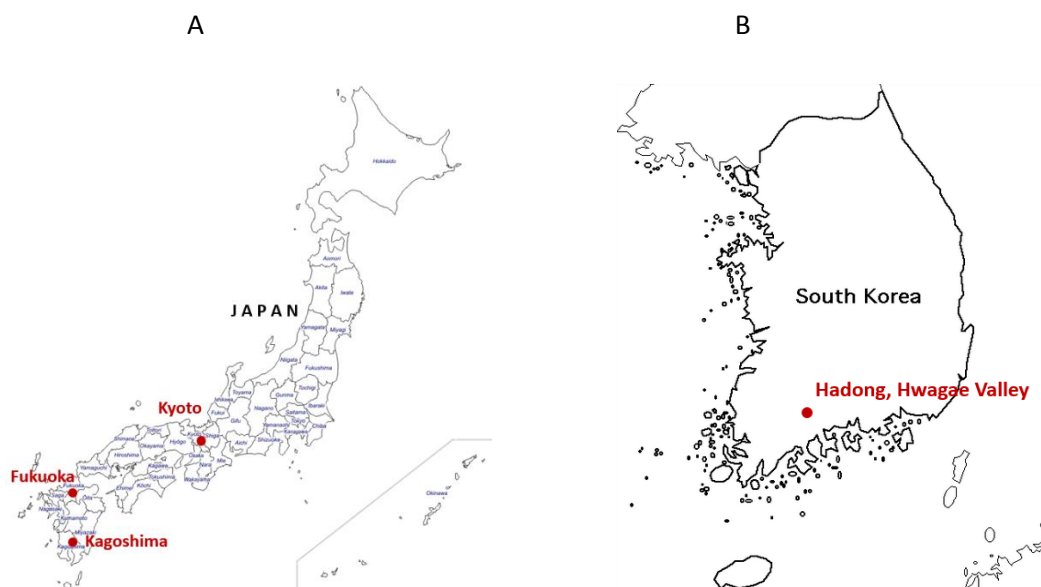


Fig. E.2. Known geographical origins of tea samples from Japan (A) and South Korea (B).

Japan

Japan is in the top of 10 tea-producing countries intended primarily for the Japanese market with a relatively small portion of tea exportation. However, some of Japanese teas are world famous and expensive, such as Gyokuro. In this study, thirteen teas from Japan were involved. The exact origins of samples were specified only for six of them: Kagoshima ($n=3$), Kyoto ($n=2$) and Fukuoka ($n=1$) as shown on Fig. E.2A. According to the Ministry of agriculture, forestry and fisheries of Japan (<http://www.maff.go.jp/e/>), these provinces are some of the biggest tea producing regions in country. The most famous fine quality Gyokuro tea is mostly growing in Fukuoka. The exact provenance for the rest six teas was unknown. Additionally, a certified reference material CRM 23 “Tea leaves” from National Institute for Environmental Studies, Japan was also included in the series of samples.

South Korea

Commercial production of green tea in South Korea is relatively recent. It began in 1970s and represents a minor amount compared to Japanese production; however this country has a strong individuality in tea cultivating and consumption. In this study, five samples of tea from a plantation in the Hadong, Hwagae valley (altitude 500 – 800 meters) were examined: one black tea (fermented), and four green teas. The geographical location of Hwagae valley can be seen on the Fig. E.2B.

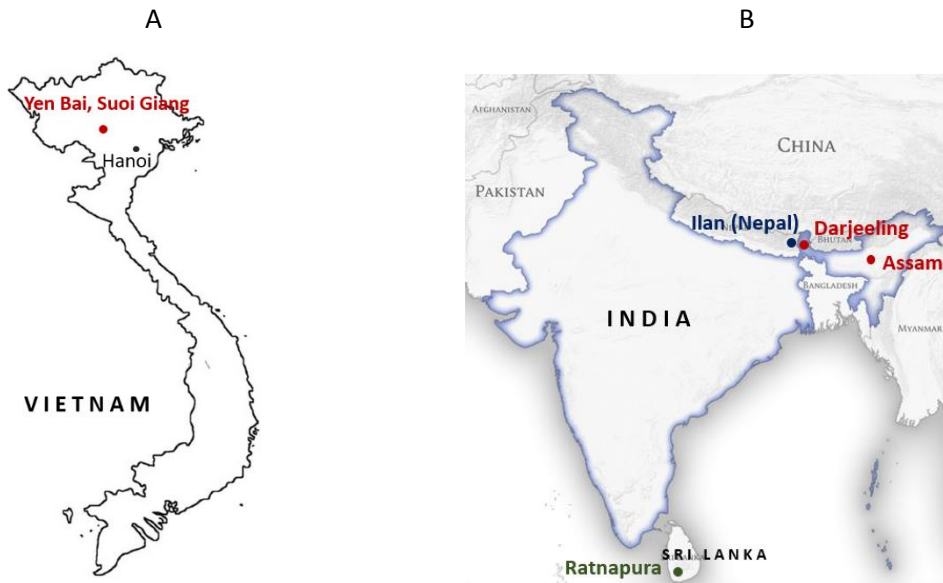


Fig. E.3. Known geographical origins of tea samples from Vietnam (A), India, Sri Lanka and Nepal (B).

Vietnam

Two green teas from a plantation on central highland in Vietnam - Suối Giàng, Văn Chấn District, Yên Bái Province, on the altitude of 1500-1700 m, located about 150 km north-west from Hanoi, were selected (Fig. E.3A). One sample was a regular “coarse plucking” tea - when along with the bud three or more mature leaves are harvested. The second sample was originated from the same plantation, however, it was a “fine plucking” tea - when only a bud and the two next tea leaves are removed.

India, Sri Lanka and Nepal

India is the second largest producer of tea in the world after China. The most famous Indian teas are from Assam and Darjeeling. A total, four Indian samples were involved in the study, one was a Darjeeling Organic tea from plantation of Gielle Khola (altitude is about 2000 m), district of Darjeeling, West Bengal state and one sample of Assam tea (Fig. E.3B). The exact provenance for the rest two teas was unknown.

Ceylon Tea is one of the main sources of foreign exchange for Sri Lanka. Among six samples of black tea, one was a low grown tea at altitude lower than 600 m from a plantation near to Ratnapura city, district of Ratnapura, Sabaragamuwa province (Fig. E.3B).

One sample of high grown white tea of Nepal origin, from a plantation geographically close to Darjeeling, was involved in the study (Fig. E.3B).



Fig. E.4. Geographical origins of tea samples from Turkey (A) and Rwanda (B).

Turkey

Tea plantations in Turkey are mostly located in the Rize Province on the eastern Black Sea coast (Fig. E.4A). Tea in Turkey is usually processed as black tea. In the present study, two samples of black tea “Rize çayı” were evaluated, one sample was certified as an “organic” tea.

Rwanda

Tea is a popular drink in Rwanda and also the largest export from the country. This study includes one green and one black tea from Kinihira, Rwanda, grown on a plateau within the altitude of 1900 m – 2500 m (Fig. E.4B).

E.2. Strontium isotopic compositions and Sr concentrations of teas

With the respect of objectives of this study, Sr isotopic compositions of all teas were determined. Sample preparation protocol following the matrix purification described in section B.1. The summary of Sr elemental content and $^{87}\text{Sr}/^{86}\text{Sr}$ ratios is presented in Table E.2, all values for individual samples are presented in Table E.3 at the end of the chapter.

The isotope ratio $^{87}\text{Sr}/^{86}\text{Sr}$ of tea leaves varied with the geographical origin to a large extent: for China 0.70532 - 0.74544; for Japan 0.70673 - 0.71070, for South Korea 0.71154 - 0.71632, for Sri Lanka 0.71345 - 0.71996, for India: 0.71345 - 0.79137, for Vietnam 0.73617 - 0.74035, for Turkey 0.70662 - 0.70671, for Rwanda 0.71381 - 0.71387, for Nepal 0.73640, and Taiwan 0.71104.

Elemental concentrations of Sr varied in the span of: 6.7 - 32.6 mg kg⁻¹ (China), 2.0 - 10.0 mg kg⁻¹ (Japan) 10.2 - 20.9 mg kg⁻¹ (South Korea), 7.3 - 15.6 mg kg⁻¹ (Sri Lanka), 9.5 - 30.4 mg kg⁻¹ (India), 7.7 - 10.4 mg kg⁻¹ (Vietnam), 16.6 - 25.1 mg kg⁻¹ (Turkey), 35.6 - 39.1 mg kg⁻¹ (Rwanda), 10.4 mg kg⁻¹ (Nepal) and 17.0 mg kg⁻¹ (Taiwan).

E.2.1. China and Taiwan

The $^{87}\text{Sr}/^{86}\text{Sr}$ ratios in Chinese teas varied greatly from 0.70532 to 0.74544, the highest value was attributed to a sample from Jiangxi, and the lowest value was found in a sample from Guangdong. The observed wide span of $^{87}\text{Sr}/^{86}\text{Sr}$ variability in Chinese tea samples is likely due to the exceptional complexity of geological structure of China, which has been formed over all geological epochs by the superposition of several intercontinental tectonic movements, which resulted in a complex lithologic constitution of the surface (Tingdong, 1980; Zhao & Cawood, 2012).

Until now, there are only few Chinese agricultural products that have been studied for Sr isotopic compositions, such as rice (Kawasaki et al., 2002; Ariyama et al., 2011), kimchi salad (Bong et al., 2012a), cabbage (Bong et al., 2012b), wheat (Liu et al. 2016; Liu et al., 2017), and onions (Hiraoka et al., 2016). And only two studies dealt with samples originated from specified geographical areas (Liu et al. 2016; Liu et al., 2017). In the study of Hiraoka et al. (2016) only provinces of sample origins are indicated, although a variability of geological settings within the same province can be significant. For example, Hiraoka et al. (2016) report the ratio $^{87}\text{Sr}/^{86}\text{Sr}$ in eleven onion samples from Yunnan (a province on southwest of China) be ranged from 0.71032 to 0.71742. In our study, four tea samples from the Yunnan province showed the $^{87}\text{Sr}/^{86}\text{Sr}$ ratio significantly higher: 0.71632 — 0.73254 (Fig. E.5A). However, $^{87}\text{Sr}/^{86}\text{Sr}$ ratios in geological rocks from Yunnan have been previously reported at a moderate high level from 0.7099 to 0.7136 (Zhou et al., 2013), and even at a relatively high level 0.7138 — 0.7170 (Zhou et al., 2001). Moreover, on the basis of kinetic and thermodynamic calculations of water/rock interactions, a theoretically possible value of about 0.745 of source rock $^{87}\text{Sr}/^{86}\text{Sr}$ in Yunnan was obtain (Zhou et al., 2001).

Table E.2. Mean values, minimum and maximum values of Sr elemental concentrations and $^{87}\text{Sr}/^{86}\text{Sr}$ ratios in tea samples.

Country	Production region / number of samples	Sr, mg/kg		$^{87}\text{Sr}/^{86}\text{Sr}$	
		range	mean value	range	mean value
China	Total / 24	6.7 - 32.6	15,1	0.70532 - 0.74544	0.71581
	Fujian / 6	8.9 - 17.8	13,1	0.70971 - 0.71909	0.71368
	Yunnan / 4	8.9 - 22.4	17,0	0.71632 - 0.73254	0.72318
	Zhejiang / 3	6.7 - 32.6	22,1	0.70809 - 0.71578	0.71076
	Anhui / 2	10.1; 10.7	10,4	0.71343; 0.71714	0.71528
	Guagdong / 2	15.8; 18.4	17,1	0.70532; 0.71073	0.70802
	Guangxi / 2	12.0; 13	12,5	0.71063; 0.71095	0.71079
	Jiangxi / 1	-	8,7	-	0.74544
	Hubei / 1	-	6,8	-	0.71173
Others / 3	13.1-27.5	18,1	0.71097 - 0.71895	0.71565	
Japan	Total / 13	2.0 - 10.0	5,7	0.70673 - 0.71070	0.70810
	Kagoshima / 3	5.0 - 10.0	7,1	0.70673 - 0.70728	0.70702
	Kyoto / 2	2.0 - 5.7	3,9	0.71046; 0.71070	0.71058
	Fukuoka / 1	-	4,9	-	0.70773
	Others / 7	3.9 - 9.7	5,7	0.70735 - 0.70867	0.70791
South Korea	Hadong / 5	10.2 - 20.9	16,5	0.71154 - 0.72947	0.71710
Sri Lanka	Total / 6	7.3 - 15.6	12,4	0.71345 - 0.71996	0.71659
	Ratnapura / 1	-	7,3	-	0.71520
	Others / 5	9.7 - 15.6	13,4	0.71345 - 0.71996	0.71686
India	Total / 4	9.5 - 30.4	16,0	0.71345 - 0.79137	0.73425
	Darjeeling / 1	-	9,6	-	0.79137
	Others / 3	11.7 - 30.4	18,2	0.71155 - 0.72081	0.71520
Vietnam	Yen Bai / 2	7.0; 10.4	8,7	0.73617; 0.74035	0.73826
Rwanda	Kinshira / 2	35.6; 39.1	37,4	0.71381; 0.71387	0,71384
Turkey	Rize / 2	16.6 -25.1	20,8	0.70662; 0.70671	0,70667
Nepal	unknown / 1	-	10,4	-	0.7364
Taiwan	unknown / 1	-	17,0	-	0.71103

Analytical uncertainties for Sr elemental analysis not exceed 5% and were calculated as RSD (%) value of individual triplicates. The analytical uncertainty for Sr isotopic data is 0.00015 calculated as the maximal SD value of individual triplicates.

On Fig. E.5A, a diagram of registered values of the $^{87}\text{Sr}/^{86}\text{Sr}$ ratio in diverse Chinese agricultural product is presented. It can be noticed that $^{87}\text{Sr}/^{86}\text{Sr}$ ratios in the teas from this study (green bars) have a wider span with more radiogenic character in comparison to those in cereals, rice and vegetables from previous studies (grey bars). Such higher values of the Sr isotope ratios in tea samples can be explained by the hypotheses that tea plantations are mostly located in mountainous areas where soils are developed under the major influence of igneous or metamorphic granitoidic rocks. In contrast, agricultural fields used for cereals, rice and vegetables are usually located in valley plains, flatlands and even temporarily flooded lowlands (for rice plantations), where soils are formed on sedimentary rocks, limestone and clay deposits. Also, applied agricultural practices may have a strong regional specification (Hiraoka et al., 2016).

The value of $^{87}\text{Sr}/^{86}\text{Sr}$ ratio of the sample from Taiwan was 0.71104 ± 0.00061 , which consistent to previous studies performed on tea (Chang et al., 2016), and coffee (Liu et al., 2014; Liu et al., 2016) and (Fig. E.5A).

E.2.2. Japan

The data for the $^{87}\text{Sr}/^{86}\text{Sr}$ ratio obtained for Japanese tea was within the interval from 0.70673 to 0.71070, which is in the range of previously reported $^{87}\text{Sr}/^{86}\text{Sr}$ ratios for brown rice (Kawasaki et al., 2002; Ariyama et al., 2011; Ariyama et al., 2012), cereals (Ariyama et al., 2011) and vegetables (Hiraoka et al., 2016, Aoyama et al., 2017) (Fig. E.5B). Results of $^{87}\text{Sr}/^{86}\text{Sr}$ in studied tea samples from the regions of Kagoshima and Kyoto are in good agreement with previously reported vegetables of the same origin (Aoyama et al., 2017). Indeed, Sr isotope ratio for tea from Kagoshima was in the range of 0.70673 – 0.70828, (n=3), which is close to values obtained for vegetables from the same prefecture 0.70786 – 0.70861, (n=10). For the Kyoto region, the $^{87}\text{Sr}/^{86}\text{Sr}$ ratio for two studied teas and six vegetables from (Aoyama et al., 2017) were 0.71046 – 0.71070 and 0.70978 – 0.701089, respectively. However, for a single tea sample from the prefecture of Fukuoka, the $^{87}\text{Sr}/^{86}\text{Sr}$ ratio was lower (0.70773) in comparison with a single vegetable sample (0.71018), (Aoyama et al., 2017).

In total, more than 700 individual samples of Japanese agricultural products were examined at different times for the Sr isotopic specification in accordance to lithological settings of regions of their origin (Kawasaki et al., 2002; Ariyama et al., 2011; Ariyama et al., 2012; Hiraoka et al., 2016; Aoyama et al., 2017). The maximal amplitude of observed $^{87}\text{Sr}/^{86}\text{Sr}$ values in vegetables and cereals across the country was noted from 0.7026 to 0.7193, at that more than 80% of the samples had their $^{87}\text{Sr}/^{86}\text{Sr}$ ratios within the range 0.704 - 0.708. It is consistent to young volcanic and basaltic

rocks which prevail in the geological structure of the archipelago (Hiraoka et al., 2016). Regarding tea samples of unknown origins involved in the experiment, the overall consistency with ratio $^{87}\text{Sr}/^{86}\text{Sr}$ in vegetables is observed (only data for Japanese tea producing regions is considered), (Aoyama et al., 2017; Hiraoka et al., 2016).

E.2.3. South Korea

The $^{87}\text{Sr}/^{86}\text{Sr}$ ratio in four studied samples from a tea plantations of Hwagae Valley was ranged from 0.71154 to 0.72947, which is in good agreement with the Sr isotope ratio obtained for Korean rice (Song et al., 2014) and cabbage (Bong et al., 2012a, b), and is divers vegetables (Song et al., 2015) (Fig. E.6A). According to Song et al. (2015), a strong correlation of the $^{87}\text{Sr}/^{86}\text{Sr}$ ratio between plants, soils fractions and bedrocks was experimentally confirmed. The typical range of $^{87}\text{Sr}/^{86}\text{Sr}$ ratio in rock samples across the south part of Korean peninsula varied from 0.704 to 0.755 with a strong dependence of lithological specifications (Song et al., 2015). The Hwagae Valley is mostly formed on Precambrian metamorphic rocks with inclusions of Mesozoic sedimentary/volcanic rocks, where the $^{87}\text{Sr}/^{86}\text{Sr}$ ratio has been reported in the interval from 0.71067 to 0.75594 (Cheong & Chang, 1997; Kwon et al., 2006). The Sr isotopic compositions of teas concurs with these findings. However, there is some degree of variability between $^{87}\text{Sr}/^{86}\text{Sr}$ ratios observed in teas originated from the same valley. A long geological process of a slow but continuous dissolution of some siliceous minerals from the earth's crust can result uneven raise the $^{87}\text{Sr}/^{86}\text{Sr}$ ratio across the valley. On the other hand, the processing of tea could involve mixing of tea leaves from different plantations during harvesting and drying.

In comparison with samples from Japan, the variability of $^{87}\text{Sr}/^{86}\text{Sr}$ ratio in South Korean samples is much wider and covers an interval from 0.720 to 0.740, which is not characteristic for the lithology of Japan (Hiraoka, 2016) and has not been found so far in any Japanese agricultural products.

E.2.4. Vietnam

Two green tea samples from the highland plantation Suối Giàng have some the highest values of $^{87}\text{Sr}/^{86}\text{Sr}$ ratio: an exclusive “fine plucking” tea – 0.73617 ± 0.00072 , and a regular “coarse plucking” tea – 0.74035 ± 0.00013 (Fig. E.5A). It is worth noting, that apart from a difference in the Sr isotope ratios, the sample of “fine plucking” tea (the pick of only the bud with two young leaves) represents smaller concentrations of Sr and Rb in comparison with the sample of “coarse plucking” tea (the pick of the bud with two and more mature leaves): concentrations of Sr were measured at 7.0 mg kg^{-1} and 10.4 mg kg^{-1} , and for Rb 70.1 mg kg^{-1} and 109.6 mg kg^{-1} , for “fine” and “coarse”

plucking teas. This show that accumulation of Rb and radiogenic Sr occurs during the whole vegetation period. The ratio of Rb/Sr, previously indicated as one of the criterion for plant's geographical origin assessment (Brunner et al., 2010), for both teas was about 10.

E.2.5. India, Sri Lanka, Nepal

Two samples of Indian tea without indication of exact origin have the Sr isotope ratio 0.71155 ± 0.00027 and 0.71324 ± 0.00019 , while tea from the state Assam has more radiogenic value of $^{87}\text{Sr}/^{86}\text{Sr}$ ratio – 0.72082 ± 0.00023 . The highest value of $^{87}\text{Sr}/^{86}\text{Sr}$ ratio for the whole series of tea samples was observed in the sample of Darjeeling tea from the same named district (state West Bengal) – 0.79137 ± 0.00054 . Lagad et al. (2013) reported the span of $^{87}\text{Sr}/^{86}\text{Sr}$ ratio for 16 Assam teas from 0.711 to 0.732, and for 11 Darjeeling teas from 0.726 to 0.829. In the geographical proximity of the Darjeeling's tea plantations, a tea from Nepal demonstrated also high radiogenic value of the $^{87}\text{Sr}/^{86}\text{Sr}$ ratio – 0.73640 ± 0.00016 .

Values of $^{87}\text{Sr}/^{86}\text{Sr}$ ratio in five samples from Sri Lanka varied between 0.71345 and 0.71996. Generally, the obtained results are in good agreement with those of regional tea and rice (Lagad et al. 2013; Lagad et al., 2017), as can be seen in Fig. E.6B.

E.2.6. Turkey

The values of $^{87}\text{Sr}/^{86}\text{Sr}$ ratio in two samples of Turkish tea from the Rize province were 0.70662 ± 0.00004 and 0.70671 ± 0.00005 . In the absence of information concerning values of $^{87}\text{Sr}/^{86}\text{Sr}$ ratios in any Turkish food products, the references in geological rocks from the region were used to compare (Fig. E.6C). According to Eyuboglu et al. (2017), the geological structure of the Rize province is mostly composed of relatively young granitic and volcanic rocks of Cretaceous / Paleocene age with minor inclusions of sedimentary rocks of Oligocene; the values of $^{87}\text{Sr}/^{86}\text{Sr}$ ratio in this province were registered in the interval of 0.7060 - 0.7068, which is generally consistent to those in studied tea samples.

E.2.7. Rwanda

Two tea samples, one green and one black tea from Kinyihira, grown on the plateau within the altitude of 1900 m – 2500 m, present the highest concentrations of Sr among all studied teas: 35.6 mg kg^{-1} and 39.0 mg kg^{-1} . The $^{87}\text{Sr}/^{86}\text{Sr}$ ratios were 0.71381 ± 0.00012 and 0.71387 ± 0.00016 . Previously, $^{87}\text{Sr}/^{86}\text{Sr}$ ratios in coffee from Rwanda were reported as 0.7114 (Rodrigues et al., 2011b) and 0.72027 (Liu et al., 2014, Liu et al., 2016), as indicated in Fig. E.6D.

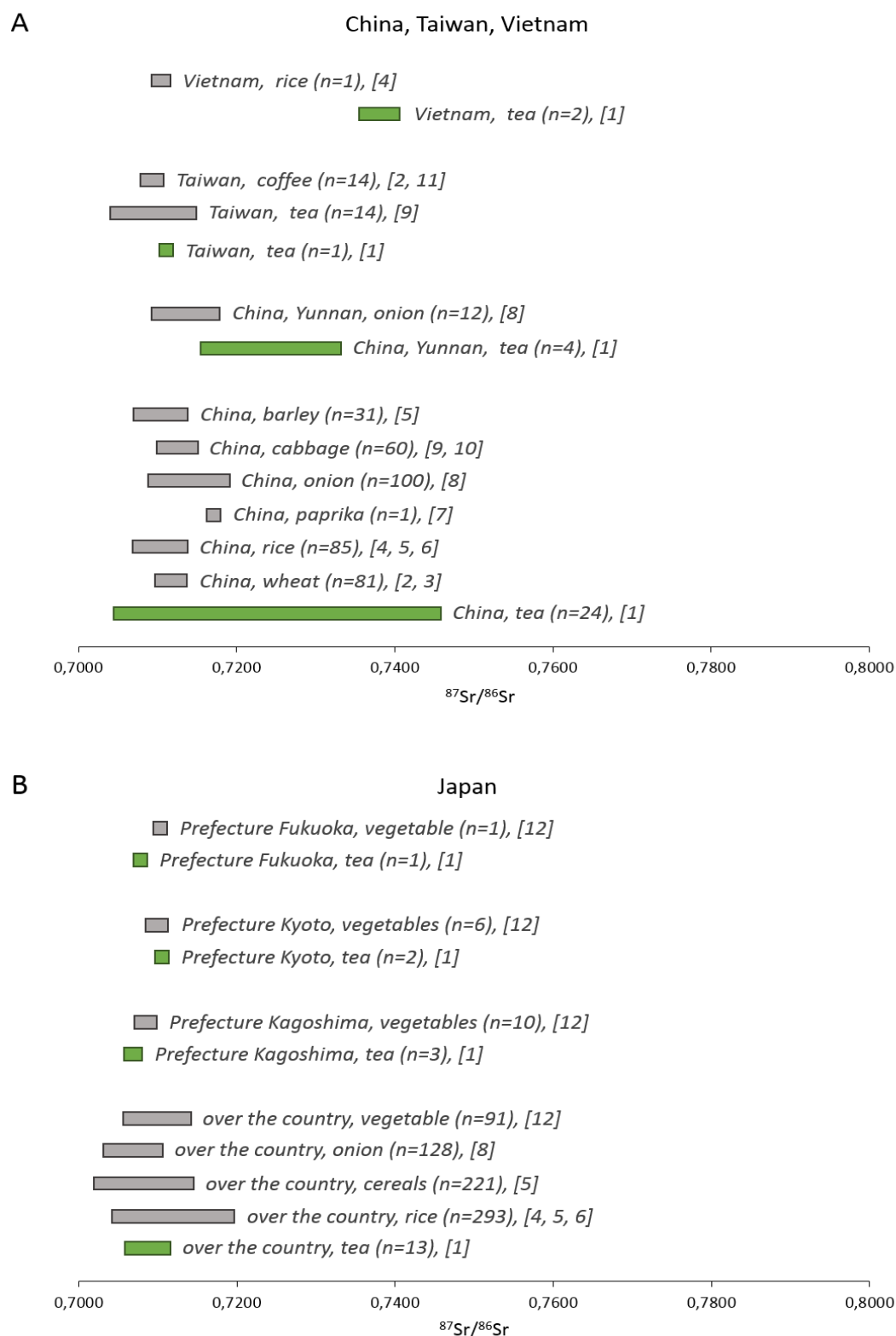


Fig. E.5. Comparison of the isotopic composition of tea samples from China, Taiwan and Vietnam (A), and Japan (B) with previously published data. References: [1] – this study; [2] – Liu et al., 2016; [3] – Liu et al., 2017; [4] – Kawasaki et al., 2002; [5] – Ariyama et al., 2011; [6] – Ariyama et al., 2012; [7] – Brunner et al., 2010; [8] – Hiraoka et al., 2016; [9] – Bong et al., 2012a; [10] – Bong et al., 2012b; [11] – Liu et al., 2014; [12] – Aoyama et al., 2017.

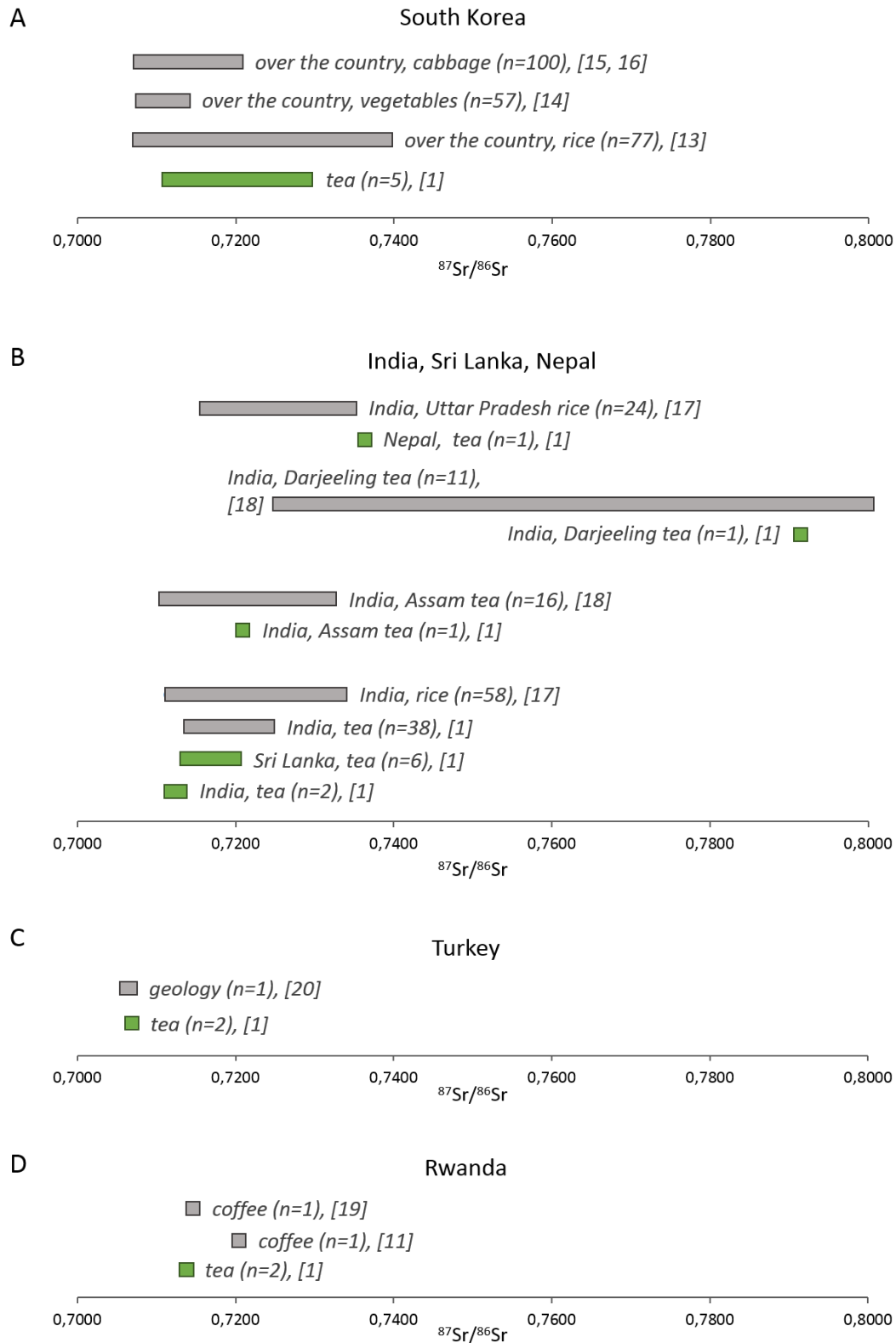


Fig. E.6. Comparison of the isotopic composition of tea samples from South Korea (A), India, Sri Lanka, Nepal (B), Turkey (C), and Rwanda (D) with previously published data. References: [1] – this study; [11] – Liu et al., 2014; [13] – Song et al., 2014; [14] – Song et al., 2015; [15] – Bong et al., 2012a; [16] – Bong et al., 2012b; [17] – Lagad et al., 2017; [18] – Lagad et al., 2013; [19] – Rodrigues et al., 2011b; [20] – Eyubogy et al., 2017.

Despite the fact that $^{87}\text{Sr}/^{86}\text{Sr}$ ratios in studied teas vary to a great extent, it is difficult to single out a specific Sr isotopic fingerprint to characterize a particular geographical origin of a series of teas due to an extensive overlapping of the majority of Sr signatures and the limited number of samples. The widest span of the values of $^{87}\text{Sr}/^{86}\text{Sr}$ ratio corresponded to the Chinese samples conceals the small indistinct Sr isotopic signatures of other teas originated from Asian countries, such Japan and South Korea. However, in the absence of Chinese samples, Japanese teas can be distinguished from South Korean samples by their lesser radiogenic Sr isotopic composition in contrast to samples from Hwagae Valley (South Korea) have the $^{87}\text{Sr}/^{86}\text{Sr}$ ratio enriched by the radiogenic isotope ^{87}Sr .

Apart from geological and pedological settings that determine the variability of Sr isotope ratios in teas, different agricultural practices (including seeding rates, irrigation methods, fertilization, and chemical control of diseases) can affect the Sr isotopic composition of a plant (Hiraoka, 2016; Aoyama et al., 2017).

The limited number of samples from other origins (India, Nepal, Sri Lanka, Vietnam, Taiwan, Turkey and Rwanda) is not allowed to estimate the discriminating potential of the $^{87}\text{Sr}/^{86}\text{Sr}$ ratio. However, some remarks can be made. Teas grown on Himalaya's highland plantations have a tendency of higher $^{87}\text{Sr}/^{86}\text{Sr}$ value, as it was observed for tea from Nepal and northern India (Assam, and Darjeeling). This hypothesis is strengthened by results of previously performed studies on tea (Lagad et al. 2013) and rice (Lagad et al. 2017) found the same trend.

E.3. Lead concentrations and lead isotopic compositions of teas

In studied teas, lead elemental and isotopic compositions were determined according to analytical procedures previously mentioned in Chapter B. Table E.4 placed at the end of the chapter reports the Pb concentrations and Pb isotope ratios in individual samples.

The only study performed on Pb isotopic compositions of 29 Chinese teas from the province of Zhejiang was available for comparison (Lu et al., 2011). In the presented experiment, there were 3 samples from the same province (Table E.4), and obtained results show close agreement with values reported in literature, as follows: $^{208}\text{Pb}/^{204}\text{Pb} = 38.283 \pm 0.050$ (38.306 ± 0.732), $^{207}\text{Pb}/^{204}\text{Pb} = 15.632 \pm 0.006$ (15.608 ± 0.249), $^{206}\text{Pb}/^{204}\text{Pb} = 18.173 \pm 0.071$ (18.155 ± 0.303), $^{206}\text{Pb}/^{207}\text{Pb} = 1.162 \pm 0.004$ (1.164 ± 0.005), in the brackets is data from Lu et al. (2011).

E.4. Lead isotopic compositions of teas from China, Japan and South Korea as signatures of the regional atmosphere and geology

Human and industrial activities in Asia is closely associated with urbanization and industrialization, and are significant sources of lead emitted into the environment through waste effluents and atmospheric emission (Cheng & Hu, 2010). The China's industrial sector is dominant in the region and it has grown greatly during last decades. Nowadays, China experiences an enormous demand of energy sources, wherein coal power plants are dominated. Mining has been carried out in China for millennia and there are a large number of active mines (Bingquan, 1995). Atmospheric particulate matter in the Asian region has been extensively described (e.g., Mukai et al., 1993, Bellhöfner & Rosman, 2001). In the past, it was affected primary by leaded gasoline in most of the sites and nowadays, the important Pb atmospheric inputs come from coal combustion and industrial activities (Mukai et al., 1993; Li et al., 2012; Xu et al., 2012). The progressive phasing out of the leaded gasoline has resulted in significant changes in the global atmospheric lead content over the last 30 years (Grousset et al., 1994; Sun et al., 2006; Li et al., 2012; Xu et al., 2012). In the absence of leaded gasoline, atmospheric Pb isotopes signatures is reflecting a Pb specification of multiplicity of sources with different proportions (Grousset et al., 1994; Bellhöfner & Rosman, 2002a, b; Chen et al., 2005).

The aim of this study was to determine the potential linkage between Pb isotopic compositions of teas originated from China, South Korea, Japan and the Pb isotopic composition of the regional atmosphere and those of predominant Pb emission sources, and then to access the sample origin classification.

E.4.1. Geographical origins of teas according to geochemical zoning of the Asian region

In 1995, Bingquan proposed a concept of geochemical zoning of China and neighboring countries based on variability of Pb isotopic compositions in ores and rocks (e.g. basalts, granites) caused by different tectonic environments and primitive heterogenetic during the geological evolution of Earth. The comparison of Pb isotopic compositions for various ores and rocks (e.g. basalts, granites) revealed that the lateral variation between different terranes is greater than the vertical variation between Earth's crust and mantle, and it can be a useful criterion for geochemical mapping. Within this context, six geochemical provinces were recognized by the differences in their Pb isotopic compositions.

Proceeding from the fact that plants are particularly susceptible to a Pb isotopic composition of the atmosphere and reflect it through the Pb uptake (section A.2.1.2. of the manuscript), and assuming that coal and ore for urbanistic and industrial purposes are transported from the nearest mines, the Pb isotopic composition of a plant is expected to be associated with those of regional ore and coal deposits. In this study, tea samples were classified with respect of the geochemical zones of their provenances (Fig. E.7). Only three geochemical provinces were concerned: Southern China Block, Yangtze Block, and Northern China Block. Details about the samples origins described in section E.1.1.

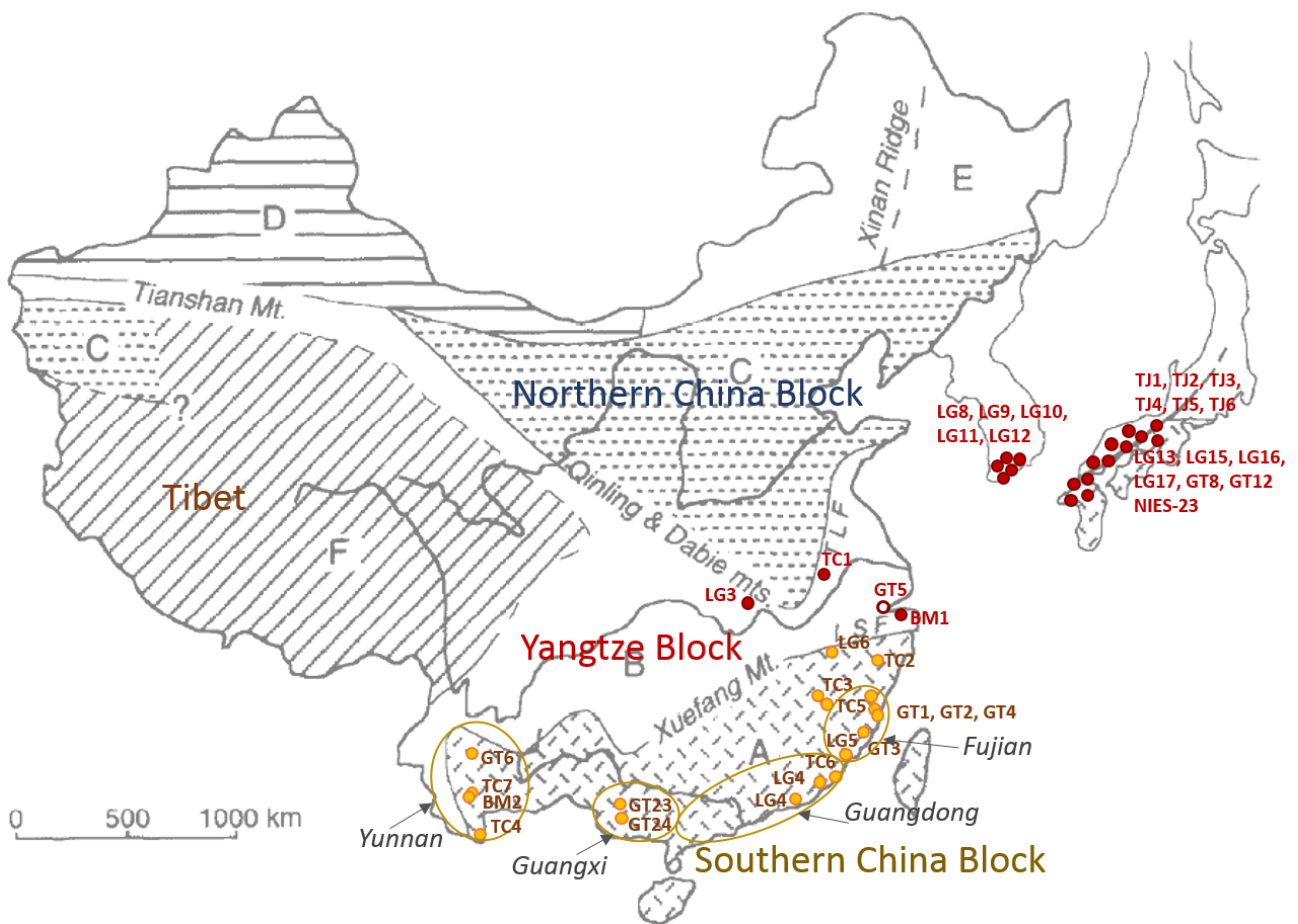


Fig.E.7. Known geographical origins of teas on a sketch map of China, South Korea and Japan with selected geochemical zones - Northern China Block (NCB), Yangtze Block (YB), and Southern China Block (SCB), modified after Bingquan (1995). Administrative provinces Yunnan, Guangxi, Guangdong and Fujian are indicated for the following discussion.

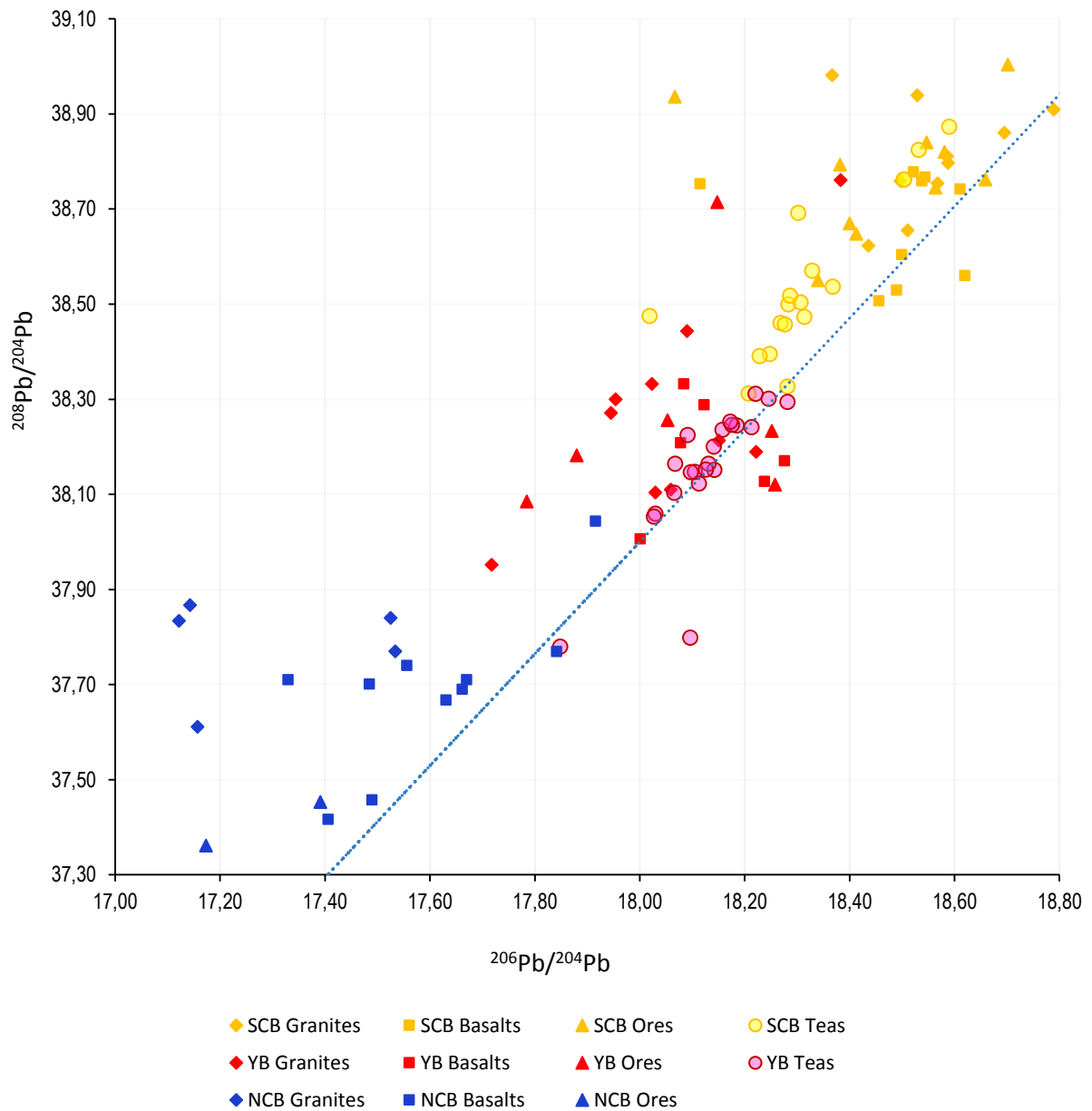


Fig. E.8. A comparison plot of $^{206}\text{Pb}/^{204}\text{Pb}$ and $^{208}\text{Pb}/^{204}\text{Pb}$ ratios determined in tea samples and previously reported ratios in basalts, granites and ores from China, South Korea and Japan. References: (Mukai et al., 1993; Bingquan, 1995; Bellhöfler & Rosman, 2001; Mukai et al., 2001). The error bars are smaller than the marks (for tea samples). The hand-drawn Pb growth curve comes from Cumming & Richards (1975). Legend includes samples and references from three geochemical provinces of China. Blue marks correspond to Northern China Block (NCB): blue rhombus - granites (NCB Granites), blue squares - basalts (NCB Basalts), blue triangles - ores (NCB Ores). Red marks correspond to Yangtze Block (YB): red rhombus - granites (YB Granites), red squares - basalts (YB Basalts), red triangles - ores (YB Ores), red circles - tea samples (YB Teas). Yellow marks correspond to Southern China Block (SCB): yellow rhombus - granites (SCB Granites), yellow squares - basalts (SCB Basalts), yellow triangles - ores (SCB Ores), yellow circles - tea samples (SCB Teas).

Each ore deposit carries a particular isotopic signature fixed at the time of its formation (Bellhöfler & Rosman, 2001). Figure E.8 displays the typical values of $^{206}\text{Pb}/^{204}\text{Pb}$ and $^{208}\text{Pb}/^{204}\text{Pb}$ ratios in natural minerals for each of the considered geochemical provinces, according to Bingquan (1995). The three-isotope plot $^{206}\text{Pb}/^{204}\text{Pb}$ vs $^{208}\text{Pb}/^{204}\text{Pb}$ is recognized as one of the preferable diagrams to trace geochemical differences in the environment (Ellam, 2010), because it provides the maximal separation between three different decay systems: isotopes ^{206}Pb and ^{208}Pb are the daughter products from the radioactive decays of ^{238}U and ^{232}Th , respectively, and the isotope ^{204}Pb is entirely a primordial nuclide and it is non-radiogenic.

Figure E.8 indicates that the $^{206}\text{Pb}/^{204}\text{Pb}$ and $^{208}\text{Pb}/^{204}\text{Pb}$ ratios evolve respecting the lead growth curve (Cumming & Richards, 1975) and constitute three individual groups according to geochemical zoning. It is noteworthy that within the same geochemical zone, Pb isotopic ratios of ore deposits are consistent with those of granites and basalts, it means that Pb signatures from naturally occurring minerals have the same nature. The growth curve records the changes of the relative isotopic weights of ^{208}Pb and ^{206}Pb , brought about by the radioactive decay of ^{232}Th and ^{238}U .

When the whole set of examined teas is juxtaposed on the diagram with the respect of geochemical zones of their origins, it can be noticed that two well-defined groups of teas are closely associated with Pb isotopic configurations of minerals and ores from corresponding geochemical zones. A relatively large number of tea samples and reference values of minerals presented on the diagram allows to observe this regularity for the samples from Yangtze Block (red symbols) and Southern China Block (yellow symbols). North China Block is characterized with a distinctive, lesser radiogenic Pb signature of ore and minerals; however, there were no samples originated from this zone.

In general, the geographical origins of studied Asian teas are consistent with Pb geochemical markers and can be distinguished on their basis on the regional scale. Hence, the observed regularities justify the hypothesis made by Bingquan (1995) that the geographic origin assignment is possible by means of Pb isotopic ratios due to the linkage to the geological settings under certain circumstances.

E.4.2. Lead isotopic signatures of teas as a record of regional atmospheric composition

As mentioned above, plants obtain an appropriate Pb isotopic composition available for bio-accumulation, primarily, through the atmosphere (section A.2). In the atmosphere, lead released by anthropogenic emitters is estimated about 100 times greater than that from natural sources (Bindler, 2011), and contributes up to 80% from global lead emission (Komárek et al., 2008; Sen et al., 2012). From Fig. E.8, no any Pb sources effected on teas can be identified. Indeed, lead contained in granites and basalts is released by natural processes of rock weathering, whilst the enrichment of the atmosphere by signatures of ores and coals predominantly emitted from various anthropogenic activities, such as mining exploitation, industry, coal combustion, vehicular exhausts and divers urban activities.

Potential sources of Pb in teas can be traced from a three-isotope plot $^{207}\text{Pb}/^{206}\text{Pb}$ vs $^{208}\text{Pb}/^{206}\text{Pb}$ considering various isotopic end-members (Fig. E.9). At first, a close examining of the $^{207}\text{Pb}/^{206}\text{Pb}$ and $^{208}\text{Pb}/^{206}\text{Pb}$ ratios was performed on a large regional scale encompassing three countries: China, Japan and South Korea. Considering Pb sources, for instance included natural geogenic values, unleaded/leaded gasoline, and coal/ore. It should be mentioned, that Chinese ores and coals will be considered together in the following discussion, because their isotopic similarity as well as the inability of determination their individual contributions to the atmosphere were already emphasized (Bellhöfner & Rosman, 2001). Unleaded gasoline commonly used in China since 2000, despite its name, contains lead in the proportions ranging from tens to hundreds of parts per billion and displayed a relatively consistent isotopic composition, and, hence, must be taken into account (Chen et al., 2005).

The geogenic end-member represented by the signatures of subsurface sediments and uncontaminated soil (Li et al., 2012). The Pb isotopic composition of tea samples demonstrates the general association with those of atmospheric aerosols of the region, partly overlapping with the signatures of coal/ore, and distinctly limited by lines represented medians of predominant regional sources. From Fig. E.9, it can be noticed that Pb isotopic signatures of teas can be explained by mixing between at least three end-members. However, Pb in teas is derived more likely from coal/ore, and, to a lesser extent, from vehicular emissions: obviously, a cloud of teas is shifted more to the coal/ore median than to this of gasoline. Within a framework of this diagram, the more precise identification of predominant Pb sources in teas is difficult to obtain.

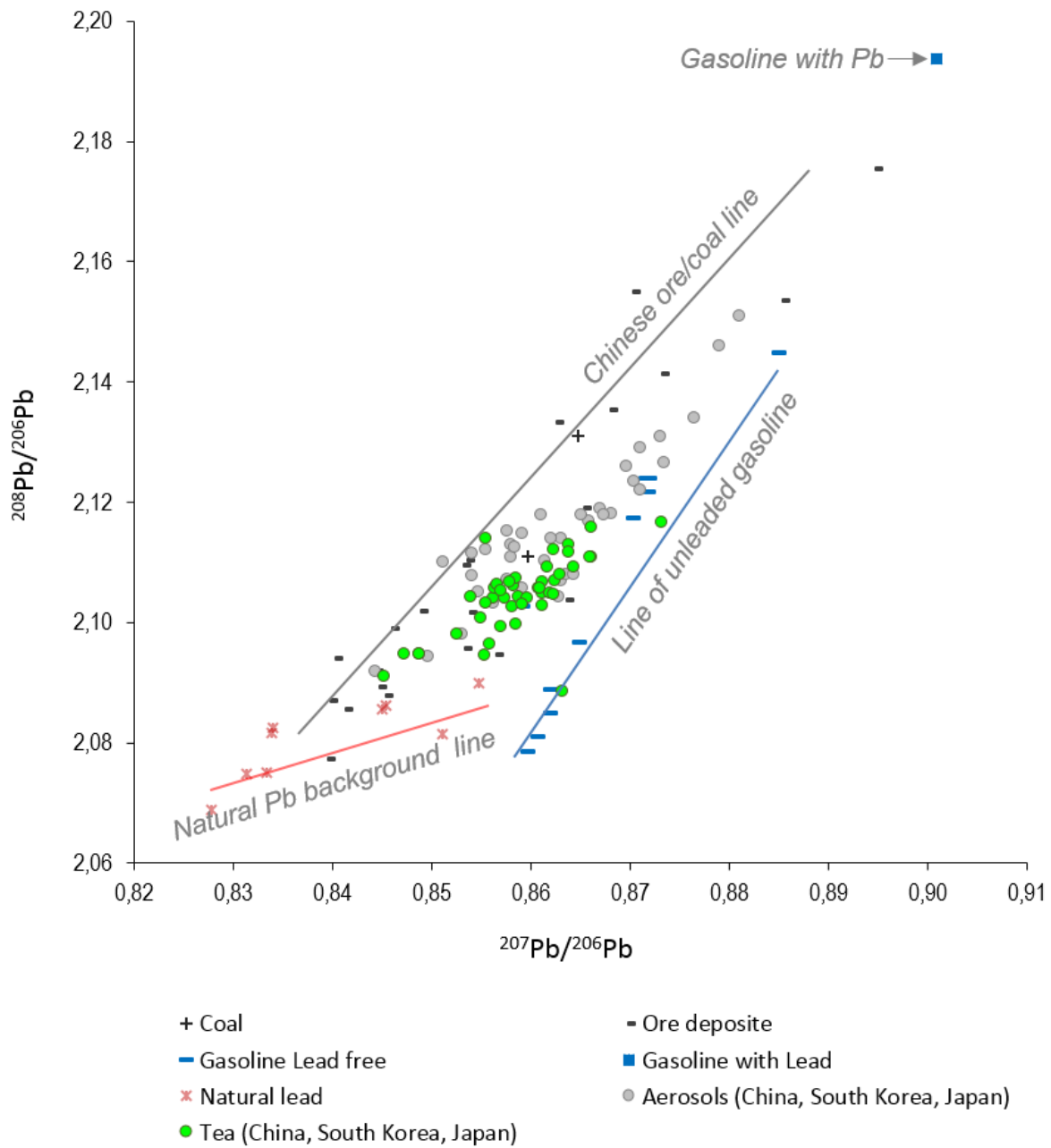


Fig. E.9. A comparison plot of $^{207}\text{Pb}/^{206}\text{Pb}$ vs $^{208}\text{Pb}/^{206}\text{Pb}$ ratios determined in tea samples and previously reported in aerosols and predominant Pb emission sources from China, South Korea and Japan. Ranges or individual isotope ratios of possible Pb sources: coal/ore, leaded and unleaded vehicle exhaust, and natural Pb isotopic ratios (Mukai et al., 1993; Bingquan, 1995; Bellhöfner & Rosman, 2001; Mukai et al., 2001; Zhu et al., 2001; Zhu et al., 2002; Chen et al., 2005; Ip et al., 2005; Xu et al., 2012; Li et al., 2012) are shown. The Pb growth curve (Cumming and Richards, 1975) is also presented in the plot. Straight lines represent uncalculated, hand-drawn trends.

E.4.3. Distinguishing of teas originated from Japan and South Korea

Pb isotopic ratios $^{207}\text{Pb}/^{206}\text{Pb}$ and $^{208}\text{Pb}/^{206}\text{Pb}$ of Japanese and South Korean tea were closely examined to perform an attempt to distinguish these teas from others of Chinese origin.

Selected Chinese teas

Samples from three administrative provinces in South China – Guangdong, Fujian, and Guangxi were selected. Guangdong, also known as the Pearl River Delta region, one of the most densely urbanized regions in the world, and also, an economic hub of China. Guangdong borders provinces of Fujian to the northeast and Guangxi to the west. These three provinces are in the top of the most important tea-producing regions of China, and geochemically assigned to the Southern China Block. A super large-scale Pb-Zn deposit, named Fankou, is located in northern Guangdong, close to the border with Guangxi province (Bi et al., 2017). In Fujian there are several Pb-Zn important deposits which contribute to impact the regional atmosphere. During decades of environmental monitoring in the Pearl River Delta region, a large data base of Pb isotopic signatures of various environmental samples was accumulated (Zhu et al., 2001; Ip et al., 2005; Cheng & Hu, 2010).

Japanese teas

From 13 teas involved in this study, only for six samples the precise geographical origins were provided: three teas from Kagoshima, two teas from Kyoto, and one sample from Fukuoka (section E.1.1). All of these three prefectures are assigned geochemically to the Yangtze Block. For the rest of teas their precise geographical origins are unknown. However, the major tea producing regions are situated on the Honshu and Kyushu islands of Japanese archipelago. The separation line between two geochemical zones, Southern China block and Yangtze block, passes through either islands and it is presented schematically on the Fig. E.7. According to Hiraoka et al. (2016), it corresponds to the Median Tectonic Line - a strike slip fault system and is the largest crustal break in southwest Japan. Thus, it is hypothetically possible for these teas to be originated from both, either Southern China block or Yangtze block.

South Korean teas

Samples used in this study are originated from Hwagae valley on the south part of the Korean Peninsula, which entirely belongs to the Yangtze geochemical block.

Discussion

On Fig. E.10, the ratios $^{207}\text{Pb}/^{206}\text{Pb}$ and $^{208}\text{Pb}/^{206}\text{Pb}$ determined in tea samples from Japan, South Korea and Chinese provinces Guangdong, Fujian, and Guangxi are presented with comparison of previously reported values in aerosols and dominant emission sources. Pb isotopic signatures in Chinese teas exhibit a coherence across aerosols originated from the region Pearle River Delta (Cheng & Hu, 2010). Additionally, the Pb composition of Chinese teas showed a similarity with isotopic patterns of surface sediments from Pearle River Estuary (not displays on Fig. E.10), ranging 0.84 - 0.85 for $^{207}\text{Pb}/^{206}\text{Pb}$, and 2.07 – 2.10 for $^{208}\text{Pb}/^{206}\text{Pb}$ (Cheng & Hu, 2010).

Japanese teas closely cluster on approximate to the Pb isotopic composition of Japanese aerosols (Fig. E.10). Additionally, the results are consistent with published data of Pb isotope composition of surface sediments from the lake Muronouchi, southern Honshu (Hosono et al., 2016), and with those in various environmental materials, such plants, water and precipitations from central Honshu (Nakano, 2016). In both studies values ranged within the interval of 0.86 - 0.87 for $^{207}\text{Pb}/^{206}\text{Pb}$, and 2.11 – 2.12 for $^{208}\text{Pb}/^{206}\text{Pb}$ (data is not displays on Fig. E.10), these areas are not remote from the prefectures of tea's sample origins.

South Korean teas are located on the plot (Fig.E.10) within the same field as Japanese teas, except one sample, which fell on the median of gasoline. Taking into account the fact that all five studied teas from South Korea were originated from the same valley, it can be assumed that this distinctive tea could be influenced by the proximity of a highway/road. Indeed, road traffic re-suspends the surface dust including the anthropogenic constituents, such depositions from previously emitted by leaded-gasoline vehicular exhausts, creates diffuse emissions, and could be an important source of secondary Pb contamination (Sun et al., 2006). The same anomaly was observed for one of the Japanese teas. Despite of the limited number of South Korean samples, the correlation between Pb isotope ratios for teas from Japan and South Korea showed a similar linear regression trend indicating the likely similarity in Pb sources. Recent studies did not reach a consensus about the identification of predominant Pb sources in the atmosphere of South Korea, although the obvious is the fact that no any environmental samples (including this study) found to be close by the Pb isotope configuration to domestic ores, which are significantly enriched by ^{208}Pb than Chinese ores and coals (Mukai et al., 1993; Mukai et al., 1994; Choi et al., 2007; Kim et al., 2013; Lim et al., 2013).

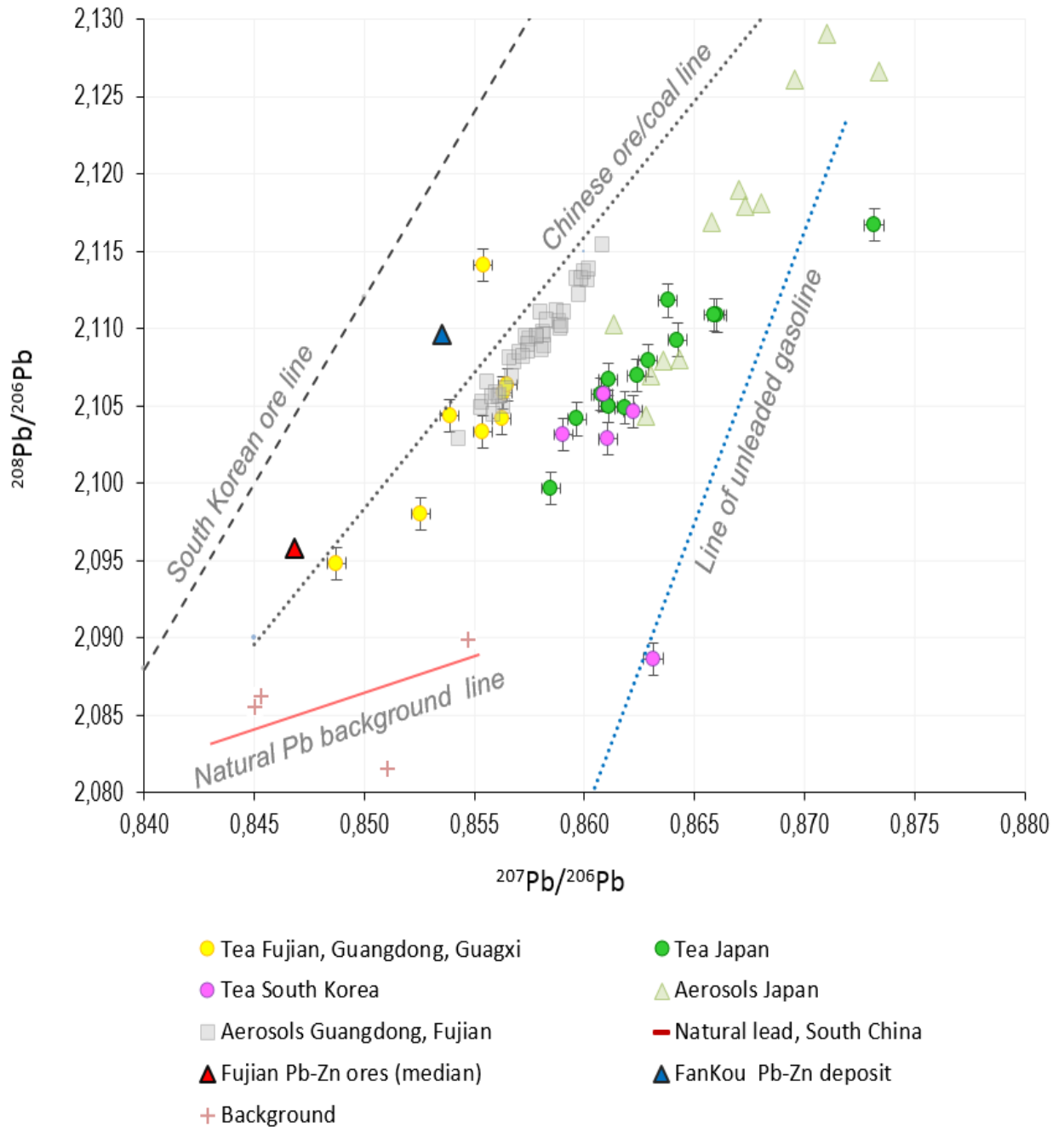


Fig. E.10. A comparison plot of $^{207}\text{Pb}/^{206}\text{Pb}$ and $^{208}\text{Pb}/^{206}\text{Pb}$ ratios determined in tea samples origin Japan, South Korea and Chinese provinces (Guangdong, Fujian and Guangxi) with previously reported ratios in aerosols and dominant Pb emission sources in regions considered. Ranges or individual isotope ratios of possible Pb sources: coal/ore, leaded and unleaded vehicle exhaust, and natural Pb isotopic ratios were taken from published studies (Mukai et al., 1993; Bellhöfler & Rosman, 2001; Mukai et al., 2001; Zhu et al., 2001; Zhu et al., 2002; Chen et al., 2005; Ip et al., 2005; Nakano et al., 2006; Choi et al., 2007; Xu et al., 2012; Li et al., 2012; Kim et al., 2013; Lim et al., 2013). The error bars of isotopic determination corresponds to maximal uncertainty of 0.05% for both ratios.

According to Jeon & Nakano (2001), Pb isotopic composition of stream waters of Central Korea testified that Pb was derived primarily from the atmosphere. To evaluate a potential impact from Pb transported by the atmospheric pathways to Korean Peninsula, and effected successively on plants, further investigations using a reliable series of samples are needed.

The observation on Fig.E.10 draws attention that atmospheric particles from Japan and from South China have distinct isotopic compositions and each group appeared to have its own mixing array. The specification of Pb composition in Japan was already reported by Mukai et al. (1994). It has been shown earlier, that about 85% of lead used for metallurgy purposes in Japan is imported from Canada, Peru, and South Africa (Mukai et al., 1993). Nakano et al. (2006) suggested that there are several significant Pb sources in the atmosphere over Japan; however, the predominant influence comes from industrial emissions (Nakano, 2016). Apparently, mixing of lead from worldwide ores and coals creates an individual Pb isotopic signature, which can be observed in Japanese atmospheric aerosols, and subsequently, in plants. Contrary, the observed closeness of Pb isotopic composition of atmospheric particles in South China and those of domestic ores and coals suggests that the local mining is predominantly used in regional metallurgy.

Here is presented the experimental evidence of the possibility trace food geographical origin with application of the geochemical zoning concept. Indeed, different continental block merger results the formation of a zone with special Pb isotopic composition, which can be transferred to plants under certain circumstances.

The variation in Pb isotopic composition in tea can be interpreted as the result of mixing between different industrial sources and old Pb pollution from leaded gasoline combustion re-emitted into the atmosphere. For those samples, where the comparison with the atmospheric particulate matter was possible, the general association of Pb isotopic signatures was observed. Since the majority of lead in the atmosphere is ultimately derived from the manufactured products formed from ores, lead stable isotopes can be a useful monitoring tool to identify plant's origin, primarily by tracing source of ore metals utilized in a given nation were the ore's national trading politics is taken into account.

E.5. Distinguishing of geographical origin of Asian teas a by means of $^{87}\text{Sr}/^{86}\text{Sr}$, lead isotope ratios and multielemental concentrations

The Sr and Pb isotope ratios completed with trace metal concentrations of 28 authentic teas originated from China, South Korea and Japan were used to classification of geographical origin.

Although the span of $^{87}\text{Sr}/^{86}\text{Sr}$ ratios in Chinese teas is extensive and some of these samples were characterized with a relatively low value of the ratio $^{87}\text{Sr}/^{86}\text{Sr}$, in general the $^{87}\text{Sr}/^{86}\text{Sr}$ ratios in China tended to be higher than those in Japan. The difference in Sr concentration was not as clear as the difference in $^{87}\text{Sr}/^{86}\text{Sr}$ ratios, however, the concentrations of Sr in Japanese teas tended to be lower than those in Chinese teas. This specific Sr-elemental and Sr-isotopic compositions of Japanese vegetables was previously reported (Hiraoka et al., 2016; Aoyama et al., 2017). The interdependence of $^{87}\text{Sr}/^{86}\text{Sr}$ ratios and Sr concentrations suggests that it may be possible to discriminate samples from China and Japan, although the fields are located sufficiently close together (Fig. E.11A).

A clearer separation of origin can be obtained for teas from Japan and South Korea, their $^{87}\text{Sr}/^{86}\text{Sr}$ ratios vary wider and shifted to higher values. The higher Sr content in South Korean samples strengthens the distinctive potential of the $^{87}\text{Sr}/^{86}\text{Sr}$ ratio and make the classification between these two origins more evident. However, a large variability of Sr concentrations and $^{87}\text{Sr}/^{86}\text{Sr}$ ratios observed in Chinese samples conceals the Sr isotopic and elemental signatures of teas from South Korea. Therefore, when using Sr-elemental and Sr-isotopic specification, only Japan-China and Japan-South Korea in the absence of Chinese samples can be distinguished.

Whilst using the Sr-elemental and Sr-isotopic signatures allows to classify the origin of tea samples according geological specifications, lead isotopic ratios characterize the difference in the atmospheric Pb compositions of the regions of origins. Figure E.11B illustrates the potential of the Pb isotopic system $^{207}\text{Pb}/^{206}\text{Pb}$ and $^{208}\text{Pb}/^{206}\text{Pb}$ in discriminating of origins. It has been previously discussed (sections E.4.2 and E.4.3 of this chapter) that the atmosphere of continental China is under the influence of domestic ores and coals used for industrial and urbanistic purposes. Contrary, Japan and South Korea import ore and coal from over the world. This develops different Pb isotopic signatures in teas of different origins. However, when examining the whole set of Chinese samples originated from different regions and provinces, the Pb isotopic compositions form a wide-ranging cloud reflecting the multitude of substantial Pb sources. The regional classification was then hindered by a considerable overlapping.

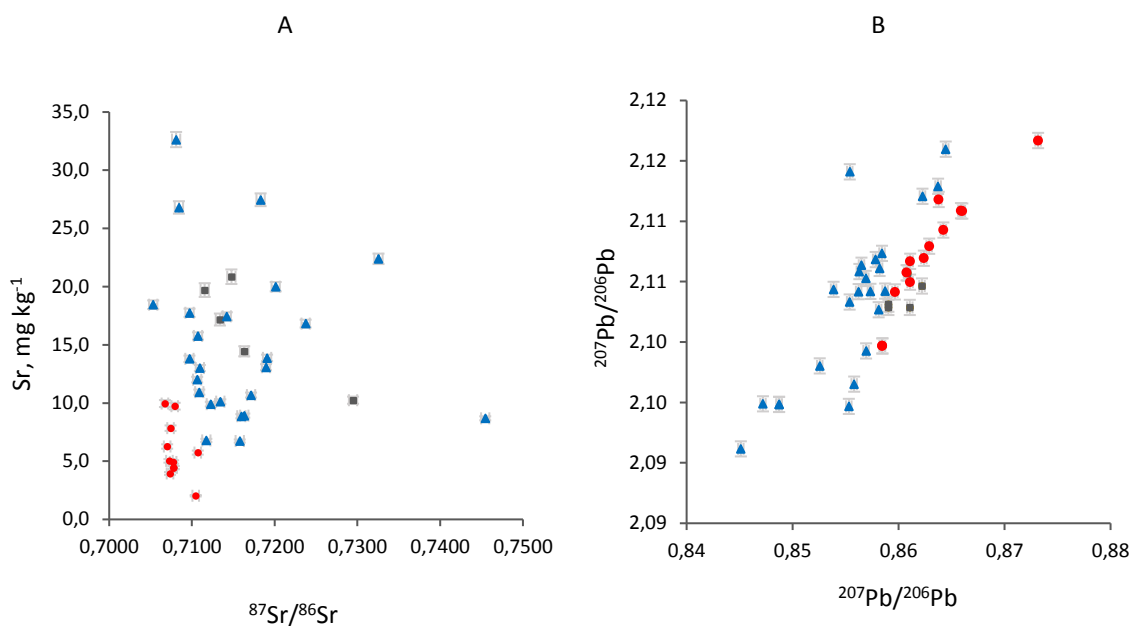


Fig. E.11. Origin differentiation in tea leaves from China (blue triangles), Japan (red circles), South Korea (gray squares) obtained by: (A) - plot of Sr concentration versus ⁸⁷Sr/⁸⁶Sr ratio; (B) - plot of ²⁰⁷Pb/²⁰⁶Pb and ²⁰⁸Pb/²⁰⁶Pb.

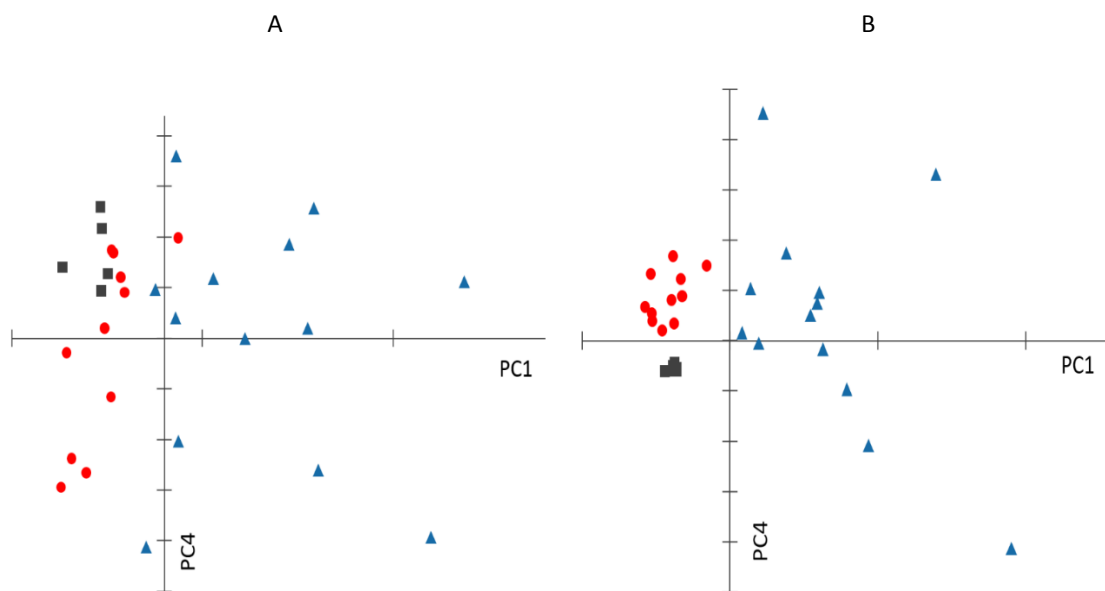


Fig. E.12. Origin differentiation of tea leaves from China (blue triangles), Japan (red circles), South Korea (gray squares) obtained by PCA: (A) - using 16 elemental concentration; (B) - using 16 elemental concentration completed with isotope ratios of Sr and Pb.

Due to the overlapping Sr and Pb isotopic patterns of tea samples, the differentiation between three countries of origins could not be done unequivocally. Therefore, a statistical analysis was applied to assess the reliable origin classification with consideration of multitude of parameters. Based on an unsupervised data reduction and calculating of a new variable (principal component) as a linear combination of the original variable, this statistical procedure is widely applied in data interpretation in different fields of the chemical analysis.

The PCA treatment was performed on the combined data of the Sr-, Pb isotopic ratios and elemental concentrations (presented in the Appendix 1), using the freeware package Excel add-in PopTools v 3.2. First, only trace element data was processed by PCA (Fig. 12A). The variables PC1 and PC4 representing respectively 33% and 15% of the total variance of the data, were selected. Such combination of the variables allowed to achieve the maximum regrouping of samples according to their origins. However, some partial overlapping can be observed, meaning that no any origins can be distinguished by using only multielemental data.

A significantly better discrimination of origins of studied teas was obtained by including of statistical weights of the $^{87}\text{Sr}/^{86}\text{Sr}$, $^{207}\text{Pb}/^{206}\text{Pb}$ and $^{208}\text{Pb}/^{206}\text{Pb}$ ratios. The results presented in Fig. E.12B with two components PC1 (32%) and PC4 (16%). Japan, South Korea and China which are three geographically distinct regions, were found to be clearly differentiated, although the dispersion of Chinese teas was still the largest if compared to Japanese and South Korean samples. This may be due to a wide variability in geology, climatic and agricultural conditions, and industrial activities across the country. Taking these factors into consideration, the use of stable isotope ratios of light elements as additional variables for the future experiments might improve the discrimination rate, and even helps to differentiate among different Chinese regions. Analyzing a larger number of tea leaves from these origins is also essential for the construction of a statistical differentiation model with a higher level of confidence.

Summarizing, the use of only one isotopic system is not enough to clearly discriminate individual countries of origin. However, a combination of two isotopic systems - one tracing the lithological settings, and the other tracing environmental ambient pollution, completed with elemental concentration gives the maximal distinctiveness for the geographical origin discrimination.

E.6. Conclusion

In the present study, the Sr isotopic compositions together with Pb isotopic ratios and elemental concentrations of 60 tea samples from over the world were determined.

Variations in $^{87}\text{Sr}/^{86}\text{Sr}$ ratios alone did not show a reliable differentiation among all countries. However, teas from regions close to Himalaya (Darjeeling, Nepal) were found the most distinguishable among all studied teas due to higher, or “radiogenic” values of $^{87}\text{Sr}/^{86}\text{Sr}$. The Sr isotope ratio of South Korean teas was also found more radiogenic as compared to Japanese ones. A differentiation of Japanese teas was achieved with respect Chinese and South Korean samples on the basis of combination of Sr concentrations and $^{87}\text{Sr}/^{86}\text{Sr}$ ratios.

Variations in Pb isotope ratios ($^{207}\text{Pb}/^{206}\text{Pb}$ and $^{208}\text{Pb}/^{206}\text{Pb}$) generally show an excellent matching between the Pb isotopic signatures of tea samples and those of the regional atmosphere. The Pb isotopic compositions ($^{208}\text{Pb}/^{204}\text{Pb}$ and $^{206}\text{Pb}/^{204}\text{Pb}$) of Chinese teas showed close similarities with the Pb specifications of regional mineral resources. Particularly, for this reason, it seems to be possible to differentiate Chinese and Japanese teas.

A well-defined differentiation was achieved among teas originated from China, South Korea and Japan by applying of the PCA analysis to whole set of data including Sr-, Pb- isotopic ratios and elemental concentrations. The presented results made advantages of combination multi-elemental and multi-isotopic approaches for food geographical origin discrimination apparent.

Here is presented also the first practical attempt to classify the food geographical origin with respect of the concept of geochemical zoning of Asia. The geographical distribution of studied teas was found consistent to Pb geochemical markers for two geochemical zones, South China Block and Yangtze Block. The observed regularities support the hypothesis that the geographic origin assignment is possible by means of Pb isotopic ratios due to the linkage to the geological settings under certain circumstances.

The obtained data on Sr and Pb isotopic ratios of authentic raw tea leaf samples from over the world can be used for informative and comparative purposes in further studies.

Table E.1. Geographical origin and provenance of studied tea samples.

Nº	Sample code	Country of producing	Type of the tea / additional information	Name of the tea	Supplier	Year	Province / City
1	GT 1	China	Green, jasmin	Jasmine tea	Supermarket	-	FUJIAN / Fuzhou
2	GT 2	China	Green, jasmin	Jasmine tea	Supermarket	-	FUJIAN / Fuzhou
3	GT 3	China	Green	OOLONG Tea	Supermarket	-	FUJIAN / Xiamen
4	GT 4	China	Green ORGANIC	Oganic Green Tea	Supermarket	-	FUJIAN / Fuzhou
5	LG 5	China	Green / Blue	Tie Guan Yin	Lydia Gautier	2013	FUJIAN / Anxi, high grown (1200m)
6	TC 5	China	Green, 60% fermentation	Shui Xian, WULONG	Terre de Chine	2013	FUJIAN / Montagne WU YI
7	TC 4	China	Green	Yunnan Vert	Terre de Chine	2013	YUNNAN / District XI SHUANG BAN NA
8	TC 7	China	Green, post fermentation	Yunnan Vert, PU-ERH	Terre de Chine	2013	YUNNAN / District LIN CANG
9	BM2	China	Red	Xia Fu Ding	Bernard Médina	-	YUNNAN / District de Lin Cang
10	GT 6	China	Green	MiniTuocha tea	Supermarket	-	YUNNAN / no information
11	BM1	China	Green	Lyne Wang	Bernard Médina	-	ZHEJIANG / Yiwu
12	TC 2	China	Green	Dao Ren Mao Feng	Terre de Chine	2013	ZHEJIANG / District JIN HUA
13	GT 5	China	Green	Lung Ching	Supermarket	-	ZHEJIANG / Hangzhou
14	TC 1	China	Green	Yan Lou Po	Terre de Chine	2013	ANHUI / District DONG ZHI
15	LG 6	China	Black	Qimen	Lydia Gautier	2013	ANHUI / Qimen, high grown (350m)
16	TC 6	China	Green, 60% fermentation	Feng Huang Dan Cong	Terre de Chine	2013	GUANG DONG / District CHAO ZHOU
17	LG 4	China	Green / Blue	Feng Huang Dan Cong	Lydia Gautier	2013	GUANGDONG / high grown (1100m)
18	GT 23	China	Green	Tyan Jen	Supermarket	-	GUANGXI / Nanning
19	GT 24	China	Green	Tyan Jen	Supermarket	-	GUANGXI / Nanning
20	TC 3	China	Green	Lu Shan Yon Wu	Terre de Chine	2013	JIANG-XI / Montagne WU YI
21	LG 3	China	Green	Mont Jing	Lydia Gautier	2013	HUBEI / District JING SHAN, high grown (900m)
22	GT 9	China	Green	No Name	Supermarket	-	no information
23	BT 11	China	Black, bergamot, orange	Hediard Blend	Supermarket	-	no information
24	GT 13	China	Green	Akbar Premium Quality Tea	Supermarket	-	no information

Table E.1. Geographical origin and provenance of studied tea samples (Continued).

No	Sample code	Country of producing	Type of the tea / additional information	Name of the tea	Supplier	Year	Provenance: Country / Province / City
25	LG 14	Japan	Green	Sencha Okumidori	Lydia Gautier	2012	KAGOSHIMA / Kirishima
26	LG 15	Japan	Green	Sencha Kashira	Lydia Gautier	2013	KAGOSHIMA / Kirishima
27	LG 17	Japan	Green	Tencha Nishi	Lydia Gautier	2013	KAGOSHIMA / Kirishima
28	LG 16	Japan	Green	Gyokuro Tawa	Lydia Gautier	2011	KYOTO / Okuyamada, Obuku
29	LG 13	Japan	Green	Sencha Motoya	Lydia Gautier	2011	KYOTO / Ishidera
30	TJ 2	Japan	Green	Gyokuro	Tamayura	2012	FUKUOKA / Yame
31	TJ 1	Japan	Green	Genmaicha	Tamayura	2012	no information
32	TJ 3	Japan	Green	Sencha	Tamayura	2012	no information
33	TJ 4	Japan	Green	Houjicha	Tamayura	2012	no information
34	TJ 5	Japan	Green	Sencha Bio	Tamayura	2012	no information
35	TJ 6	Japan	Green	Matcha	Tamayura	2012	no information
36	GT 8	Japan	Green	No Name	Supermarket	-	no information
37	CRM 23	Japan	Green	Certified Reference Materia	NIES	-	no information
38	LG 8	South Korea	Black	Uri cha	Lydia Gautier	2013	HADONG / Hwagae, mid-high grown (500-800m)
39	LG 9	South Korea	Green	Woojeon	Lydia Gautier	2013	HADONG / Hwagae, mid-high grown (500-800m)
40	LG 10	South Korea	Green	Sejak	Lydia Gautier	2013	HADONG / Hwagae, mid-high grown (500-800m)
41	LG 11	South Korea	Green	Jungjak	Lydia Gautier	2013	HADONG / Hwagae, mid-high grown (500-800m)
42	LG 12	South Korea	Green	Daejak	Lydia Gautier	2013	HADONG / Hwagae, mid-high grown (500-800m)

Table E.1. Geographical origin and provenance of studied tea samples (Continued).

No	Sample code	Country of producing	Type of the tea / additional information	Name of the tea	Supplier	Year	Provenance: Country / Province / City
45	LG 19	Sri Lanka	Black	Vithanakande	Lydia Gautier	-	Ceylon / RATNAPURA / Low grown (<600m)
46	BT 18	Sri Lanka	Black	Hyleys	Supermarket	-	Ceylon / no information
47	BT 19	Sri Lanka	Black	Golden Ceylon	Supermarket	-	Ceylon / no information
48	BT 20	Sri Lanka	Black	Basilur	Supermarket	-	Ceylon / no information
49	BT 21	Sri Lanka	Black	Basilur Tipson	Supermarket	-	Ceylon / no information
50	BT 22	Sri Lanka	Black	Akbar Gold	Supermarket	-	Ceylon / no information
51	LG 18	India	Black Tea ORGANIC	Darjeeling bio	Lydia Gautier	2013	WEST BENGAL / Darjeeling, Gielle Khola
52	BT 17	India	Black	Assam	Supermarket	-	no information
53	BT 10	India	Black	Le Morning	Supermarket	-	no information
54	BT 16	India	Black	Princess Noori	Supermarket	-	no information
55	LG 7	Nepal	White	Shangri la	Lydia Gautier	2011	ILAN / Steep Himalayan slope, high grown (1200-2000 m)
56	LG 1	Rwanda	Black	Sorwathé	Lydia Gautier	2012	KINIHIRA / high grown (1900m - 2500m), alpine plateau
57	LG 2	Rwanda	Green	Sorwathé	Lydia Gautier	2012	KINIHIRA / high grown (1900m - 2500m), alpine plateau
58	BT 14	Turkey	Black	Caykur Filiz Çayı	Supermarket	-	Turkey / RIZE / Çay İşletmeleri Genel Müd
59	BT 15	Turkey	Black ORGANIC	Organic Caykur Rize	Supermarket	-	Turkey / RIZE / Çay İşletmeleri Genel Müd
60	GT 7	Taiwan	Green, mint	Jhihuo OOLONG	Supermarket	-	Taiwan / no information

Table E.3. Sr concentrations and $^{87}\text{Sr}/^{86}\text{Sr}$ in teas.

No	Sample code	Provenance (Short)	Li, mg/kg	Rb, mg/kg	Sr, mg/kg	$^{87}\text{Sr}/^{86}\text{Sr}$
1	GT 1	China / Fujian	0,15	89,4	17,4	0,71421
2	GT 2	China / Fujian	0,11	77,2	9,90	0,71228
3	GT 3	China / Fujian	0,10	100	10,9	0,71089
4	GT 4	China / Fujian	0,05	169	8,87	0,71597
5	LG 5	China / Fujian	0,03	68,4	17,8	0,70971
6	TC 5	China / Fujian	0,18	57,5	13,9	0,71909
7	TC 4	China / Yunnan	0,04	54,1	8,92	0,71632
8	TC 7	China / Yunnan	0,22	111	22,4	0,73254
9	BM 2	China / Yunnan	0,06	86,4	16,8	0,72374
10	GT 6	China / Yunnan	0,13	161	20,0	0,72012
11	BM 1	China / Zhejiang	0,07	44,4	32,6	0,70809
12	TC 2	China / Zhejiang	0,14	45,6	26,8	0,70843
13	GT 5	China / Zhejiang	0,03	50,2	6,73	0,71578
14	TC 1	China / Anhui	0,10	35,3	10,1	0,71343
15	LG 6	China / Anhui	0,05	64,9	10,7	0,71714
16	TC 6	China / Guagdong	0,12	55,1	18,4	0,70532
17	LG 4	China / Guagdong	0,03	128	15,8	0,71073
18	GT 23	China / Guangxi	0,03	93,0	13,0	0,71095
19	GT 24	China / Guangxi	0,03	101	12,0	0,71063
20	TC 3	China / Jiangxi	0,21	121	8,69	0,74544
21	LG 3	China / Hubei	0,05	61,0	6,78	0,71174
22	GT 9	China / no information	0,07	97,6	27,5	0,71830
23	BT 11	China / no information	0,09	66,9	13,1	0,71895
24	GT 13	China / no information	0,08	95,1	13,8	0,70969
25	LG 14	Japan / Kagoshima	0,02	41,2	9,95	0,70673
26	LG 15	Japan / Kagoshima	0,03	39,4	5,03	0,70728
27	LG 17	Japan / Kagoshima	0,08	40,1	6,27	0,70703
28	LG 16	Japan / Kyoto	0,09	24,1	2,03	0,71046
29	LG 13	Japan / Kyoto	0,26	9,67	5,74	0,71070
30	TJ 2	Japan / Fukuoka	0,30	22,4	4,93	0,70773
31	TJ 1	Japan / no information	0,29	22,2	9,73	0,70792
32	TJ 3	Japan / no information	0,20	20,8	3,95	0,70735
33	TJ 4	Japan / no information	0,08	25,1	7,84	0,70741
34	TJ 5	Japan / no information	0,16	11,7	4,46	0,70778
35	TJ 6	Japan / no information	0,22	35,3	4,44	0,70779
36	GT 8	Japan / no information	0,05	16,8	5,47	0,70847
37	CRM 23	Japan / no information	0,20	20,5	4,21	0,70867

Analytical uncertainties for elemental analysis are not exceed 5% and were calculated as RSD (%) value of individual triplicates. The analytical uncertainty for Sr isotopic data is 0.00015 calculated as the maximal SD value of individual triplicates.

Table E.3. Sr concentrations and $^{87}\text{Sr}/^{86}\text{Sr}$ in teas (Continued).

No	Sample code	Provenance (Short)	Li, mg/kg	Rb, mg/kg	Sr, mg/kg	$^{87}\text{Sr}/^{86}\text{Sr}$
38	LG 8	South Korea / Hadong	0,032	25,088	17,173	0,71338
39	LG 9	South Korea / Hadong	0,034	24,902	10,241	0,72947
40	LG 10	South Korea / Hadong	0,032	21,475	14,442	0,71632
41	LG 11	South Korea / Hadong	0,018	24,013	19,705	0,71154
42	LG 12	South Korea / Hadong	0,028	25,585	20,851	0,71477
43	LG 20	Vietnam / Yen Bai	0,010	70,151	7,008	0,74035
44	LG 21	Vietnam / Yen Bai	0,027	109,601	10,405	0,73617
45	LG 19	Ceylon / no information	0,019	42,881	7,324	0,71520
46	BT 18	Ceylon / no information	0,026	40,800	15,630	0,71781
47	BT 19	Ceylon / no information	0,018	37,813	14,321	0,71658
48	BT 20	Ceylon / no information	0,016	41,904	14,184	0,71996
49	BT 21	Ceylon / no information	0,020	35,630	13,054	0,71345
50	BT 22	Ceylon / no information	0,021	41,387	9,670	0,71652
51	LG 18	India / Darjeeling	0,043	58,303	9,562	0,79137
52	BT 17	India / no information	0,039	43,594	11,683	0,72081
53	BT 10	India / Ceylon	0,020	42,035	12,464	0,71155
54	BT 16	India / Ceylon	0,053	55,886	30,388	0,71324
55	LG 7	Nepal / Ilan	0,022	125,967	10,370	0,73640
56	LG 1	Rwanda / Kinyira	0,056	70,369	39,092	0,71381
57	LG 2	Rwanda / Kinyira	0,029	24,369	35,639	0,71387
58	BT 14	Turkey / Rize	0,063	33,048	16,571	0,70671
59	BT 15	Turkey / Rize	0,062	22,522	25,100	0,70662
60	GT 7	Taiwan / no information	0,263	14,336	16,987	0,71104

Analytical uncertainties for elemental analysis are not exceed 5% and were calculated as RSD (%) value of individual triplicates. The analytical uncertainty for Sr isotopic data is 0.00015 calculated as the maximal SD value of individual triplicates.

Table E.4. Pb concentrations and Pb isotopic ratios in teas.

№	Sample code	Pb, mg/kg	$^{208}\text{Pb}/^{204}\text{Pb}$	$^{207}\text{Pb}/^{204}\text{Pb}$	$^{206}\text{Pb}/^{204}\text{Pb}$	$^{208}\text{Pb}/^{206}\text{Pb}$	$^{207}\text{Pb}/^{206}\text{Pb}$	$^{206}\text{Pb}/^{207}\text{Pb}$
1	GT 1	1,43	38,457	15,649	18,277	2,1042	0,8562	1,1679
2	GT 2	0,93	38,499	15,650	18,283	2,1058	0,8563	1,1678
3	GT 3	0,89	38,503	15,659	18,307	2,1033	0,8554	1,1690
4	GT 4	0,84	38,518	15,662	18,287	2,1064	0,8565	1,1675
5	LG 5	0,64	38,692	15,655	18,302	2,1141	0,8554	1,1690
6	TC 5	2,05	38,570	15,650	18,329	2,1044	0,8539	1,1711
7	TC 4	0,11	38,824	15,701	18,532	2,0949	0,8472	1,1803
8	TC 7	0,60	38,762	15,704	18,504	2,0948	0,8487	1,1782
9	BM 2	0,24	38,873	15,710	18,590	2,0912	0,8451	1,1832
10	GT 6	1,89	38,475	15,671	18,019	2,1160	0,8661	1,1546
11	BM 1	0,78	38,311	15,635	18,221	2,1027	0,8581	1,1653
12	TC 2	0,79	38,312	15,635	18,207	2,1042	0,8587	1,1645
13	GT 5	0,45	38,225	15,626	18,091	2,1129	0,8637	1,1577
14	TC 1	1,11	38,301	15,635	18,245	2,0993	0,8569	1,1669
15	LG 6	0,54	38,390	15,644	18,229	2,1061	0,8582	1,1652
16	TC 6	0,48	38,762	15,704	18,504	2,0948	0,8487	1,1782
17	LG 4	0,44	38,537	15,659	18,368	2,0980	0,8526	1,1729
18	GT 23	0,80	38,395	15,645	18,248	2,1042	0,8573	1,1663
19	GT 24	0,66	38,460	15,654	18,269	2,1053	0,8569	1,1669
20	TC 3	1,29	38,327	15,646	18,282	2,0965	0,8558	1,1684
21	LG 3	0,64	38,295	15,637	18,282	2,0947	0,8553	1,1691
22	GT 9	0,94	38,521	15,692	18,280	2,1073	0,8584	1,1649
23	BT 11	0,86	38,319	15,644	18,243	2,1121	0,8623	1,1597
24	GT 13	1,35	38,389	15,639	18,231	2,1068	0,8578	1,1657
25	LG 14	0,04	38,154	15,620	18,109	2,1069	0,8625	1,1593
26	LG 15	0,05	38,241	15,636	18,213	2,0997	0,8585	1,1648
27	LG 17	0,10	38,059	15,615	18,030	2,1108	0,8660	1,1547
28	LG 16	0,19	38,164	15,612	18,131	2,1050	0,8611	1,1613
29	LG 13	0,23	37,780	15,585	17,848	2,1167	0,8732	1,1452
30	TJ 2	0,16	38,103	15,613	18,066	2,1093	0,8642	1,1571
31	TJ 1	0,11	38,235	15,630	18,158	2,1057	0,8608	1,1617
32	TJ 3	0,23	38,246	15,626	18,176	2,1042	0,8597	1,1632
33	TJ 4	0,16	38,147	15,614	18,105	2,1069	0,8624	1,1595
34	TJ 5	0,08	38,146	15,616	18,098	2,1079	0,8629	1,1589
35	TJ 6	0,19	38,053	15,609	18,027	2,1109	0,8659	1,1548
36	GT 8	0,12	38,253	15,622	18,173	2,1067	0,8611	1,1613
37	CRM 23	0,15	38,164	15,610	18,067	2,1118	0,8638	1,1577

Analytical uncertainties for elemental analysis are not exceed 5% and were calculated as RSD (%) value of individual triplicates. Uncertainties of Pb isotopic determination related to complete process of sample preparation including digestion and column separation were estimated on independently prepared triplicates of samples (RSD): 530 ppm ($^{208}\text{Pb}/^{204}\text{Pb}$), 240 ppm ($^{207}\text{Pb}/^{204}\text{Pb}$), 560 ppm ($^{206}\text{Pb}/^{204}\text{Pb}$), 560 ppm ($^{208}\text{Pb}/^{206}\text{Pb}$), 450 ppm ($^{207}\text{Pb}/^{206}\text{Pb}$).

Table E.4. Pb concentrations and Pb isotope ratios in teas (Continued).

№	Sample code	Pb, mg/kg	$^{208}\text{Pb}/^{204}\text{Pb}$	$^{207}\text{Pb}/^{204}\text{Pb}$	$^{206}\text{Pb}/^{204}\text{Pb}$	$^{208}\text{Pb}/^{206}\text{Pb}$	$^{207}\text{Pb}/^{206}\text{Pb}$	$^{206}\text{Pb}/^{207}\text{Pb}$
38	LG 8	0,20	38,122	15,618	18,113	2,1046	0,8622	1,1598
39	LG 9	0,18	37,799	15,619	18,096	2,0887	0,8631	1,1585
40	LG 10	0,23	38,200	15,617	18,141	2,1057	0,8608	1,1616
41	LG 11	0,09	38,244	15,621	18,185	2,1031	0,8590	1,1640
42	LG 12	0,12	38,152	15,622	18,142	2,1029	0,8611	1,1613
43	LG 20	0,02	ND	ND	ND	ND	ND	ND
44	LG 21	0,36	38,473	15,657	18,314	2,1008	0,8550	1,1696
45	LG 19	0,17	37,900	15,622	17,971	2,1090	0,8693	1,1503
46	BT 18	0,17	37,967	15,650	18,062	2,1044	0,8681	1,1519
47	BT 19	0,44	38,148	15,627	17,907	2,1285	0,8727	1,1459
48	BT 20	0,16	37,758	15,611	17,826	2,1181	0,8758	1,1418
49	BT 21	0,26	38,172	15,650	18,086	2,1105	0,8653	1,1556
50	BT 22	0,18	37,879	15,629	17,943	2,1110	0,8710	1,1480
51	LG 18	0,13	38,399	15,672	18,273	2,1014	0,8576	1,1659
52	BT 17	0,49	37,476	15,592	17,526	2,1378	0,8897	1,1239
53	BT 10	0,17	37,674	15,606	17,728	2,1248	0,8803	1,1359
54	BT 16	0,45	37,680	15,601	17,695	2,1299	0,8817	1,1342
55	LG 7	0,24	37,685	15,612	17,689	2,1303	0,8826	1,1330
56	LG 1	0,27	37,966	15,624	17,990	2,1104	0,8685	1,1514
57	LG 2	0,43	37,765	15,597	17,841	2,1168	0,8743	1,1438
58	BT 14	0,32	38,232	15,621	18,279	2,0935	0,8557	1,1686
59	BT 15	0,36	38,115	15,615	18,153	2,1019	0,8611	1,1613
60	GT 7	0,54	38,267	15,632	18,141	2,1094	0,8617	1,1605

Analytical uncertainties for elemental analysis are not exceed 5% and were calculated as RSD (%) value of individual triplicates. Uncertainties of Pb isotopic determination related to complete process of sample preparation including digestion and column separation were estimated on independently prepared triplicates of samples (RSD): 530 ppm ($^{208}\text{Pb}/^{204}\text{Pb}$), 240 ppm ($^{207}\text{Pb}/^{204}\text{Pb}$), 560 ppm ($^{206}\text{Pb}/^{204}\text{Pb}$), 560 ppm ($^{208}\text{Pb}/^{206}\text{Pb}$), 450 ppm ($^{207}\text{Pb}/^{206}\text{Pb}$).

General conclusion

Perspectives

General conclusion and Perspectives

This dissertation has been focused on the applications of Sr- and Pb- isotope ratios for tracing the geographical origin of foods. For the first time, a large series of authentic Bordeaux wines, European dry-cured hams of the known brands, different salts, and original Asian teas were examined for Sr isotopic specification as well as with Pb isotope determination. The general observation noticed a strong influence on Sr- and Pb- isotopic composition of food products from the environment of origin and suggest that these isotopes are certainly powerful traceability markers, owing to their peculiarities which allows to discriminate samples with different origins and characteristics. A valuable information about the exposure pathways of Pb ambient pollution accumulated in plants is also presented and may serve to investigate the Pb geochemical cycle in the environment. The main findings and perspectives concluded from this doctoral work are summarized below:

Wine

Lead and strontium isotopic specifications were determined in a series of 43 prestigious Bordeaux wines in the context of their application for wine authenticity and provenance assessment.

This study of Sr content, the first of its kind performed on Bordeaux wines, revealed moderate variabilities in Sr elemental and isotopic compositions of wines from this region caused by its particular geological and pedological settings. Negligible variations of the $^{87}\text{Sr}/^{86}\text{Sr}$ ratio were observed in wines within the same production chain. The results obtained through the examined varietal blended wines and wines from different vintages allow to evidence a distinctive characteristic for authenticity tracing of Bordeaux wines with precise specifications of different viticultural sub-regions and even individual wineries. The unique binary Sr pattern combining elemental and isotopic information integrates at first the lithological signature of a vineyard, and then includes also specific signatures of traditional viticultural and winemaking practices. All things considered, the Sr binary fingerprint can be recognized as a powerful provenance tracer for Bordeaux wines, and has been successfully tested on mislabeled Bordeaux wines.

The Pb isotopes determination is the second study of such scale performed on Bordeaux wines. The results obtained with Bordeaux wines shown good agreement with a previous survey of Medina et al. (2000) and together the two studies provide the unique record of Pb isotopic signatures of the Bordeaux wine in the period from 1895 to 2015. Today, the contribution from leaded gasoline in wine has almost disappeared, the Pb isotopes are fairly homogeneous within the whole region and are influenced primarily by airborne lead of natural origin. Taking into account the compositional

difference of lead isotopic signatures on a continental scale, this tracer can be a useful tool to detect counterfeited "Bordeaux" wines produced outside of the homonymous territory.

Perspectives:

The Sr elemental-isotopic fingerprint of wine is a terroir-inherent and winemaking-related tracer, which reflects accurately and precisely the whole ensemble of geological, pedological, climatic, atmospheric specifications combined with national traditions of viticulture and winemaking. Being reinforced by trace elemental concentrations, this authentic pattern can be used for geographical origin assessment when considering possible fraud involving branded Bordeaux wines. In the future, it will be interesting to create a representative regional Sr isotopic map with specifications of individual wineries, as it has been done for Italian Lambrusco PDO wines (Durante et al., 2018), to be able to verify the declared origin of a wine without the presence of authentic reference samples.

Tea

The Sr and Pb isotope ratios together with trace elemental concentrations were determined in 60 tea samples across a wide range of producing countries. The variations in $^{87}\text{Sr}/^{86}\text{Sr}$ ratios did not show a reliable differentiation among all countries with the exception of tea originating from Japan and Himalaya, demonstrating a strong pronounced specific Sr binary composition. In other cases, when applying alone the $^{87}\text{Sr}/^{86}\text{Sr}$ ratio, it was difficult to have a clear distinction for the provenance interpretation due to the great variability and complexity of geological settings over the studied origins.

In the contrary, when using Pb isotopic specification of teas provided, a very useful information could be obtained addressing to sample's geographical provenance due to the direct linkage with the environment of origin through locally available Pb emission sources. An excellent matching between the Pb isotopic signatures of teas and those of the regional atmosphere was observed for teas from China and Japan.

For the first time, the concept of geochemical zoning of Asia was practically applied for the food geographic origin classification. The observed regularities reliably confirmed that the geographic origin assignment is possible by means of Pb isotopic ratios due to the linkage to the geological settings under certain circumstances.

The comprehensive multi-elemental and multi-isotopic approach completed with statistical data treatment has been successfully applied for classification of teas from China, Japan and South Korea.

Perspectives:

By the tea study case a very important outcome can be highlighted: it is highly possible that origins of any food products from a region with specific atmospheric Pb composition can be traced and identified by Pb isotope ratios. This tracer will be a sensitive descriptor when consider a large geographic scale, for example, origins of Europe, Australia, North America, China.

The elimination of such significant permanent source of Pb-pollution as leaded gasoline, has globally altered the atmospheric lead isotopic signatures: if before they reflected in a greater extent lead from lower radiogenic, geologically ancient mines, which have been commonly used for many years to produce anti-knock additive to gasoline, now they are slowly returning to geogenic values and reflect more regional Pb-sources of lead. The restriction of leaded gasoline was realized gradually around the world. Therefore, the Pb isotope ratios could be useful criteria to distinguish food product from regions under a tetraethyl lead ban and those where it is still being in use, on used or has been banned recently. However, such indicator also signal that the substantial level of Pb in the atmosphere is maintained now by the various of industrial and urbanistic emissions.

Ham

The study of Sr isotopic specification in dry-cured ham is the first of its kind for prepared meat products, and it is the most complete record of determined trace elements of Iberian, Bayonne, Parma and San Daniele dry-cured hams. Based on the obtained results, it can be concluded that the discrimination among the different origin for dry-cured ham is the result of both raw meat elemental/isotopic content and processing practices.

As regard to regional classification, the most notable particularities can be attributed to the French Bayonne ham. Its highly specific elemental and Sr isotopic composition is due to the mineral salt from regional mine Salies-de- Béarn used for its production. Other investigated hams origin Spain, Portugal and Italy, salted with sea salt, demonstrated non distinguishable Sr isotopic composition.

Perspectives:

Further studies involving larger homogeneous sample selections are required to evaluate the salt contribution to the elemental and Sr isotopic composition of dry-cured hams and explain a slight variabilities observed in the hams salted with sea salt (origin from Spain, Portugal and Italy), likely caused by the row meat elemental composition. Such research could establish specific characteristics of cured meat products for authenticity tracing purposes, provenance confirmation and/or counterfeit detection.

Areas which merit a particular attention

The definitive assignment of food provenance remains a complex challenge. Several factors should be considered as part of the context for successful interpreting of origin by means of Sr- and Pb isotope ratios:

- Assess to a database involving representative number of authentic samples which can represent the maximally entire Sr isotopic variability of the area;
- Use Pb-isotopes to trace food provenance and authenticity is only valid if carried out in relation to a region with clearly defined Pb emission sources and if time trends are studied;
- Features of regional climates, dust transportation, environmental trends caused by climate change and anthropogenic impact must be taken into consideration depending on the region;
- Evaluate the impact of human activity, norms and regulations of agricultural practices as well as national trading politics of export and import of mineral resources. These needs to be taken into account also.

Perspectives for Aquitaine's regional food products

The ensemble of isotopic and elemental results obtained for Aquitaine regional food products (Bordeaux wines, Bayonne ham, and salt from Salies-de-Bearn) is of strong interest since it highlights a certain compositional specification which can be used in development of a regional food protection schema. Indeed, the concept of PDO, PGI, TDS, and AOC presupposes that food originates from a specific geographical area with clear distinct characteristics and defined process of the preparation. The tracing of Sr and Pb isotope ratios in such products may serve for detection imitation or mislabeling products and, thus, protect the regional food market.

The present research emphasizes the importance of the Sr and Pb isotopic approaches for being involved in the future in modern legislative interactions aimed at guaranteeing food authenticity and geographical origin, and protecting customers and producers from possible frauds.

Appendix

1. Selected trace elements in Bordeaux

2. Trace metals in teas origin China, Japan and South Korea

3. Scientific contribution

4. Curriculum Vitae

Appendix 1

Selected trace elements in Bordeaux wines

Trace element concentrations are an important characteristics of wine quality. First of all, they are useful criterions to control toxicological risks, food regulations norms, vinification process and wine stability (Kruzlikova et al., 2013). Secondly, the elemental fingerprinting of wine is widely applied for discrimination according to geographical origin (Médina et al., 2013; González, A. & De La Guardia, 2013b; Cozzolino & Smyth, 2013). The elemental composition in wine depends on natural factors such as the types of ground and underground waters, vineyard soil, and climatic conditions, what is described by the concept of terroir (Almeida & Vasconcelos, 2003b; Greenough et al., 2005; Galani-Nikolakaki & Kallithrakas-Kontos, 2007; Kment et al., 2005; Rodrigues et al., 2011c; Zou et al., 2012; Kruzlikova et al., 2013; Geană et al., 2013; Šelih et al., 2014; Hopfer et al., 2015; Pepi & Vaccaro, 2018; Pepi et al., 2018). Apart from this, several alternative circumstances may effect on the elemental composition of wines, and render the correlation between a wine and its terroir more complex:

- a) Anthropogenic sources, that represent the influence from environmental contaminations: wines from vineyards located close to roads / highways or situated in industrial areas, generally contain higher levels of Cd and Pb due to vehicular exhaust or other industrial emissions to air, water and soil (Pohl, 2007; Vystavna et al., 2015).
- b) Agricultural practices: an application of certain fertilizers on vines (containing Fe-, B-, Mn-, Cu-, Zn-compounds) and inorganic pesticides / herbicides (containing As-, Cd- compounds, etc.) leads to increasing of concentrations of these metals in wine (Pohl, 2007; Vystavna et al., 2015).
- c) Features of winemaking processes: the wine contamination may occur due to the direct contact of wine with materials and equipment of production and storing (Pohl, 2007), also adding of special yeasts, sulfites or bentonite during vinification can change the elemental composition of wine (Médina et al., 2013; Šelih et al., 2014; Geană et al. 2013; Hopfer et al., 2015).

With the framework of this study, the concentrations of sixteen selected elements (Li, B, Al, V, Fe, Mn, Co, Ni, Cu, Zn, Rb, Sr, Cd, Cs, Ba and Pb) were quantified in a large selection of authentic Bordeaux wines and wines with suspicious Bordeaux origin purchased in China (detailed description is provided in paragraph C.1.1) with the goal to access the distinctive elemental fingerprint of authentic Bordeaux wines, and then evaluate whether it is a performant criterion for

identification of imitated wines. The second goal was an appraising the possibility of studied Bordeaux wineries differentiation by means of wine elemental content.

1. Elemental profiles of studied wines

The trace metal analysis was performed using Q-ICP-MS NexION. The operating parameters and details of the analytical procedure are described in Chapter B. A summary table of the mean elemental concentrations is presented in Table 1.1.

For a comparative evaluation of mean concentrations of selected elements, the studied wines were integrated into two groups according to their origins. The first group, named "Bordeaux authentic", includes 43 wines from Pomerol, Saint-Émilion, Pessac-Léognan and Pauillac. The second group, called "Bordeaux imitation", includes 14 wines of suspicious Bordeaux origin and sold as "Bordeaux" in China. Box plots on Fig. 1.1 graphically present elemental ranges for two studied groups, where: the red horizontal bars correspond to the medians for each individual group, the boxes correspond to the interquartile ranges (IQR) of concentrations, and their vertical height indicates the degree of dispersion between minimal and maximal concentrations within the range of IQR. Two limiting vertical whiskers outside of the boxes extend the intervals to the highest and to the lowest limits with the consideration of the $1.5 \times \text{IQR}$. The extreme values of concentrations pointed by red circles.

According to obtained results, concentrations of considered elements in wines were found in the trace quantities, meaning that their level did not exceed 100 mg L^{-1} . Among the selected elements determined in authentic Bordeaux wines, boron was the most abundant element followed by Rb, Fe, Mn, Al, Zn, Sr, Ba, the concentrations of these elements were about from 0.1 to 10 mg L^{-1} . Other elements were presented on the level below of 0.1 mg L^{-1} .

In terms of safety levels, the concentrations of all studied elements were within the limits imposed in the International code of oenological practices (OIV code).

Boron is an essential element in vine plants. It can enter wines from the soil: boron-rich soils are the result of either marine sediments or boron rich minerals (Hopfer et al., 2015). Also, boron is an important constituent of mineral fertilizers applied on vineyards (Goldammer, 2013), of specific treatments of musts and wines (Galani-Nikolakaki & Kallithrakas-Kontos, 2007). The range of B concentrations in authentic Bordeaux varies between 3.2 and 11.8 mg L^{-1} , for suspicious Bordeaux the range is $1.5\text{-}15 \text{ mg L}^{-1}$.

Manganese, in small amounts, is a natural constituent of grapes and wines (Geană et al., 2013). The amount found in wines depends on the soil composition and the use of herbicides (Galani-

Nikolakaki & Kallithrakas-Kontos, 2007). In our study, measured Mn concentrations are homogeneously ranged between 0.40 and 2.2 mg L⁻¹ for Bordeaux wines, while the second group of suspicious wines had the higher and the more dispersed range from 0.91 to 7.11 mg L⁻¹.

Iron found in wine can be originated from several sources: from the soil, from fertilizers (Goldammer, 2013), and from Fe-containing treatment during vinification (Pohl, 2007). The concentrations of Fe in the group of authentic Bordeaux wines ranged between 0.3 and 4.8 mg L⁻¹, for suspicious Bordeaux the variation was from 1.9 to 7.5 mg L⁻¹. For a sample with the highest level of Mn – 7.1 mg L⁻¹, the highest level of Fe was also observed – 7.5 mg L⁻¹ (Table 1.1). This observation is in agreement with a previous study (Galani-Nikolakaki & Kallithrakas-Kontos, 2007). Such correlation was also noted for one sample from the group of Chinese wines, where the elevated concentrations of both elements were observed: 4.1 mg L⁻¹ for Mn and 7.8 mg L⁻¹ for Fe (Table 1.1).

Cobalt and **Nickel** often are transferred into wine from stainless steel winery equipment, or certain type of glass bottles (Galani-Nikolakaki & Kallithrakas-Kontos, 2007). The levels of Co in both groups are relatively homogeneous and not exceed 1.25 µg L⁻¹. The Ni content in authentic Bordeaux wines ranged between 14.2 and 70.6 µg L⁻¹ with an average of 21.2 µg L⁻¹, and had the highest content in wines from Pauillac. All authentic Bordeaux wines were characterized by a relatively low variability of Ni concentrations within the same winery. In contrast, Ni measured in suspicious Bordeaux achieve a maximal level of 125 µg L⁻¹ with the averaged content nearly 47 µg L⁻¹. In Chinese wines, Ni was detected at a relatively high level as well: 45, 58, and 166 µg L⁻¹.

Vanadium concentrations in studied wines are characterized by a high variability, from 0.29 to 280 µg L⁻¹ for authentic wines, and from 6.7 to 123 µg L⁻¹ in suspicious wines. For Bordeaux, the tendency of framing of concentrations in a certain defined interval depending on the wineries was observed, which might be related to the use of the stainless steel winery equipment.

Copper is an essential element for vines. Plants uptake Cu which occurs naturally or as a consequence of agricultural practices, such as applying of copper-based fungicides to control the vine downy mildew (Geană et al., 2013; Goldammer, 2013; Vystavna et al., 2017). The span of Cu concentrations in studied wines is relatively large, changing from 0.02 to 0.35 mg L⁻¹ for authentic Bordeaux, and from 0.06 to 1.10 mg L⁻¹ for mislabeled “Bordeaux”.

Zinc is also an essential element for vines, however, it's source in wine is predominantly from fungicides, insecticides and technological equipment (Galani-Nikolakaki & Kallithrakas-Kontos, 2007; Goldammer, 2013; Vystavna et al., 2017). The Zn content in studied samples varied without a significant differences: in authentic Bordeaux - 0.27-3.07 µg L⁻¹, in mislabeled Bordeaux - 0.40-

2.24 $\mu\text{g L}^{-1}$. However, the higher level of Zn has been found in the vintage wines from Pomerol - about 3 $\mu\text{g L}^{-1}$ in the wines produced in 1969 and 1973. Further, during 1978-1992 the concentrations of Zn have decreased up to a level of about 1 $\mu\text{g L}^{-1}$, and since 2000 are consistently decreasing (with an exception of year 2009). Three samples of mislabeled "Bordeaux" produced in 2007-2009, have the Zn concentrations being on a level significantly higher than it has been found in the authentic Bordeaux - about 2 $\mu\text{g L}^{-1}$. This phenomenon can be explain by a more intensive use of Zn-based fungicides or insecticides or by a more significant pollutant load of the atmosphere by heavy metals in the past years, which therefore ultimately falls on wine (Médina et al., 2013). The same trend was observed for Pb and Cd concentrations and will be discussed below.

Lead and Cadmium in authentic Bordeaux wines varied within a range from 4.4 to 163.1 $\mu\text{g L}^{-1}$ and from 0.2 to 1.9 $\mu\text{g L}^{-1}$, respectively. For the suspicious Bordeaux wines, intervals of concentrations were: 8.6-44.4 $\mu\text{g L}^{-1}$ and 0.2-5.5 $\mu\text{g L}^{-1}$, for Pb and Cd respectively. It is notable, that French wines from older vintage present a higher level of those elements, which can be seen on the example of wines from Pomerol. Evidently, the Pb concentrations exponentially decreased in 40 years from 163 $\mu\text{g L}^{-1}$ down to about 18 $\mu\text{g L}^{-1}$ (section C.3.2.1, Fig. C.7) and the Cd concentrations present the same decreasing trend from 1.8 down to 0.3 $\mu\text{g L}^{-1}$. Since around the 2000s, all studied Bordeaux wines have Pb concentrations below 30 $\mu\text{g kg}^{-1}$ and Cd concentrations below 0.5 $\mu\text{g L}^{-1}$. In contrast, the samples of suspicious Bordeaux demonstrate higher levels of these elements without any visible trends of Pb- Cd-decreasing during the period of wine's declared production 1998-2009. Moreover, the Pb and Cd concentrations in suspicious Bordeaux do not match levels of these elements in authentic wines if considering the same period of production.

In literature, the similar temporal depending trend of changing of Pb concentrations was described (Rosman et al., 1998; Médina et al., 2000). Apart from that, a strong dependency of Pb concentration in wine from regional Pb sources was reported (Vystavna et al., 2017). A more detailed discussions about Pb concentrations in studied Bordeaux wine can be seen in section C.3.3.1 of this manuscript.

Cesium and Barium are the elements, whose concentrations do not differ significantly between two studied wine groups. Levels of Cs in authentic and suspicious Bordeaux ranged between 1.7 and 5.9 $\mu\text{g L}^{-1}$, and between 2.5 and 7.7 $\mu\text{g L}^{-1}$, respectively, with an exception of two high values measured in the suspicious group - 27.4 and 36.6 $\mu\text{g L}^{-1}$. For most samples in both groups, the concentrations of Ba ranged in an interval of 0.07-0.30 mg L^{-1} (with one exception of 0.52 mg L^{-1}).

Aluminum in excessive quantities can bring toxicity and facilitate wine instability. The concentrations of Al did not change considerably between these two compared groups, respecting

the safe limit (OIV), and ranged in intervals of 0.13-2.56 mg L⁻¹ and 0.27-1.72 mg L⁻¹ for authentic and suspicious Bordeaux respectively.

Lithium in small amounts is the natural constituent of grapes, mostly originating from soil and does not seem to be influenced by the wine production process (Geană et al., 2013). In certain cases, it might migrate to the wine from glass bottles during prolonged storage (Galani-Nikolakaki & Kallithrakas-Kontos, 2007). In our study, measured values of Li ranged between 1.8 and 21.7 µg L⁻¹ for authentic Bordeaux wines, and between 8.8 and 85.8 µg L⁻¹ for wines of suspicious Bordeaux provenance.

Rubidium as lithium, is mostly transferred into wine from the vineyard soil and so far has not been found to be contaminant during the vinification process. Rubidium was observed in authentic Bordeaux group on the level of concentrations from 0.80 to 2.95 mg L⁻¹. In the group of suspicious wines, Rb concentrations didn't differ from these values, with only one sample measured at 7.02 mg L⁻¹ ("Mislabelled Pauillac", Table 1.1). Such a high Rb concentration was observed in group of Chinese wine: 7.88 mg L⁻¹ ("China red wine", Table 1.1).

Strontium as lithium and rubidium, is mostly originated in wine from the soil, which makes it of interest to be used for geographical classifications of wines. Several studies were devoted to the correlation between Sr isotopic composition of soil, grapes and wine (more details in Chapter A). Concentrations of Sr in authentic Bordeaux wines varied from 0.11 to 0.52 mg L⁻¹ and did not change significantly within the same winery (section C.2.2, Fig. C.2), which was consistent with Koreňovská et al. (2005). In contrast, wines from the suspicious Bordeaux group were characterized by a greater span of Sr concentration values: 0.29-1.52 mg L⁻¹. Such high Sr concentrations were also observed in the group of Chinese wines from this work: 0.70, 1.47 and 2.16 mg L⁻¹.

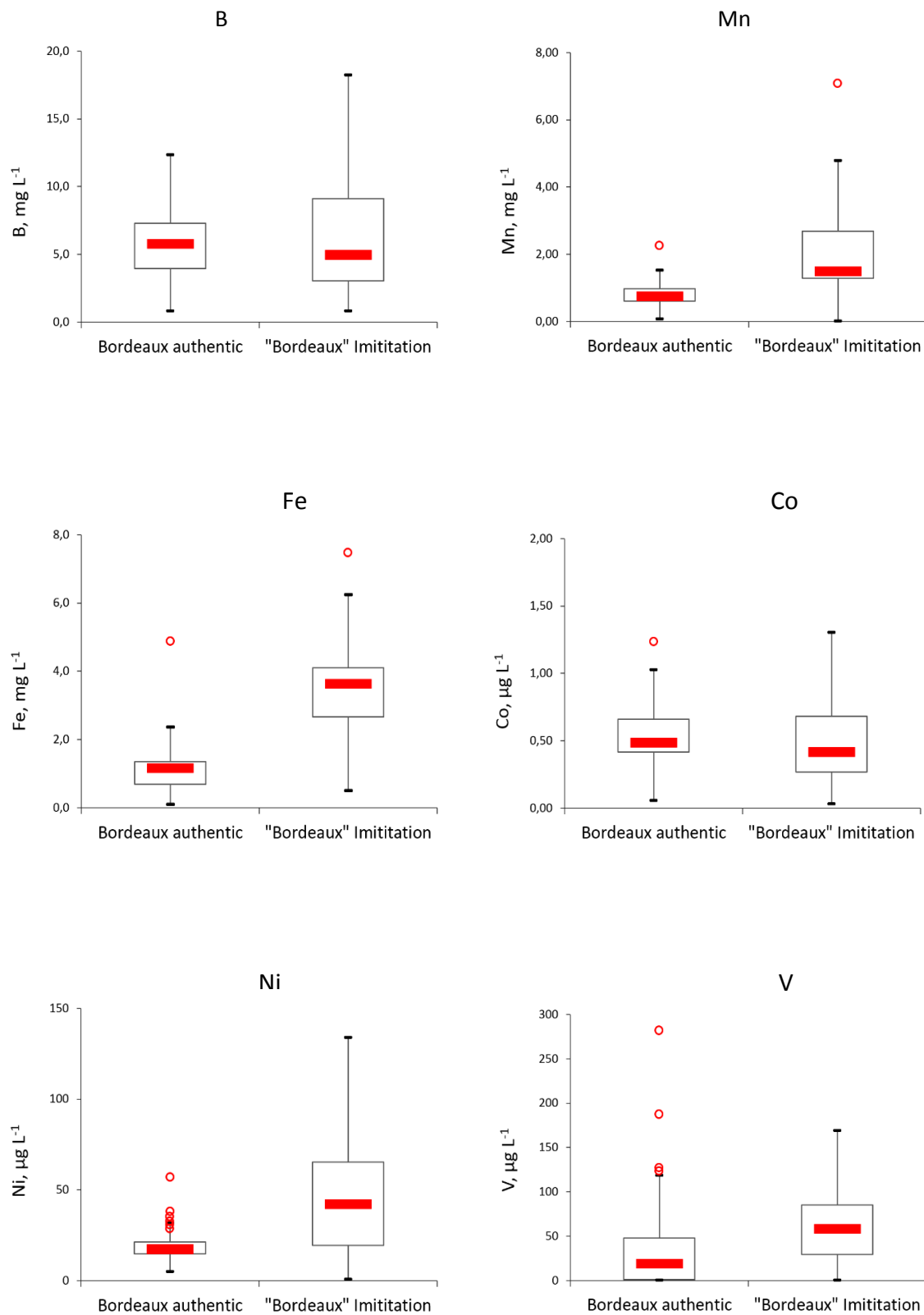


Fig. 1.1. Comparison of elemental concentrations in authentic and imitated Bordeaux wines.

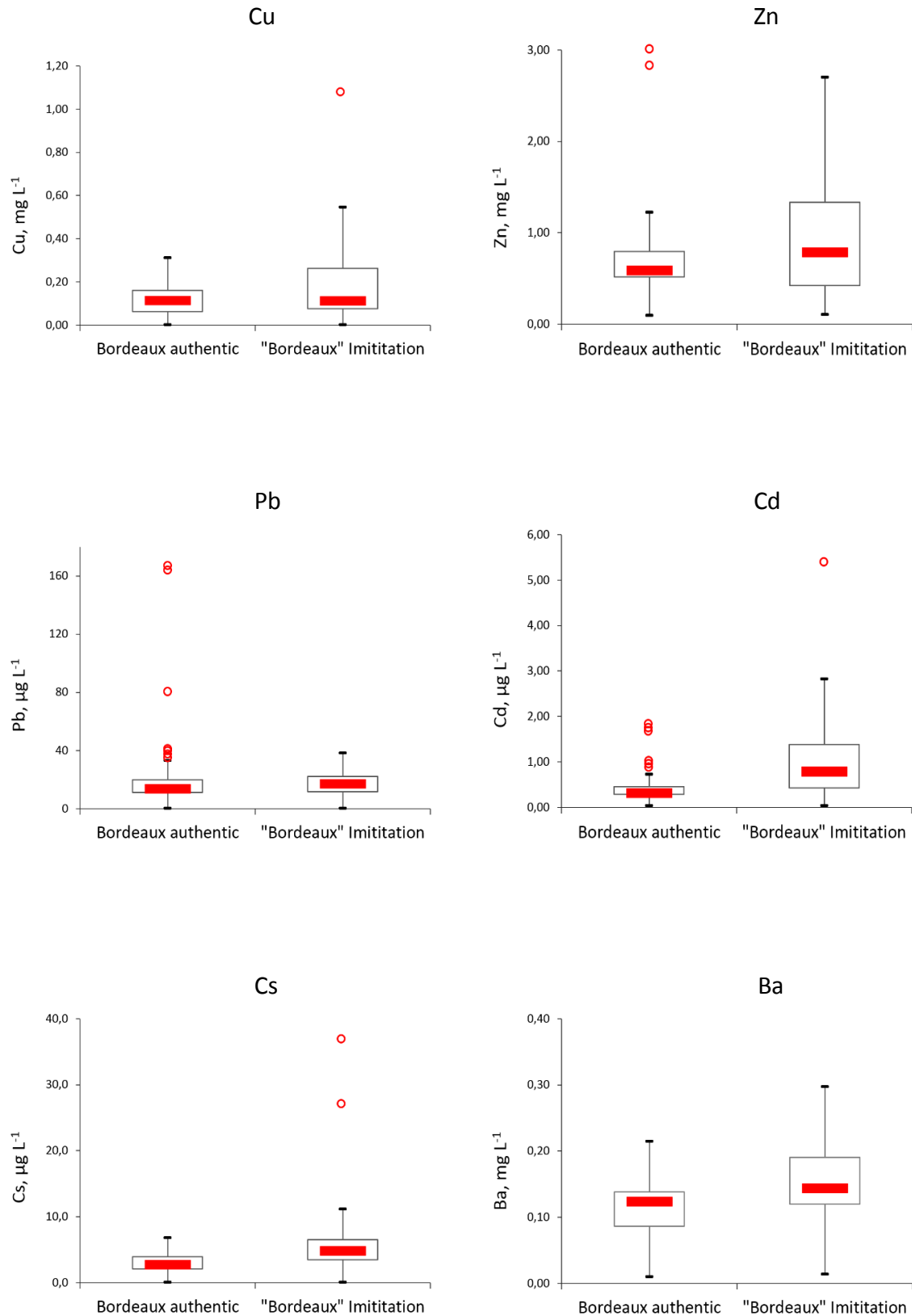


Fig. 1.1. Comparison of elemental concentrations in authentic and imitated Bordeaux wines (Continuation).

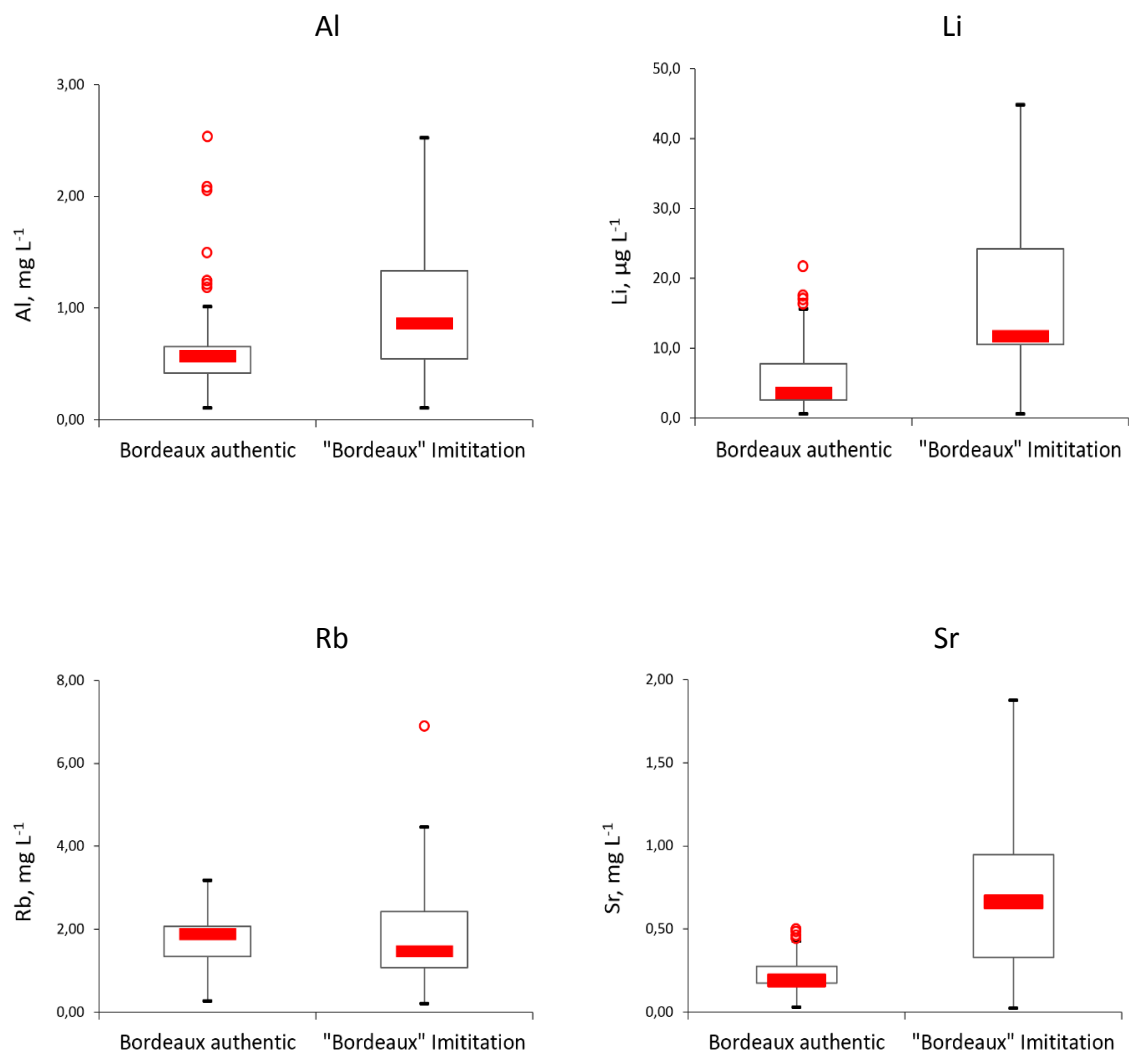


Fig. 1.1. Comparison of elemental concentrations in authentic and imitated Bordeaux wines (Continuation).

Table 1.1. Concentrations of selected elements in the studied wines.

Appellation Provenance	Year	Li $\mu\text{g L}^{-1}$	B mg L^{-1}	Al mg L^{-1}	V $\mu\text{g L}^{-1}$	Mn mg L^{-1}	Fe mg L^{-1}	Co $\mu\text{g L}^{-1}$	Ni $\mu\text{g L}^{-1}$
Pomerol	1969	14,8	9,38	0,47	1,22	0,79	4,79	1,24	36,6
Château 1	1973	7,02	7,52	0,58	1,07	1,13	3,16	0,85	32,9
red wine	1978	4,01	6,70	0,45	1,35	2,22	1,84	0,72	18,0
Bordeaux	1979	21,7	6,85	0,95	1,33	0,83	3,67	0,83	21,2
France	1989	9,82	7,07	0,29	1,60	1,00	1,29	0,90	19,2
	1992	16,2	6,99	0,68	4,02	1,16	2,37	0,64	14,2
	2002	16,0	9,91	0,58	1,62	0,59	1,33	0,63	24,2
	2003	15,2	11,8	0,49	2,45	0,58	1,47	0,78	23,4
	2004	16,9	10,3	0,64	1,68	0,57	1,31	0,65	17,5
	2009	11,8	9,47	0,44	1,34	0,67	1,02	0,74	18,9
	2010	8,48	9,21	1,17	1,56	0,66	1,06	0,67	17,5
	Mean	12,9	8,65	0,61	1,75	0,93	2,12	0,79	22,2
	SD	5,17	1,71	0,25	0,84	0,48	1,25	0,18	6,90
	Min value	4,01	6,70	0,29	1,07	0,57	1,02	0,63	14,2
	Max value	21,70	11,76	1,17	4	2,22	4,79	1,24	36,6
Saint-Emilion	2011	6,36	8,91	1,45	96,5	0,95	1,24	0,59	20,9
Château 2	2011	6,77	9,02	2,00	184	0,95	1,55	0,63	21,8
red wine	2011	9,19	7,90	2,03	119	0,97	1,41	0,77	28,3
Bordeaux	2011	9,91	8,12	2,56	281	0,99	1,70	0,89	30,9
France	Mean	8,06	8,49	2,01	170	0,96	1,48	0,72	25,5
	SD	1,76	0,56	0,45	82,5	0,02	0,19	0,14	4,91
	Min value	6,36	7,90	1,45	96,5	0,95	1,24	0,59	20,9
	Max value	9,91	9,02	2,56	281	0,99	1,70	0,89	30,9
Pessac-Léognan	2010	5,35	3,97	0,15	0,38	0,46	0,28	0,39	10,1
Château 3	2010	6,45	3,53	0,15	0,64	0,47	0,50	0,28	9,86
white wine	2010	3,94	3,52	0,21	0,82	0,73	0,50	0,42	13,9
Bordeaux	2011	2,80	3,23	0,15	0,47	0,70	0,38	0,47	11,6
France	2011	3,44	3,40	0,46	2,44	0,73	1,24	0,44	14,7
	2012	4,51	3,50	0,27	0,58	0,41	0,59	0,29	9,77
	2012	2,09	3,43	0,13	0,29	0,40	0,35	0,21	8,87
	2012	1,81	3,46	0,13	0,86	0,57	0,48	0,29	8,33
	2012	3,17	3,32	0,52	1,13	0,43	0,81	0,36	12,9
	Average	3,73	3,48	0,24	0,85	0,55	0,57	0,35	11,1
	SD	1,51	0,21	0,15	0,65	0,14	0,30	0,09	2,28
	Min value	1,81	3,23	0,13	0,29	0,40	0,28	0,21	8,3
	Max value	6,45	3,97	0,52	2	0,73	1,24	0,47	14,7

Analytical uncertainties for elemental analysis not exceed 5% and were calculated as RSD (%) value of individual triplicates.

Table 1.1. Concentrations of selected elements in the studied wines (Continuation).

Appellation Provenance	Year	Cu $\mu\text{g L}^{-1}$	Zn mg L^{-1}	Sr mg L^{-1}	Rb mg L^{-1}	Cd $\mu\text{g L}^{-1}$	Cs $\mu\text{g L}^{-1}$	Ba mg L^{-1}	Pb $\mu\text{g L}^{-1}$
Pomerol	1969	44,8	2,82	0,43	2,06	1,87	2,05	0,20	163
Château 1	1973	124	3,07	0,32	2,09	1,27	3,60	0,14	161
red wine	1978	127	1,19	0,34	1,95	1,74	3,52	0,17	84,7
Bordeaux	1979	155	1,00	0,36	2,10	1,83	4,81	0,17	37,1
France	1989	145	1,00	0,35	2,61	0,70	5,15	0,13	34,6
	1992	211	1,17	0,32	2,06	0,67	3,68	0,12	34,0
	2002	176	0,77	0,42	2,22	0,38	4,71	0,17	29,5
	2003	191	0,91	0,46	2,70	0,37	5,74	0,19	24,4
	2004	332	0,64	0,41	2,54	0,54	5,27	0,15	22,1
	2009	114	1,11	0,43	2,95	0,33	5,23	0,14	16,7
	2010	170	0,78	0,52	2,93	0,51	5,91	0,19	18,0
	Mean	163	1,31	0,39	2,38	0,93	4,52	0,16	56,9
	SD	71,6	0,82	0,06	0,37	0,62	1,17	0,03	55,2
	Min value	44,8	0,64	0,32	1,95	0,33	2,05	0,12	16,7
	Max value	332	3,07	0,52	2,95	1,87	5,91	0,20	163
Saint-Emillion	2011	52,5	0,49	0,16	1,86	0,27	5,08	0,08	5,17
Château 2	2011	123	0,51	0,16	1,87	0,29	5,10	0,09	4,91
red wine	2011	67,4	0,59	0,18	1,85	0,16	4,25	0,08	4,39
Bordeaux	2011	148	0,66	0,19	1,85	0,38	4,37	0,10	5,30
France	Mean	97,7	0,56	0,17	1,86	0,28	4,70	0,09	4,94
	SD	45,2	0,08	0,01	0,01	0,09	0,45	0,01	0,40
	Min value	52,5	0,49	0,16	1,85	0,16	4,25	0,08	4,39
	Max value	148	0,66	0,19	1,87	0,38	5,10	0,10	5,30
Pessac-Léognan	2010	64,8	0,68	0,15	1,36	0,36	2,01	0,08	10,1
Château 3	2010	184,9	0,86	0,17	0,88	0,49	1,66	0,09	15,7
white wine	2010	81,6	0,87	0,14	1,11	0,89	2,71	0,09	15,1
Bordeaux	2011	42,0	0,82	0,12	0,80	0,41	1,78	0,08	12,3
France	2011	74,3	0,27	0,23	0,81	0,43	1,81	0,09	16,2
	2012	21,8	0,49	0,16	1,04	0,32	1,87	0,07	12,3
	2012	59,2	0,53	0,14	1,28	0,29	1,77	0,08	9,37
	2012	80,4	0,54	0,11	0,91	0,29	1,76	0,07	10,5
	2012	62,2	0,65	0,20	1,00	0,38	1,96	0,09	14,0
	Average	74,6	0,63	0,16	1,02	0,43	1,92	0,08	12,8
	SD	45,5	0,20	0,04	0,20	0,19	0,31	0,01	2,53
	Min value	21,8	0,27	0,11	0,80	0,29	1,66	0,07	9,37
	Max value	185	0,87	0,23	1,36	0,89	2,71	0,09	16,2

Analytical uncertainties for elemental analysis not exceed 5% and were calculated as RSD (%) value of individual triplicates.

Table 1.1. Concentrations of selected elements in the studied wines (Continuation).

Appellation Provenance	Sample ID	Li $\mu\text{g L}^{-1}$	B mg L^{-1}	Al mg L^{-1}	V $\mu\text{g L}^{-1}$	Mn mg L^{-1}	Fe mg L^{-1}	Co $\mu\text{g L}^{-1}$	Ni $\mu\text{g L}^{-1}$
Pessac-Léognan	2009	2,08	5,24	0,54	40,0	1,28	1,39	0,63	18,0
Château 3	2009	2,09	5,14	0,58	42,4	1,13	1,13	0,49	15,6
red wine	2009	2,75	6,49	0,57	31,2	1,37	0,56	0,49	16,5
Bordeaux	2009	2,50	5,77	0,63	51,7	0,75	1,11	0,46	17,7
France	2009	2,38	6,79	0,43	24,6	1,39	0,86	0,85	16,2
	2010	2,46	3,93	0,36	12,0	0,66	0,46	0,40	14,9
	2010	2,20	3,80	0,46	41,1	0,58	0,49	0,46	14,3
	2010	2,53	5,37	0,56	30,4	0,87	0,90	0,42	18,2
	2010	2,51	5,88	0,41	18,9	0,78	0,78	0,41	17,2
	2011	3,59	6,41	0,72	77,7	0,66	1,30	0,46	15,0
	2011	3,54	5,95	0,40	43,8	0,64	1,15	0,47	15,4
	2011	4,18	6,56	0,59	81,1	0,58	1,25	0,43	15,2
	2011	2,62	3,45	0,62	125	0,69	1,53	0,52	16,7
	2011	2,33	5,17	0,65	38,8	1,12	0,27	0,49	14,8
	2011	2,64	5,51	0,66	68,3	0,72	1,22	0,46	17,7
	Average	2,69	5,43	0,55	48,5	0,88	0,96	0,50	16,2
	SD	0,60	1,03	0,11	29,1	0,29	0,38	0,11	1,30
	Min value	2,08	3,45	0,36	12,0	0,58	0,27	0,40	14,3
	Max value	4,18	6,79	0,72	125	1,39	1,53	0,85	18,2
Pauillac	2004	2,73	5,03	0,63	44,7	0,78	1,23	0,30	42,5
Château 4	2005	2,64	5,67	0,63	69,8	0,82	1,14	0,34	45,7
red wine	2006	6,59	5,19	1,20	38,5	0,83	1,16	0,36	37,3
Bordeaux	2007	3,57	5,13	1,19	62,0	1,00	1,24	0,48	70,6
France	Average	3,88	5,26	0,92	54	0,86	1,19	0,37	49,0
	SD	1,85	0,28	0,33	14,6	0,10	0,05	0,08	14,8
	Min value	2,64	5,03	0,63	38,5	0,78	1,14	0,30	37,3
	Max value	6,59	5,67	1,20	70	1,00	1,24	0,48	70,6
Misslabeled	2004	11,7	12,1	0,77	57,6	1,50	1,94	1,08	20,0
Pauillac	2005	14,3	8,85	0,83	12,4	1,29	2,99	0,49	19,0
Unknown	2006	26,6	9,37	0,92	65,1	0,91	3,56	0,23	18,9
	2007	11,0	9,65	0,90	89,8	1,40	3,09	0,75	15,6
	Average	15,9	9,99	0,85	56	1,28	2,90	0,64	18,4
	SD	7,31	1,44	0,07	32,28	0,26	0,68	0,36	1,93
	Min value	11,0	8,85	0,77	12,4	0,91	1,94	0,23	15,6
	Max value	26,64	12,09	0,92	90	1,50	3,56	1,08	20,0

Analytical uncertainties for elemental analysis not exceed 5% and were calculated as RSD (%) value of individual triplicates.

Table 1.1. Concentrations of selected elements in the studied wines (Continuation).

Appellation Provenance	Sample ID	Cu $\mu\text{g L}^{-1}$	Zn mg L^{-1}	Sr mg L^{-1}	Rb mg L^{-1}	Cd $\mu\text{g L}^{-1}$	Cs $\mu\text{g L}^{-1}$	Ba mg L^{-1}	Pb $\mu\text{g L}^{-1}$
Pessac-Léognan	2009	38,3	0,54	0,20	2,04	0,28	2,18	0,12	12,9
Château 3	2009	23,0	0,55	0,18	2,14	0,29	2,73	0,15	13,2
red wine	2009	119	0,69	0,22	2,04	0,31	2,49	0,17	13,8
Bordeaux	2009	61,3	0,66	0,21	2,01	0,27	2,36	0,13	11,1
France	2009	76,6	0,57	0,19	2,39	0,30	2,79	0,13	11,5
	2010	83,4	0,50	0,18	1,69	0,30	2,71	0,12	12,4
	2010	70,7	0,44	0,18	2,04	0,29	3,19	0,12	11,0
	2010	138	0,53	0,19	1,89	0,24	2,69	0,13	10,1
	2010	72,2	0,53	0,18	1,90	0,26	2,79	0,14	11,2
	2011	53,4	0,57	0,20	1,80	0,28	2,71	0,13	17,5
	2011	39,8	0,48	0,19	1,77	0,24	2,67	0,12	12,4
	2011	118	0,41	0,20	1,97	0,26	2,90	0,13	13,2
	2011	150	0,59	0,20	1,77	0,35	2,83	0,13	17,7
	2011	82,9	0,53	0,18	2,11	0,32	2,73	0,13	12,4
	2011	180	0,60	0,21	2,02	0,33	2,34	0,13	10,3
	Average	87,2	0,55	0,19	2,0	0,29	2,67	0,13	12,7
	SD	45,0	0,07	0,01	0,2	0,03	0,25	0,01	2,26
	Min value	23,0	0,41	0,18	1,7	0,24	2,18	0,12	10,1
	Max value	180	0,69	0,22	2,39	0,35	3,19	0,17	17,7
Pauillac	2004	295	0,43	0,17	1,23	0,34	2,11	0,07	18,3
Château 4	2005	351	0,54	0,17	1,35	0,35	2,12	0,07	16,8
red wine	2006	261	0,47	0,19	1,35	0,32	2,02	0,08	21,5
Bordeaux	2007	217	0,48	0,18	1,17	0,40	1,84	0,09	27,8
France	Average	281	0,48	0,18	1,27	0,35	2,02	0,08	21,1
	SD	56,5	0,04	0,01	0,09	0,03	0,13	0,01	4,90
	Min value	217	0,43	0,17	1,17	0,32	1,84	0,07	16,8
	Max value	351	0,54	0,19	1,35	0,40	2,12	0,09	27,8
Misslabeled	2004	1095	0,92	1,52	1,42	0,50	3,11	0,13	11,6
Pauillac	2005	351	0,76	0,74	1,05	0,23	5,42	0,19	14,6
Unknown	2006	58,6	0,40	0,89	1,14	0,23	7,67	0,11	19,1
	2007	80,7	0,45	0,95	7,02	0,34	36,6	0,28	8,60
	Average	396	0,63	1,02	2,66	0,33	13,2	0,18	13,5
	SD	484	0,25	0,35	2,91	0,12	15,7	0,07	4,46
	Min value	59	0,40	0,74	1,05	0,23	3,11	0,11	8,60
	Max value	1095	0,92	1,52	7,02	0,50	36,60	0,28	19,1

Analytical uncertainties for elemental analysis not exceed 5% and were calculated as RSD (%) value of individual triplicates.

Table 1.1. Concentrations of selected elements in the studied wines (Continuation).

Appellation Provenance	Sample ID	Li $\mu\text{g L}^{-1}$	B mg L^{-1}	Al mg L^{-1}	V $\mu\text{g L}^{-1}$	Mn mg L^{-1}	Fe mg L^{-1}	Co $\mu\text{g L}^{-1}$	Ni $\mu\text{g L}^{-1}$
Bordeaux	1998	8,79	4,56	0,70	123	1,30	4,05	0,28	34,0
Mislabeled red wine	2005	21,8	5,17	1,22	58,4	1,87	3,79	0,61	52,5
	2006	47,0	7,67	0,91	44,4	1,48	2,00	0,26	26,5
Unknown	2007	53,1	6,75	1,45	48,4	2,90	3,99	0,49	97,9
	2007	10,9	2,15	1,72	41,6	2,48	3,40	0,51	78,1
	2008	11,7	1,48	0,56	6,66	3,02	2,35	0,19	42,2
	2009	13,6	2,23	1,70	69,6	7,11	7,54	0,89	125
	2009	10,3	4,33	0,53	96,1	1,27	4,20	0,34	41,9
	-	10,2	3,83	0,27	12,5	2,02	3,73	0,29	43,9
	-	10,7	4,75	0,52	98,3	1,32	4,15	0,34	47,8
	Average	19,8	4,29	0,96	59,9	2,48	3,92	0,42	59,0
	SD	16,4	1,98	0,53	37,5	1,75	1,48	0,21	31,4
	Min value	8,79	1,48	0,27	6,66	1,27	2,00	0,19	26,5
	Max value	53,1	7,67	1,72	123	7,11	7,54	0,89	125
China red wine	-	43,2	5,84	1,38	74,5	3,09	5,34	0,50	57,8
	-	51,0	15,1	3,19	81,1	4,10	7,84	4,91	166
	-	85,8	9,30	1,36	17,9	2,25	4,09	0,42	44,7
	Average	60,0	10,1	1,98	57,8	3,15	5,76	1,94	89,5
	SD	22,7	4,70	1,05	34,7	0,92	1,91	2,57	66,7
	Min value	43,2	5,84	1,36	17,9	2,25	4,09	0,42	44,7
	Max value	85,8	15,13	3,19	81	4,10	7,84	4,91	166

Analytical uncertainties for elemental analysis not exceed 5% and were calculated as RSD (%) value of individual triplicates.

Table 1.1. Concentrations of selected elements in the studied wines (Continuation).

Appellation Provenance	Sample ID	Cu $\mu\text{g L}^{-1}$	Zn mg L^{-1}	Sr mg L^{-1}	Rb mg L^{-1}	Cd $\mu\text{g L}^{-1}$	Cs $\mu\text{g L}^{-1}$	Ba mg L^{-1}	Pb $\mu\text{g L}^{-1}$
Bordeaux	1998	103	0,93	0,37	2,15	0,49	4,87	0,20	16,3
Mislabeled red wine	2005	73,2	0,63	0,81	1,51	0,80	3,54	0,13	25,4
	2006	261	0,46	1,45	1,10	5,46	4,17	0,14	11,9
Unknown	2007	116	0,81	0,94	3,28	2,63	27,4	0,15	44,4
	2007	58,1	0,40	0,53	0,92	1,38	3,45	0,10	23,1
	2008	110	0,23	0,29	0,89	1,34	2,53	0,07	10,3
	2009	99,2	0,82	0,59	1,44	1,40	3,90	0,13	21,5
	2009	161	1,74	0,33	2,19	0,86	4,79	0,15	18,7
	-	267	2,15	0,31	2,67	0,77	4,89	0,24	15,3
	-	172	2,24	0,33	2,19	0,73	4,88	0,16	17,9
	Average	142	1,04	0,60	1,83	1,59	6,44	0,15	20,5
	SD	72,9	0,73	0,37	0,79	1,49	7,39	0,05	9,66
	Min value	58,1	0,23	0,29	0,89	0,49	2,53	0,07	10,3
	Max value	267	2,24	1,45	3,28	5,46	27,4	0,24	44,4
China red wine	-	88,2	0,83	0,70	1,30	5,31	5,69	0,12	33,7
	-	116	0,77	2,16	7,88	3,72	46,7	0,52	54,6
	-	75,2	0,70	1,47	2,13	1,74	6,91	0,14	28,2
	Average	93,0	0,77	1,44	3,77	3,59	19,8	0,26	38,9
	SD	20,6	0,07	0,73	3,58	1,79	23,4	0,23	13,9
	Min value	75,2	0,70	0,70	1,30	1,74	5,69	0,12	28,2
	Max value	116	0,83	2,16	7,88	5,31	46,7	0,52	54,6

Analytical uncertainties for elemental analysis not exceed 5% and were calculated as RSD (%) value of individual triplicates.

Appendix 2

Trace metals in teas origin China, Japan and South Korea

Elemental analysis is the first and necessary step of advanced isotopic determination, and widely applied to food classification purposes (Szefer, 2007).

The concentrations of following elements (Mn, Fe, Rb, Zn, Ba, Sr, Cu, Ni, Pb, Cr, Co, V, Li, As, Cd and Be) were determined using Q-ICP-MS and presented in Table 2.1. As can be seen, among 15 elements, Mn is the most abundant, contrary to lowest contents of Be, Cd, Li and As. Levels of Rb, Ba, Pb and V in Japanese and South Korean teas were comparable, but lower than that in Chinese teas. Teas from China exhibits the highest content of Fe, ranging from 152 to 342 mg kg⁻¹, whilst the other origins show lower levels (from 84 to 110 mg kg⁻¹). Concentrations of Rb in Japanese and South Korean teas are not exceed of 41 mg kg⁻¹, while in Chinese samples, Rb ranged from 82 to 169 mg kg⁻¹. Barium in Chinese teas was found about two times higher than in samples from Japan and South Korea, ranging in intervals of 19-48 mg kg⁻¹ and 9-21 mg kg⁻¹, respectively. Also, teas from China demonstrated the higher level of V (140-441 mg kg⁻¹), whilst in teas of other origins vanadium was detected below the level of 100 mg kg⁻¹. Contents of Zn, Cu, Sr and Ni do not vary significantly throughout three examined origins, and were consistent with previously reported (McKenzie et al., 2006; Herrador & Gonzalez, 2001). Mean concentrations of Cr, also do not change significantly among different origins, however, individual samples from Chinese province Yunnan present elevated concentrations of this element (708-947 µg kg⁻¹).

The lower contents of metals, which elevated concentrations may cause a health risk, such Pb, Cd, and As, were found in South Korean tea at the levels of 0.18 mg kg⁻¹, 19 µg kg⁻¹, and 28 µg kg⁻¹, respectively) and in Japanese teas concentrations were 0.15 mg kg⁻¹, 25 µg kg⁻¹, and 22 µg kg⁻¹, respectively), in contrary to slightly higher concentrations in Chinese teas: 0.80 mg kg⁻¹, 40 µg kg⁻¹, and 74 µg kg⁻¹, respectively. The interval of Pb concentrations in Chinese samples ranges from 0.11 mg kg⁻¹ to 2.05 mg kg⁻¹, and is consistent with research of Zhong et al. (2016) for teas of the same origin: 0.11-1.93 mg kg⁻¹. The Cd content of all studied samples ranged from 10 µg kg⁻¹ to 95 µg kg⁻¹, was in agreement to those in green tea from China and Japan ranging between 51 and 114 µg kg⁻¹. (Marcos et al., 1998). Arsenic has been already reported in tea leaves to be at such levels, mean values for green and black teas were 134 µg kg⁻¹ and 58 µg kg⁻¹, respectively (Mania et al., 2014). Although, according to authors (Marcos et al., 1998; Mania et al., 2014; Zhong et al., 2016), aforesaid concentrations should not pose a significant health threat to consumers even with

some elevated levels, the contamination of tea leaves by Pb remains an issue of concern, and practices should be developed to avoid problems in the future (Brzezicha-Cirocka et al., 2016).

Table 2.1. Mean, minimum and maximum values of metal content in tea samples origin of China, Japan and South Korea.

Element	China			Japan			South Korea		
	mean	min	max	mean	min	max	mean	min	max
Mn, mg/kg	727	511	1337	675	292	1380	498	385	863
Fe, mg/kg	152	85,4	342	84,0	60,3	110,3	97,8	79,0	101
Rb, mg/kg	81,8	35,3	169	22,4	9,7	41,2	24,9	21,5	25,6
Zn, mg/kg	30,0	8,6	60,8	29,6	14,7	37,6	27,4	20,5	28,3
Ba,mg/kg	18,9	5,4	48,3	8,9	3,2	21,0	15,6	14,8	21,1
Sr, mg/kg	13,4	6,7	32,6	5,0	2,0	10,0	17,2	10,2	20,9
Cu, mg/kg	12,5	3,2	21,4	7,0	4,6	10,0	6,2	4,9	7,6
Ni, mg/kg	4,0	1,0	11,3	5,6	1,4	9,5	6,9	4,5	7,3
Pb, mg/kg	0,80	0,11	2,05	0,15	0,04	0,23	0,18	0,09	0,23
Cr, µg/kg	312	63,3	947	105	45,9	204	150	96,9	183
Co, µg/kg	189	37,2	512	180	31,6	392	153	123	166
V, µg/kg	140	30,4	441	46,8	17,7	102	87,1	68,5	90,4
Li, µg/kg	78,0	30,3	217	156	19,3	300	31,6	17,7	34,1
As, µg/kg	74,0	41,3	188	22,2	15,4	92,1	28,2	16,2	37,5
Cd, µg/kg	40,1	17,2	95,2	25,1	10,4	61,5	18,8	14,6	24,9
Be, µg/kg	8,5	4,0	32,7	4,7	2,9	17,0	3,8	2,9	3,9

Analytical uncertainties for elemental analysis not exceed 5% and were calculated as RSD (%) value of individual triplicates.

The minimal levels of Sr, the element which directly related to soil, were attributed to Japanese teas. Taking into account that Japanese samples were origin from different regions across the country, this characteristic may be important for regional classification. The minimal levels of Li and Rb were determined in tea from the Hwagae valley, South Korea and also reflected the regional geologic specification. Elements with elevated concentrations in Chinese teas, Fe, Cr, Pb, Co, Cu, Cd, Zn, most likely, reflected an intensive industrial development of China. The measured elemental concentrations in tea leaves were used to differentiate the tea origins using PCA analysis (section E.5 of the manuscript).

Appendix 3

Scientific contribution within the framework of the project “Food traceability”, 2013-2018

Conferences and congresses

1. S. Bérail, O.F.X. Donard, E. Epova, C. Pécheyran, J. Malherbe, B. Medina, L. Sarthou, (2013). TRACABILITÉ DES VINS/ DU CONTENU AU CONTENANT PAR L'ANALYSE ÉLÉMENTAIRE AND ISOTOPIQUES EN ULTRA-TRACES // Wine Track 2013, Journée Scientifique et Professionnelle sur la Traçabilité des Vins et Spiritueux, 30 octobre 2013, Bordeaux – France // *Oral (Fr.)*.
2. E. Epova, S. Bérail, J. Barre, B. Medina, L. Sarthou, O.F.X. Donard, (2014). MULTIELEMENT AND ISOTOPE ANALYSIS IN TRACEABILITY AND AUTHENTICITY OF WINE // Trace Elements in Food (TEF-5) - 5th International IUPAC Symposium for Trace Elements in Food: 6th - 9th May 2014, Copenhagen - Denmark // *Oral (Eng.)*.
3. E. Epova, S. Bérail, J. Barre, B. Medina, L. Sarthou, O.F.X. Donard, (2014). COULD STRONTIUM AND LEAD ISOTOPES BE TRACERS FOR AUTHENTICITY AND TRACEABILITY OF BORDEAUX WINES? // 8th International Franco-Spanish Workshop on Bio-Inorganic Analytical Chemistry: 7-10 of July 2014, Pau - France // *Oral (Eng.)*.
4. O.F.X. Donard, N. Estrade, S. Bérail, E. Epova, D. Amouroux, J. Koschorreck, H. Rüdell, (2015). ASSESSING HISTORICAL HG CONTAMINATION OF MAIN GERMAN RIVERS USING HG ISOTOPES // European Winter Conference on Plasma Spectrochemistry (EWCPS 2015), 22-26 February 2015, Münster - Germany // *Oral (Eng.)*.
5. M.R. Silis, E. Epova, O.F.X. Donard, S. Bérail, M. Valiente, (2015). TRACE-ELEMENT COMPOSITION AND STABLE-ISOTOPIC RATIO FOR GEOGRAPHICAL ORIGIN ASSIGNMENT OF IBERIAN, FRENCH, ITALIAN AND PORTUGUESE DRY-CURED HAM // CMJS 2015 - VIII Congrès Mondial du Jambon Sec, VIII-th Dry Cured Ham World Congress, 25 & 26 June 2015, TOULOUSE - France // *Poster (Eng.)*.
6. E. Epova, S. Bérail, J. Barre, Z. Pedrero Zayas, B. Medina, L. Sarthou, O.F.X. Donard, (2015). AUTHENTICITY TESTING OF BORDEAUX WINE: ANALYTICAL STRATEGY USING COMBINED NON-TRADITIONAL STABLE ISOTOPES DETERMINED BY ICP/ MC/ MS (INDUCTIVE COUPLED PLASMA / MULTICOLLECTION / MASS-SPECTROMETRY) // EUROANALYSIS 2015, the XVIII-th European Conference in Analytical Chemistry, 6th to 10th September 2015, Bordeaux – France // *Poster (Eng.)*.
7. E. Epova, S. Bérail, B. Medina, L. Sarthou, O.F.X. Donard, (2015). ANALYTICAL STRATEGY FOR AUTHENTICITY TESTING OF WINE AND TEA SAMPLES USING COMBINED NON-TRADITIONAL STABLE ISOTOPES DETERMINED BY ICP-MC-MS // Recent Advances in Food Analysis (RAFA 2015) 7th International Symposium, 3th- 6th November 2015, PRAGUE – Czech Republic // *Oral (Eng.)*.

8. E. Epova, S. Bérail, L. Sarthou, O.F.X. Donard, (2015). LES EMPREINTES ISOTOPIQUES ET MULTIELEMENTAIRES SUR L'AUTHENTIFICATION ET LE TRACAGE D'ORIGINE GEOGRAPHIQUE DU JAMBON DE BAYONNE // XVII-ème Comité Scientifique et Technique RYPAGENA, 10 Decembre 2015, Arzacq – France // *Oral (Fr.)*
9. E. Epova, S. Bérail, J. Malherbe, L. Sarthou, O.F.X. Donard, (2016). AUTHENTIFICATION ET TRACAGE D'ORIGINE GÉOGRAPHIQUE DU JAMBON DE BAYONNE PAR EMPRENTES ISOTOPIQUES AND MULTIÉLÉMENTAIRES // SPECTR'ATOM 2016, 23-27 May 2016 Pau – France // *Poster (Fr.)*
10. E. Epova, S. Bérail, B. Médina, J. Barre, J. Malherbe, O.F.X. Donard, (2016). POTENTIAL OF MULTI-ELEMENT ISOTOPIIC APPROACH FOR GEOGRAPHICAL ORIGIN DISCRIMINATION OF TEA 2nd IMEKOFOODS Promoting Objective and Measurable Food Quality & Safety, 2-5 October 2016 Benevento - Italy // *Oral (Eng.)*
11. M. Valiente, E. Epova, M. Restituyo, S. Bérail, O.F.X. Donard, (2017). DETERMINACIÓN ISOTÓPICA DEL ORIGEN DEL JAMÓN CURADO PROCEDENTE DE ITALIA, FRANCIA, PORTUGAL Y ESPAÑA. RELACIONES CON EL ORIGEN DE LA SAL EMPLEADA EN LA SALAZÓN. IX Congreso Mundial del Jamón Curado, 7-9 Junio 2017 Toledo – Spain // *Poster Presentation - Sp.*
12. E. Epova, S. Bérail, B. Medina, L. Sarthou, O.F.X. Donard, (2017). APPLICATION OF STRONTIUM AND LEAD ISOTOPES RATIOS FOR AUTHENTICITY TESTING OF PRESTIGEOS WINES, TEAS AND DRY-CURED HAMS // Isotopes 2017, 9-14 July 2017 Ascona – Switzerland // *Oral (Eng.)*
13. E. Epova, S. Bérail, B. Medina, L. Sarthou, O.F.X. Donard, (2017). NON-TRADITIONAL STABLE ISOTOPES – A NEW HORIZON IN AUTHENTICITY CONFIRMATION AND TRACING THE GEOGRAPHICAL ORIGIN OF FOOD // Goldschmidt, 13-18 August 2017 Paris – France // *Oral (Eng.)*
14. E. Epova, S. Bérail, T. Zuliani, B. Medina, O.F.X. Donard (2017). NON-TRADITIONAL STABLE ISOTOPE TECHNIQUES FOR VERIFYING THE DECLARED GEOGRAPHICAL ORIGIN OF WINE. 3rd IMEKOFOODS Promoting Objective and Measurable Food Quality & Safety, 1-4 October 2017 Thessaloniki – Greece // *Oral (Eng.)*
15. B. Medina, N. Grijalba, E. Epova, C. Péchyran, O.F.X. Donard (2017). UTILISATION DES ÉLÉMENTS MINÉRAUX POUR GARANTIR L'AUTHENTICITÉ DES VIN. 15^e matinée des œnologues de Bordeaux, 14 Avril 2017 Bordeaux – France // *Oral (Fr.)*
16. E. Epova, S. Bérail, T. Zuliani, B. Médina, F. Séby, V. Vaccina, L. Sarthou, O.F.X. Donard (2017). RAPPORTS ISOTOPIQUES DU Sr ET Pb ET ORIGINE DU VIN. Wine Track 2017, Journée Scientifique et Professionnelle sur la Traçabilité des Vins et Spiritueux, 30 octobre 2017, Pau – France // *Oral (Fr.)*
17. O.F.X. Donard (2018). POTENTIEL DES ISOTOPES NON TRADITIONNELS POUR UNE RESOLUTION GEOGRAPHIQUES HAUTE RESOLUTION DANS LES VINS: UN NOUVEL ATOUT. OVI 2018, Journée Scientifique, Organisation Internationale de la Vigne et du Vin, 10 avril 2018, Paris – France // *Oral (Fr.)*

*-The presenting author is underlined

Article published:

1. Epova, E.N., Bérail, S., Zuliani, T., Malherbe, J., Sarthou, S., Valiente, M., & Donard, O.F.X. (2018). $^{87}\text{Sr}/^{86}\text{Sr}$ isotope ratio and multielemental signatures as indicators of origin of European cured hams: The role of salt. *Food Chemistry*, 246, 313-322.

Articles submitted:

2. Epova, E.N., Bérail, S., Barre, J., Séby, F., Vacchina, V., Medina, B., Sarthou, L., & Donard, O.F.X. (2018c). Lead elemental and isotopic signatures of Bordeaux wines for authenticity and geographical origin. *Food Chemistry (submitted)*.
3. Epova, E.N., Bérail, S., Séby, F., Bareille, G., Vacchina, V., Médina, B., Sarthou, L., & Donard, O.F.X. (2018b). Strontium elemental and isotopic signatures of Bordeaux wines for authenticity and geographical origin. *Food Chemistry (submitted)*.
4. Vacchina, V., Epova, E.N., Bérail, Medina, B., Donard, O.F.X. & S., Séby, F. (2018). Total As and As speciation from worldwide collected red wine samples. *Food Additives and Contaminants - Part B (submitted)*.

Articles in preparation:

1. Epova, E.N., Bérail, S., Barre, J., Medina, B., Sarthou, L., & Donard, O.F.X. Geogenic and anthropogenic lead isotope signatures in tea from China, South Korea and Japan: Potential for use for geographic origin traceability. / *in preparation for "Science of the Total Environment"*.
2. Epova, E.N., Bérail, S., Barre, J., Medina, B., Sarthou, L., & Donard, O.F.X. Multi-elemental composition, strontium and lead isotope ratios for geographic origin assessment of tea. / *in preparation*.
3. Epova, E.N., Bérail, S., Baltrons, O., Séby, F., Vacchina, V., Medina, B., Sarthou, L., & Donard, O.F.X. Multielemental fingerprints of Bordeaux wines for authenticity and geographical origin. / *in preparation for "Food Chemistry"*.
4. Analytical method of Sr isotope determination in food samples. / *in preparation*.
5. Analytical method of Pb isotope determination in food samples. / *in preparation*.

Ekaterina EPOVA, neé POLEKH

5 Allée Corot

64140 LONS

Mobile : 07 87 62 65 78

Email : ekaterina.epova@univ-pau.fr

Nationalité : Française, Russe; Age: 44

Languages : Français, Anglais, Russe

Diplômes		
1996	Université d'Irkoutsk, Irkoutsk, Russie (options Chimie analytique, Mention : très bien).	M.S. en Chimie
1992	Université d'Etat d'Irkoutsk, Irkoutsk, Russie.	B.S. en Chimie
EMPLOI ACTUEL		
11/2012	Présent	<p>Chargé de projet de recherche, Laboratoires des Pyrénées et des Landes (Lagor).</p> <p><i>Traçabilité des produits alimentaires AOC par isotopie des métaux lourds (Sr, Pb). Dans le cadre de ce projet :</i> réalisation étude bibliographique avec définition des axes de recherche, planification et réalisation d'expérimentations, développement et conception des protocoles expérimentaux pour l'analyse élémentaire et isotopique de haute précision, analyse et traitement de données, contrôle et qualité, rédaction de rapports et d'articles scientifiques. Maîtrise des techniques : analyse isotopique par spectrométrie de masse à plasma à couplage induit multi-collection (MC-ICP-MS); l'instrumentation : NuPlasma2 (Nu Instrument); NexION (Perkin Elmer).</p>
EMPLOIS PRECEDENTS		
06/2016	12/2016	<p>Chercheur Ingénieur à UPPA-IPREM-LCABIE, Pau.</p> <p>Continuation de projet "<i>Traçabilité des produits alimentaires par isotopie des métaux lourds (Sr, Pb)</i>" dans le cadre du « Programme CRA MARSS »</p>
06/2010	10/2012	<p>Ingénieur-chimiste à UPPA-IPREM-LCABIE, Pau.</p> <p>Analyse isotopique et multi-élémentaire ICP-MS des échantillons environnementaux et biologiques pour des projets en cours, recherches documentaires, réalisation d'analyses, contrôle et qualité. Instrumentation : NexION et DRC II (Perkin Elmer). Expérience en chromatographie en phase liquide (HPLC) et la chromatographie en phase gazeuse (CPG).</p>
1/2002	4/2006	<p>Assistant de recherche, faculté de chimie, Centre de la qualité de l'eau, Université de Trent, Peterborough, Ontario, Canada.</p> <p>Analyse multi-élémentaire ICP-MS des substances environnementales et biologiques pour des projets en cours. Analyse de routine et traitement de données. L'instrumentation : Element2 (Finnigan), DRC (Perkin Elmer).</p>
8/1996	9/2001	<p>Ingénieur-chimiste à l'Institut de Limnologie, Irkoutsk, Russie.</p> <p>Assistance techniques de préparation. Expérience en: chromatographie (HPLC) ; spectrométrie d'absorption atomique (AAS), spectrométrie d'émission atomique (AES) ; ICP-MS ; colorimétrie ; titrage.</p>

PUBLICATIONS SELECTIONNEES :**COMPTE RENDU :**

- I. Articles dans des journaux – 8 articles publiés and 3 soumis
- II. Résumés de présentations dans des conférences – 25
- III. Références citées – 67 (15.01.2018)

ARTICLES SELECTIONNES DANS DES JOURNAUX SCIENTIFIQUES :

E. N. Epova, S. Bérail, T. Zuliani, J. Malherbe, L. Sarthou, M. Valiente, O.F.X. Donard.

$^{87}\text{Sr}/^{86}\text{Sr}$ ISOTOPE RATIO AND MULTIELEMENTAL SIGNATURES AS INDICATORS OF ORIGIN OF EUROPEAN CURED HAMS: THE ROLE OF SALT // *Food Chemistry* **246**, 313-322 (2018)

I.E. Vasilyeva, E.V. Shabanova, N.N. Pakhomova, and E.N. Epova

ATOMIC EMISSION DETERMINATION OF MICROELEMENTAL COMPOSITION OF DIATOMS // *Chinese Journal of Geochemistry* **25**, Suppl., 201-202 (2006).

S. A. Watmough, P. J. Dillon, and E. N. Epova

METAL PARTITIONING AND UPTAKE IN CENTRAL ONTARIO FORESTS // *Environmental Pollution* **134**, No 3, 493-502 (2005).

V. N. Epov, D. Lariviere, E.N. Epova, and R. D. Evans

POLYATOMIC INTERFERENCES PRODUCED BY MACROELEMENTS DURING DIRECT MULTI-ELEMENTAL HYDROCHEMICAL ANALYSES // *Geostandards and Geoanalytical Research* **28**, No 2, 213-224 (2004).

V. N. Epov, I. E. Vasil'eva, A. N. Suturin, V. I. Lozhkin, and E. N. Epova

DETERMINATION OF TRACE ELEMENTS IN LAKE BAIKAL WATER USING INDUCTIVELY COUPLED PLASMA MASS SPECTROMETRY // *Journal of Analytical Chemistry* **54**, No 11, 1170-1175 (1999).

V. N. Epov, I. E. Vasil'eva, V. I. Lozhkin, E. N. Epova, L. F. Paradina, and A. N. Suturin

DETERMINATION OF MACROELEMENTS IN LAKE BAIKAL WATER USING INDUCTIVELY COUPLED PLASMA MASS SPECTROMETRY // *Journal of Analytical Chemistry* **54**, No 9, 943-948 (1999).

References

1. Åberg, G. (1995). The use of natural strontium isotopes as tracers in environmental studies. In J. Černý, M. Novák, T. Pačes, & R.K. Wieder (Eds.), *Biogeochemical monitoring in small catchments* (pp. 309–322). Kluwer Academic Publisher.
2. Adamo, P., Zampella, M., Quézel, C.R., Aversano, R., Dal Piaz, F., De Tommasi, N., Frusciante, L., Iorizzo, M., Lepore, L., & Carputo, D. (2012). Biological and geochemical markers of the geographical origin and genetic identity of potatoes. *Journal of Geochemical Exploration*, *121*, 62–68.
3. Adamsen, C.E., Møller, J.K.S., Laursen, K., Olsen, K., & Skibsted, L.H. (2006a). Zn-porphyrin formation in cured meat products: Effect of added salt and nitrite. *Meat Science*, *72*, 672–679.
4. Adamsen, C.E., Møller, J.K.S., Parolari, G., Gabba, L., & Skibsted, L.H. (2006b). Changes in Zn-porphyrin and proteinous pigments in italian dry-cured ham during processing and maturation. *Meat Science*, *74*, 373–379.
5. Albarède, F., Telouk, P., Blichert-Toft, J., Boyet, M., Agraniér, A., & Nelson, B. (2004). Precise and accurate isotopic measurements using multiple-collector ICPMS. *Geochimica et Cosmochimica Acta*, *68*(12), 2725–2744.
6. Allègre, C.J., Louvat, P., Gaillardet, J., Meynadier, L., Rad, S., & Capmas, F. (2010). The fundamental role of island arc weathering in the oceanic Sr isotope budget. *Earth and Planetary Science Letters*, *292*, 51–56.
7. Almeida, C.M.R., & Vasconcelos, M.T.S.D. (1999a). Determination of lead isotope ratios in port wine by inductively coupled mass spectrometry after pretreatment by UV-irradiation. *Analytica Chimica Acta*, *396*, 45–53.
8. Almeida, C.M.R., & Vasconcelos, M.T.S.D. (1999b). UV-irradiation and MW-digestion pretreatment of Port wine suitable for the determination of lead isotope ratios by inductively coupled plasma mass spectrometry. *Journal of Analytical Atomic Spectrometry*, *14*, 1815–1821.
9. Almeida, C.M.R., & Vasconcelos, M.T.S.D. (2001). ICP-MS determination of strontium isotope ratio in wine in order to be used as a fingerprint of its regional origin. *Journal of Analytical Atomic Spectrometry*, *16*, 607–611.
10. Almeida, C.M.R., & Vasconcelos, M.T.S.D. (2003a). Lead contamination in Portuguese red wines from the Douro region: from the vineyard to the final product. *Journal of Agricultural and Food Chemistry*, *51*, 3012–3023.
11. Almeida, C.M.R., & Vasconcelos, M.T.S.D. (2003b). Multielement composition of wines and their precursors including provenance soil and their potentialities as fingerprints of wine origin. *Journal of Agricultural and Food Chemistry*, *51*, 4788–4798.
12. Almeida, C.M.R., & Vasconcelos, M.T.S.D. (2004). Does the winemaking process influence the wine $^{87}\text{Sr}/^{86}\text{Sr}$? A case study. *Food Chemistry*, *85*, 7–12.
13. Aoyama, K., Nakano, T., Shin, K.-C., Izawa, A., & Morita, S. (2017). Variation of strontium stable isotope ratios and origins of strontium in Japanese vegetables and comparison with Chinese vegetables. *Food Chemistry*, *237*, 1186–1195.
14. Ariyama, K., Shinozaki, M., & Kawasaki, A. (2012). Determination of the geographic origin of rice by chemometrics with strontium and lead isotope ratios and multielement concentrations. *Journal of Agricultural and Food Chemistry*, *60*, 1628–1634.
15. Ariyama, K., Shinozaki, M., Kawasaki, A., & Ishida, Y. (2011). Strontium and lead isotope analyses for determining the geographic origins of grains. *Analytical Science*, *27*, 709–713.
16. Asahara, Y., Ishiguro, H., Tanaka, T., Yamamoto, K., Mimura, M., Minami, M., & Yoshida, H. (2006). Application of Sr isotopes to geochemical mapping and provenance analysis: The case of Aichi Prefecture, central Japan. *Applied Geochemistry*, *21*(3), 419–436.
17. Asfaha, D.G., Quézel, C.R., Thomas, F., Horacek, M., Wimmer, B., Heiss, G., Dekant, C., Deters-Itzelsberger, P., Hoelzl, S., Rummel, S., Brach-Papa, C., et al. (2011). Combining isotopic signatures of $n(^{87}\text{Sr})/n(^{86}\text{Sr})$ and light stable elements (C, N, O, S) with multi-elemental profiling for the authentication of provenance of European cereal samples. *Journal of Cereal Science*, *53*, 170–177.
18. Augagneur, S., Medina, B., & Grousset, F. (1997). Measurement of lead isotope ratios in wine by ICP-MS and its applications to the determination of lead concentration by isotope dilution. *Fresenius Journal of Analytical Chemistry*, *357*, 1149–1152.

19. Baffi, C., & Trincherini, P. R. (2016). Food traceability using the $^{87}\text{Sr}/^{86}\text{Sr}$ isotopic ratio mass spectrometry. *European Food Research and Technology*, 242(9), 1411-1439.
20. Bailey, S.W., Hornbeck, J.W., Charles, T., Driscoll, C.T. & Gaudette, H.E. (1996). Calcium inputs and transport in a base-poor forest ecosystem as interpreted by Sr isotopes. *Water Resources Research*, 32(3), 707-719.
21. Balcaen, L., De Schrijver, I., Moens, L., & Vanhaecke, F. (2005). Determination of the $^{87}\text{Sr}/^{86}\text{Sr}$ isotope ratio in USGS silicate reference materials by multi-collector ICP-mass spectrometry. *International Journal of Mass Spectrometry*, 242, 251-255.
22. Balcaen, L., Moens, L., & Vanhaecke, F. (2010). Determination of isotope ratios of metals (and metalloids) by means of inductively coupled plasma-mass spectrometry for provenancing purposes — A review. *Spectrochimica Acta Part B*, 65, 769-786.
23. Banner, J. (2004). Radiogenic isotopes: systematics and applications to earth surface processes and chemical stratigraphy. *Earth-Science Reviews*, 65, 141-194.
24. Barbaste, M., Halicz, L., Galy A., Medina, B., Emteborg, H., Adams, F.C., & Lobinski, R. (2001). Evaluation of the accuracy of the determination of lead isotope ratios in wine by ICP MS using quadrupole, multicollector magnetic sector and time-of-flight analyzers. *Talanta*, 54, 307-317.
25. Barbaste, M., Robinson, K., Guilfoyle, S., Medina, B., & Lobinski, R. (2002). Precise determination of the strontium isotope ratios in wine by coupled plasma sector field multicollector mass (ICP-SF-MC-MS). *Journal of Analytical Atomic Spectrometry*, 17, 135-137.
26. Baroni, M.V., Podio, N.S., Badini, R.G., Inga, M., Ostera, H.A., Cagnoni, M., Gallegos, E., Gautier, E., Peral-García, P., Hoogewerff, J., & Wunderlin, D.A. (2011). How much do soil and water contribute to the composition of meat? A case study: Meat from three areas of Argentina. *Journal of Agricultural and Food Chemistry*, 59(20), 11117-11128.
27. Barre, J. (2013). Evaluation de la contamination atmosphérique des écosystèmes en utilisant la composition isotopique de plomb et du mercure dans les lichens. Thèse. Ecole doctorale des sciences exactes et de leurs applications. UPPA. Pau.
28. Bataille, C.P., & Bowen, G.J. (2012). Mapping $^{87}\text{Sr}/^{86}\text{Sr}$ variations in bedrock and water for large scale provenance studies. *Chemical Geology*, 304-305, 39-52.
29. Bataille, C.P., Brennan, S.R., Hartmann, J., Moosdorf, N., Wooller, M.J., & Bowen, G.J. (2014). A geostatistical framework for predicting variations in strontium concentrations and isotope ratios in Alaskan rivers. *Chemical Geology*, 389(11), 1-15.
30. Beard, B. L., & Johnson, C. M. (2000). Strontium isotope composition of skeletal material can determine the birthplace and geographic mobility of humans and animals. *Journal of Forensic Sciences*, 45(5), 1049-1061.
31. Bellhöfler, A., & Rosman, K.J.R (2001). Isotopic source signatures for atmospheric lead: The Northern Hemisphere. *Geochimica et Cosmochimica Acta*, 65(11), 1727-1740.
32. Bellhöfler, A., & Rosman, K.J.R. (2002a). Isotopic source signatures for atmospheric lead: The Southern Hemisphere. *Geochimica et Cosmochimica Acta*, 66(8), 1375-1386.
33. Bellhöfler, A., Rosman, K.J.R. (2002b). The temporal stability in lead isotopic signatures at selected sites in the Southern and Northern Hemispheres. *Geochimica et Cosmochimica Acta*, 66(8), 1375-1386.
34. Bellhöfler, A.F. & Rosman, K.J.R. (2001). Lead isotopic ratios in European atmospheric aerosols. *Physics and Chemistry of the Earth. Part B*, 26(10), 835-838.
35. Bernat, M., & Church, T. M. (1989). Uranium and thorium decay series in the modern marine environment. In P. Fritz & J.-Ch. Fontes (Eds.), *Handbook of Environmental Isotope Geochemistry* (pp. 357-383). Elsevier Science.
36. Bi, X.-Y., Li, Z.-G., Wang, S.-X., Zhang, L., Xu, R., Liu, J.-L., Hong-Mei Yang, H.-M., & Guo, M.-Z. (2017). Lead isotopic compositions of selected coals, Pb/Zn ores and fuels in China and the application for source tracing. *Environmental and Science Technology*, 51, 13502-13508.
37. Billström, K. (2008). Radiogenic isotopes and their applications within a range of scientific fields. *Seminarios de la sociedad Española de mineralogía. Volumen 5. Instrumental techniques applied to mineralogía and geochemistry. Zaragoza*, 111-131.
38. Bindler, R. (2011). Contaminated lead environments of man: reviewing the lead isotopic evidence in sediments, peat, and soils for the temporal and spatial patterns of atmospheric lead pollution in Sweden. *Environmental Geochemistry and Health*, 33, 311-329.
39. Bingquan, Z. (1995). The mapping of geochemical provinces in China based on Pb isotopes. *Journal of Geochemical Exploration*, 55, 171-181.

40. Bong, Y.-S., Gautam, M. K., La, M.-R., & Lee, A.-R. (2012a). Geographical origin of Korean and Chinese kimchi determined by multiple elements. *Bioscience, Biotechnology, and Biochemistry*, 76(11), 2096–2100.
41. Bong, Y.-S., Shin, W.-J., Gautam, M. K., Jeong, Y.-J., & Lee, A.-R. (2012b). Determining the geographical origin of Chinese cabbages using multielement composition and strontium isotope ratio analyses. *Food Chemistry*, 135, 2666–2674.
42. Bontempo, L., Larcher, R., Camin, F., Hölzl, S., Rossman, A., Horn, P., & Nicolini, G. (2011). Elemental and isotopic characterisation of typical Italian alpine cheeses. *International Dairy Journal*, 21, 441–446.
43. Bourrouilh, R. (2006). Geology and terroirs of the Bordeaux wines, France. *Bollettino della Società Geologica Italiana, Volume special*, 6, 63–74.
44. Bowen, G.J. (2010). Isoscapes: Spatial Pattern in Isotopic Biogeochemistry. *Annual Review of Earth and Planetary Sciences*, 38, 161–87.
45. Brach-Papa, C., Van Bocxstaele, M., Ponzevera, E., & Quéte, C.R. (2009). Fit for purpose validated method for the determination of the strontium isotopic signature in mineral water samples by multi-collector inductively coupled plasma mass spectrometry. *Spectrochimica Acta Part B*, 64, 229–234.
46. Brännvall, M.-L., Bindler, R., Emteryd, O., & Renberg, I. (2001). Four thousand years of atmospheric lead pollution in northern Europe: a summary from Swedish lake sediments. *Journal of Paleolimnology*, 25, 421–435.
47. Braschi, E., Marchionni, S., Priori, S., Casalini, M., Tommasini, S., Natarelli, L., Buccianti, A., Bucelli, P., Costantini, E.A.C., & Conticelli, S. (2018). Tracing the $^{87}\text{Sr}/^{86}\text{Sr}$ from rocks and soils to vine and wine: An experimental study on geologic and pedologic characterisation of vineyards using radiogenic isotope of heavy elements. *Science of the Total Environment*, 628–629, 1317–1327.
48. Brenot, A., Baran, N., Petelet-Giraud, E., & Négrel, P. (2008). Interaction between different water bodies in a small catchment in the Paris basin (Bréville, France): Tracing of multiple Sr sources through Sr isotopes coupled with Mg/Sr and Ca/Sr ratios. *Applied Geochemistry*, 23, 58–75.
49. Brunner, M., Katona, R., Stefánka, Z., & Prohaska, T. (2010). Determination of the geographical origin of processed spice using multielement and isotopic pattern on the example of Szegedi paprika. *European Food Research and Technology*, 231, 623–634.
50. Brzezicha-Cirocka, J., Grembecka, M., & Szefer, P. (2016). Monitoring of essential and heavy metals in green tea from different geographical origins. *Environmental Monitoring and Assessment*, 188(3), 183.
51. Camin, F., Boner, M., Bontempo, L., Fauhl-Hassek, C., Kelly, S.D., Riedl, J., & Rossmann, A. (2017). Stable isotope techniques for verifying the declared geographical origin of food in legal cases. *Trends in Food Science & Technology*, 61, 176–187.
52. Camin, F., Bontempo, L., Perini, M., & Piasentier, E. (2016). Stable isotope ratio analysis for assessing the authenticity of food of animal origin. *Comprehensive Reviews in Food Science and Food Safety*, 15, 868–877.
53. Capo, R. C., Stewart, B.W., & Chadwick O.A. (1998). Strontium isotopes as tracers of ecosystem processes: theory and methods. *Geoderma*, 82, 197–225.
54. Catarino, S., Moreira, C., Kaya, A., de Sousa, R.B., Curvelo-Garcia, A., de Pinho, M., & Ricardo-da-Silva, J. (2016). Effect of new and conventional technological processes on the terroir marker $^{87}\text{Sr}/^{86}\text{Sr}$. *BIO Web of Conferences*, 7, 02003. DOI: 10.1051/bioconf/20160702003.
55. Chang, C.-T., You, C.-F., Aggarwal, S.K., Chung, C.-H., Chao, H.-C., & Liu, H.-C. (2016). Boron and strontium isotope ratios and major/trace elements concentrations in tea leaves at four major tea growing gardens in Taiwan. *Environmental Geochemistry and Health*, 38, 737–748.
56. Chang, X., Fu S., Liu, H., Chen, N., Zhao, X., Zhu, B., & Tu, X. (2011). Identification of products of geographical origin based on geochemical zoning. *Chinese Journal of Geochemistry*, 30, 138–144.
57. Chaudhuri, S., & Clauer, N. (1992). Signatures of radiogenic isotopes in deep subsurface waters in continents. In N. Clauer, & S. Chaudhuri (Eds.), *Lecture notes in earth sciences* (pp. 497–529). Berlin: Springer.
58. Chen, J.M., Tan, M.G., Li, Y.L., Zhang, Y.M., Lu, W.W., Tong, Y.P., Zhang, G.L., & Li, Y., (2005). A lead isotope record of Shanghai atmospheric lead emissions in total suspended particles during the period of phasing out of leaded gasoline. *Atmospheric Environment*, 39, 1245–1253.
59. Cheng, H., & Hu, Y. (2010). Lead (Pb) isotopic fingerprinting and its applications in lead pollution studies in China: A review. *Environmental Pollution*, 158, 1134–1146.
60. Cheong, C.S., & Chang, H.W. (1997). Sr, Nd, and Pb isotope systematics of granitic rocks in the central Ogcheon belt, Korea. *Geochemical Journal*, 31, 17–36.

61. Chesson, L.A., Tipple, B.J., Mackey, G.N., Hynek, S.A., Fernandez, D.P., & Ehleringer, J.R. (2012). Strontium isotopes in tap water from the coterminous USA. *Ecosphere*, 3(7) 1-17.
62. Choi, M.-S., Yi, H.-I., Shou Ye Yang, S.Y., Lee, C.-B., & Cha, H.-J. (2007). Identification of Pb sources in Yellow Sea sediments using stable Pb isotope ratios. *Marine Chemistry*, 107, 255–274.
63. Cloquet, C., Carignan, J., & Libourela, G. (2006). Atmospheric pollutant dispersion around an urban area using trace metal concentrations and Pb isotopic compositions in epiphytic lichens. *Atmospheric Environment*, 40, 574–587.
64. Codling, E.E., Chaney, R.L., & Green, C.E. (2015). Accumulation of lead and arsenic by carrots grown on lead-arsenate contaminated orchard soils. *Journal of Plant Nutrition*, 38(4), 509-525.
65. Codling, E.E., Chaney, R.L., & Green, C.E. (2016). Accumulation of lead and arsenic by potato grown on lead-arsenate-contaminated orchard soils. *Communications in Soil Science and Plant Analysis*, 47(6), 799-807.
66. Coelho, I., Castanheira, I., Bordado, J.M., Donard, O., & Silva, J.A.L. (2017). Recent developments and trends in the application of strontium and its isotopes in biological related fields. *Trends in Analytical Chemistry*, 90, 45–61.
67. Consortium du Jambon de Bayonne. URL: <http://www.jambon-de-bayonne.com/en/>. Accessed 01 April 2018.
68. Consorzio del Prosciutto di Parma. URL: <http://www.prosciuttodiparma.com>. Accessed 01 April 2018.
69. Consorzio del Prosciutto di San Daniele. URL: <http://www.prosciuttosandaniele.it/>. 01 April 2018.
70. Cozzolino, D., & Smyth, H. (2013). Analytical and chemometric-based methods to monitor and evaluate wine protected designation. In M. De La Guardia & A. González (Eds.), *Food protected designation of origin, 1st ed., Methodologies and Applications. Comprehensive Analytical Chemistry, Volume 60* (358-408). Elsevier. Amsterdam.
71. Crews, H. M., Massey, R. C., & McWeeny, D. J. (1988). Some applications of isotope analysis of lead in food by ICP-MS. *Journal of Research of the National Bureau of Standards*, 93(3), 464-466.
72. Crittenden, R.G., Andrew, A.S., LeFournour, M., Young, M.D., Middleton, H., & Stockmann, R. (2007). Determining the geographic origin of milk in Australasia using multi-element stable isotope ratio analysis. *International Dairy Journal*, 17, 421–428.
73. Cumming, G.L., & Richards, J.R. (1975). Ore lead isotope ratios in a continuously changing Earth. *Earth and Planetary Science Letters*, 28(2), 155-171.
74. Curnelle, R. (1983). Evolution structuro-sédimentaire du Trias et de l'Infra-Lias d'Aquitaine. *Bulletin des centres de recherches Exploration-production Elf-Aquitaine*, 7(1), 69 -99.
75. Danezis, G. P., Tsagkaris, A. S., Camin, F., Brusic, V., & Georgiou, C. A. (2016). Food authentication: Techniques, trends & emerging approaches. *Trends in Analytical Chemistry*, 85, 123–132.
76. Davies, B.E. (1995). Lead. In B.J. Alloway (Edt.), *Heavy metals in soils* (pp. 206-224). Springer Netherlands.
77. Dean, J. R., Ebdon, L., & Massey, R. C. (1990). Isotope ratio and isotope dilution analysis of lead in wine by inductively coupled plasma mass spectrometry. *Food Additives and Contaminants*, 7, 109-116.
78. Dean, J.R., Ebdon, L., & Massey, R.C. (1987). Selection of mode for the measurement of lead isotope ratios by inductively coupled plasma mass spectrometry and its application to milk powder analysis. *Journal of Analytical Atomic Spectrometry*, 2, 369-374.
79. Degryse, P., De Muynck, D., Delporte, S., Boyen, S., Jadoul, L., De Winne, J., Ivaneanu, T., & Vanhaecke F. (2012). Strontium isotopic analysis as an experimental auxiliary technique in forensic identification of human remains. *Analytical Methods*, 4, 2674-2679.
80. Dehelean, A., & Voica, C. (2012). Determination of lead and strontium isotope ratios in wines by inductively coupled plasma mass spectrometry. *Romanian Journal of Physics*, 57(7-8), 1194-1203.
81. Denominación de Origen Jamón de Huelva. URL: <http://www.mapama.gob.es>. Accessed 01 April 2018.
82. Di Paola-Naranjo, R.D., Baroni, M.V., Podio, N.S., Rubinstein, H.R., Fabani, M.P., Badini R.G., Inga, M., Ostera, H.A., Cagnoni, M., Gallegos, E., Gautier, E., Peral-García, P., Hoogewer, J., & Wunderlin D.A. (2011). Fingerprints for main varieties of argentinean wines: Terroir differentiation by inorganic, organic, and stable isotopic analyses coupled to chemometrics. *Journal of Agricultural and Food Chemistry*, 2011, 59, 7854–7865.
83. Drivelos, S.A., & Georgiou, C.A. (2012). Multi-element and multi-isotope ratio analysis to determine the geographical origin of foods in the European Union. *Trends in Analytical Chemistry* 40, 38-51.
84. Durante, C., Baschieri, C., Bertacchini, L., Bertelli, D., Cocchi, M., Marchetti, A., Manzini, D., Papotti, G., & Sighinolfi, S. (2015). An analytical approach to Sr isotope ratio determination in Lambrusco wines for geographical traceability purposes. *Food Chemistry*, 173, 557–563.

85. Durante, C., Baschieri, C., Bertacchini, L., Cocchi, M., Sighinolfi, S., Silvestri, M., & Marchetti, A. (2013). Geographical traceability based on $^{87}\text{Sr}/^{86}\text{Sr}$ indicator: A first approach for PDO Lambrusco wines from Modena. *Food Chemistry*, *141*, 2779–2787.
86. Durante, C., Bertacchini, L., Bontempo, L., Camin, F., Manzini, D., Lambertini, P., Marchetti, A., & Paolini, M. (2016). From soil to grape and wine: Variation of light and heavy elements isotope ratios. *Food Chemistry*, *210*, 648–659.
87. Durante, C., Bertacchini, L., Cocchi, M., Manzini, D., Marchetti, A., Rossi, M.C., Sighinolfi, S., & Tassi, L. (2018). Development of $^{87}\text{Sr}/^{86}\text{Sr}$ maps as targeted strategy to support wine quality. *Food Chemistry*, *255*, 139–146.
88. Elbaz-Poulichet, F., Holliger, P., Huang, W.W., & Martin J.-M. (1984). Lead Cycling in Estuaries, Illustrated by the Gironde Estuary, France. *Nature*, *308*, 409–414.
89. Epova, E.N., Bérail, S., Barre, J., Medina, B., Sarthou, L., & Donard, O.F.X. (2018d). Multi-elemental composition, strontium and lead isotope ratios for geographic origin assessment of tea. (*in preparation*).
90. Epova, E.N., Bérail, S., Barre, J., Séby, F., Vacchina, V., Medina, B., Sarthou, L., & Donard, O.F.X. (2018c). Lead elemental and isotopic signatures of Bordeaux wines for authenticity and geographical origin. *Food Chemistry* (submitted).
91. Epova, E.N., Bérail, S., Séby, F., Bareille, G., Vacchina, V., Médina, B., Sarthou, L., & Donard, O.F.X. (2018b). Strontium elemental and isotopic signatures of Bordeaux wines for authenticity and geographical origin. *Food Chemistry* (submitted).
92. Epova, E.N., Bérail, S., Zuliani, T., Malherbe, J., Sarthou, S., Valiente, M., & Donard, O.F.X. (2018a). $^{87}\text{Sr}/^{86}\text{Sr}$ isotope ratio and multielemental signatures as indicators of origin of European cured hams: The role of salt. *Food Chemistry*, *246*, 313–322.
93. Ettler, V., Mihaljevič, M., & Komárek, M. (2004). ICP-MS measurements of lead isotopic ratios in soils heavily contaminated by lead smelting: tracing the sources of pollution. *Analytical and Bioanalytical Chemistry*, *378*, 311–317.
94. European Commission Regulation (EC) No 466/2001 of 8 March 2001 setting maximum levels for certain contaminants in foodstuffs (Text with EEA relevance) URL: <https://publications.europa.eu>. Accessed 01 April 2018.
95. Evans, J.A., Montgomery, J., Wildman, G., & Boulton, N. (2010). Spatial variations in biosphere $^{87}\text{Sr}/^{86}\text{Sr}$ in Britain. *Journal of the Geological Society*, *167*(1), 1–4.
96. Evans, J.A., Pashley, V., Richards, G.J., Brereton, N., & Knowles, T.G. (2015). Geogenic lead isotope signatures from meat products in Great Britain: Potential for use in food authentication and supply chain traceability. *Science of the Total Environment*, *537*, 447–452.
97. Eyuboglu, Y., Dudas, F.O., Thorkelson, D.J., & Santosh, M. (2017). Eocene granitoids of northern Turkey: Polybaric magmatism in an evolving arc–slab window system. *Gondwana Research*, *50*, 311–345.
98. Faure, G. (1986). *Principles of Isotope Geology*. (2nd ed.). New York: John Wiley & Sons. (Chapter 8).
99. Faure, G., & Powell, J. L. (1972). *Strontium Isotope Geology* (1st ed.). Berlin: Springer-Verlag. (Chapter 1, 4).
100. Feng, J., Wang, Y., Zhao, J., Zhu, L., Bian, X., & Zhang, W. (2011). Source attributions of heavy metals in rice plant along highway in Eastern China. *Journal of Environmental Sciences*, *23*(7), 1158–1164.
101. Fernandes, J.R., Pereira, L., Jorge, P., Moreira, L., Gonçalves, H., Coelho, L., Alexandre, D., Eiras-Dias, J., Brazão, J., Clímaco, P., Baleiras-Couto, M., Catarino, S., Graça, A., & Martins-Lopes, P. (2015). Wine fingerprinting using a bio-geochemical approach. *BIO Web of Conferences*, *5*, 02021. DOI: 10.1051/bioconf/20150502021.
102. Ferrari, G., Lambertini, P., Manzini, D., Marchetti, A., Sighinolfi, S., & Della Casa, G. (2007). Evaluation of the oxidation state and metal concentration in the adipose tissue of Parma ham. *Meat Science*, *75*, 337–342.
103. Fortunato, G., & Wunderli, S. (2003). Evaluation of the combined measurement uncertainty in isotope dilution by MC-ICP-MS. *Analytical and Bioanalytical Chemistry*, *377*, 111–116.
104. Fortunato, G., Mumic, K., Wunderli, S., Pillonel, L., Bosset, J.O., & Gremaud G. (2004). Application of strontium isotope abundance ratios measured by MC-ICP-MS for food authentication. *Journal of Analytical Atomic Spectrometry*, *19*, 227–234.
105. FP6-TRACE project-website: URL: <http://www.foodreg.com/index.php/sample-projects-menu-item/trace> Accessed 01 April 2018.
106. Franke, B.M., Gremaud, G., Hadorn, R., & Kreuzer, M. (2005). Geographic origin of meat—elements of an analytical approach to its authentication. *European Food Research and Technology*, *221*, 493–503.
107. Franke, B.M., Koslitz, S., Micaux, F., Piantini, U., Maury, V., Pfammatter, E., Wunderli, S., Gremaud, G.,

- Bosset, J.-O., Hadorn, R., & Kreuzer, M. (2008). Tracing the geographic origin of poultry meat and dried beef with oxygen and strontium isotope ratios. *European Food Research and Technology*, 226, 761–769.
108. Frei, K.M., & Frei, R. (2011). The geographic distribution of strontium isotopes in Danish surface waters – A base for provenance studies in archaeology, hydrology and agriculture. *Applied Geochemistry*, 26(3), 326–340.
109. Frei, R., & Frei, K.M. (2013). The geographic distribution of Sr isotopes from surface waters and soil extracts over the island of Bornholm (Denmark) – A base for provenance studies in archaeology and agriculture. *Applied Geochemistry*, 38, 147–160.
110. Galani-Nikolakaki, S., & Kallithrakas-Kontos, N.G. (2007). Element content in wines. In P. Szefer & J.O. Nriagu (Eds.), *Mineral components in food* (pp.323–338). CRC Press, Taylor and Francis group.
111. Galvis-Sánchez, A.C., Lopes, J. A., Delgadillo, I., & Rangel, A.O.S.S. (2013). Sea salt. In M. De La Guardia & A. González (Eds.), *Food protected designation of origin, 1st ed., Methodologies and Applications. Comprehensive Analytical Chemistry, Volume 60 (1st ed.)* (pp.719–740). Elsevier.
112. Geană, E.-I., Sandru, C., Stanciu, V., & Ionete, R.E. (2017). Elemental profile and ⁸⁷Sr/⁸⁶Sr isotope ratio as fingerprints for geographical traceability of wines: an approach on Romanian wines. *Food Analytical Methods*, 10(1), 63–73.
113. Geană, I., Iordache, A., Ionete, R., Marinescu, A., Ranca, A., & Culea, M. (2013). Geographical origin identification of Romanian wines by ICP-MS elemental analysis. *Food Chemistry*, 138, 1125–1134.
114. Ghezzi, L., Arienzo, I., Bucciante, A., Demarchi, G., & Petrini, R. (2018). Highly radiogenic Sr-isotopic signature and trace element content of grape musts from northern Piedmont vineyards (Italy). *European Food and Research and Technology*, doi.org/10.1007/s00217-017-3022-z.
115. Goldammer, T. (2013). *Grape Grower's Handbook*. (1st ed.). Apex Publishers, (Chapters 17, 18).
116. González, A. & De La Guardia, M., (2013a). Basic chemometric tools. In M. De La Guardia & A. González (Eds.), *Food protected designation of origin, 1st ed., Methodologies and Applications. Comprehensive Analytical Chemistry, Volume 60 (1st ed.)* (pp.299–315). Elsevier.
117. González, A. & De La Guardia, M., (2013b). Mineral profile. In M. De La Guardia & A. González (Eds.), *Food protected designation of origin, 1st ed., Methodologies and Applications. Comprehensive Analytical Chemistry, Volume 60* (pp. 51–76). Elsevier. Amsterdam.
118. González, A., & Guardia, de la, M. (2013c). *Food protected designation of origin. Methodologies and Applications. Comprehensive Analytical Chemistry*. (1st ed.). Amsterdam: Elsevier.
119. González, A., Armenta, S., & de la Guardia, M. (2009). Trace-element composition and stable-isotope ratio for discrimination of foods with Protected Designation of Origin. *Trends in Analytical Chemistry*, 28(11), 1295–1311.
120. Goossens, J., De Smaele, T., Moens, L., & Dams, R. (1993). Accurate determination of lead in wines by inductively coupled plasma mass spectrometry. *Fresenius Journal of Analytical Chemistry*, 347, 119–125.
121. Goossens, J., Moens, L., & Dams, R. (1994). Determination of lead by flow-injection inductively coupled plasma mass spectrometry comparing several calibration techniques. *Analytica Chimica Acta*, 293, 171–181.
122. Graustein, W.C. (1989). ⁸⁷Sr/⁸⁶Sr ratios measure the sources and flow of strontium in terrestrial ecosystems. In P.W. Rundel, J.R. Ehleringer, & K.A. Nagy (Eds.), *Stable Isotopes in Ecological Research* (pp. 491– 511). New York: Springer-Verlag.
123. Green, G.P., Bestland, E.A., & Walker, G.S. (2004). Distinguishing sources of base cations in irrigated and natural soils: evidence from strontium isotopes. *Biogeochemistry*, 68(2), 199–225.
124. Greenough, J.D., Mallory-Greenough, L.M., & Fryer, B.J. (2005). Geology and Wine 9: Regional Trace Element Fingerprinting of Canadian Wines. *Journal of geological association of Canada*, 32(3), 129–137.
125. Grousset, F.E., & Biscaye, P.E. (2005). Tracing dust sources and transport patterns using Sr, Nd and Pb isotopes. *Chemical Geology* 222, 149– 167.
126. Grousset, F.E., Quérel, C.R., Thomas, B., Buat-Ménard, P., Donard, O.F.X., & Bucher, A. (1994). Transient Pb isotopic signatures in the Western European atmosphere. *Environmental Science & Technology*, 28, 1605–1608.
127. Han, C., Burn-Nunes, L.J., Lee, K., Chang, C., Kang, J.-H., Han, Y., Hur, S.D., & Hong, S. (2015). Determination of lead isotopes in a new Greenland deep ice core at the sub-pico gram per gram level by thermal ionization mass spectrometry using an improved decontamination method. *Talanta*, 140, 20–28.
128. Hartman, G., & Richards, M. (2014). Mapping and defining sources of variability in bioavailable strontium isotope ratios in the Eastern Mediterranean. *Geochimica et Cosmochimica Acta*, 126, 250–264.

129. He, M. L., Wehr, U., & Rambeck, W. A. (2010). Effect of low doses of dietary rare earth elements on growth performance of broilers. *Journal of Animal Physiology and Animal Nutrition*, *94*, 86–92.
130. Herrador, M.A., & Gonzalez, A.G. (2001). Pattern recognition procedures for differentiation of Green, Black and Oolong teas according to their metal content from inductively coupled plasma atomic emission spectrometry. *Talanta*, *53*, 1249-1257.
131. Hiraoka, H., Morita S., Izawa, A., Aoyama, K., Shin, K.C., & Nakano, T. (2016). Tracing the geographical origin of onions by strontium isotope ratio and strontium content. *Analytical Sciences*, *32*(7), 781-8.
132. Hobson, K.A., Barnett-Johnson, R., & Cerling, T. (2010). Using Isoscapes to track animal migration. In J.B. West, G.J. Bowen, T.E. Dawson & K.P. Tu (Eds.), *Isoscapes: Understanding movement, pattern, and process on Earth through isotope mapping* (pp. 273-298). New York: Springer.
133. Hopfer, H., Nelson, J., Collins, T.S., Heymann, H., Susan E. & Ebeler, S.E. (2015). The combined impact of vineyard origin and processing winery on the elemental profile of red wines. *Food Chemistry*, *172*, 486–496.
134. Horn, P., Hölzl, S., Todt W., & Matthies, D. (1998). Isotope abundance ratios of Sr in wine provenance determinations, in a tree-root activity study, and of Pb in a pollution study on tree-rings. *Isotopes in Environmental and Health Studies*, *34*(1-2), 31-42.
135. Horn, P., Schaaf, P., Holbach, B., Höltl, S., & Eschnauer, H. (1993). $^{87}\text{Sr}/^{86}\text{Sr}$ from rock and soil into vine and wine. *Zeitschrift für Lebensmittel-Untersuchung und-Forschung*, *196*, 407-409.
136. Horsky, M., Irrgeher, J., & Prohaska, T. (2016). Evaluation strategies and uncertainty calculation of isotope amount ratios measured by MC ICP-MS on the example of Sr. *Analytical and Bioanalytical Chemistry*, *408*(2), 351–367.
137. Horwitz, E.P., Chiarizia, R., & Dietz, M.L. (1992). A novel strontium-selective extraction chromatographic resin. *Journal Solvent Extraction and Ion Exchange*, *10*(2), 313-336.
138. Hu, X., & Ding, Z. (2009). Lead/Cadmium Contamination and Lead Isotopic Ratios in Vegetables Grown in Peri-Urban and Mining/Smelting Contaminated Sites in Nanjing, China. *Bulletin of Environmental Contamination and Toxicology*, *82*, 80–84.
139. Huygens, D., Vidican, R., Rotar, I., & Carlier, L. (2012). Safe food for all European consumers: The farm to table principle - 50 Years. Common Agricultural Policy. *Bulletin UASVM Agriculture*, *69*(1), 1-10.
140. Ip, C.C.M., Li, X.D., Zhang, G., Farmer, J.G., Wai, O.W.H., & Li, Y.S. (2004). Over one hundred years of trace metal fluxes in the sediments of the Pearl River Estuary, South China. *Environmental Pollution*, *132*, 157–172.
141. Irrgeher J., & Prohaska T. (2016). Application of non-traditional stable isotopes in analytical ecogeochemistry assessed by MC ICP-MS - A critical review. *Analytical and Bioanalytical Chemistry*, *408*, 369-385.
142. Janin, M., Medini, S., & Techer, I. (2014). Methods for PDO olive oils traceability: state of art and discussion about the possible contribution of strontium isotopic tool. *European Food Research and Technology*, *239*, 745–754.
143. Jeon, S.-R., & Nakano, T. (2001). Geochemical comparison of stream water, rain water, and watershed geology in Central Korea. *Water, Air, and Soil Pollution*, *130*, 739-744.
144. Jiménez-Colmenero, F., Ventanas, J., & Toldrá, F. (2010). Nutritional composition of dry-cured ham and its role in a healthy diet. *Meat Science*, *84*, 585–593.
145. Jones, C., Jenkyns, U.C., Coe, A. L., & Hesselbo, S.P. (1994). Strontium isotopic variations in Jurassic and Cretaceous seawater. *Geochimica et Cosmochimica Acta*, *58*(14), 3061-3074.
146. Kabata-Pendias, A. (2010). *Trace Elements in Soils and Plants*. (4th ed). New York: CRC Press, Taylor & Francis Group. (Chapter 7).
147. Kaufmann, A. (1988). Lead in wine. *Food Additives and Contaminants*, *15*(4), 437-445.
148. Kawasaki, A., Oda, H., & Hirata, T. (2002). Determination of strontium isotope ratio of brown rice for estimating its provenance. *Journal of Soil Science and Plant Nutrition*, *48*(5), 635 - 640.
149. Kelly, S., Heaton, K., & Hoogewerff, J. (2005). Tracing the geographical origin of food: The application of multi-element and multi-isotope analysis. *Trends in Food Science & Technology*, *16*, 555-567.
150. Kendall, C., Eric, A., & Caldwell, E.A. (1998). Fundamentals of Isotope geochemistry. In C. Kendall & J.J. McDonnell (Eds.), *Isotope tracers in catchments hydrology* (pp. 51-86). Elsevier Science.
151. Kendall, C., Sklash, M. G., & Bullen, T. D. (1995). Isotope Tracers of Water and Solute Sources in Catchments. In: S. Trudgill (Ed.), *Solute modelling in catchment systems* (pp. 261-303). New York: John Wiley and Sons.
152. Kennedy, M.J., Chadwick, O.A., Vitousek, F.M., Derry, L.A., & Hendricks D.M. (1998). Changing sources of base cations during ecosystem development, Hawaiian Islands. *Geology*, *26*(11), 1015-1018.

153. Kim, J.S., Hwang, I.M., Lee, G.H., Park, Y.M., Choi, J.Y., Jamila, N., Khan, N., & Kim, K.S. (2017). Geographical origin authentication of pork using *multi-element* and multivariate data analyses. *Meat Science*, *123*, 13-20.
154. Kim, Y.H., Kim, K.J., Kim, E.H., Park, J.J., Kim, S.M., & Seok, K.S. (2013). Lead isotope ratios as a tracer for lead contamination sources: A lake Andong case study. *Web of Conferences*, DOI: 10.1051/e3sconf/20130133001.
155. Kment, P., Mihaljevič, M., Ettler, V., Sebek, O., Strnad, L., & Rohlova, L. (2005). Differentiation of Czech wines using multielement composition – A comparison with vineyard soil. *Food Chemistry*, *91*, 157–165.
156. Koepnick, R.B., Burke, W.H., Denison, R.E., Hetherington, E.A., Nelson, H.F., Otto, J.B., & Waite, L.E. (1985). Construction of the seawater $^{87}\text{Sr}/^{86}\text{Sr}$ curve for the Cenozoic and Cretaceous: supporting data. *Chemical Geology (Isotope Geoscience Section)*, *58*, 55-81.
157. Komárek, M., Ettler, V., Chrastný, V., & Mihaljevič M. (2008). Lead isotopes in environmental sciences: A review. *Environment International*, *34*, 562–577.
158. Kootker L.M., van Lanen, R.J., Kars, H., & Davies, G.R. (2016). Strontium isoscapes in The Netherlands. Spatial variations in $^{87}\text{Sr}/^{86}\text{Sr}$ as a proxy for palaeomobility. *Journal of Archaeological Science*, *6*, 1-13.
159. Koreňovská, M., & Suhaj, M. (2005). Identification of some Slovakian and European wines origin by the use of factor analysis of elemental data. *European Food Research and Technology*, *221*(3), 550-558.
160. Kreitals, N.M., & Watling, R.J. (2014). Multi-element analysis using inductively coupled plasma mass spectrometry and inductively coupled plasma atomic emission spectroscopy for provenancing of animals at the continental scale. *Forensic Science International*, *244*, 116-121.
161. Kruzlicova, D., Fiket, Ž., & Kniewald, G. (2013). Classification of Croatian wine varieties using multivariate analysis of data obtained by high resolution ICP-MS analysis. *Food Research International*, *54*, 621–626.
162. Kwon, S.T., Cheong, C.S., & Sagong, H. (2006). Rb-Sr isotopic study of the Hwacheon granite in northern Gyeonggi massif, Korea: a case of spurious Rb-Sr whole rock age. *Geosciences Journal*, *10*, 137–143.
163. Lagad, R.A., Alamelu, D., Laskar, A.H., Rai, V.K., Singh, S.K., Aggarwal, S.K. (2013). Isotope signature study of the tea samples produced at four different regions in India. *Analytical Methods*, *5*, 1604–1611.
164. Lagad, R.A., Singh, S.K., & Rai, V.K. (2017). Rare earth elements and $^{87}\text{Sr}/^{86}\text{Sr}$ isotopic characterization of Indian Basmati rice as potential tool for its geographical authenticity. *Food Chemistry*, *217*, 254–265.
165. Lahd Geagea, M., Stille, P., Gauthier-Lafaye, F., Perrone, Th., & Aubert, D. (2008). Baseline determination of the atmospheric Pb, Sr and Nd isotopic compositions in the Rhine valley, Vosges mountains (France) and the Central Swiss Alps. *Applied Geochemistry*, *23*, 1703–1714.
166. Larcher, R., Nicolini, G., & Pangrazzi, P. (2003). Isotope ratios of lead in Italian wines by inductively coupled plasma mass spectrometry. *Journal of Agricultural and Food Chemistry*, *51*, 5956-5961.
167. Lecat, B., Brouard, J., & Chapuis, C. (2016). Fraud and counterfeit wines in France: an overview and perspectives. *British Food Journal*, *119*(1), 84-104.
168. Li, H.B., Yu, S., Li, G.L., & Deng, H. (2012). Lead contamination and source in Shanghai in the past century using dated sediment cores from urban park lakes. *Chemosphere*, *88*, 1161–1169.
169. Lim, D., Jung, S.W., Choi, M.S., Kang, S.M., Jung, H.S., & Choi, J.Y. (2013). Historical record of metal accumulation and lead source in the southeastern coastal region of Korea. *Marine Pollution Bulletin*, *74*, 441–445.
170. Lim, M.P., & McBride, M.B (2015). Arsenic and lead uptake by Brassicas grown on an old orchard site. *Journal of Hazardous Materials*, *299*, 656–663.
171. Liu, H., Wei, Y., Lu, H., Wei, S., Jiang, T., Zhang, Y., & Guo, B. (2016). Combination of the $^{87}\text{Sr}/^{86}\text{Sr}$ ratio and light stable isotopic values ($\delta^{13}\text{C}$, $\delta^{15}\text{N}$ and δD) for identifying the geographical origin of winter wheat in China. *Food Chemistry*, *212*, 367–373.
172. Liu, H., Wei, Y., Lu, H., Wei, S., Jiang, T., Zhang, Y., Ban, J., & Guo, B. (2017). The determination and application of $^{87}\text{Sr}/^{86}\text{Sr}$ ratio in verifying geographical origin of wheat. *Journal of Mass Spectrometry*, *52*, 248-253.
173. Liu, H.-C., You, C.-F., Chen, C.-Y., Liu, Y.-C., & Chung, M.-T. (2014). Geographic determination of coffee beans using multi-element analysis and isotope ratios of boron and strontium. *Food Chemistry*, *142*, 439–445.
174. Lu, Y., Yang, H., Ma, L., Chen, X., & Wang, Q. (2011). Application of Pb isotopic tracing technique to constraining the source of Pb in the West Lake Longjing tea. *Chinese Journal of Geochemistry*, *30*, 554-562.
175. Lucarini, M., Sacconi, G., D’Evoli, L., Tufi, S., Aguzzi, A., Gabrielli, P., Marletta, L., Lombardi-Boccia, G. (2013). Micronutrients in Italian ham: A survey of traditional products. *Food Chemistry*, *140*, 837-842.

176. Mackay, A.K., Taylor, M.P., Munksgaard, N.C., Hudson-Edwards, K.A., & Burn-Nunes, L. (2013). Identification of environmental lead sources and pathways in a mining and smelting town: Mount Isa, Australia. *Environmental Pollution*, *180*, 304–311.
177. Maneux, E., Grousset, F. E., P. Buat-Ménard, P., Lavaux, G., P. Rimmelin, P., & Lapaquellerie, Y. (1999). Temporal patterns of the wet deposition of Zn, Cu, Ni, Cd and Pb: the Arcachon Lagoon (France). *Water, Air, and Soil Pollution*, *114*, 95–120.
178. Mania, M., Szynal, T., Rebeniak, M., Wojciechowska-Mazurek, M., Starska K., & Strzelecka, A. (2014). Human exposure assessment to different arsenic species in tea. *Roczniki Państwowego Zakładu Higieny*, *65*(4), 281–286.
179. Marchionni, S., Braschi, E., Tommasini, S., Bollati, A., Cifelli, F., Mulinacci, N., Mattei, M., Conticelli, S. (2013). High-precision $^{87}\text{Sr}/^{86}\text{Sr}$ analyses in wines and their use as a geological fingerprint for tracing geographic provenance. *Journal of Agricultural and Food Chemistry*, *61*, 6822–6831.
180. Marchionni, S., Buccianti, A., Bollati, A., Braschi, E., Cifelli, F., Molin, P., Parotto, M., Mattei, M., Tommasini, S., Conticelli, S. (2016). Conservation of $^{87}\text{Sr}/^{86}\text{Sr}$ isotopic ratios during the winemaking processes of 'Red' wines to validate their use as geographic tracer. *Food Chemistry*, *190*, 777–785.
181. Marcos, A., Fischer, A., Rea, G., & Hill, S.J. (1998). Preliminary study using trace element concentrations and a chemometrics approach to determine geographical origin of tea. *Journal of Analytical Atomic Spectrometry*, *13*, 521–525.
182. Marguá, E., Iglesias, M., Queralt, I., & Hidalgo, M. (2006). Lead isotope ratio measurements by ICP-QMS to identify metal accumulation in vegetation specimens growing in mining environments. *Science of the Total Environment*, *367*, 988–998.
183. Martin, J., Bareille, G., Berail, S., Pecheyran, C., Daverat, F., Bru, N., Tabouret, H., & Donard, O. (2013). Spatial and temporal variations in otolith chemistry and relationships with water chemistry: a useful tool to distinguish Atlantic salmon *Salmo salar* parr from different natal streams. *Journal of Fish Biology*, *82*, 1556–1581.
184. Martins, P., Madeira, M., Monteiro, F., de Sousa, B., Curvelo-Garcia, A.S., & Catarino, S. (2014). $^{87}\text{Sr}/^{86}\text{Sr}$ ratio in vineyard soils from Portuguese denominations of origin and its potential for origin authentication. *Journal International des Sciences de la Vigne et du Vin*, *48*(1), 21–29.
185. Maurer, A.-F., Galer, S.J.G., Knipper, C., Beierlein, L., Nunn, E.V., Peters, D., Tütken T., Alt, K.W., & Schöne, B.R. (2012). Bioavailable $^{87}\text{Sr}/^{86}\text{Sr}$ in different environmental samples — Effects of anthropogenic contamination and implications for isoscapes in past migration studies. *Science of the Total Environment*, *433*, 216–229.
186. McKenzie, J.S., Jurado, J.M., & de Pablos, F. (2010). Characterisation of tea leaves according to their total mineral content by means of probabilistic neural networks. *Food Chemistry*, *123*, 859–864.
187. Médina, B., Augagneur, S., Barbaste, M., Grousset, F.E., & Buat-Ménard, P. (2000). Influence of atmospheric pollution on the lead content of wines. *Food Additives and Contaminants*, *17*(6), 435–445.
188. Médina, B., Salagoity, M.H., Guyon, F., Gaye, J., Hubert, P., & Guillaume, F. (2013). Using new analytical approaches to verify the origin of wine. In: P. Brereton (Ed.), *New analytical approaches for verifying the origin of food* (pp. 149–188). Woodhead Publishing.
189. Medini, S., Janin, M., Verdoux, P., & Techer, I. (2015). Methodological development for $^{87}\text{Sr}/^{86}\text{Sr}$ measurement in olive oil and preliminary discussion of its use for geographical traceability of PDO Nîmes (France). *Food Chemistry*, *171*, 78–83.
190. Meija, J., Yang, L., Mester, Z., & Sturgeon, R. (2012). Correction of instrumental mass discrimination for isotope ratio determination with multi-collector inductively coupled plasma mass spectrometry. In F. Vanhaecke & P. Degryse (Eds.), *Isotopic Analysis: Fundamentals and applications using ICP-MS* (pp. 113–137). Wiley-VCH Verlag GmbH & Co.
191. Mercurio, M., Grilli, E., Odierna, P., Morra, V., Prohaska, T., Coppola, E., Grifa C., Buondonno, A., & Langella, A. (2014). A 'Geo-Pedo-Fingerprint' (GPF) as a tracer to detect univocal parent material-to-wine production chain in high quality vineyard districts, Campi Flegrei (Southern Italy). *Geoderma*, *230–231*, 64–78.
192. Mihaljevič, M., Ettler, V., Sebek, O., Strnad, L., & Chrastný, V. (2006). Lead isotopic signatures of wine and vineyard soils—tracers of lead origin. *Journal of Geochemical Exploration*, *88*, 130–133.
193. Mihaljevič, M., Ettler, V., Vaněk, A., Penížek, V., Svoboda, M., Kříbek, B., Sracek, O., Mapani, B.S., & Kamona, A.F. (2015). Trace elements and the lead isotopic record in marula (*Sclerocarya birrea*) tree rings and soils near the Tsumeb smelter, Namibia. *Water, Air, & Soil Pollution*, *226*(6), 177.

194. Miller, O.L., Solomon, D.K., Fernandez, D.P., Cerling, T.E., & Bowling, D.R. (2014). Evaluating the use of strontium isotopes in tree rings to record the isotopic signal of dust deposited on the Wasatch Mountains. *Applied Geochemistry*, 50, 53-65.
195. Ministry of agriculture, forestry and fisheries of Japan. URL: <http://www.maff.go.jp/e/>. Accessed 01 April 2018.
196. Monna, F., Ben Othman, D., & Luck, J.M. (1995). Pb isotopes and Pb, Zn and Cd concentrations in the rivers feeding a coastal pond (Thau, southern France): constraints on the origin(s) and flux(es) of metals. *The Science of the Total Environment*, 166, 19-34.
197. Monna, F., Lancelot, J., Croudace, I.W., Cundy, A.B., & Lewis J.T. (1997). Pb Isotopic composition of airborne particulate material from France and the Southern United Kingdom: implications for Pb pollution sources in urban areas. *Environmental Science and Technology*, 31(8), 2277–2286.
198. Montgomery, J., Evans, J.A., & Wildman, G. (2006). $^{87}\text{Sr}/^{86}\text{Sr}$ isotope composition of bottled British mineral waters for environmental and forensic purposes. *Applied Geochemistry*, 21, 1626–1634.
199. Mukai, H., Furuta, N., Fujii, T., Amb, Y., Sakamoto, K., & Hashimoto, Y. (1993). Characterization of sources of lead in the urban air of Asia using ratios of stable lead isotopes. *Environmental Science & Technology*, 27, 1347–1356.
200. Mukai, H., Tanaka, A., & Fujii, T. (1994). Lead isotope ratios of airborne particulate matter as tracers of long-range transport of air pollutants around Japan. *Journal of Geophysical Research*, 99(D2), 3717-3726.
201. Mukai, H., Zeng, Y., Hong, Y., Tang, J., Guo, S., Xue, H., Sun, Z., Zhou, J., Xue, D., Zhao, J., Zhai, G., Gu, J., & Zhai, P. (2001). Regional characteristics of sulfur and lead isotope ratios in the atmosphere at several Chinese urban sites. *Environmental Science & Technology*, 35(6), 1064–1071.
202. Nakano, T. (2016). Potential uses of stable isotope ratios of Sr, Nd, and Pb in geological materials for environmental studies. *Proceedings of the Japan Academy, Series B*, 92(6), 167-184.
203. Nakano, T., Morohashi, S., Yasuda, H., Sakai, M., Aizawa, S., Shichi, K., Morisawa, T., Takahashi, M., Sanada, M., Matsuura, Y., Sakai, H., Akama, A., Okada, N. (2006). Determination of seasonal and regional variation in the provenance of dissolved cations in rain in Japan based on Sr and Pb isotopes. *Atmospheric Environment*, 40, 7409–7420.
204. Nakano, T., Tanaka, T., Tsujimura, M., & Matsutani, J. (1993). Strontium isotopes in soil-plant-atmosphere continuum (SPAC). *Tracers in hydrology*, 215, 73-78.
205. Nakano, T., Yokoo, Y., & Yamanaka, M. (2001). Strontium isotope constraint on the provenance of basic cations in soil water and stream water in the Kawakami volcanic watershed, central Japan. *Hydrological Processes*, 15, 1859–1875.
206. Ndung'u, K., Hibdon, S., Véron, & A., Flegel, A.R. (2011). Lead isotopes reveal different sources of lead in balsamic and other vinegars. *Science of the Total Environment*, 409, 2754–2760.
207. Novak, M., Mikova, J., Krachler, M., Kosler, J., Erbanova, L., Prechova, E., Jackova, I., & Fottova, D. (2010). Radial distribution of lead and lead isotopes in stem wood of Norway spruce: a reliable archive of pollution trends in Central Europe. *Geochimica et Cosmochimica Acta*, 74, 4207–4218.
208. Nriagu, J.O. (1989). A global assessment of natural sources of atmospheric trace metals. *Nature*, 338, 47-49.
209. O'Brien, E. (2011). Chronology of Leaded Gasoline / Leaded Petrol History - Knowledge of the dangers of lead in petrol / gasoline; Steps taken and not taken, to phase out leaded petrol; Steps remaining to achieve global leaded petrol phase - out. A Report for the lead education and abatement design group. URL: http://www.lead.org.au/Chronology-Making_Leaded_Petrol_History.pdf . Accessed 01 April 2018.
210. Oda, H., Kawasaki, A., & Hirata, T. (2002). Determining the rice provenance using binary isotope signatures along with cadmium content. 17th World Congress of soil science, August 14-21, 2002, Thailand/ Book of abstracts, 2018-1 - 2018-10.
211. OIV code. Maximum acceptable limits. The International Organisation of Vine and Wine. URL: <http://www.oiv.int/public/medias/3741/e-code-annex-maximum-acceptable-limits.pdf>. Accessed 01 April 2018.
212. Ordóñez, J.A., & De La Noz, L. (2007). Mediterranean products. In Toldrá, F. (Ed.), *Handbook of fermented meat and poultry* (pp. 333-347). Wiley-Blackwell.
213. Ortega, G.S., Pécheyran, C., Bérail, S., & Donard, O.F.X. (2012). A fit-for purpose procedure for lead isotopic ratio determination in crude oil, asphaltene and kerogen samples by MC-ICPMS. *Journal of Analytical Atomic Spectrometry*, 27, 1447-1456.
214. Pacyna, J.M., & Pacyna, E.G. (2001). An assessment of global and regional emissions of trace metals to the atmosphere from anthropogenic sources worldwide. *Environmental Reviews*, 9(4), 269-298.

215. Pattee, O.H., & Pain, D.J. (2002). Lead in the Environment. In Hoffman D.J., Rattner, B.A., Burton G.A. Jr., Clairins J. Jr. (Eds.), *Handbook of Ecotoxicologie* (pp. 373-408). CRC Press.
216. Pepi, S., & Vaccaro, C. (2018). Geochemical fingerprints of "Prosecco" wine based on major and trace elements. *Environmental Geochemistry and Health*, 40(2), 833-847.
217. Pepi, S., Grisenti, P., Sansone, L., Chicca, M., & Vaccaro, C. (2018). Chemical elements as fingerprints of geographical origin in cultivars of *Vitis vinifera* L. raised on the same SO₄ rootstock. *Environmental Science and Pollution Research*, 25(1), 490-506.
218. Perini, M., Camin, F., Sánchez Del Pulgar, J., & Piasentier, E. (2013). Effect of origin, breeding and processing conditions on the isotope ratios of bioelements in dry-cured ham. *Food Chemistry*, 136, 1543–1550.
219. Petrini, R., Sansone, L., Slejko, F.F., Buccianti, A., Marcuzzo, P., & Tomasi, D. (2015). The ⁸⁷Sr/⁸⁶Sr strontium isotopic systematics applied to Glera vineyards: A tracer for the geographical origin of the Prosecco. *Food Chemistry*, 170, 138–144.
220. Petrova, I., Aasen, I.M., Rustad, T., Eikevik, T.M. (2015) Manufacture of dry-cured ham: a review. Part 1. Biochemical changes during the technological process. *European Food Research and Technology*, 241, 587–599.
221. Pillonel, L., Badertscher, R., Froidevaux, R., Haberhauer, G., Hölzl, S., Horn, P., Jakob, A., Pfammatter, E., Piantini, U., Rossmann, A., Tabacchi, R., & Bosset, J.O. (2003). Stable isotope ratios, major, trace and radioactive elements in emmental cheeses of different origins. *Lebensmittel-Wissenschaft und Technologie*, 36, 615–623.
222. Pohl, P. (2007). What do metals tell us about wine? *Trends in Analytical Chemistry*, 26(9), 941-949.
223. Porder, S., Paytan, A., & Hadly, E.A. (2003). Mapping the origin of faunal assemblages using strontium isotopes. *Paleobiology*, 29(2), 197-204.
224. Pourcelot, L., Stille, P., Aubert, D., Solovitch-Vella, N., & Gauthier-Lafaye, F. (2008). Comparative behaviour of recently deposited radiostrontium and atmospheric common strontium in soils (Vosges Mountains, France). *Applied Geochemistry*, 23, 2880–2887.
225. Prohaska, T., Wenzel, W.W., & Stingeder, G. (2005). ICP-MS-based tracing of metal sources and mobility in a soil depth profile via the isotopic variation of Sr and Pb. *International Journal of Mass Spectrometry*, 242, 243–250.
226. Rees, G., Kelly, S.D., Cairns, P., Ueckermann, H., Hölzl, S., Rossmann, A., & Scotter, M.J. (2016). Verifying the geographical origin of poultry: The application of stable isotope and trace element (SITE) analysis. *Food Control*, 67, 144–154.
227. Reid, L.M., O'Donnell, C.P., & Downey, G. (2006). Recent technological advances for the determination of food authenticity. *Trends in Food Science & Technology* 17, pp. 344–353.
228. Reimann, C., Flem, B., Fabian, K., Birke, M., Ladenberger, A., Negrel, P., Demetriades, A., & Hoogewerff, J. (2012). The GEMAS Project Team 1. Lead and lead isotopes in agricultural soils of Europe – The continental perspective. *Applied Geochemistry* 27, 532–542.
229. Resano, M. & Vanhaecke, F. (2012). Forensic applications. In F. Vanhaecke & P. Degryse (Eds.), *Isotopic Analysis: Fundamentals and applications using ICP-MS* (pp. 391-418). Wiley-VCH Verlag GmbH & Co.
230. Rich, S., Manning, S.W., Degryse, P., Vanhaecke, F., & Van Lerberghe, K. (2012). Strontium isotopic and tree-ring signatures of *Cedrus brevifolia* in Cyprus. *Journal of Analytical Atomic Spectrometry*, 27, 796-806.
231. Richardson, G.M., Garrett, R., Mitchell, I., Mah-Paulson, M., & Hackbarth, T. (2001). Critical review on natural global and regional emissions of six trace metals to the atmosphere. Final report. Geological Survey of Canada. Ottawa. 59 pages.
232. Rodrigues, C., Brunner, M., Steiman, S., Bowen, G.J., Nogueira, J.M.F., Gautz, L., Prohaska, T., & Máguas, C. (2011a). Isotopes as tracers of the Hawaiian coffee-producing regions. *Journal of Agricultural and Food Chemistry*, 59, 10239–10246.
233. Rodrigues, C., Máguas, C., & Prohaska, T. (2011b). Strontium and oxygen isotope fingerprinting of green coffee beans and its potential to proof authenticity of coffee. *European Food Research and Technology*, 232, 361–373.
234. Rodrigues, C., Maia, R., Ribeirinho, M., Hildebrandt, P., Gautz, L., Prohaska, T., & Máguas C. (2013). Coffee. In M. de la Guardia & A. Gonzálves (Eds.), *Food protected designation of origin methodologies and applications. Comprehensive Analytical Chemistry*, 60, 573–598.
235. Rodrigues, S.M., Otero, M., Alves, A.A., Coimbra, J., Coimbra, M.A., Pereira, E., & Duarte, A.C. (2011c). Elemental analysis for categorization of wines and authentication of their certified brand of origin. *Journal of Food Composition and Analysis*, 24, 548–562.

236. Rodushkin, I., Baxter, D.C., Engström, E., Hoogewerff, J., Horn, P., Papesch, W., Watling, J., Latkoczy, C., van der Peijl, G., Berends-Montero, S., Ehleringer, J., & Zdanowicz, V. (2011). Elemental and isotopic characterization of cane and beet sugars. *Journal of Food Composition and Analysis*, *24*, 70–78.
237. Rodushkin, I., Bergmanc, T., Douglas, G., Engström, E., Sörlin, D., & Baxter, D.C. (2007). Authentication of Kalix (N.E. Sweden) vendace caviar using inductively coupled plasma-based analytical techniques: Evaluation of different approaches. *Analytica Chimica Acta*, *583*, 310–318.
238. Rodushkin, I., Ödman, F., & Appelblad, P.K. (1999). Multielement determination and lead isotope ratio measurement in alcoholic beverages by high resolution inductively coupled plasma mass spectrometry. *Journal of Food Composition and Analysis*, *12*, 243–257.
239. Rosman, K.J.R., Chisholm, W., Boutron, C.F., Candelone, J.P., & Hohg, S. (1994). Isotopic evidence to account for changes in the concentration of lead in Greenland snow between 1960 and 1988. *Geochimica et Cosmochimica Acta*, *58*(15), 3265–3269.
240. Rosman, K.J.R., Chisholm, W., Jimi, S., Candelone, J.-P., Boutron, C.F., Teissedre, P.-L., & Adams F.C. (1998). Lead concentrations and isotopic signatures in vintages of French wine between 1950 and 1991. *Environmental Research, Section A*, *78*, 161–167.
241. Rosner, M. (2010). Geochemical and instrumental fundamentals for accurate and precise strontium isotope data of food samples: comment on “Determination of the strontium isotope ratio by ICP-MS ginseng as a tracer of regional origin” (Choi et al., 2008). *Food Chemistry*, *121*, 918–92.
242. Rossmann, A., Haberhauer, G., Hölzl, S., Horn, P., Pichlmayer, F., & Voerkelius, S. (2000). The potential of multielement stable isotope analysis for regional origin assignment of butter. *European Food Research and Technology*, *211*, 32–40.
243. Rummel, S., Dekant, C.H., Hölzl, S., Kelly, S.D., Baxter, M., Marigheto, N., Quetel, C.R., Larcher, R., Nicolini, G., Fröschl, H., Ueckermann, H., & Hoogewerff, J. (2012). Sr isotope measurements in beef—analytical challenge and first results. *Analytical Bioanalytical Chemistry*, *402*, 2837–2848.
244. Rummel, S., Hoelzl, S., & Horn, P. (2010). The combination of stable isotope abundance ratios of H, C, N and S with $^{87}\text{Sr}/^{86}\text{Sr}$ for geographical origin assignment of orange juices. *Food Chemistry*, *118*, 890–900.
245. Šelih, V.S., Šala, M., & Drgan, V. (2014). Multi-element analysis of wines by ICP-MS and ICP-OES and their classification according to geographical origin in Slovenia. *Food Chemistry*, *153*, 414–423.
246. Sen, I.S., Peucker-Ehrenbrink, B. (2012). Anthropogenic disturbance of element cycles at the Earth’s surface. *Environmental Science & Technology*, *46*, 8601–8609.
247. Sherman, L.S., Blum, J.D., Dvonch, J.T., Gratz, L.E., & Landis, M.S. (2015). The use of Pb, Sr, and Hg isotopes in Great Lakes precipitation as a tool for pollution source attribution. *Science of the Total Environment*, *502*, 362–374.
248. Somers, T.C., & Evans, M.E. (1974). Wine Quality: Correlations with color, density and anthocyanin equilibria in a group of young red wines. *Journal of the Science of Food and Agriculture*, *25*, 1369–1379.
249. Song, B.-Y., Gautam, M.K., Ryu, J.-S., Lee, D., & Lee, K.-S. (2015). Effects of bedrock on the chemical and Sr isotopic compositions of plants. *Environmental Earth Sciences*, *74*, 829–837.
250. Song, B.-Y., Ryu, J.-S., Shin, H.S., & Lee, K.-S. (2014). Determination of the Source of Bioavailable Sr Using $^{87}\text{Sr}/^{86}\text{Sr}$ Tracers: A Case Study of Hot Pepper and Rice. *Journal of Agricultural and Food Chemistry*, *62*, 9232–9238.
251. Sracek, O., Mapani, B.S., & Kamona, A.F. (2015). Trace elements and the lead isotopic record in marula (*Sclerocarya birrea*) tree rings and soils near the Tsumeb smelter, Namibia. *Water, Air, & Soil Pollution*, *226*(6), 177.
252. Stockley, C.S., & Lee, T.H. (1995). Much ado about Lead in Wine? An Australian Review. *Journal of Wine Research*, *6*(1), 5–17.
253. Stockley, C.S., Smith, L.H., Tiller, K.J; Gulson, B.L., Osborn, C.D’A., & Lee, T. (2003). Lead in wine: a case study on two varieties at two wineries in South Australia. *Australian Journal of Grape and Wine Research*, *9*, 47–55.
254. Sun, Y., Zhuang, G., Zhang, W., Wang, Y., & Zhuang, Y. (2006). Characteristics and sources of lead pollution after phasing out leaded gasoline in Beijing. *Atmospheric Environment*, *40*(16), 2973–2985.
255. Swoboda, S., Brunner, M., Boulyga, S. F., Galler, P., Horacek, M., & Prohaska, T. (2008). Identification of marchfeld asparagus using Sr isotope ratio measurements by MC-ICP-MS. *Analytical Bioanalytical Chemistry*, *390*, 487–494.
256. Szefer P. (2007). Chemometric techniques in analytical evaluation of food quality. In P. Szefer & J.O. Nriagu (Eds.), *Mineral components in foods* (pp.69–122). CRC Press, Taylor & Francis. London.
257. Szostek, K., Mądrzyk, K., & Cienkosz-Stepańczyk, B. (2015). Strontium isotopes as an indicator of human migration – easy questions, difficult answers. *Anthropological Review*, *78*(2), 133–156.

258. Tchaikovsky, A., Zitek, A., Irrgeher, J., Opper, C., Sarne, J., Scheiber, R., & Prohaska, T. (2015). $^{87}\text{Sr}/^{86}\text{Sr}$ isotope pattern as a tool for provenancing of sturgeon caviar. 7-th International Symposium on Recent Advances In Food Analysis, Nov 3-6, 2015, Prague, Czech Republic/ Book of abstracts, P.134.
259. Techer, I., Lancelot, J., Descroix, F., & Guyot, B. (2011). About Sr isotopes in coffee 'Bourbon Pointu' of the Réunion Island. *Food Chemistry*, *126*, 718–724.
260. Techer, I., Medini, S., Janin, M., & Arregui, M. (2017). Impact of agricultural practice on the Sr isotopic composition of food products: Application to discriminate the geographic origin of olives and olive oil. *Applied Geochemistry*, *82*, 1-14.
261. Tescione, I., Marchionni, S., Matte, M., Tassi, F., Romano, C., & Conticelli, S. (2015). A comparative $^{87}\text{Sr}/^{86}\text{Sr}$ study in red and white wines to validate its use as geochemical tracer for the geographical origin of wine. *Procedia Earth and Planetary Science*, *13*, 169 – 172.
262. Teutsch, N., Erel, Y., Halicz, L., & Banin A. (2001). Distribution of natural and anthropogenic lead in Mediterranean soils. *Geochimica et Cosmochimica Acta*, *65*(17), 2853–2864.
263. Tian, X., Emteborg, H., Barbaste, M., & Adams, F. (2000). Accuracy and precision of lead isotope ratios in wines measured by axial inductively coupled plasma time-of-flight mass spectrometry. *Journal of Analytical Atomic Spectrometry*, *2000*, *15*, 829-835.
264. Tian, Y., Yan, C., Zhang, T., Tang, H., Li, H., Yu, J., Bernarde, J., Chen, L., Martin, S., Delepine-Gilon, N., Bocková, J., Veis, P., Chen, Y., & Yua, J. (2017). Classification of wines according to their production regions with the contained trace elements using laser-induced breakdown spectroscopy. *Spectrochimica Acta Part B*, *135*, 91–101.
265. Tingdong, L. (1980). The development of geological structures in China. *GeoJournal*, *4*(6), 487-497.
266. Vanhaecke F., & Degryse P. (2012). *Isotopic Analysis: Fundamentals and Applications Using ICP-MS*. Wiley-VCH. 550 pp.
267. Vanhaecke, F. & Kuzer, K. (2012). The isotopic compositions of the elements. In F. Vanhaecke & P. Degryse (Eds.), *Isotopic Analysis: Fundamentals and applications using ICP-MS* (pp. 1-29). Wiley-VCH Verlag GmbH & Co.
268. Veizer, J. (1989). Strontium isotopes in seawater through time. *Annual Review of Earth and Planetary Sciences*, *17*, 141-167.
269. Veysseyre, A., Bollhöfer, A.F., Rosman, K.J.R., Ferrari, C.P., & Boutron, C.F. (2001). Tracing the origin of pollution in French alpine snow and aerosols using lead isotopic ratios. *Environmental Sciences and Technology*, *35*, 4463-4469.
270. Veysseyre, R.M. (2010). The graphical presentation of lead isotope data for environmental source apportionment. *Science of the Total Environment*, *408*, 3490–3492.
271. Vinciguerra, V., Stevenson, R., Pedneault, K., Poirier, A., Hélie, J.-F., & Widory, D. (2016). Strontium isotope characterization of wines from Quebec, Canada. *Food Chemistry*, *210*, 121–128.
272. Voerkelius, S., Lorenz, G.D., Rummel, S., Quétel, C.R., Heiss G., Baxter, M., Brach-Papa, C., Deters-Itzelsberger, P., Hoelzl, S., Hoogewerff, J., Ponzevera, E., Van Bocxstaele, & M., Ueckermann, H. (2010). Strontium isotopic signatures of natural mineral waters, the reference to a simple geological map and its potential for authentication of food. *Food Chemistry*, *118*, 933–940.
273. Vogl, J., & Pritzkow, W. (2012). Reference materials in isotopic analysis. In F. Vanhaecke & P. Degryse (Eds.), *Isotopic Analysis: Fundamentals and applications using ICP-MS* (pp. 77-91). Wiley-VCH Verlag GmbH & Co.
274. Vorster, C., Greeff, L., & Coetsee, P.P. (2010). The determination of $^{11}\text{B}/^{10}\text{B}$ and $^{87}\text{Sr}/^{86}\text{Sr}$ isotope ratios by quadrupole-Based ICP-MS for the fingerprinting of South African wine. *South African Journal of Chemistry*, *63*, 207–214.
275. Vystavna, Y., Zaichenko, L., Klimenko, N., & Rätsep, R. (2017). Trace metals transfer during vine cultivation and winemaking processes. *Science of Food and Agriculture*, *97*, 4520–4525.
276. Vystavna, Y., Pätsep, P., Klymenko, N., Drozd, O., Pidlisnyuk, B., & Klymenko, M. (2015). Comparison of soil-to-root transfer and translocation coefficients of trace elements in vines of Chardonnay and Muscat white grown in the same vineyard. *Scientia Horticulturae*, *192*, 89–96.
277. Waight, T., Baker, J., & Peate, D. (2002). Sr isotope ratio measurements by double-focusing MC-ICPMS: techniques, observations and pitfalls. *International Journal of Mass Spectrometry*, *221*, 229–244.
278. Walczyk, T. (2004). TIMS versus multicollector-ICP-MS: coexistence or struggle for survival? *Analytical and Bioanalytical Chemistry*, *378*, 229–231.
279. Watmough S.A. (1999). Monitoring historical changes in soil and atmospheric trace metal levels by dendrochemical analysis. *Environmental Pollution*, *106*, 391-403.

280. Weis, D., Kieffer, B., Maerschalk, C., Barling, J., de Jong, J., Williams, G.A., Hanano, D., Pretorius, W., Mattielli, N., & Scoates, J.S. (2006). High-precision isotopic characterization of USGS reference materials by TIMS and MC-ICP-MS. *Geochemistry Geophysics Geosystems*, 7(8), 1-30.
281. WHO/FAO (2012). Joint FAO/WHO food standard programme codex committee on contaminants in foods. In *6-th session, Maastricht, The Netherlands, 26-30 March 2012 CF/6 INF/1*. URL: ftp://ftp.fao.org/codex/meetings/cccf/cccf6/cf06_INF6.pdf. Accessed 01 April 2018.
282. Wieser, M., Schwiters, J., & Douthitt, C. (2012). Multi-collector inductively coupled plasma mass spectrometry. In F. Vanhaecke & P. Degryse (Eds.), *Isotopic Analysis: Fundamentals and applications using ICP-MS* (pp. 77-91). Wiley-VCH Verlag GmbH & Co.
283. Wilson, J.E. (1999). *Terroir: The role of geology, climate and culture in the making of French Wines* (1st ed.). University of California Press, (Chapters 5, 6).
284. Xu, H.M., Cao, J.J., Ho, K.F., Ding, H., Han, Y.M., Wang, G.H., Chowa, J.C., Watson, J.G., Khol, S.D., Qiang, J., & Li, W.T. (2012). Lead concentrations in fine particulate matter after the phasing out of leaded gasoline in Xi'an, China. *Atmospheric Environment*, 46, 217-224.
285. Xu, H.M., Cao, J.J., Ho, K.F., Ding, H., Han, Y.M., Wang, G.H., Chow, J.C., Watson, J.G., Khol, S.D., Qiang, J., & Li, W.T. (2012). Lead concentrations in fine particulate matter after the phasing out of leaded gasoline in Xi'an, China. *Atmospheric Environment*, 46, 217-224.
286. Yip, Y., Lam, J.C., & Tong, W. (2008). Applications of lead isotope ratio measurements. *Trends in Analytical Chemistry*, 27(5), 460-480.
287. Zampella, M., Quérel, C.R., Paredes, E., Asfaha, D.G., Vingiani, S., & Adamo, P. (2011). Soil properties, strontium isotopic signatures and multi-element profiles to authenticate the origin of vegetables from small-scale regions: illustration with early potatoes from southern Italy. *Rapid Communications in Mass Spectrometry*, 25, 2721-2731.
288. Zannella, C., Carucci, F., Aversano, R., Prohaska, T., Vingiani, S., Carputo, D., & Adamo, P. (2017). Genetic and geochemical signatures to prevent frauds and counterfeit of high-quality asparagus and pistachio. *Food Chemistry*, 237, 545-552.
289. Zhao, G. & Cawood, P.A. (2012). Precambrian Geology of China. *Precambrian Research* 222-223, 1-502.
290. Zhao, Y., Wang, D., & Yang, S. (2016). Effect of organic and conventional rearing system on the mineral content of pork. *Meat Science*, 118, 103-107.
291. Zhao, Y., Zhang, B., Chen, G., Chen, A., Yang, S., & Ye, Z. (2014). Recent developments in application of stable isotope analysis on agro-product authenticity and traceability. *Food Chemistry*, 145, 300-305.
292. Zhong, W.-S., Ren, T., & Zhao, L.-J. (2016). Determination of Pb (Lead), Cd (Cadmium), Cr (Chromium), Cu (Copper), and Ni (Nickel) in Chinese tea with high-resolution continuum source graphite furnace atomic absorption spectrometry. *Journal of Food and Drug Analysis*, 24(1), 46-55.
293. Zhou, C., Wei, C., Gou, J., & Li, C. (2001). The Source of Metals in the Qilinchang Zn-Pb Deposit, Northeastern Yunnan, China: Pb-Sr Isotope Constraints. *Economic Geology*, 96(3), 583-598.
294. Zhou, J.-X., Huang, Z.-L., Gao, J.-G. & Yan, Z.-F. (2013). Geological and C-O-S-Pb-Sr isotopic constraints on the origin of the Qingshan carbonate-hosted Pb-Zn deposit, Southwest China. *International Geology Review*, 55(7), 904-916.
295. Zhu, B.-Q., Chen, Y.-W. & Chang, X.-Y. (2002). Application of Pb isotopic mapping to environment evaluation in China. *Chemical Speciation & Bioavailability*, 14(1-4), 49-56.
296. Zhu, B.-Q., Chen, Y.-W., & Peng, J.-H. (2001). Lead isotope geochemistry of the urban environment in the Pearl River Delta. *Applied Geochemistry*, 16, 409-417.
297. Zou, J.-F., Peng, Z.-X., Du, H.-J., Duan, C.-Q., Reeves, M.J., & Qiu-Hong Pan, Q.-H. (2012). Elemental patterns of wines, grapes, and vineyard soils from Chinese wine-producing regions and their association. *American Journal of Enology and Viticulture*, 63(2), 232-240.

